THE *LEGIONELLA PNEUMOPHILA* EFFECTOR PROTEIN, LEGC7, DISRUPTS YEAST ENDOSOMAL DYNAMICS

by

KEVIN MICHAEL O'BRIEN

(Under the Direction of Vincent Starai)

ABSTRACT

Legionella pneumophila are facultative intracellular bacteria and accidental human pathogens that can cause a severe and deadly pneumonia known as Legionnaires' disease. In order to establish and maintain an intracellular niche within host cells, *Legionella* utilize a type IVB secretion system to inject around 300 effector proteins into the eukaryotic host, to manipulate pathways and processes to the benefit of the bacterium. One such effector protein, LegC7, was originally identified as causing cell death when expressed in yeast, and was noted to disrupt vesicle trafficking. In this work we demonstrate that LegC7 specifically disrupts the localization of cargos that traffic through the endosomal system, while leaving alternative trafficking pathways unaltered. We also demonstrate that the toxicity of LegC7 is reduced or eliminated upon deletion of a subset of early endosome trafficking genes, centered on the early endosome Rab GTPase *VPS21* and the early endosome tethering complex CORVET. Expression of LegC7 causes a mislocalization of Vps8p, the Rab binding subunit of the CORVET complex, and LegC7-RFP displays a high degree of colocalization with this subunit. Thus, disruption of the CORVET complex likely explains the specific endosomal disruption that occurs upon LegC7 expression. Disruption of the normal endosome maturation pathway likely prevents progression of the infected phagosome into the

traditional lysosomal fusion pathway. Finally, we show that LegC7 is degraded upon deletion of the ER glycosylated protein chaperone *EMP47,* which was detected as interacting with LegC7 based on mass spectrometry. This evidence, along with the observation that LegC7-RFP is not mislocalized upon deletion of endosome trafficking genes, suggests the LegC7 disrupts endosome trafficking indirectly. Mutant versions of LegC7 show that endosomal disruption and toxicity are two distinct events, with the toxicity attributed to the interaction with Emp47p. A model of LegC7 acting in the ER fits with the high degree of manipulation that *Legionella* is known to exert on the ER to Golgi trafficking pathway during infection. This work suggests a more involved role of glycosylated proteins and the Emp47p chaperone in the proper functioning of the eukaryotic endosomal system.

INDEX WORDS: *Legionella pneumophila*, *Saccharomyces cerevisiae*, Effector Protein, LegC7, Endosomes, CORVET, Emp47p, Vps21p, Vesicle Trafficking

THE *LEGIONELLA PNEUMOPHILA* EFFECTOR PROTEIN, LEGC7, DISRUPTS YEAST ENDOSOMAL DYNAMICS

by

KEVIN O'BRIEN

A.B. College of the Holy Cross, 2011

A Dissertation Submitted to the Graduate Faculty of The University of Georgia in Partial Fulfillment of the Requirements for the Degree

DOCTOR OF PHILOSOPHY

ATHENS, GEORGIA

2016

THE *LEGIONELLA PNEUMOPHILA* EFFECTOR PROTEIN, LEGC7, DISRUPTS YEAST ENDOSOMAL DYNAMICS

by

KEVIN MICHAEL O'BRIEN

Major Professor:	Vincent Starai
Committee:	Eric Lafontaine Walter Schmidt Eric Stabb

Electronic Version Approved:

Suzanne Barbour
Dean of the Graduate School
The University of Georgia
May 2016

DEDICATION

I am dedicating my thesis to my parents Robert and Karen O'Brien. Without their years of sacrifice and encouragement, I would have been unable to pursue a career in research. They instilled in me the values of dedication, hard work, curiosity, and a love of learning.

ACKNOWLEDGEMENTS

Many people deserve credit and thanks for their support which has allowed me to reach this stage in my career. I would first like to thank my amazing wife Marisa, who has continually supported me throughout graduate school. It has been through her love and encouragement that I have been able to reach this milestone in my life. I owe a tremendous debt of gratitude to my advisor, Dr. Vincent Starai, for training and mentoring me throughout graduate school. It is through his enthusiasm and dedication to my personal development that I am able to write this thesis. I thank my committee members: Eric Lafontaine, Walter Schmidt, and Eric Stabb for their efforts to critique and improve my work. They have continually pushed me to improve both my scientific thinking and research aims. I am grateful to Eric Lafontaine and Mary Hondalus as well as past and present members of their laboratories for their helpful comments and critiques of my research. I have had the pleasure of working with a number of talented and dedicated undergraduates over the years including: Chetan Hebbale, Elizabeth Lindsay, Ivelisse Resto-Garay, and Margret Steward. They have not only collected crucial data but more importantly have instilled in me a dedication to mentoring and disseminating scientific knowledge.

TABLE OF CONTENTS

Page

ACKNOWLEDGEMENTS……v

CHAPTER

1. INTRODUCTION AND LITERATURE REVIEW……1
2. THE *LEGIONELLA PNEUMOPHILA* EFFECTOR PROTEIN, LEGC7, ALTERS YEAST ENDOSOMAL TRAFFICKING……37
3. THE *LEGIONELLA PNEUMOPHILA* EFFECTOR PROTEIN, LEGC7, ALTERS THE LOCALIZATION OF THE CORVET COMPLEX……66
4. THE *LEGIONELLA PNEUMOPHILA* EFFECTOR PROTEIN, LEGC7, REQUIRES THE GLYCOSYLATED PROTEIN CHAPERONE EMP47P FOR STABILITY AND TOXICITY IN YEAST……102
5. CONCLUSIONS……177

REFERENCES……187

APPENDIX 1……215

CHAPTER 1

INTRODUCTION AND LITERATURE REVIEW

LEGIONELLA PNEUMOPHILA

Legionella taxonomy

Although bacteria from the genus *Legionella* were first isolated in 1944, the genus was not officially established until a severe pneumonia outbreak occurred at the American Legion convention in Philadelphia in 1976 (Tatlock 1944, Brenner 1979). The bacteria had been responsible for causing a severe pneumonia amongst conference attendees, killing 34 and sending over 100 to the hospital; it was later discovered to have spread through contaminated water that had been aerosolized and dispersed in the air conditioning system (Fraser 1977). *Legionella pneumophila* are classified as gammaproteobacteria in the order Legionellales that contains two families: Legionellaceae and Coxiellaceae, the latter of which contains the important human pathogen *Coxiella burnetii* (Benson 1998). *Legionella* utilize amino acids as their major growth substrates, specifically cysteine and serine which are converted into pyruvate and fed into the TCA cycle for energy (Pine 1979). More than 50 different species of *Legionella* have been defined to date, though most research is focused on *Legionella pneumophila* which accounts for an estimated 90% of clinical presentations (Marston 1994). While most investigation has been focused on *Legionella pneumophila,* other clinically relevant species exist such as *Legionella longbeachae,* which was originally identified in Long Beach California and accounts for a significant number of *Legionella* infections in Australia. Unlike other species of *Legionella* that inhabit aquatic

environments, *Legionella longbeachae* is found in soil leading to concerns of *Legionella longbeachae* infection through contact with contaminated soil (Steele 1989). Sporadic reports of disease caused by *Legionella* species other than *Legionella pneumophila* and *Legionella longbeachae* would indicate that other members of the *Legionella* genus are in fact able to cause disease, though the total number of infections or public health concern remains unclear (Fields 2002). As such, the remainder of this review will focus specifically on *Legionella pneumophila* and the term *Legionella* will be used as shorthand for this species, not the genus.

Legionella pneumophila microbiology

Legionella pneumophila are Gram-negative facultative intracellular bacteria that are found ubiquitously in aquatic environments including both man-made and natural water systems such as lakes, ponds, and cooling towers (Fliermans 1981). *Legionella* invade and colonize a wide variety of different amoeba and protists in their normal aquatic habitat but have never been described as being able to replicate outside of host organisms in the natural environment (Hagele 2000). Important amoeba hosts include species within the genera of *Hartmanella, Naeglaria,* and *Acanthamoeba,* though over 15 natural hosts have been described and likely more exist (Hagele 2000). In a laboratory setting, *Legionella* has an even wider host range including mice, monkeys, moths, a range of mammalian cell types, and *Caenorhabditis elegans* (Fujio 1992, Fitzgeorge 1983, Harding 2012, and Brassinga 2013). *Legionella* can also be cultured in free-living form in a laboratory environment on buffered-charcoal yeast extract with iron and cysteine as the important constituents (Pine 1979).

Legionellosis

When contaminated water is aerosolized and inhaled by susceptible individuals, *Legionella* can infect alveolar macrophages leading to disease states known broadly as legionellosis. Legionellosis contains two subcategories of infection: Legionnaire's disease, which presents as a severe pneumonia and Pontiac fever, which is a self-limiting flu-like illness (Frasier 1977, Glick 1978). Around 1,000 cases of legionellosis are described each year though the true number is estimated to be as high as 20,000 (Marston 1994). Humans are thought to be dead-end hosts for *Legionella* as no human-to-human transmission has ever been recorded. Nonetheless infections by *Legionella* still pose public health concerns due to the aerosolized mechanism of the *Legionella* infections, which results in community outbreaks of pneumonia that are thought to represent up to 15% of the community acquired pneumonia cases documented each year (Butler 1998). Mortality rates due to legionellosis are estimated around 25% for those whom require hospitalization (Marston 1994). Risk factors for Legionaries' disease include diabetes, compromised immunity, renal disease, heavy smoking, or other respiratory complications such as chronic obstructive pulmonary disease (Marston 1994).

Legionella invasion

The first step to *Legionella* invasion of host cells is attachment of the bacteria to the cell surface. $PilE_L$ a subunit of the pili, and RtxA, which shares sequence similarity to the repeats in structural toxin gene (RTA) are required for attachment of *Legionella* to both amoeba and human cell lines (Strom 1993, Cirillo 2002). Other genes such as major outer membrane protein (MOMP), and *Legionella* collagen-like protein (Lcl) have also been shown to be important for adherence to host cells (Bellinger-Kawahara 1990, Newton

2008). Host factors are also important for attachment of *Legionella* to cell surfaces including the galactose/N-acetylgalactosamine-inhibitable lectin (Gal/GalNAc), which is required for attachment of *Legionella* to *Hartmannella vermiformis* (Venkataraman 1997). A complicating factor in studying *Legionella* is that many processes, including attachment, appear to be host specific as the interaction with Gal/GalNAc seems dispensable for attachment to other host organisms (Harb 1998). Attachment of *Legionella* to human macrophage cells can occur through complement dependent and independent pathways (Payne 1987, Gibson 1994). MOMP appears to be the major protein on *Legionella* that modulates attachment to macrophages by complement dependent systems (Shin 2012). Once attached, the bacterium is engulfed by a special type of phagocytosis known as coiling phagocytosis that involves a pseudopod wrapping around the bacterium before uptake (Horwitz 1984). Coiling phagocytosis has been observed in both amoeba hosts and macrophage hosts of *Legionella,* though heat killed *Legionella* are also engulfed in this manner, leading to confusion as to the significance of this entry method (Horwitz 1984). *Legionella* are also phagocytosed by conventional phagocytosis (Elliot 1986, Rechnitzer 1989). In either case, actin is necessary for entry of *Legionella* into the host cell as prevention of actin polymerization impairs phagocytosis of *Legionella* (Elliot 1986, Lu 2005). In summary, entry of *Legionella* appears to be moderated by alternative mechanisms depending on host type though the process appears to be actin dependent in all circumstances. This highlights a general caveat of the *Legionella* literature: while infection of different host organisms is often similar, it cannot be assumed that all *Legionella* infections proceed by the same pathways and result in the same host cell manipulations.

Legionella Containing Vacuole

Once inside the host cell, the infected phagosome known as the *Legionella* containing vacuole (LCV) becomes the replicative niche for *Legionella* and avoids acidification and fusion with the lysosome (Horwitz 1984). Within 15 minutes of host cell entry, endoplasmic reticulum (ER)-derived vesicles fuse with the membrane of the LCV; important ER markers such as Rab1, Arf1, and Sec22 are seen to localize to the LCV membrane (Horwitz 1983, Kagan 2002, Derre 2004, Kagan 2004). Mitochondria are also recruited to the exterior of the LCV (Horwitz 1983, Swanson 1995). Shortly after uptake, ribosomes stud the surface of the LCV though no mechanistic explanation exists on how they are recruited (Berger 1994). A large number of host pathways are commandeered to ensure survival of the host cell and maintain the replicative niche. The LCV gains the early endosome lipid marker phosphatidylinositol 3-phosphate [PI(3)P] within 1 minute of uptake but loses the marker quickly and gains the normally Golgi localized PI(4)P within 30 minutes (Weber 2014). The mature LCV maintains a high concentration of PI(4)P which helps to explain both the recruitment of ER derived vesicles and the observations that a number of *Legionella* effectors bind to PI(4)P, which allows for anchoring of effector proteins to the LCV (Dolinsky 2014, Del Campo 2013, Hilbi 2011). Proteomic analysis of the LCV has found an interesting mixture of proteins on the mature LCV. Results from macrophages and amoeba hosts are broadly in agreement pointing to similar overall infection mechanisms (Hoffmann 2013, Urwyler 2008). In macrophages, nearly 25% of host derived LCV proteins were mitochondrial in origin, and 16% were designated as ER derived. It is also interesting to note that less than 4% of total host-derived LCV proteins were identified as endosome specific, highlighting the separation of the LCV from the

traditional maturation pathway (Hoffmann 2013). The high percentage of ER related proteins found on the LCV demonstrates the crucial nature of the ER-to-Golgi trafficking pathway in *Legionella* pathogenesis; this fits with the observation that siRNA knockdown of certain ER trafficking genes result in replication defects (Dorer 2003).

Secretion Systems

Legionella encode at least 5 different secretion systems: the Type IVB Dot/Icm (Defective in organelle trafficking/Intracellular multiplication) system, the *Legionella* secretion pathway (Lsp) type II secretion system, the *Legionella* secretion system (Lss) type I secretion system, a twin arginine transporter (TAT) system, and a type IVA secretion system named *Legionella virB/virD*-like type IV secretion system (Lvh). The type IVB Dot/Icm system is responsible for secretion of a majority of the effector proteins into the host cell while the Lsp type II system is also important for full pathogenicity of the bacterium. Both of these systems will be discussed in depth below. The functions and roles of the latter three systems in *Legionella* infections are not well characterized. The Lss type I secretion system was identified based on gene homology to other type I secretion systems but appears to be dispensable for infection leading to the question of whether or not it actually functions in *Legionella* cells (Jacobi 2003). Another more recent report indicates that the Lss system might function in host cell invasion, though this effect may be host specific (Fuche 2014). The TAT system appears to be important for environmental survival, biofilm formation, and for survival of the bacterium in the host cell (De Buck 2004, Rossier 2005). The type IVA Lvh system is able to partially compensate for mutants in the type IVB Dot/Icm system leading to the hypothesis that it functions either as an alternate

secretion pathway for some effectors, functions in certain hosts, or functions under specific environmental conditions (Bandyopadhyay 2007).

The Lsp Type II secretion system is required for full virulence of *Legionella* in host cells (Hales 1999, Soderberg 2008). The Lsp system appears to mainly function in relation to metabolic survival and environmental persistence of *Legionella* compared to the central focus on intracellular replication of the Dot/Icm system. As such, *Legionella* strains bearing Lsp system mutantions are defective for persistence traits such as low temperature survival and motility (Soderberg 2004, Soderberg 2008, Stewart 2003). Proteins that are secreted by type II secretion systems bear distinct secretion signals at the N-terminus leading to the bioinformatics prediction of at least 27 Lsp secreted proteins from *Legionella* (DebRoy 2006). Important proteins secreted by this system include ProA, a zinc metalloprotease, phospholipase C, and lysophospholipase A (Aragon 2002, Rossier 2001, Rossier 2004).

The Dot/Icm type IVB secretion is the best studied secretion system in *Legionella* as it functions to secrete the vast majority of the effector proteins that are important for survival of *Legionella* in host cells (Vogel 1998, Horwitz 1987, Marra 1992). Type IV secretion systems come in three varieties: those used in conjugative transfer of plasmid DNA between bacteria as epitomized by the secretion system of *Agrobacterium tumefaciens* (Type IVA), those used for uptake of DNA without direct bacterial contact, and those used for secretion of proteins such as the Dot/Icm system from *Legionella* (Type IVB) (Cascales 2003). The *Legionella* Dot/Icm system was the founding member of the type IVB secretion system group that now includes secretion systems from organisms within genera such as *Wolbachia, Coxiella,* and *Rickettsia* (Masui 2000, Zusman 2003). There are at least 27

Dot/Icm genes found on two chromosomal regions (Matthews 2000, Vogal 1998, Segal 1998). The exact structure of the Dot/Icm secretion system has yet to be determined but evidence suggests that DotC, D, F, G, and H serve as the membrane spanning domains of the complex with DotH localizing to the outer membrane (Vincent 2006, Kubori 2014). A second complex containing DotL, M, N, S, and W is thought to act as the Type 4 coupling complex which provides energy in the form of ATP to secrete proteins; DotL serves the essential role of effector protein recognition (Vincent 2006). IcmS and IcmW are thought to function as chaperones that recognize effector proteins, and in support of this role IcmS and IcmW bind to DotL (Ninio 2009, Sutherland 2012).

There are roughly 300 effector proteins that have been verified or are predicted to be secreted effector proteins of *Legionella,* meaning that 10% of the *Legionella* genome is devoted to effector protein genes which underscores the important role of these genes in host invasion and survival (Burnstein 2009, Luo 2004, Heidtman 2009, Lifshitza 2013). Many of these effector proteins appear to have been acquired via horizontal gene transfer due to the presence of eukaryotic motifs (de Felipe 2005, Costa 2014). Another important factor in *Legionella* effector evolution appears to have been domain swapping between effector genes resulting in the evolution of novel effectors from different combinations of building blocks leading to the observation that while *Legionella* species largely do not share effector protein genes they do share many of the same functional motifs (Burstein 2016). The C-terminus appears to be important for the secretion of many of the effectors though no definite secretion signal exists, making the identification of effectors difficult (Nagai 2005). The presence of an internal signal sequence on an effector was also recently reported leaving open the possibility that different signal sequences temporally control the

release of effectors (Jeong 2015). Individual deletions of effector protein genes usually do not cause any phenotypic change in the ability of *Legionella* to survive or replicate in host cells; this is due to the suspected redundancy of many of the effectors but results in difficulty in identifying the roles of effectors in traditional genetic experiments (Dorer 2006). The only effectors that demonstrate phenotypic defects upon deletion are those that are related to stability of the LCV (Creasey 2012). The Dot/Icm system is essential for survival in host cells, and as such deletion of Dot/Icm system genes result in an inability of the LCV to separate from the traditional phagosome-lysosome fusion pathway resulting in bacterial destruction by the host cell (Horwitz 1983).

Legionella tightly regulates the expression of effector proteins in order to ensure proper timing of host invasion, manipulation, and egress. Around 40 effector genes have been identified as regulated by the response regulator PmrA, though that number is likely higher (Zusman 2007). The CpxR regulation system was identified as regulating another 9 effector proteins (Altman 2008). Finally a system termed the LetA-RsmYZ-CsrA has been identified and controls the regulation of up to 279 genes, some of them effector proteins. This system will be discussed in more depth below (Rasis 2009).

Manipulation of the Host Cell

A large number of host pathways are modulated and manipulated by *Legionella* in order to promote LCV formation, LCV stability, host cell viability, and *Legionella* metabolism. While the functions and targets of many of the 300 effector proteins remain unclear, some effector protein activities have been described in detail. One of the major pathways manipulated by *Legionella* is the ER-to-Golgi trafficking pathway during which

ER-derived material is recruited to coat the LCV membrane through a concerted effort of a number of effector proteins (Swanson 1995).

Mitochondria are recruited to the LCV membrane early in infection and though it is still unclear what role mitochondria play in intracellular survival of *Legionella,* a few effector proteins have been demonstrated to alter mitochondrial dynamics (Horwitz 1983, Tilney 2001). LncP has been described as a mitochondrial inner membrane transporter that might function to modulate mitochondrial activity towards some bacterial benefit (Dolezal 2012). LegS2 shares similarity with the enzyme sphingosine-1-phosphate lyase but contains a mitochondrial localization motif which suggests the ability to localize and manipulate mitochondrial function (Degtyer 2009). Interestingly, LegS2 results in a depletion of sphingosine which in turn prevents the initiation of autophagy (Rolando 2016).

Legionella manipulates ubquitination of host membranes to modulate signaling pathways as well as provide nutrients for growth (Price 2011, Manske 2014). LegU1 functions to tag ubiquitin to BAT3 which signals for this protein to be degraded, leading to the inability of BAT3 to signal for apoptosis (Ensminger 2010). GobX was described as localizing to Golgi membranes and possessing ubiquitin ligase activity (Lin 2015). AnkB, a *Legionella* effector protein that contains an F-box domain, is farnesylated by host machinery anchoring it to the LCV membrane and allowing interaction with the host protein Skp1 to form an ubiquitin ligase (Ivanov 2010, Price 2010). This complex is thought to promote ubiquitination of host proteins that are then degraded by the proteasome. The resulting peptides are thought to be transported into the LCV and used as metabolites by *Legionella* (Price 2011). In support of this hypothesis, phenotypic defects

due to *ankB* deletion can be bypassed by supplementation of amino acids, specifically serine and cysteine, into growth media (Price 2011). LubX was found to promote the ubiquitination of another *Legionella* effector protein of unknown function, SidH; this indicates that in addition to manipulating proteasomal degradation for nutrient acquisition, *Legionella* may also use this pathway to degrade its own effector proteins as a form of self-regulation (Kubori 2010). Acquisition of iron, a crucial cofactor for cells, is thought to be acquired via the effector protein MavN (Isaac 2015).

VESICLE TRAFFICKING AND MANIPULATION BY *LEGIONELLA* EFFECTORS

Vesicle Trafficking

One of the key differentiating characteristics of eukaryotes and prokaryotes is the presence of distinct membrane bound organelles in the former. Movement of protein and lipid cargo to and from these organelles via vesicle intermediates requires stringent control to ensure that cargo is delivered to the proper compartment at the appropriate time. Membrane fusion is a multi-step process involving a number of protein and lipid components to ensure the specificity of cargo delivery and promote non-leaky fusion of a vesicle to a target compartment (Figure 1.1). In general, the process of vesicle traffic can be broken into 4 distinct steps: budding, transit, tethering, and fusion (Cai 2007). Vesicle budding is driven in large part by the accumulation of coat proteins and adaptor protein complexes that function to induce membrane curvature and eventual budding as well as functioning in cargo selection (Cai 2007). Once a vesicle has budded from a membrane, it generally traffics to its target membrane by association with a motor protein such as kinesin or dynein (Matanis 2002). Tethering is the initial contact between a vesicle and its target compartment. This is mediated by a tethering complex, which is anchored to the

membrane of the target compartment either directly or through an interaction with a Rab GTPase (Whyte 2002). Fusion, the final step in the membrane trafficking pathway, involves the mixing of lipid bilayers and eventual luminal content mixing; this step is promoted by SNARE complex formation (Sollner 1993). Due to the importance of the specificity and timing of these events, vesicle trafficking pathways are highly manipulated by intracellular pathogens such as *Legionella.*

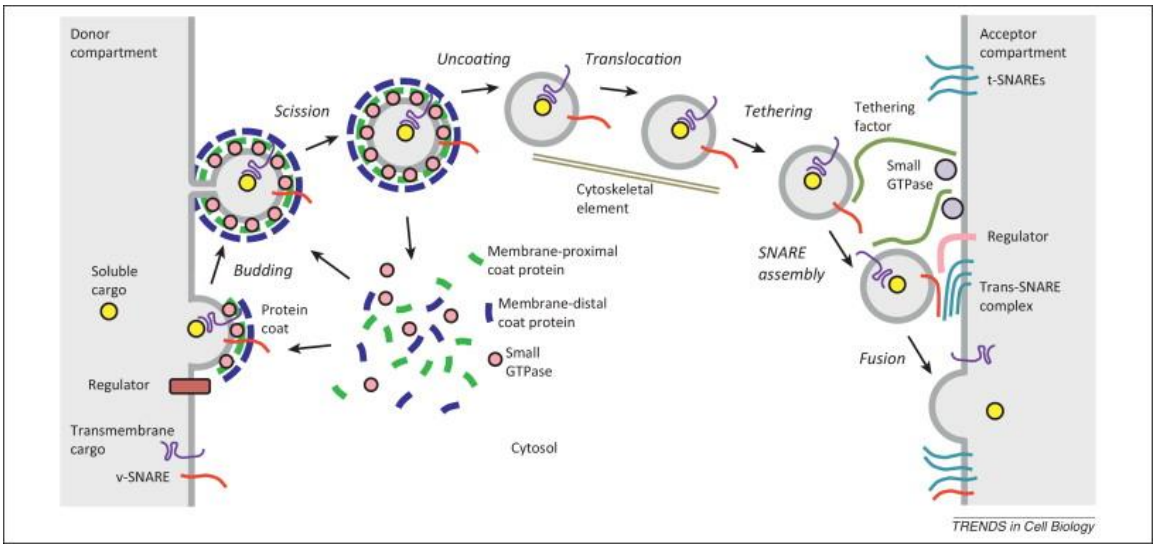

Figure 1.1: Vesicle trafficking in eukaryotic cells. The four major steps of vesicle fusion are demonstrated; budding, transport, tethering, and fusion. Figure adapted from Bonifacino and Glick 2004.

Rab GTPases

Rab GTPases (Rabs) are small GTPases in the Ras superfamily that undergo cycles of activation and inactivation in respect to their ability to bind and hydrolyze GTP to GDP (Stenmark 2009). Rabs play a crucial role in membrane trafficking due to their specific localization to certain cellular membranes. Rab GTPases are prenylated at cysteine

residues found at their C-termini to allow membrane association; the prenylation event does not explain membrane specificity, an event that likely requires the assistance of proteins that bind to specific Rab GTPases (Alexandrov 1994). The prenylation event occurs when the Rab binds to a Rab escort protein (REP) which promotes association with Rab-geranylgeranyltransferase (Rab-GGT), catalyzing the addition of the prenyl group to the Rab which can now become membrane associated through this hydrophobic posttranslational modification (Andres 1993, Alexandrov 1994). Rab activation through GTP binding is promoted by a guanine-nucleotide exchange factor (GEF). It is the active GTP-bound form of the Rab GTPase that generally is important for the recruitment of tethering complexes to the organelle membrane. Eventually a GTP-hydrolysis activator protein (GAP) results in the hydrolysis of GTP to GDP and the inactivation of the Rab (Scheffzek 1997). Inactive Rabs are bound by GDP-dissociation inhibitors (GDI), which results in the removal of the Rab from the organelle membrane by masking the prenyl group (Soldati 1993, Ullrich 1993). The Rab can then be reinserted into a membrane when a GDP-dissociation factor (GDF) acts to dissociate the GDI and promote reinsertion of the Rab GTPase into a membrane (Rak 2003).

Rab GTPases share conserved structural domains that are important for function. The N-terminus of the Rab contains structural elements that are involved in nucleotide binding and overall regulation. The P-loop is involved in overall structural coordination and binding of the guanine nucleotide. The switch 1 and switch 2 regions are responsible for the activation and inactivation cycle of the Rab and undergo dramatic rearrangements during different nucleotide binding states (Schlichting 1990). These regions at the N-terminus are highly conserved amongst Rabs. This is contrasted with the C-terminus,

which is highly divergent but contains a variation of a di-cystine motif needed for prenylation and membrane association (Seabra 1992).

Yeast early endosomes are enriched with the Rab GTPase Vps21p (Singer-Kruger 1994 and Horazdovsky 1994, Gerrard 2000). Three paralogs of this gene exist in yeast, *VPS21*(Y*PT51*), Y*PT52*, and Y*PT53*; Vps21p is the major functional Rab at early endosomes as demonstrated by experiments where deletion of *YPT52* or *YPT53* result in only minor defects in endosomal traffic compared to *VPS21* deletion (Singer-Kruger 1994, Nickerson 2012). Ypt52p appears to have similar functionality to Vps21p but is highly negatively regulated; Ypt52p is bound by the protein Roy1p (repressor of Ypt52 1), resulting in no Ypt52p activity (Liu 2011). Roy1p is hypothesized to act as an overflow switch that inhibits Ypt52p activity under normal conditions but allows for immediate increase of endosomal fusion when necessary. *YPT53* is not expressed under normal cellular conditions but is induced upon nutrient stress and appears to have a broader functionality than either Vps21p or Ypt52p (Singer-Kruger 1994, Nickerson 2012, Nakatsukasa 2014).

Vps21p is activated by the GEFs Vps9p and Muk1p (Burd 1996, Hama 1999, Paulsel 2013). Vps21p is inactivated by the GAPs Msb3p and to a lesser extent its paralog Msb4p (Nickerson 2012, Lachmann 2012). Msb3p is recruited to endosomes in part through the actions of the biogenesis of lysosome related organelle complex 1 (BLOC-1) complex that also binds to active GTP bound, Vps21p (Rana 2013, Peter 2013). The BLOC complexes are a series of three related complexes found in mammalian cells termed BLOC-1,-2,-3 and are responsible for Hermansky-Pudlak syndrome, a disorder of melanosomes and lysosomal related organelles (Falcon-Perez 2002, Nazarian 2003). In yeast only a single BLOC complex, BLOC-1, has been described. BLOC-1 functions in endosome maturation and

consists of 6 members: Bls1p, Snn1p, Bli1p, Kxd1p, Cnl1p, and Vab2p, all distinctly related to their mammalian homologs (Hayes 2011). Mammals also encode three Rab5 isoforms (Rab5a, Rab5b, and Rab5c). As in yeast Rab5a (Vps21p) is the predominate Rab GTPase on early endosomes, and Rab5c(Ypt53p) is not required under normal growth conditions (Gorvel 1991, Bucci 1995, Chen 2009).

The Rab GTPase Ypt7p functions in late endosome fusion, vacuole fusion, fusion of Golgi derived AP-3 vesicles to the vacuole, and autophagosome/vacuole fusion (Kirisako 1999, Haas 1995, Schimmoller 1993). Ypt7p is activated by the Mon1/Ccz1 complex in yeast and mammalian cells (Nordmann 2010, Wang 2002). The Mon1/Ccz1 complex localizes to early endosomes in part due to an interaction with PI(3)P (Poteryaev 2010). Msb3p has been shown to have GAP activity towards Ypt7p in addition to Vps21p; Ypt7p is also inactivated by the GAP Gyp7p (GAP for Ypt7) (Nickerson 2012, Vollmer 1999).

A number of *Legionella* effector proteins target host Rab GTPases. The effector protein SidM binds to PI(4)P, anchoring this effector to the LCV, where it activates and recruits Rab1, the Rab GTPase that functions in ER to Golgi traffic (Murata 2006, Machner 2006, Machner 2007). A second effector protein, LepB, can then inactivate Rab1 causing its release from the LCV (Ingmundson 2007). SidM also functions to AMPylate Rab1 which prevents inactivation by LepB or normal host cell factors until Rab1 is de-AMPylated by another effector protein, SidD; this AMPylation event is also crucial for localization of Rab1 to the LCV (Neunuebel 2011, Chen 2013, Hardiman 2014). The AMPylation activity of SidM was demonstrated on numerous other Rab GTPases *in vitro* though it is unclear if this broad activity is relevant *in vivo.* LidA binds to Rab1 regardless of AMPylation status and prevents inactivation of Rab1 (Neunuebel 2011). AnkX catalyzes the addition of a

phosphocholine to Rab1, which disrupts traffic, while the effector Lem3 removes this modification (Tan 2011, Goody 2012, Pan 2008, Campanacci 2013). In addition to Rab1, Arf1 is a small GTPase that promotes ER-to-Golgi traffic; the effector protein RalF activates this small GTPase and localizes this protein to the LCV membrane (Nagai 2002). Two effectors LidA and PieE have been reported to each bind to at least 10 Rab GTPases including Rab1, the early endosome Rab5, and the late endosome Rab7 (Mousnier 2014, Schoebel 2011). It remains unclear the rationale behind binding to such a large number of Rab GTPases, though these proteins have been termed supereffectors or metaeffectors and might play a role in modulating the activities of other *Legionella* effectors. Manipulation of both Rab1 and Arf1 provide at least a partial explanation for the recruitment of ER-derived vesicles to the LCV. VipD functions as a lipase, which is activated by binding to Rab5 and is able to hydrolyze phosphatidylethanoamine, phosphtytidylcholine, and PI(3)P, resulting in the avoidance of LCV entry into the phagosome maturation pathway (Shohdy 2005, Zhu 2013, Gaspar 2014).

Tethering Complexes

Tethering complexes function to physically link a donor and acceptor vesicle and in some instances, can function to promote additional steps in the fusion process. There are two general types of tethering complexes, the multi-subunit tethering complexes (MTCs) and the coiled-coil tethers (Lupashin 2005, Brocker 2010). MTCs have been comparatively better studied, and a number of distinct MTCs are known to exist in the cell, localizing to distinct organelles and promoting specific fusion events. MTCs are comprised of multiple protein subunits and display an ability to bind to Rab GTPases; these complexes play a more involved role in the fusion process compared to coiled coil tethers. These complexes

include members such as the homotypic fusion and vacuole protein sorting (HOPS) complex, which functions in late endosome and vacuole fusion; the class C core vacuole/endosome tethering (CORVET) complex which functions in early endosome fusion; and the Golgi-associated retrograde protein (GARP) complex which functions in retrograde, endosome to Golgi traffic among other complexes (reviewed in Yu 2010).

Collectively called Vps Class C complexes, the CORVET (class C core vacuole/endosome tethering) and HOPS (homotypic fusion and protein sorting) tethering complexes function to promote endosomal and vacuole fusion events; the CORVET complex functions at the early endosome and the HOPS complex functions at the late endosome and vacuole (Balderhaar 2013). These closely related complexes share 4 core subunits (Vps11p, Vps16p, Vps18p, and Vps33p) and each contains two additional Rab binding subunits, Vps3p and Vps8p in the CORVET complex and Vps39p and Vps41p in the HOPS complex (Seals 2000). The structure of the HOPS complex reveals a seahorse shaped structure with one Rab binding subunit on each end leading to the hypothesis that the complex binds Rab GTPases on two opposing membranes thus serving as a physical bridge between vesicles (Brocker 2012). Though no structure has been solved for the CORVET complex, the similarity between the complex compositions and similar immunoprecipitation patterns has led to a hypothesis that both complexes adopt the same structure (Ostrowicz 2010). Analysis of the mammalian HOPS complex revealed that the overall structural topology was conserved compared to the yeast complex, however the mammalian HOPS complex contains an additional member the Rab7 interacting lysosomal protein (RILP) subunit (van der Kant 2015, Cantalupo 2001). In addition to the RILP subunit, mammalian cells encode two isoforms of Vps33 (Vps33A and Vps33B) and Vps16

(Vps16A and Vps16B); it appears that the mammalian CORVET and HOPS complexes only incorporate Vps33A and Vps16A (Perini 2014, Akbar 2009, Kim 2001). Vps33B and Vps16B appear to function in the formation of more specialized structures like platelet α-granules though their exact role in mammalian cells has yet to be defined (Lo 2005).

Vps33p is a SM-like protein that has been implicated in binding to the assembled vacuolar SNARE complex (Subramanian 2004, Stroupe 2006). Vps33p appears to bind only to the assembled Qa,b,c (Vam3p, Vam7p, and Nyv1p) or quaternary SNARE complex rather than individual SNARE domains; binding of the SNARE complex prevents early disassembly by Sec18p (Lobingier 2012, Xu 2010). In addition to prevention of SNARE complex disassembly, HOPS also functions to ensure proper SNARE complex formation (Starai 2008). Vps33p binds to the SNARE motifs of Vam3p and Nyv1p, which are found on opposing membranes, thus serving to promote proper trans-SNARE complex formation (Baker 2015).

In addition to the SNARE binding capabilities of Vps33p, two additional interactions between core complex members and SNAREs have been demonstrated. Vps16p binds to the Habc domain of Vam3p during vacuole fusion (Lobingier 2012, Lurick 2015). The N-terminal region of Vam7p has also been shown to bind to either Vps16p or Vps18p (Kramer 2011). SNARE binding by the Vps Class C core complex members has only been demonstrated within the context of the HOPS complex; it remains to be seen if similar interactions occur in the CORVET complex, but based on the similarity of the complexes, it is likely that the Vps Class C core complex members play similar SNARE binding roles at the early endosome.

HOPS

The HOPS complex contains the subunits Vps39p and Vps41p; both of which bind to Ypt7p, Vps39p binds both GDP and GTP bound Ypt7p while Vps41p preferentially binds the GTP bound form of Ypt7p (Brett 2008). Little is known about how the HOPS complex assembles, but Vps39p appears to nucleate HOPS assembly as it localizes to Ypt7p positive membranes before Vps41p, which appears to be recruited to the complex after initial Vps39p/Ypt7p interaction (Auffarth 2014).

The HOPS complex participates in the fusion of vesicles to the vacuole from a number of distinct pathways and as such, HOPS is highly regulated, mainly through the Vps41p subunit, to promote specific fusion events. In general, Vps41p, which preferentially binds to active Ypt7p, is thought to function in the promotion of homotypic vacuole fusion and late endosome to vacuole fusion by preventing inactivation of Ypt7p (Cabrera 2009, Hickey 2009). Vps41p directly binds to Apl5p, a member of the AP-3 coat complex, thereby linking AP-3 vesicle fusion and the HOPS complex (Angers 2009). Vps41p contains a membrane curvature motif known as an amphipathic lipid-packing sensor (ALPS) motif which is inserted into the membrane on small highly curved membranes such as late endosomes; this motif, along with the Apl5 interaction motif, is exposed on large, less curved, structures such as the vacuole, providing evidence as to why AP-3 vesicles fuse only with the vacuole (Cabrera 2010). The kinase Yck3p phosphorylates Vps41p and prevents reinsertion of the ALPS motif into the membrane thus promoting AP-3 vesicle fusion (LaGrassa 2005). Vps41p also directly interacts with Arl8p on phagosomes, an interaction that explains the role of HOPS in autophagosome/vacuole fusion (Saski 2013). A second protein pleckstrin homology domain containing protein family member 1

(PLEKHM 1) also binds to the HOPS complex and interacts with LC3 on autophagosomes providing a second link between HOPS and autophagosome/vacuole fusion (McEwan 2015). Taken together these data argue for a central role of Vps41p in directing fusion specificity of the HOPS complex.

CORVET

The CORVET complex contains Vps3p and Vps8p, which interact with the early endosome Rab Vps21p, giving the complex specificity towards early endosome fusion (Peplowska 2007, Markgraf 2009). Vps8p binds to only GTP bound Vps21p, while Vps3p can bind to nucleotide free, GDP, or GTP bound Vps21p, mimicking the Rab binding patterns of Vps39p and Vps41p (Peplowska 2007). The CORVET complex localizes independently of other early endosome proteins such as Vac1p and Vps45p and can tether Vps21p positive endosomes *in vitro* (Balderhaar 2013). All subunits of the CORVET complex from yeast have clear homologs in higher eukaryotes except for Vps3p. The identity of a Vps3p homolog has been the subject of speculation but recently a protein, Tgfbrap1, was identified as a Vps3p functional homolog in the mammalian CORVET complex (Perini 2014).

GARP/EARP

The Golgi-associated retrograde protein (GARP) complex is a tethering complex made up of four members: Vps51p, Vps52p, Vps53p, and Vps54p (Conibear 2000, Conibear 2003). This complex assembles on late Golgi membranes and modulates fusion of retrograde traffic, endosome-to-Golgi traffic (Siniossoglou 2001). This pathway is important for the retrieval of a number of proteins including cargo receptors such as Vps10p that are essential for proper trafficking of endosomal directed cargos (Marcusson

1994). Vps51p binds to the retrograde SNARE Tlg1p linking the tethering complex to SNARE complex formation (Siniossoglou 2001). The endosome-associated recycling protein (EARP) complex is a newly identified tethering complex that functions at mammalian endosomes (Schindler 2015). This complex shares 3 subunits with the GARP complex: Ang2, Vps52, and Vps53. In EARP, syndetin replaces Vps54 and results in localization of the complex to endosomes where it functions in endocytic recycling in higher eukaryotes, it is unclear if a similar complex functions in yeast.

SNARES

Soluble N-ethylmaleimide-sensitive factor (NSF) attachment protein receptor (SNARE) proteins contain heptad repeats that interact to form a tetrameric helical bundle and through this interaction promote membrane fusion (Sollner 1993). A fusogenic SNARE complex requires a total of 4 SNARE helices to form into a complete complex; generally each SNARE protein contains one SNARE motif however there are examples of SNAREs containing two motifs (Sollner 1993). SNAREs are classified as either Q-or R-SNAREs depending on the residue found at the middle, or 0 layer, of the tetrameric bundle; *in vivo* membrane fusion requires the formation of a bundle between three Q-SNARE motifs and 1 R-SNARE motif (Fasshauer 1998, Sollner 1993). Most SNAREs contain a transmembrane domain anchoring them to membranes though some require modifications such as farnesylation or palmitolation for membrane association (Fukasawa 2004, Dietrich 2004). N-terminal regulatory domains known as Habc domains are found on many SNAREs and function to autoinhibit SNARE complex assembly, these domains are also targeted by a number of SNARE binding proteins, which also function in SNARE complex assembly and regulation (Misura 2000, Munson 2000, Paumet 2005).

SNAREs undergo a cycle by which the tetrameric helical bundle is formed after a fusion event and then exists on the target membrane in a non-fusogenic and stable complex called the cis-SNARE complex, so named for the fact that all four SNAREs currently reside on the same membrane (Malsam 2008). This complex is recycled by the action of NSF, a hexameric AAA ATPase, and alpha-soluble NSF attachment protein (α-SNAP) which modulates NSF attachment to the cis-SNARE complex (Block 1988, Weidman 1989). NSF and α-SNAP were identified as Sec18 and Sec17 in yeast, respectively (Mayer 1996).

The SNARE complex that promotes early endosome fusion consists of Syn8p, Pep12p, Ykt6p, and Vti1p (Gerrard 2000, von Mollard 1997, Lewis 2002, Kweon 2003). Mammalian endosome fusion is moderated by syntaxin13, vti1a, syntaxin6, and VAMP4 (Brandhorst 2006, Zwilling 2007). The SNARE complex that is responsible for late endosome and vacuole fusion consists of Nyv1p, Vam3p, Vam7p, and Vti1p (Ungermann 1999).

Legionella encodes *lse1* which functions as a SNARE mimic that can promote ER-to-Golgi SNARE pairing, likely helping to fuse ER-derived vesicles with the LCV (King 2015). In addition to directly mimicking SNARE proteins, the recruitment of Rab1 to the LCV, described previously, promotes the creation of abnormal SNARE complexes between plasma membrane and ER SNAREs that nonetheless promote vesicle fusion between ER vesicles and the LCV (Arasaki 2012). The effector proteins LepA and LepB are similar in structure to SNARE proteins and might function to hijack normal host exocytic machinery for bacterial egress (Chen 2004).

Sec1-Munc-18 like Proteins

Another class of important SNARE binding proteins are known as Sec1-Munc-18 like (SM) proteins that function to promote SNARE complex assembly as well as protect SNARE complexes from disassembly (Carr 1999, Scott 2004, Rodkey 2008). SM proteins can both bind to single SNAREs as well as assembled SNARE complexes (Deak 2009). SM proteins function in the protection of assembled SNARE complexes from NSF mediated disassembly (Xu 2010). Rather than simply acting to protect formed SNARE complexes from disassembly, it is now well established that SM proteins play more active roles in SNARE complex assembly, acting to directly nucleate proper SNARE complexes by functioning as scaffolds (Demircioglu 2014). Consistent with this scaffolding role is the observation that mutants in the SNARE-binding groove of SM proteins do not promote efficient fusion events (Weber-Boyvat 2011). SM proteins do not only function in nucleation of SNARE complex assembly but they also function to proofread complexes to ensure proper fusogenic SNARE complexes; this nucleated assembly greatly increases the speed of SNARE complex assembly (Starai 2008, Scott 2004). The N-terminal Habc domain found on some SNAREs appears to represent an important binding and regulation site between SNAREs and SM proteins (Burkhardt 2008).

Lipids

Lipids play important roles in membrane fusion including the recruitment of protein fusion factors and promoting proper membrane curvature. One very important class of lipids are the phosphoinositides (PtdIns). PtdIns have an inositol headgroup attached to a glycerol phosphate backbone, the inositol group can be phosphorylated in the 3, 4, or 5 positions or combinations therein, and these different phosphorylation patterns serve as

targets for a variety of protein interaction motifs (Lemmon 2008). PtdIns make up a small percentage of total cellular lipids, but phosphorylated versions are specifically enriched on particular cellular membranes and play important roles in recruiting specific fusion related proteins to those cellular compartments (Odorizzi 2000). PI(4,5)P_2 is enriched at the plasma membrane, PI(3)P is enriched on early endosomes, and PI(3,5)P_2 becomes enriched on late endosomes and vacuoles/lysosomes (Padron 2003, Gillooly 2000).

Phosphatindylinositol 3-phosphate [PI(3)P] is an important lipid marker found primarily on the early endosome and early autophagosome (Gillooly 2000). Two protein motifs specifically bind to PI(3)P and help to localize proteins necessary for early endosome fusion. The FYVE domain is found on important endosomal proteins such as Vac1p and Vps27p (Peterson 1999, Misra 1999). A second motif, the phox-homology (PX) domain also binds to PI(3)P though with lower affinity than the FYVE domain (Ellson 2002). PI(3)P is synthesized from PtInds by the action of Vps34p, a PI(3)P kinase. Vps34p exists in two complexes in the cell. One complex is comprised of Vps34p, Vps15p, Vps30p, and Vps38p and functions in PI(3)P synthesis at the early endosome while a second complex made of Vps34p, Vps15p, Vps30p, and Apg14p functions to synthesize PI(3)P on autophagosomes (Kihara 2001). The regulatory subunit Vps15p is found in both complexes and acts to activate Vps34p kinase activity (Stack 1995).

Vac1p is a protein that is found on endosomes, localized to early endosomes by its FYVE domain (Weisman 1992). Vac1p binds to GTP bound Vps21p and Vps45p and shows a genetic interaction with the SNARE, *PEP12* (Tall 1999, Peterson 1998). The mammalian homolog, rabenosyn-5, also contains a FYVE domain and binds to both Rab5, Rab4, and Vps45 and is thought to function in coordination of recycling and anterograde endosome

maturation (Nielson 2000, de Renzis 2002, Morrison 2008). Overexpression of *VAC1* can compensate for CORVET deletions in only the endocytic pathway, indicating that Vac1p might function in fusion of endocytic vesicles to the early endosome (Cabrera 2013). Vac1p was demonstrated to bind to the CORVET/HOPS core complex member Vps11p *in vivo* though it remains unclear what relevance this has to Vac1p functionality (Peterson 2001).

During endosome maturation, the protein Fab1p is recruited to early endosomes through its FYVE domain and converts PI(3)P into PI(3,5)P_2 which becomes enriched on late endosomes and vacuoles accounting for the alteration in PtdIns identity of endosomes during maturation (Cabezas 2006, Cooke 1998). PI(3)P synthesis is also negatively regulated in higher eukaryotes; two proteins, SORF-1 and SORF-2, act to inhibit PI(3)P synthesis at the early endosome thus preventing over enrichment which leads to fusion defects, it is unclear if yeast contain homologs of these genes (Liu 2016).

The lipid PI(4)P is normally found enriched on the Golgi and serves to recruit a number of host factors that promote ER-to-Golgi traffic (Di Paolo 2006). PI(4)P is enriched in the LCV membrane and serves to recruit both secreted *Legionella* effectors as well as host proteins (Weber 2014). The effectors SidF and LppA can both synthesize PI(4)P from various PI precursors (Weber 2014, Hsu 2012). SidF hydrolyzes PI(3,4)P_2 and PI(3,4,5)P_3 to PI(4)P and is responsible for the majority of PI(4)P enrichment on the LCV. The effector SidP hydrolyses PI(3)P, which serves as an important early endosome marker that recruits endosome trafficking machinery, to PtIdns. Removal of PI(3)P from the LCV plays a major role in preventing LCV entry into a phagosomal maturation pathway (Toulabi 2013). RavZ is recruited to new autophagosomes via a PI(3)P interaction motif and functions to inhibit autophagy by irreversibly hydrolyzing a bond within Atg8 in such a way as to inhibit

conjugation to Atg7 and Atg3 thus preventing autophagosome formation (Choy 2012, Horenkamp 2015).

ESCRT

The endosomal complex required for transport (ESCRT) pathway is comprised of 5 protein complexes that function in the degradation of membrane proteins; each of the 5 complexes is recruited by the previous complex (Reviewed in Schuh 2014). Protein targets of this pathway are modified with ubiquitin (Ub) and sorted into intraluminal vesicles (ILVs) which are ultimately delivered to the vacuolar/lysosomal lumen upon vacuole/late endosome fusion (Katzmann 2001). ILV formation begins on early endosomes though late endosomes contain much denser accumulations of ILVs formed during the maturation process (Raiborg 2002). The ESCRT pathway results in vesicle scission from within the budneck of a vesicle; the ESCRT pathway or ESCRT components have been implicated in other membrane scission including cytokinesis and viral budding, two more examples where vesicle scission must be accomplished from within the budneck (Weiss 2011, Carlton 2007, Morita 2007). Unlike proteasomal degradation of proteins, a single Ub is sufficient for entry into the ESCRT pathway (Haglund 2003). The first complex that acts is ESCRT-0 comprised of Vps27p and Hse1p (Bilodeau 2002). Both members of this complex can bind Ub which serves as a link between the early endosome and initial cargo selection (Bilodeau 2003). Vps27p directly binds to Stp22p, a member of ESCRT-I, which in turn recruits the remainder of ESCRT-I made up of Mvb12p, Srn2p, and Vps28p (Katzmann 2001, Chu 2006). ESCRT-II is comprised of Vps25p, Snf8p, and Vps36p and is recruited though an interaction between Vps28p and Vps36p (Babst 2002, Hierro 2004, Teo 2006). ESCRT-III which is comprised of Did4p, Vps20p, Vps24p, and Snf7p is recruited due to an

interaction between Vps25p and Vps20p (Babst 2002, Bowers 2004). Finally the Vps4 complex, or ESCRT-IV, is made up of Vps4p, Vps60p, and Vta1p and is recruited through interaction with the N-termini of ESCRT-III members (Babst 1998, Yu 2008).

ESCRT-0 functions to initiate the pathway and anchors the pathway at the early endosome due to the FYVE domain found on Vps27p (Bilodeau 2003). ESCRT-0 binds to clathrin resulting in early association with the plasma membrane and possibly Golgi vesicles indicating that ESCRT-0 functions before early endosome biogenesis (Mayers 2013, Raiborg 2001, Flores-Rodriguez 2015). ESCRT-I also functions in cargo binding through Ub interaction and associates weakly with the membrane (Katzmann 2003, Kostelansky 2006). ESCRT-II seems to function primarily by bridging the early cargo binding complexes to ESCRT-III though it also interacts with PI(3)P providing additional localization cues (Babst 2002, Slagsvold 2005).

ESCRT-III is the complex primarily responsible for membrane invagination. Vps20p binds to the ESCRT-II member Vps25p and is thought to initiate the resulting ESCRT-III cascade (Teo 2004). Vps20p is then thought to nucleate the assembly of the most numerous complex member, Snf7p, which polymerizes until this polymer is capped by Vps24p and Did4p (Saksena 2009, Teis 2008). The AAA ATPase Vps4p and associated complex members are then recruited to the membrane by interactions with the N-termini of ESCRT-III members and promote the dissociation of the ESCRT members (Babst 1998, Yu 2008, Scott 2005). Conflicting reports exist as to the importance in Vps4p activity in the process of membrane scission; some evidence suggests that Vps4p induced depolymerization of Snf7p is directly responsible for membrane scission while other reports indicate it has a dispensable role (Wollert 2009, Saksena 2009). No definitive

answer exists for how ILV membrane scission actually occurs the process likely entails the constriction of the budneck due to Snf7p (Lata 2008, Henne 2012).

ENDOSOME DYNAMICS

Endosome maturation

Endosomes undergo a maturation process from early to late ending ultimately with fusion to the vacuole. Endosomes can be differentiated morphologically with early endosomes displaying a tubular structure and late endosomes being round and enriched in ILVs that are formed primarily through the activity of the ESCRT complexes; early and late endosomes also contain different lipid compositions and late endosomes contain a more acidic luminal pH due to the activity of V-ATPases (Huotari 2011). It is thought that the major factor in endosome maturation is Rab conversion, the loss of Rab5 (Vps21p) on early endosomes and enrichment of Rab7 (Ypt7p) on late endosomes; indeed the proper recruitment of Ypt7p requires the inactivation of Vps21p (Rink 2005, Rana 2015). In yeast, Vps9p acts as a GEF towards Vps21p, the active Vps21p binds to BLOC-1 which in turn recruits Msb3p, the primary Vps21p GAP thus ultimately inactivating Vps21p (Rana 2015). The Mon1/Ccz1 complex that acts as a GEF towards Ypt7p is recruited to early endosomes through a PI(3)P interaction thus recruiting and activating Ypt7p to the maturing endosome (Poteryaev 2010). Finally PI(3)P is converted to $PI(3,5)P_2$ through the actions of Fab1p which is recruited to the early endosome through a FYVE domain; loss of PI(3)P and gain of $PI(3,5)P_2$ results in differential protein binding (Gary 1998). Many accessory factors such as Vac1p, CORVET, and HOPS are recruited to the endosome through their Rab interactions demonstrating how Rab conversion can have a major effect on the total protein composition of the endosome.

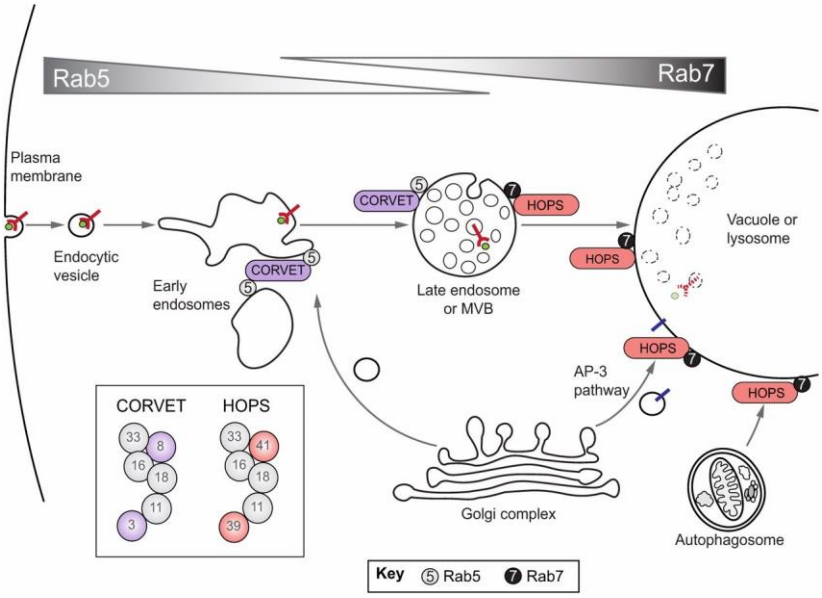

Figure 1.2: Endosome maturation. The process of endosome maturation is delineated including the crucial process of Rab conversion. Figure adapted from: Balderhaar 2013a.

Early Endosomes and Subpopulations

Early endosomes are found near the cell periphery and are weakly acidic (Maxfield 1987, Nielson 1999). The early endosome has distinct structural features including tubular projections and rounded vesicular lobes; these structural features appear to segregate sorting pathways with cargo destined for recycling localizing to the tubular regions and cargo destined for lysosomal degradation enriched in the vesicular regions (Gruenberg 1989, Gruenberg 2001, Goldstein 1985).

There are subpopulations of early endosomes in mammalian cells that appear to play distinct roles in sorting and recycling cargos. At least three major subpopulations of early endosomes in mammals are thought to exist. Two subpopulations are defined by the distinct Rab5 interaction proteins APPL1 and EEA1 (Miaczynska 2004). These different

populations of endosomes contain distinct cargos and retain distinct functions. It was noticed that APPL endosomes can occasionally convert into EEA1 endosomes, leading to the hypothesis that APPL endosomes represented an early stage of endosome maturation (Zoncu 2009). This hypothesis has since been shown to be an oversimplification as only a small percentage of APPL endosomes ever convert to EEA1 positive endosomes (Kalaidzidis 2015). A third endosome subpopulation is defined by the protein WDFY2; this subpopulation of endosomes is thought to have important roles in signaling pathways, including the insulin pathway (Walz 2010).

Different pathways appear to be responsible for the transport of different model cargos although some overlap has been observed. The transferrin (Tf) receptor is thought to traffic almost entirely within the APPL endosome subpopulation epidermal growth factor receptor (EGFR) traffic appears to not demonstrate a preference (Kalaidzidis 2015).

Endosome subpopulations in yeast are less clear; the early endosome receives cargo from both endocytic vesicles as well as Golgi derived vesicles; recent evidence suggests that these two pathways do not immediately converge and instead at least two early endosome subpopulations exist in yeast (Toshima 2014). The first indication that two subpopulations of endosomes exist in yeast came from the observation that deletion of *VPS21* did not entirely disrupt endosomal traffic and instead resulted in the accumulation of two distinct sets of cargo vesicles (Gerrard 2000). More recently it was demonstrated that one subpopulation of early endosomes contained both Golgi and endocytic cargo while another population contained only Golgi derived cargo; one population relies on the presence of Vps21p for fusion and the other population appears to fuse independently of Vps21p and contains the AP-3 complex, which had previously been described as only functioning in

direct Golgi to vacuole transport (Toshima 2014). Ultimately these two endosome subpopulations converge and become dependent on Vps21p for fusion; it remains unclear exactly when these pathways converge. It also remains unclear what, if any, additional fusion factors are required to promote fusion at the earliest stages of these pathways though the evidence showing that Vps45p and Vac1p act upstream of the CORVET complex makes these proteins prime potential targets for promoting fusion in these early populations (Balderhaar 2013).

YEAST AS A MODEL SYSTEM

As *Legionella* secretes around 300 effector proteins into host cells and deletion of any individual effector protein gene generally does not result in a growth phenotype, it is difficult to discern the roles of individual effectors during infection. By isolating individual effectors it becomes easier to identify the activity and targets of these proteins. We utilize the budding yeast, *Saccharomyces cerevisiae,* as a model system; the trafficking pathways in yeast are highly conserved and yeast are easy to manipulate genetically and biochemically (Feyder 2015). The use of yeast as a model system to study *Legionella* effectors has been well established in the literature with information from yeast studies later being validated in higher eukaryotes (Shohdy 2005, Campodonico 2005). Due to the wide range of eukaryotic hosts, *Legionella* frequently targets highly conserved proteins and pathways, making the use of model systems particularly applicable.

Trafficking Pathways to the Yeast Vacuole

Yeast vacuoles are prominent organelles that occupy the majority of space in the yeast cell. Vacuoles serve as the main degradative compartment in yeast cells, often drawing comparisons to the mammalian lysosome though the yeast vacuole functions in a

variety of other non-degradative functions such as osmotic regulation and metabolite storage drawing a distinction between lysosomes and serving to illustrate their central role in yeast cell physiology (Li 2009). The vacuole and assays involving vacuole fusion have long been used to identify and characterize fusion factor mutants, including the large class of vacuole protein sorting (*vps*) mutants (Raymond 1992, Seeley 2002).

Three major pathways exist for the transport of biosynthetic material to the vacuole. The AP-3 pathway, representing a direct Golgi to vacuole fusion event, is defined by vesicles containing the adaptor protein AP-3 (Darsow 1998). This pathway is also known as the alkaline phosphatase (ALP) pathway after the enzyme that was first described to traffic in this manner though other important cargos exist such as the vacuolar SNARE Vam3p (Klionsky 1989, Cowles 1997). This fusion pathway relies on the vacuolar Rab Ypt7p and the late endosome and vacuole tethering complex, HOPS (Bowers 2005).

The cytoplasm to vacuole targeting pathway (CVT) is a pathway that delivers vacuolar proteases to the vacuole; cargos of this pathway are synthesized in the cytosol in pro-enzyme forms where they oligomerize and are encapsulated into autophagosome-like organelles (Trumbly 1983, Kim 1997, Suzuki 2001). Many of the genes required for delivery of CVT cargo to the vacuole are also required for autophagy, demonstrating the large overlap between these two processes (Scott 1996). Important differences exist between autophagy and the CVT pathway, including the observation that the CVT pathway functions during normal growth conditions while autophagy is upregulated during nutrient stress conditions; there are also distinct CVT and autophagy specific genes (Baba 1997, Kawamata 2005). The CVT pathway is highly specific and only a few known cargos traffic

through this pathway including Ape1, Ams1, and Ape4 (Suzuki 2002, Hutchins 2001, Yuga 2011).

Most biosynthetic cargo is trafficked to the vacuole via the endosomal pathway. Cargo from late Golgi compartments is loaded into AP-1 containing vesicles that fuse to endosomes (Yeung 1999). Many vacuolar proteases such as carboxypeptidase Y traffic to the vacuole via endosomal intermediates modulated by interactions with cargo receptors such as Vps10p (Marcusson 1994).

LEGC7

LegC7 was originally identified as a *Legionella* effector predicted to contain coiled coil domains and a transmembrane spanning region that resulted in cell death upon expression in yeast, as such it was termed yeast lethal factor A (YlfA) (Campodonico 2005). LegC7 has a paralog termed YlfB/LegC2 that is 41% identical and 62% similar at the amino acid level but does not result in toxicity when expressed in yeast (Campodonico 2005). LegC7 is secreted into host cells in a Dot/Icm dependent manner verifying it as a true *Legionella* effector protein. It was also seen that deletion of LegC7 or LegC7 and LegC2 did not impair intracellular growth of *Legionella* in either murine macrophages or *A. castellanii*; as mentioned earlier this result is not particularly surprising as deletions of *Legionella* effector protein genes generally do not cause growth defects (Campodonico 2005). In CHO FcγRII, cells GFP-LegC7 was found to colocalize with ER proteins such as the TRAPP complex (Campodonico 2005, de Felipe 2008). LegC7 is found in all sequenced *Legionella pneumophila* strains unlike many other effector proteins, suggesting a conserved function (Chien 2004, Fraser 1977, Aurell 2003, Glockner 2008, D'Auria 2010, Schroeder 2010).

LegC3, another coiled coil containing effector protein from *Legionella,* is able to disrupt homotypic vacuole fusion (Bennett 2013). LegC7 lacking the first 144 amino acids (LegC7ΔTM) is unable to inhibit vacuole fusion, pointing to a difference in activity between these proteins (Bennett 2013). While LegC7 and LegC3 do not share any significant sequence similarity, they both are categorized as *Legionella* effector proteins that contain coiled coil domains. A partial crystal structure of LegC3, lacking its transmembrane domain, was solved showing that LegC3 forms an extended helical arm capped by a rigid 4 helix domain (Yao 2014).

Further work with LegC7 indicted that expression of LegC7 in yeast results in aberrant secretion of roughly 30% of total CPY-Invertase, a normally vacuole-directed protein, indicating a general defect in trafficking (de Felipe 2008). Expression of LegC7-GFP caused accumulations of vesicular material on the yeast vacuole, which also contained LegC7, leading the authors to suspect that this structure was a Class E like compartment (de Felipe 2008). Class E compartments represent non-functional multivesicular endosomes (MVEs) (Raymond 1992).

Expression of LegC7 as well as LegC2 is regulated by the LetA-RsmYZ-CsrA regulatory cascade (Rasis 2009). When the cells reach stationary phase, LetS phosphorylates LetA which in turn allows for expression of the sRNAs RsmY and RsmZ, which in turn bind to CsrA. CsrA is normally bound to mRNAs of genes such as LegC7. Thus binding of CsrA by RsmY and RsmZ results in functional mRNAs from regulated genes (Rasis 2009). A number of the effectors regulated by this system are known to have an effect on vesicular trafficking such as LegC7, RalF, and VipA (Nevo 2014 and Rasis 2009). Research on life stage specific proteomes of *Legionella* found that LegC7 was produced only

during the exponential phase of *Legionella* growth, along with many other verified effector proteins (Aurass 2016).

In an attempt to characterize host factors that are important for *Legionella* infections, an approach called insertional mutagenesis and depletion (iMAD) was developed (O'Connor 2013). This approach utilized transposon mutagenesis to knockout particular *Legionella* effectors; these transposon-mutagenized cells were then used to infect *Drosophila* cells that had been treated with siRNA to one of 5 early secretory pathway genes (*sar1, arf1, sec22, rab1*, or *bet5*). Previously it had been shown that knockdown on any one of these genes did not impair *Legionella* replication in cells, but knocking down two of these genes did result in growth defects (Dorer 2006). The rationale for the screen is that if the effector targets the same pathway of the knockdown then no growth defect will be observed. If, however, the effector targets a second pathway then growth will be inhibited because *Legionella* cannot grow when two of the above pathways are disrupted. It was also reasoned that based on the pattern of inhibition, effectors could be grouped into functional classes. Deletions of LegC7 caused growth defects when *sar1*, *sec22*, or *rab1* were depleted. No growth defect was observed in cells where *arf1* and *bet5* were silenced. The authors grouped the screened effectors into 14 functional groups, though LegC7 was not classified into any of these groups.

By studying bacterial effector proteins that manipulate eukaryotic physiology we hope to gain insight into the normal functioning of these pathways. The dynamic nature of endosomes makes them challenging to study with traditional cell biology techniques that often rely on static capture or examination of organelles. By studying an effector such as LegC7 that induces a defect in endosome trafficking, we hope to gain insight into the

regulation of endosome fusion and the recruitment of endosome fusion factors. These experiments will not only provide information about how *Legionella* is able to manipulate host cells during infection but also provide information about how these processes work in normal host cells.

CHAPTER 2

THE *LEGIONELLA PNEUMOPHILA* EFFECTOR PROTEIN, LEGC7, ALTERS YEAST ENDOSOMAL TRAFFICKING

O'Brien KM, Lindsay EL, Starai VJ. The *Legionella pneumophila* Effector Protein, LegC7, Alters Yeast Endosomal Trafficking. *PLoS ONE*. 2015;10(2):e0116824. doi:10.1371/journal.pone.0116824.
Reprinted with Permission from publisher

ABSTRACT

The intracellular pathogen, *Legionella pneumophila,* relies on numerous secreted effector proteins to manipulate host endomembrane trafficking events during pathogenesis, thereby preventing fusion of the bacteria-laden phagosome with host endolysosomal compartments, and thus escaping degradation. Upon expression in the surrogate eukaryotic model *Saccharomyces cerevisiae*, we find that the *L. pneumophila* LegC7/YlfA effector protein disrupts the delivery of both biosynthetic and endocytic cargo to the yeast vacuole. We demonstrate that the effects of LegC7 are specific to the endosome:vacuole delivery pathways; LegC7 expression does not disrupt other known vacuole-directed pathways. Deletions of the ESCRT-0 complex member, *VPS27*, provide resistance to the LegC7 toxicity, providing a possible target for LegC7 function *in vivo*. Furthermore, a single amino acid substitution in LegC7 abrogates both its toxicity and ability to alter endosomal traffic *in vivo*, thereby identifying a critical functional domain. LegC7 likely inhibits endosomal trafficking during *L. pneumophila* pathogenesis to prevent entry of the phagosome into the endosomal maturation pathway and eventual fusion with the lysosome.

INTRODUCTION

Legionella pneumophila are ubiquitous aquatic bacteria and obligate intracellular pathogens that infect a variety of phylogenetically diverse aquatic amoebae and protists (Fields 1986, Fliermans 1981). *Legionella* are opportunistic pathogens of humans, able to infect and invade human alveolar macrophages if contaminated water is aerosolized and inhaled, causing a severe form of pneumonia known as Legionnaires' disease, as well as the milder, self-limiting infection, Pontiac fever (Kaufmann 1981, McDade 1977).

Legionella pneumophila requires a type IVb secretion system (Dot/Icm; defective in organelle trafficking/intracellular multiplication) for intracellular survival (Horwitz 1983), which allows the translocation of nearly 300 known and predicted effector proteins into the host cell (Burnstein 2009, Luo 2004, Heidtman 2009, Lifshitza 2013). Many of these proteins are thought to directly disrupt normal host membrane trafficking pathways in order to both prevent the lysosomal

degradation of *Legionella*, and to promote the synthesis of the specialized intracellular replicative niche termed the *Legionella*-containing vacuole (LCV) (Kagan 2004, de Felipe 2008, Bennett 2013). The LCV is composed of both plasma membrane and ER membrane components, which requires both a major diversion of ER-derived vesicles from normal trafficking pathways, and the aberrant SNARE protein-dependent fusion of those membranes (Bennett 2013, Paumet 2009, Tilney 2001, Swanson 1995).

A number of the *Legionella* effector proteins contain motifs with high similarity to eukaryotic proteins, and are thought to function by manipulating eukaryotic host cell events by mimicking or modulating host proteins. (Chen 2004, de Felipe 2005, Neunuebel 2011). Some of the effectors thought to directly alter host cell membrane trafficking events contain coiled coil motifs (LegC) including LegC2, LegC3, and LegC7 [de Felipe 2008, Bennett 2013, Campodonico 2005]. LegC7/YlfA was originally identified as a *Legionella* effector protein that resulted in cell death upon expression in the budding yeast *Saccharomyces cerevisiae* [Campodonico 2005]. It was also found that expression of LegC7 resulted in vesicular accumulations on the yeast vacuole and aberrant secretion of CPY-Invertase, inducing an apparent a yeast class E vacuolar protein sorting (VPS) phenotype [de Felipe 2008, Campodonico 2005, Raymond 1992]. As there is a high degree of conservation amongst genes involved in cellular transport and fusion across eukaryotic biology, these studies provided essential information into the function of LegC7/YlfA during *Legionella* pathogenesis.

The yeast endosomal trafficking pathway serves as an important hub that links the processes of endocytosis and vacuole-directed biosynthetic traffic; vesicles derived from the Golgi or plasma membrane fuse to establish early endosomes that undergo a conserved maturation process, which ultimately concludes with the fusion of late endosomes with the degradative vacuole (reviewed in Huotari 2011). To solve the topology "problem" in the degradation of integral membrane proteins, the yeast multivesicular endosome/body (MVB) is a specialized late-stage

maturing endosome characterized by the presence of intraluminal vesicles (ILVs) that contain membrane proteins bound for degradation in the yeast vacuole [Nickerson 2006]. ILVs are formed due to the action of a highly conserved protein-sorting complex called the endosomal sorting complex required for transport (ESCRT) complex (reviewed in [Schuh 2014]), which functions by recognizing and packaging ubiquitin modified membrane proteins into ILVs for degradation in the vacuole lumen [Katzmann 2001, Kolling 1994]. Deletion of many of the ESCRT genes, or class E VPS genes, results in a malformed MVB and aberrant secretion of CPY-Invertase, a normally vacuolar directed protein [Raymond 1992, Robinson 1988, Rothman 1989].

As expression of LegC7 results in an apparent class E phenotype in yeast cells, we hypothesized that LegC7 exerts its toxic effect at some point in the endosomal trafficking pathway and that likely one or more of the class E genes are required for the toxicity of LegC7. Herein, we show that deletion of the yeast ESCRT-0 gene, *VPS27*, results in a decrease in LegC7 toxicity. Furthermore, we see that LegC7 causes a severe disruption of both vacuole-directed biosynthetic traffic and endocytic cargo pathways, while not disrupting alternative vacuolar transport pathways. Localization to, and formation of, class E compartments, disruption of both biosynthetic and endocytic traffic, and genetic interaction with an ESCRT protein all indicate that LegC7 functions to modulate endosomal traffic. These data help provide a deeper understanding of LegC7 function in eukaryotic cells.

MATERIALS AND METHODS

Yeast strains and plasmid construction

Yeast strain SEY6210 (MATα *his3-Δ200 trp1-Δ901 leu2-3,112 ura3-52 lys2-801 suc2-Δ9*) was used for GFP-Vam3 and Ste3-GFP localization studies. Yeast strain BY4742 (MATα *his3Δ1 leu2Δ0 lys2Δ0 ura3Δ0*) was used for all other studies, and a full list of strains and plasmids used are included in Table 2.1.

The creation of a galactose inducible yeast expression vector in pYES2/NTc for *LEGC7* expression, pVJS52, was previously described [Bennett 2013]. For some experiments, the *URA3* locus on this plasmid was converted to *LYS2* via standard lithium acetate transformation methods and homologous recombination with HindIII-digested pM2660 [Voth 2003], resulting in pVJS53.

To create GFP-LegC7 expression vectors via gap repair, *LEGC7* was amplified using primers GFPC7_R and GFPC7_F, and the resulting amplicon was co-transformed with linearized pGO36 plasmid (a generous gift from Dr. Alexey Merz, University of Washington-Seattle) [Odorizzi 1998] into BY4742, creating pVJS59. GFP-Vps27 was created in the same manner, using primers GFPVps27_F and GFPVps27_R.

A plasmid for the purification of GST-Vps27 was constructed by amplifying *VPS27* from BY4742 genomic DNA using primers Vps27BamHI_F and Vps27XhoI_R, digested with BamHI and XhoI, and ligated into plasmid pET-42a (Novagen) digested with the same enzymes, resulting in pVJS56.

Recombinant protein purification

LegC7ΔTM protein was purified as previously described [Bennett 2013], except that the final elution from chitin beads was performed for 48 h at 22 °C. Eluted protein was dialyzed into PS buffer (20mM PIPES-KOH, pH 6.8, 200mM sorbitol) containing 300mM KCl. Antibodies against LegC7ΔTM were raised in rabbits using a standard protocol and subsequent serum used for Western blots at a 1:5000 dilution (Rockland Immunochemicals, Inc).

GST-Vps27 was purified by standard glutathione affinity chromatography, using pVJS56 as the expression vector. Eluted protein was dialyzed into PS buffer containing 150mM KCl.

Random mutagenesis of *LEGC7*

In order to locate regions of *LEGC7* required for toxicity in yeast, BY4742 harboring pVJS52 was grown in selective media at 30°C for 18 h, and 1 OD_{600} unit was harvested by centrifugation. This pellet was washed with 1M sterile sodium phosphate buffer, pH 7.0, suspended in 1mL of the

same buffer, and the chemical mutagen ethyl methanesulfonate (EMS) was added to 2% (v/v). After shaking at 30°C for 1 h, 1 mL of 1M sodium thiophosphate was added, and the cells were plated directly to CSM-uracil plates containing 2% galactose. Plasmids were isolated from each resulting colony. These plasmids were re-introduced into BY4742; plasmids that were no longer inhibitory, but expressed full length LegC7 by immunodetection, were sequenced (Georgia Genomics Facility, University of Georgia).

Site-directed mutagenesis of pVJS52 was carried out via standard PCR techniques with the following primer pairs: C7N242_F/C7N242_R (LegC7^{N242I}), C7N242D_R/C7N242D_F (LegC7^{N242D}), C7N242Q_R/C7N242Q_F (LegC7^{N242Q}), C7N242L_F/C7N242L_R (LegC7^{N242L}), C7N242A_F/C7N242A_R (LegC7^{N242A}), or C7N242R_R/C7N242R_F (LegC7^{N242R}) (Table 2.2).

Lucifer Yellow uptake assay

Cells were grown for 18 hours at 30°C in CSM-uracil with 2% glucose, collected by centrifugation, washed with sterile water, suspended in CSM-uracil with 2% galactose and grown for 16 hours at 30°C. 1.0 OD_{600} unit of cells were harvested by centrifugation and suspended in 100µL fresh CSM-uracil containing 2% galactose. Lucifer Yellow was added to 8mg/mL and samples were incubated for 2 h at 30 °C. Ice-cold Lucifer Yellow stop buffer (50mM potassium phosphate, pH 7.5, 10mM sodium azide) was added with mixing, and cells were pelleted. Samples were washed 3 additional times with Lucifer Yellow stop buffer to ensure removal of extracellular dye. Samples were suspended in 100µL Lucifer Yellow stop buffer, mixed with an equal volume of a 0.6% agar solution, and mounted for fluorescence microscopy.

RESULTS

LegC7 N242I is no longer toxic when expressed in yeast

As LegC7 expression is known to be toxic upon expression in yeast [Campodonico 2005], identification of residues critical for this activity *in vivo* would likely be important for understanding the mechanism of LegC7-mediated toxicity. Therefore, we mutagenized yeast

containing a galactose-inducible *LEGC7* plasmid using ethyl methanesulfonate (EMS). Plasmids that were no longer inhibitory were sequenced, and one plasmid contained a single nucleotide transversion at position 725 that produced a mutant protein substituting an isoleucine for asparagine at amino acid position 242 (LegC7^{N242I}). This single nucleotide transversion strongly reduced the toxicity of *LEGC7* expression *in vivo* (Figure 2.1A); immunoblots confirmed that LegC7^{N242I} was expressed to levels similar to (or greater than) LegC7 expression (Figure 2.1B).

In attempt to dissect the function of N242 in LegC7, we used site directed mutagenesis to introduce a number of other amino acids into this position, including a conservative change (N242Q), charged residues (N242R and N242D), and hydrophobic residues (N242A or N242L). Interestingly, only mutation of N242 to hydrophobic residues (N242I or N242L) resulted in abrogation of LegC7 toxicity; N242A shows a very slight reversal phenotype (Figure 2.1C). This particular residue (N242) is predicted to be one of the first residues of the second putative coiled coil region, based on *in silico* models (Figure 2.1D). Just prior to the second coiled coil domain of LegC7, probability models of coiled coil structure predict a sharp decrease in coiled coil domain formation probability (Figure 2.1E, left panel, red arrow). When replacing asparagine 242 with isoleucine, however, this *in silico* model predicts that the disordered region is eliminated (Figure 2.1E, middle panel, red arrow); replacing N242 with a residue that did not reduce LegC7 toxicity showed coiled coil probabilities similar to the wild type protein (Figure 2.1E, right panel, red arrow). Based on these coiled coil prediction methods, asparagine 242 may be essential for the proper folding of either the second coiled coil domain or small loop region just upstream of this domain. A previous report identified that this coiled coil domain is essential for LegC7 toxicity, but was based on large deletions in this region [Campodonico 2005]. Therefore, we have identified a single residue in LegC7 responsible for LegC7 function *in vivo*.

LegC7 disrupts endosome to vacuole traffic

It is known that expression of LegC7 in yeast induces a vacuolar protein-sorting defect based upon the observed mis-sorting and extracellular secretion of a vacuole-directed CPY-invertase fusion protein when *LEGC7*$^{+}$ is expressed [de Felipe 2008]. In order to further characterize the protein sorting defects induced by LegC7 in yeast, we examined the endosomal trafficking patterns of several well-defined yeast proteins upon *LEGC7*$^{+}$ expression. Carboxypeptidase S (CPS) is a vacuolar protease known to traffic to the vacuole via the CPY (Golgi-endosome-multi-vesicular body) route [Odorizzi 1998]. Accordingly, yeast cells harboring GFP-tagged CPS protein in the absence of LegC7 show a distinct localization of GFP-CPS to the vacuole lumen (Figure 2.2A). Upon expression of *LEGC7*, however, GFP-CPS is strongly localized to the cell periphery in a diffuse punctate pattern (Figure 2.2A, 2.S1A). In confirmation that the LegC7^{N242I} protein is no longer active *in vivo*, cells expressing LegC7^{N242I} deliver GFP-CPS to the vacuole lumen, as in wild type strains (Figures 2.2A, 2.S1A).

In order to confirm delivery of GFP-CPS was disrupted in strains expressing LegC7, we took advantage of the fact that the GFP-CPS protein is known to be cleaved upon delivery to the proteolytic vacuole, resulting in an easily-detectable size shift upon immunoblot for GFP [McNatt 2007]. Strains expressing LegC7 show a clear accumulation of the full length GFP-CPS fusion protein (Figure 2.2B). In contrast, strains harboring the inactive LegC7^{N242I} protein or vector control plasmid show complete conversion of the GFP-CPS protein to the lower molecular weight GFP (Figure 2.2B), confirming the observation that delivery of GFP-CPS to the vacuole is drastically altered in *LEGC7*$^{+}$ strains (Figure 2.2A).

In order to examine LegC7's effect on the delivery of another well characterized membrane protein to the vacuole, we examined the trafficking of the Sna3p protein, which is sorted to the MVB membrane via its close association with, and ubiquitination by, the ubiquitin ligase Rsp5p [MacDonald 2012]. Sna3p is then packaged into ILVs at the MVB and localized to the vacuole lumen

upon MVB:vacuole fusion [McNatt 2007]. As expected, Sna3-GFP was localized to the vacuole lumen in yeast strains lacking LegC7 (Figure 2.2C). Expression of LegC7, however, resulted in the striking accumulation of Sna3-GFP in either peripherally-localized punctae, or in a diffuse cytosolic staining pattern (Figures 2.2C, 2.S1B). Expression of LegC7^{N242I}, does not affect normal vacuolar localization of Sna3-GFP (Figures 2.2C, 2.S1B), confirming that this mutant derivative of LegC7 has lost *in vivo* function.

LegC7 expression is known to induce a class E phenotype in yeast upon expression, leading to vacuole protein sorting defects and aberrant protein secretion of biosynthetic traffic through the MVB [de Felipe 2008]. Therefore, we hypothesized that LegC7 may also induce defects in the delivery of endocytic cargo to the vacuole. In order to assay for endocytic defects in the presence of LegC7, we measured the ability of yeast to accumulate the soluble fluorescent dye, Lucifer Yellow (LY). LY is known to enter yeast via endocytosis, and is delivered to the vacuole where it accumulates [Riezman 1985]. Under galactose growth conditions, yeast accumulates LY in the vacuole, as expected (Figure 2.2D). In contrast, strains expressing LegC7 fail to accumulate LY in the vacuole, but rather display a cytoplasmic accumulation phenotype (Figures 2.2D, 2.S1C); LegC7^{N242I} does not block endocytic delivery of LY to the vacuole (Figures 2.2D, 2.S1C). Furthermore, when we attempted to stain the yeast vacuolar membrane of LegC7-expressing strains with the fluorescent styryl dye, FM4-64, we observed accumulations of the dye in punctate structures lining the plasma membrane, staining not seen in either vector control or LegC7^{N424I}-expressing strains, highly reminiscent of the structures seen to accumulate GFP-CPS and Sna3-GFP (Figures 2.2E, 2.S1D). These results strongly suggest a defect in endocytic delivery of FM4-64 to the vacuole in strains expressing LegC7. Recent work from our laboratory has shown normal FM4-64 staining patterns of the vacuole in LegC7-expressing strains [Bennett 2013], however those images were taken three hours post-induction. After a 16h galactose induction, strains harboring LegC7 display these clear defects in FM4-64 delivery to the vacuole. Taken together, these data show that

LegC7 either delays or inhibits normal endosomal traffic to the vacuole, from both biosynthetic and endocytic pathways.

In order to examine the effects of LegC7 on the disruption of receptor-mediated endocytosis, we utilized the a factor pheromone receptor, Ste3p, fused to GFP [Prosser 2010]. Without the appropriate ligand, Ste3 is constitutively endocytosed and delivered to the vacuole [Roth 1998]. Under galactose growth conditions Ste3-GFP accumulates in the vacuole as expected (Figure 2.2F). When LegC7 is expressed, however, Ste3-GFP accumulates in a single, small compartment on the vacuolar periphery, reminiscent of a class E compartment (Figures 2.2F, 2.S1E). In order to more explicitly define whether LegC7 prevents the endocytic uptake of Ste3-GFP, we utilized a strain with the 4 clathrin-binding adaptor proteins (Ent1p, Ent2p, Yap1801p, and Yap1802p) deleted and complimented with an epsin N-terminal homology domain (4Δ + pENTH1), a strain previously shown to be defective in the uptake of Ste3-GFP from the plasma membrane via endocytosis [Prosser 2010, Maldonado-Baez 2008]. In this strain background, Ste3-GFP accumulated at the plasma membrane as expected (Figure 2.2F). The clear distinction between the plasma membrane accumulations of Ste3-GFP in the strain defective for endocytic uptake (4Δ + pENTH1) and the strain expressing LegC7 show that LegC7 does not disrupt the physical process of endocytosis, but rather prevents the proper vacuolar delivery of the endocytosed Ste3-GFP cargo.

In order to determine if the disruption in endosomal trafficking was due simply to LegC7-induced cell death, we stained cells with propidium iodide (PI) which is only internalized upon cell membrane disruption after cell death [Krishan 1975]. We found that after the standard 16 hour galactose induction period, cells expressing the vector control plasmid showed that approximately 94% of the cells excluded PI, compared to nearly all of the yeast cells subjected to excess heat (Figure. 2.S2A). Strains expressing LegC7 show PI staining levels indistinguishable from vector control strains, suggesting that the observed endosome trafficking defects are not due to widespread cell death induced by LegC7 (Figure 2.S2A).

LegC7 does not inhibit endosome-independent traffic to the vacuole

The yeast vacuole receives cargo from at least 3 pathways (Reviewed in [Reggiori 2013]): the endocytic/vacuolar protein-sorting pathway (CPY pathway) [Raymond 1992], directly from the Golgi in an AP-3 adapter complex-dependent manner (ALP pathway) [Cowles 1997], and directly from the cytosol via autophagic processes [Klionsky 1992]. Of these three pathways, however, only the endocytic/CPY pathway utilizes endosomal intermediate vesicles for vacuolar delivery, and we therefore sought to measure the effects of LegC7 on vacuolar trafficking pathways that do not require endosomal intermediates.

The vacuolar SNARE, Vam3p, traffics directly from the Golgi to the vacuole through the AP-3/ALP pathway; no interaction with the endocytic pathway is observed [Darsow 1998]. Yeast strains expressing GFP-Vam3p show a clear localization of Vam3p to the vacuolar membrane (Figure 2.3A). Strains expressing LegC7 show no obvious defect in GFP-Vam3 trafficking (Figures 2.3A, 2.S2B), in contrast to our previous data showing disruption of known endosomal traffic from the Golgi to the vacuole (Figures 2.2A,C).

As a marker for the delivery of cytosolic components to the vacuole via a specialized autophagic process known as cytosol-to-vacuole targeting (Cvt), we measured the maturation of the vacuolar aminopeptidase, Ape1p. This protein is produced in a cytosolic proenzyme form, selectively encapsulated by an autophagosomal membrane, and delivered to the vacuole for proteolytic processing and enzymatic activation [Klionsky 1992]. This processing can be easily observed via immunoblot, and wild type yeast shows the expected maturation of the Ape1p polypeptide, confirming normal Cvt trafficking. Expression of LegC7 does not disrupt the maturation of Ape1p while strains lacking Atg19p, the Ape1 receptor required for proper Ape1 delivery to the vacuole, result in an accumulation of unprocessed precursor (Figure 2.3B) [Leber 2001, Scott 2001]. These data indicate that the inhibitory effects of LegC7 on trafficking pathways are specific to endosomal traffic, and not the result of general trafficking or vacuolar defects.

Deletions in *vps27* reduce LegC7 toxicity

Previous reports have indicated that low-level expression of LegC7 results in the formation of so-called "class E" compartments, and that LegC7-GFP is localized to these compartments [de Felipe 2008]. Furthermore, LegC7 was reported to induce the aberrant secretion of CPY-Invertase, a protein that should be directed to the vacuole via the CPY pathway [de Felipe 2008, Campodonico 2005]. As these results phenocopy known class E trafficking mutants in yeast, we hypothesized that one or more class E VPS genes may be required for LegC7 toxicity, even though deletions of individual class E genes did not cause major disruptions in LegC7-GFP localization [de Felipe 2008].

We assayed LegC7 toxicity in each of the single deletions of the 13 originally-identified class E mutants (*vps4Δ, vps20Δ, vps23Δ, vps24Δ, vps25Δ, vps27Δ, vps28Δ, vps36Δ, bro1Δ, snf7Δ, snf8Δ, srn2Δ,* and *did4Δ*) [Raymond 1992] and *hse1Δ*. These genes define many of the proteins that comprise the various ESCRT complexes and accessory factors which are required for both the biogenesis of the MVB, and in the proteolytic turnover of ubiquitinated proteins; their functions in this pathway is highly ordered process. Interestingly, deletion of only the ESCRT-0 member *vps27* resulted in a partial reversal of toxicity of LegC7 (Figure 2.4A); no other single class E gene deletion affected LegC7 toxicity (Figure 2.S3).

As a member of the ESCRT-0 complex, Vps27p is a multifunctional protein that binds ubiquitinated proteins, binds to endosomal phosphatidylinositol 3-phosphate (PI3P) via its FYVE (Fab-1, YOTB, Vac1, and EEA-1) domain, and recruits the ESCRT-I complex to the endosome via direct interactions with Vps23p [Raiborg 2001, Bache 2003, Lu 2003]. ESCRT-0 functions as 1:1 heterodimer of Vps27p and Hse1p [Prag 2007, Ren 2009]. Surprisingly, the *hse1Δ* single deletion strain did not reduce the toxicity of LegC7 (Figure 2.S3), and the double deletion strain (*hse1Δ vps27Δ*) did not show any additional reversal of LegC7 toxicity beyond the effect of the *vps27Δ* deletion (2.SI3). Given that *hse1Δ* strains are not resistant to LegC7, nor are any ESCRT mutants

downstream of Vps27 function, the *vps27*-mediated reversal of LegC7 toxicity is likely due to a specific function, and not a direct result of defective ESCRT complex activity.

As Vps27p functions to target ubiquitinated membrane proteins bound for vacuolar turnover, we hypothesized that suppression of LegC7 toxicity in *vps27Δ* strains may be due to either mislocalization of LegC7, or altered proteolytic turnover of LegC7 *in vivo*. GFP-LegC7 localizes to vesicular accumulations reminiscent of class E compartments, confirming a previous report (Figure 2.4B, [de Felipe 2008]). The localization of GFP-LegC7 is not drastically altered in Δ*vps27* strains, which is also consistent with this report (Figures 2.4B, 2.S4A [de Felipe 2008]). Given that ESCRT complex proteins are important in regulating membrane protein turnover, we measured LegC7 turnover in *vps27Δ* strains. After 60 minutes of incubation, LegC7 is near undetectable in wild type yeast extracts (Figure 2.S4B). In *vps27Δ* strains, however, there appears to be less LegC7 present at all timepoints taken (Figure. 2.S4B), when compared to wild type. Therefore, LegC7 levels in *vps27Δ* strains are reduced either through enhanced proteolytic turnover, or through a reduction in expression. Interestingly, Sec18p, a protein that should degrade over the course of this assay [Belle 2006], also appears to degrade more quickly in *vps27Δ* strains, while Sec17p remains stable over the assay in both strains (Figure 2.S4B). Therefore, it appears that some proteins may turnover more quickly in *vps*27Δ strains, and lower levels of LegC7 *in vivo* may explain the resistance of *vps27Δ* strains to LegC7 expression.

It is known that *vps27Δ* strains have defects in delivery of endosomal traffic to the vacuole, presumably due to an aberrant MVB function [Raymond 1992]. When we observed the trafficking of the endosomal cargoes Sna3-GFP and GFP-CPS in *vps27Δ* strains, we noted the expected punctate trafficking defect of Sna3-GFP, similar to that seen in LegC7-expressing strains (Figure. 2.4C, 2.S4C and D, 2.2C). Additionally, GFP-CPS accumulated on the vacuolar membrane in *vps27Δ* strains, and was not delivered to the vacuolar lumen (Figures 2.4C,2.S4D). To measure whether or not LegC7 and Vps27p interact directly, we purified GST-Vps27p and attempted to pull-down recombinant

LegC7ΔTM [Bennett 2013]. We did not detect an interaction between GST-Vps27 and LegC7ΔTM *in vitro* (Figure 2.S5A), although either the transmembrane domain or short N terminal region of LegC7 could be required for interaction of these two proteins, or LegC7ΔTM may require ubiquitination for this interaction to occur. Consistent with the lack of a direct biochemical interaction, LegC7 did not disrupt the overall localization of GFP-Vps27 (Figures 2.4D, 2.S5B).

Interestingly, LegC7 expression in the *vps27Δ* background did not induce the fragmented punctate pattern of GFP-CPS localization seen previously (Figure 2.2A), suggesting that LegC7 may function after Vps27p, as LegC7 is unable to induce additional trafficking defects downstream of the relevant effects imparted by the deletion of *vps27*. Therefore, LegC7 appears to be directly involved in altering protein traffic via the endosome-MVB-vacuole route.

DISCUSSION

In order to survive intracellularly, *Legionella* separates the LCV from the standard endosomal maturation pathway thus avoiding LCV-lysosome fusion [Horwitz 1983]. To this end, *Legionella* secretes a number of effector proteins that appear to directly manipulate endolysosomal compartments. For example, VipD misregulates the early endosomal Rab-family GTPase, Rab5, to promote intracellular survival of the bacterium [Ku 2012, Gaspar 2014]. Our lab has also characterized another *Legionella* coiled coil containing protein, LegC3, that causes vacuolar fragmentation upon expression in yeast and prevents homotypic vacuole fusion *in vitro* pointing to this protein's probable role in manipulating host endolysosomal pathways [Bennett 2013]. Due to the importance of separating the LCV from the endosomal pathway and *Legionella'*s broad host range we speculate that other uncharacterized *Legionella* effectors also function to manipulate different aspects of host endosomal systems.

When expressed in yeast, LegC7 disrupts biosynthetic vacuole-directed cargo that emanate from the Golgi, such as CPS and Sna3p. In both cases, the predominant phenotype consists of numerous punctate structures that localize to the cell periphery. Because these proteins are

trafficked via similar mechanisms, we suspect that both GFP-CPS and Sna3-GFP are accumulating in the same physiological compartments; perhaps early endosomes that are unable to either mature or fuse to downstream compartments. In addition, by following fluid-phase endocytosis with the soluble dye Lucifer Yellow, we find that yeast cells expressing LegC7 accumulate this marker within the cytosol. Therefore, LegC7 does not completely prevent endocytosis, as the dye is still able to enter the cell, but the LY-containing endosomes fail to deliver their cargo to the vacuole. Interestingly, strains deleted for *vps21* and *ypt52*, the major Rab-family GTPases of the early endocytic pathway, are also reported to display a similar LY accumulation phenotype [Singer-Kruger 1994]; this phenotypic similarity to LegC7-expressing strains further suggests that LegC7 may be capable of modulating the early endocytic pathway. It is unknown, however, whether LegC7 directly manipulates these Rab GTPases or the fusion events they catalyze, and therefore requires further study. Upon LegC7 expression, the fluorescent styryl dye, FM4-64 was not seen to accumulate in yeast vacuole membranes, but instead was contained within punctate structures around the cell periphery. The localization pattern observed with FM4-64 mirrors the aberrant accumulation of GFP-CPS and Sna3-GFP in LegC7-expressing cells, leading us to hypothesize that these structures represent the same physiological compartment. Using a GFP tagged version of the a-Factor, Ste3p, we determined that LegC7 also prevented proper vacuolar delivery of receptor mediated endocytic cargoes yet did not disrupt the actual endocytic event.

Our data indicates that LegC7 manipulates traffic involving endosomal maturation, however we wondered if the effects of LegC7 were specific to the endosomal system, or rather represented a global disruption of traffic. As the yeast vacuole receives cargo from at least two other pathways we sought to determine if LegC7 disrupted these pathways as well. In order the probe the ALP pathway which moves cargo directly from the late Golgi to the vacuole in an AP-3 dependent manner we utilized GFP-Vam3, a well-characterized vacuolar SNARE that is known to traffic through the ALP pathway. Localization of GFP-Vam3 was not disrupted by LegC7 expression, nor

was the processing of a Cvt-delivered protein, Ape1p. These data indicate that LegC7 specifically disrupts cargo that is required to traffic through endosomes to vacuoles, while not disrupting global cellular trafficking events.

Mutation of the asparagine 242 of LegC7 to either isoleucine or leucine results in a non-toxic derivative of LegC7 that also lacks the endocytic disruption phenotypes of wild type LegC7. Based on *in silico* calculations, this residue is predicted to fall in the very beginning of the putative second coiled-coil domain of LegC7. Furthermore, models predict that replacing this residue with a large aliphatic amino acid alters the predicted linking region between coiled coil region 1 and 2, suggesting that the presence of this domain is critical for proper LegC7 folding or function *in vivo*. In support of these data, early studies with LegC7 found that large deletions of this central coiled-coil domain produced a non-toxic protein, and that the C-terminal coiled-coil domain of LegC7 was not important for toxicity [Campodonico 2005]. As the elimination of LegC7 toxicity in our study is fairly specific, we suspect that significant structural changes are induced in LegC7^{N242I}, but will not be fully appreciated until crystallographic data are obtained. Recently, the N-terminal portion of a related *Legionella* effector protein, LegC3, was crystallized, resulting in a structure that did not share close homology with any currently known structure [Yao 2014]. As this crystal structure did not match *in silico* predictions, the structure of LegC7 may provide a new role for the N242 residue in LegC7 function.

Finally, we find that deletions of *VPS27*, and ESCRT-0 complex member, partially reversed the toxic effects of *LEGC7* expression. This effect is not the result of mislocalization of LegC7, but could be explained by the reduction of LegC7 levels through enhanced proteolytic turnover or reduced LegC7 expression in *vps27Δ* backgrounds*;* direct interactions between Vps27p and LegC7 *in vitro* were not detected. Furthermore, we were unable to detect any suppression of LegC7 toxicity in *hse1Δ* deletions, which may rule out a function of the intact ESCRT-0 complex in this reversal. It is also possible that Vps27p recruits either a secondary protein required for LegC7

function *in vivo*, or Vps27p plays an as yet undescribed role in an endosomal maturation pathway that LegC7 can exploit. There is a hypothesized link between the ESCRT pathway, which removes membrane surface area of the MVB, and the endocytic fusion pathway, which increases the surface area of the MVB [Progida 2007, Solinger 2012]. Perhaps Vps27p, with the earliest function in the yeast ESCRT pathway, serves a role in promoting endosomal fusion or maturation to ensure sufficient surface area of the MVB for proper downstream ESCRT function. It is clear, however, that no other class E protein activity is required for LegC7 toxicity or localization, and we therefore do not believe that LegC7 is directly modulating overall ESCRT function.

The modulation of host endosomal traffic would likely be an important goal for *Legionella*, in both its attempt to evade the normal host endomembrane system, and in the construction of the LCV during infection. It should be noted that *Legionella* strains lacking LegC7 are not defective in macrophage proliferation studies [Campodonico 2005], and therefore LegC7-specific activities during *Legionella* infection remain unclear. Identification of the yeast target protein(s) of LegC7 will likely provide essential insight into the role of this effector protein during the intracellular lifecycle of *Legionella*.

ACKNOWLEDGMENTS

We would like to thank Drs. Daniel Nickerson, Alexey Merz, Derek Prosser, Daniel Klionsky, Beverly Wendland, William Wickner, and Greg Odorizzi for thoughtful gifts of strains and plasmids, as well as helpful comments.

Table 2.1: Strains and plasmids used in this study

Strain	Genotype	Source
BY4742	MATα *his3Δ1 leu2Δ0 lys2Δ0 ura3Δ0*	[Brachmann 1998]
SEY6210	MATα *his3-Δ200 trp1-Δ901 leu2-3,112 ura3-52 lys2-801 suc2-Δ9*	[Robinson 1988]
BY4742 *vps27Δ*	BY4742 *vps27Δ::KANMX6*	GE Healthcare Dharmacon
BY4742 *hse1Δ*	BY4742 *hse1Δ*::KANMX6	GE Healthcare Dharmacon
BY4742 *vps27Δ hse1Δ*	BY4742 *vps27Δ*::KANMX6 *hse1Δ::NATMX*	This Study
BY4742 *srn2Δ*	BY4742 *srn2Δ::KANMX6*	GE Healthcare Dharmacon
BY4742 *vps36Δ*	BY4742 *vps36Δ::KANMX6*	GE Healthcare Dharmacon
BY4742 *snf8Δ*	BY4742 *snf8Δ::KANMX6*	GE Healthcare Dharmacon
BY4742 *vps25Δ*	BY4742 *vps25Δ::KANMX6*	GE Healthcare Dharmacon
BY4742 *vps20Δ*	BY4742 *vps20Δ::KANMX6*	GE Healthcare Dharmacon
BY4742 *vps24Δ*	BY4742 *vps24Δ::KANMX6*	GE Healthcare Dharmacon
BY4742 *did4Δ*	BY4742 *did4Δ::KANMX6*	GE Healthcare Dharmacon
BY4742 *vps4Δ*	BY4742 *vps4Δ::KANMX6*	GE Healthcare Dharmacon
BY4742 *vps28Δ*	BY4742 vps28*::KANMX6*	GE Healthcare Dharmacon
BY4742 *snf7Δ*	BY4742 *snf7Δ::KANMX6*	GE Healthcare Dharmacon
BY4742 *bro1Δ*	BY4742 *bro1Δ::KANMX6*	GE Healthcare Dharmacon
BY4742 *vps23Δ*	BY4742 *vps23Δ::KANMX6*	GE Healthcare Dharmacon
BWY640	SEY6210 *vam3Δ*::HIS3 pPRS306 GFP-GFP-Vam3	[Wang 2002]
BWY2858	SEY6210 Ste3-GFP::KAN	[Prosser 2010]
BWY3400	SEY6210 *ent1Δ*::LEU2 *ent2*ΔHIS3 *yap1801*Δ::HIS3 *yap1802*Δ::LEU2 Ste3-GFP::KAN +pBW0778[pRS414::*ent1*(aa1-151)]	[Prosser 2010]

Plasmid	Characteristics	Source
pVJS52	pYES2/NT C, *legC7*, *ura3*	[Bennett 2013]
pVJS53	pYES2/NT C, *legC7, lys2*	This Study
pVJS54	pYES2/NT C, *legC7N242I, ura3*	This Study
pVJS55	pYES2/NT C, *legC7N242I, lys2*	This Study
pGO36	pRS416, URA3	[Odorizzi 1998]
pMM134	pRS416, Sna3-GFP	[McNatt 2007]
pGO45	pRS416, GFP-CPS	[Odorizzi 1998]
pVJS47	pTYB12 LEGC7ΔTM	[Bennett 2013]
pVJS56	pET42a, GST-VPS27	This Study
pVJS57	GFP-Vps27 (pGO36)	This Study
pMM2660	*ura3* to *lys2* converter	GE Healthcare Dharmacon
pVJS59	GFP-LegC7(pGO36)	This Study

Table 2.2: Primers used in this study

Primer Name	Sequence*
LegC3-KpnI	5’-GTAGAA*GGTACC*CGTGATTATGTTTTTGGCCAAC-3’
LegC3-XbaI	5’-GGTGGT*TCTAGA*GCTCCATTGAAATTTTATTGACAG-3’
GFPC7_F	5'-ATGGATGAACTATACAAGTCCGGACTCAGATCTATGGCTACTAATGAAACAG-3'
GFPC7_R	5'-GCTTTAGTCAATTAAAGATCTCGAGCTCAAGCTTCGAATTCTGCAGTCGAC-3'
C7N242_F	5'-CTGATTTATTGGAAAAAATTCAAAAGGAATTGTCAAAA-3'
C7N242_R	5'-CTGATTTATTGGAAAAAATTCAAAAGGAATTGTCAAAA-3'
Vps27BamH1_F	5'-GGAGGA*GGATCC*GACAGTATGTCCGTTAGCACGCC-3'
Vps27Xho1_R	5'-GGAACTGCTAATAGAGCTTTAATA*CTCGA*GGGAGGA-3'
C7N242Q_F	5'-CTGATTTATTGGAAAAACAACAAAAGGAATTGTCAAAA-3'
C7N242Q_R	5'-CTGATTTATTGGAAAAACAACAAAAGGAATTGTCAAAA-3'
C7N242R_F	5'-CTGATTTATTGGAAAAACGTCAAAAGGAATTGTCAAAA-3'
C7N242R_R	5'-CTGATTTATTGGAAAAACGTCAAAAGGAATTGTCAAAA-3'
C7N242D_F	5'-CTGATTTATTGGAAAAAGATCAAAAGGAATTGTCAAAA-3'
C7N242D_R	5'-CTGATTTATTGGAAAAAGATCAAAAGGAATTGTCAAAA-3'
C7N242L_F	5'-CTGATTTATTGGAAAAACTTCAAAAGGAATTGTCAAAA-3'
C7N242L_R	5'-CTGATTTATTGGAAAAACTTCAAAAGGAATTGTCAAAA-3'
C7N242A_F	5’- CTGATTTATTGGAAAAAGCTCAAAAGGAATTGTCAAAA-3’
C7N242A_R	5’- CTGATTTATTGGAAAAAGCTCAAAAGGAATTGTCAAAA-3’
Vps27GFP_F	5'-ATGGATGAACTATACAAGTCCGGACTCAGATCTATGTCCGTTAGCACGCCAAG-3'
Vps27GFP_R	5'-GGAACTGCTAATAGAGCTTTAAAGATCTCGAGCTCAAGCTTCGAATTCTGCAGTCGAC-3'

*****Italics denote introduced restriction sequences

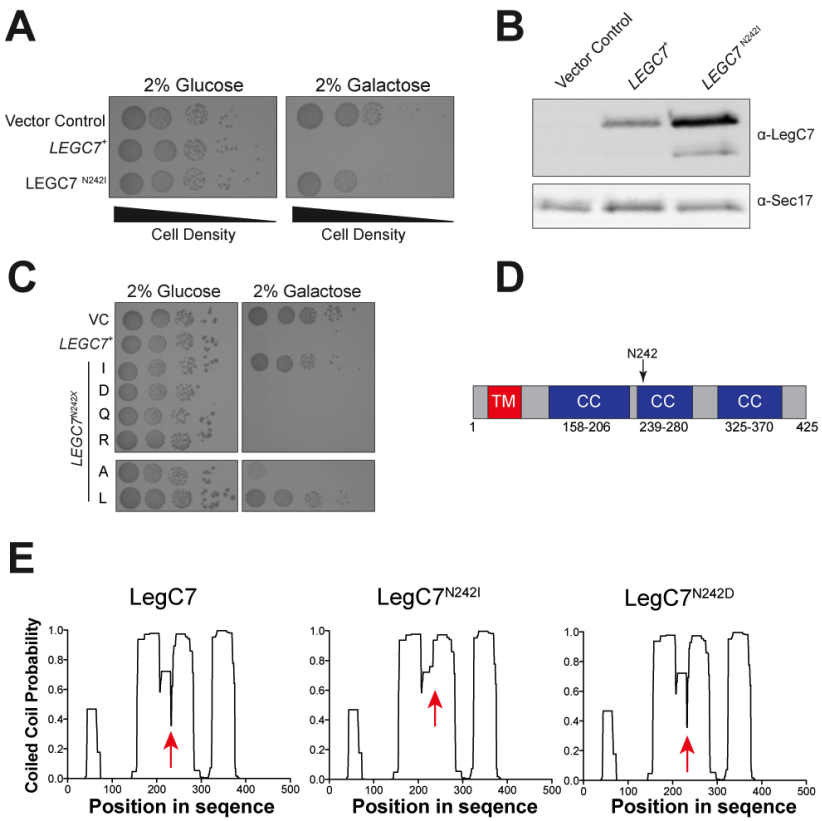

Figure 2.1: Residue N242 is required for LegC7 toxicity in yeast**.**
(A) BY4742 yeast strains harboring the galactose-inducible control plasmid pYES2/NT C, pVJS52 (*LEGC7*$^{+}$), or pVJS54 (*LEGC7*^{N242I}) were spotted onto CSM-uracil medium supplemented with either 2% glucose or 2% galactose with 10-fold serial dilutions from a starting culture of OD_{600}=1.0. Plates were incubated for 72 h at 30°C. (B) Strains from (A) were grown in for 24 h in CSM-uracil supplemented with 2% glucose at 30 °C, washed in ddH_2O, suspended in fresh CSM-uracil/2% galactose, and incubated at 30°C for 16 h. Equal fractions of each strain were harvested, total protein was extracted [von de Haar 2007], and 30µl from each sample was separated by SDS-PAGE. Samples were immunoblotted for LegC7 (rabbit 1:5000) or Sec17p (Rabbit, 1:1000) [Wang 2003] (loading control). (C) The *LEGC7*$^{+}$ plasmid, pVJS52, was mutagenized via site-directed mutagenesis (Materials and Methods), transformed into BY4742, and spotted onto CSM-uracil medium containing either 2% glucose or 2% galactose in 10-fold serial dilutions. (D) Diagram of the predicted LegC7 protein structure indicating transmembrane domain (TM, red) and three predicted coiled coil domains (CC, blue). Transmembrane prediction was calculated with TMHMM Server v.2.0 (http://www.cbs.dtu.dk/services/TMHMM/,) and coiled coil predictions were calculated with COILS (http://toolkit.tuebingen.mpg.de/pcoils) with a window size of 21, weighting, and an iterated matrix. (E) Coiled coil probability prediction of LegC7 containing either N, I, or D at position 242 were run as in (D)**.** Probabilities at each position were plotted and the predicted disordered region between predicted coiled coil regions 1 and 2 is marked (red arrow).

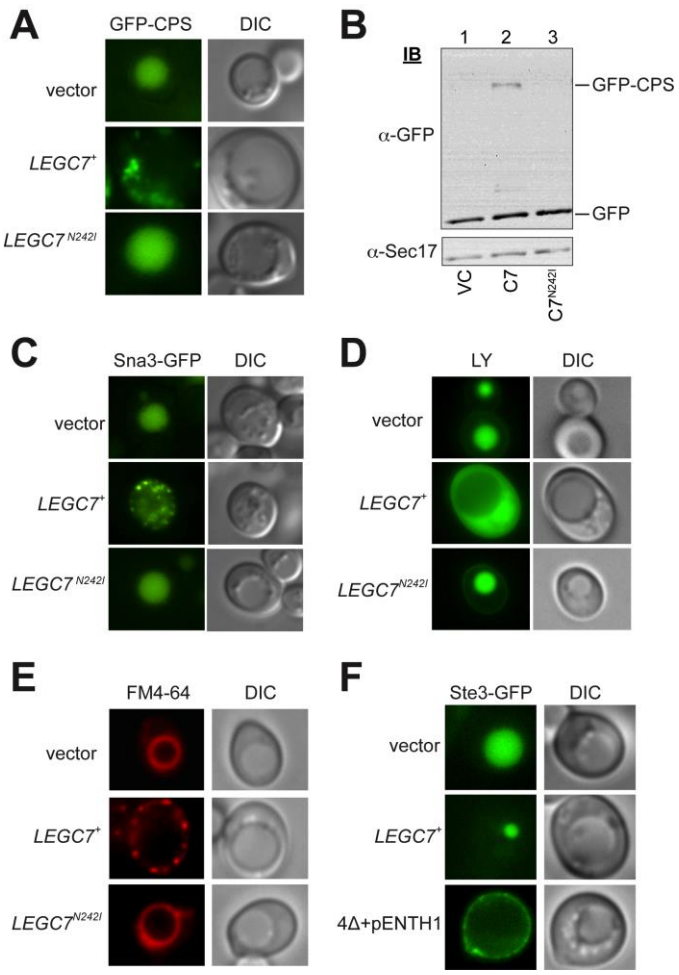

Figure 2.2: LegC7 induces endosome:vacuole trafficking defects**.**
(A) BY4742 yeast strains harboring GFP-CPS and either the vector control, *LEGC7+*, or *LEGC7N242I* plasmids were grown in selective media supplemented with 2% glucose at 30 °C, washed in ddH_2O, suspended in fresh CSM-uracil/2% galactose, incubated at 30°C for 16 h, then visualized. (B) Equal portions of total proteins were extracted from strains in (A), then immunoblotted for GFP and Sec17p (loading control). (C) BY4742 yeast strains containing GFP-Sna3 and either the vector control, *LEGC7+*, or *LEGC7N242I* plasmids were grown as in (A), then visualized.
(D) Cells containing the vector control, *LEGC7+*, or *LEGC7N242I* plasmids were incubated with Lucifer Yellow (Materials and Methods), and then visualized. (E) Strains from (D) were grown in selective media supplemented with 2% glucose at 30 °C, washed in ddH_2O, suspended in fresh CSM-uracil/2% galactose, incubated at 30°C for 16 h, then stained with the yeast vacuolar marker FM4-64 [Vida 1995] and visualized. (F) Wild type SEY6210 or Δ4+ENTH (Table 2.1) strains harboring Ste3-GFP and either the vector control or *LEGC7+* plasmids were grown as in (A) and then visualized.

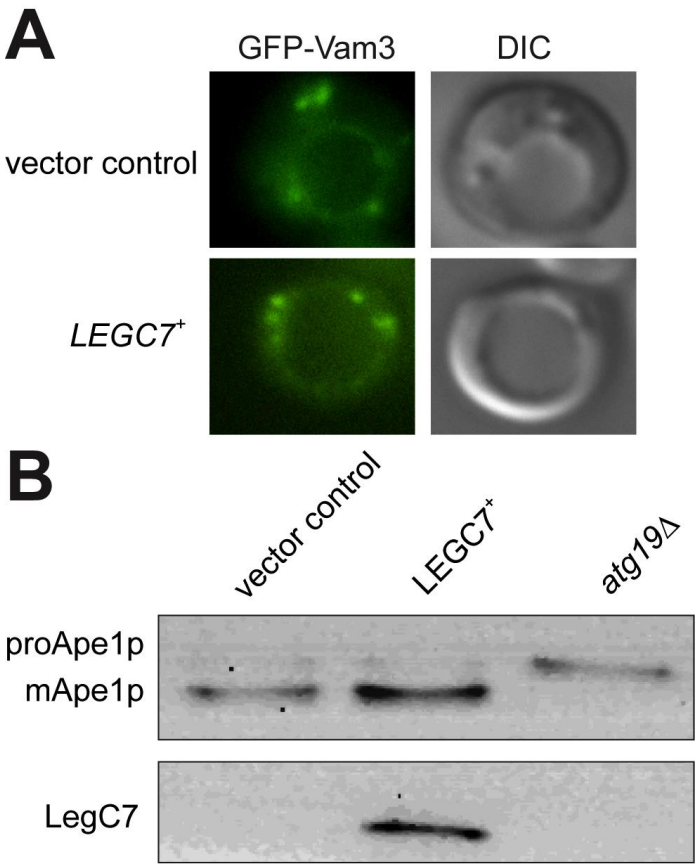

Figure 2.3: LegC7 does not delay non-endosomal vacuolar traffic**.**
(A) Wild type yeast strains expressing GFP-Vam3 [Wang 2002] and expressing either *LEGC7*$^{+}$ or *LEGC7*^{N242I} were grown in selective media supplemented with 2% glucose at 30 °C, washed in ddH_2O, suspended in fresh CSM-uracil-lysine/2% galactose, incubated at 30°C for 16 h, then visualized. (B) Wild type or *atg19Δ* cells expressing either *LEGC7*$^{+}$ or *LEGC7*^{N242I} were grown in selective media containing 2% glucose at 30 °C, washed in ddH_2O, suspended in fresh CSM-uracil/2% galactose, incubated at 30°C for 16 h, and total proteins were extracted from equal fractions. Proteins were separated and immunoblotted for Ape1p (Rabbit 1:2000) [Klionsky 1992] and LegC7.

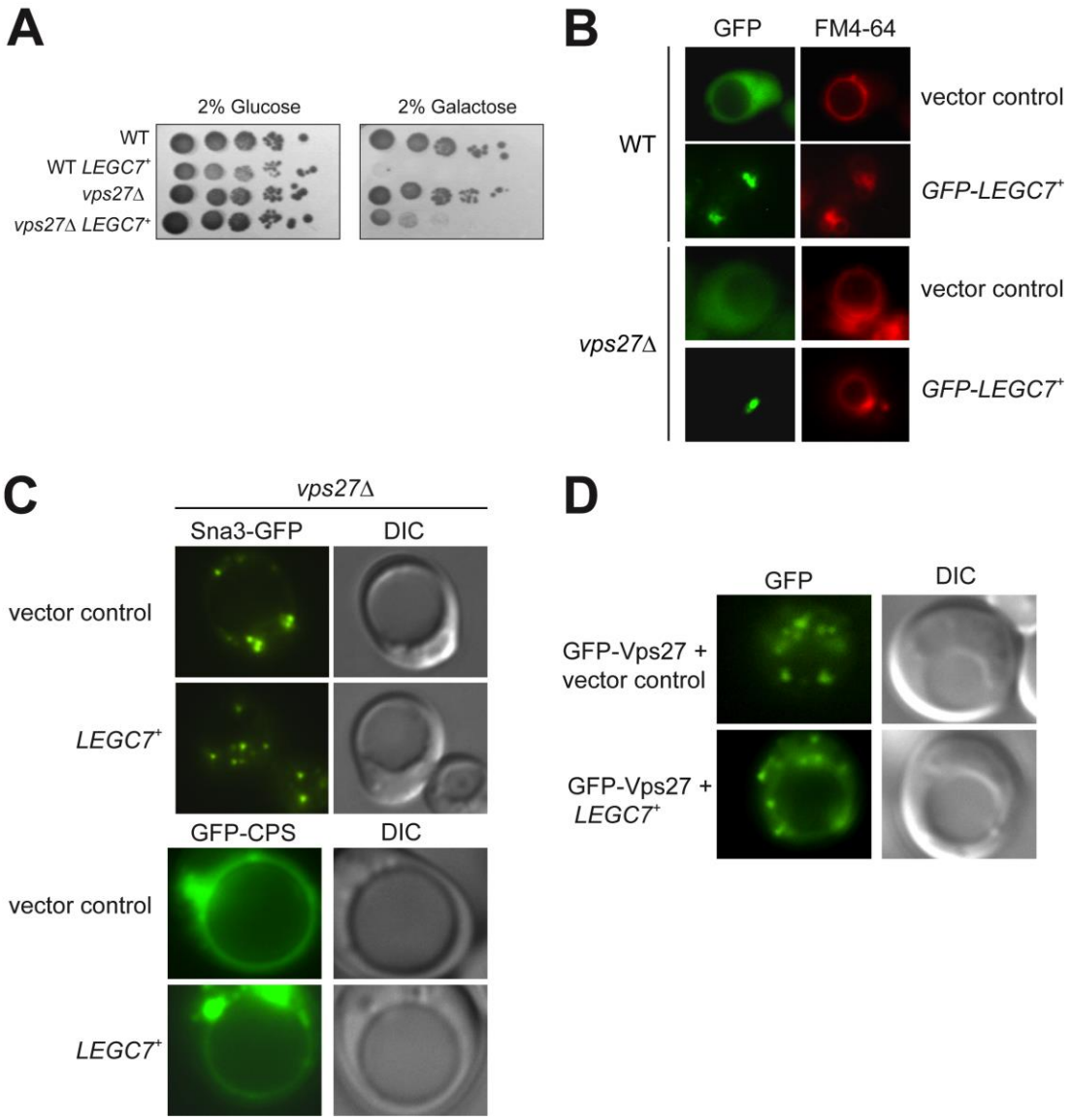

Figure 2.4: Deletion of *VPS27* reduces LegC7 toxicity**.**
(A) BY4742 or *vps27Δ* strains harboring either the control or *LEGC7+* plasmids were spotted onto CSM-Ura plates containing 2% glucose or 2% galactose in 10-fold serial dilutions (starting OD_{600} = 1.0) and grown at 30°C for 96h. (B) BY4742 or *vps27Δ* strains expressing GFP or GFP-LegC7 were grown in selective media supplemented with 2% glucose at 30 °C, stained with FM4-64, and visualized for GFP and FM4-64 fluorescence. (C) Yeast *vps27Δ* strains expressing either GFP-CPS or Sna3-GFP harboring the *LEGC7+* expression plasmid or vector control were grown in selective media supplemented with 2% glucose at 30 °C, washed in ddH_2O, suspended in fresh CSM-uracil-lysine/2% galactose, incubated at 30°C for 16 h, then visualized. (D) Cells expressing GFP-Vps27 and LegC7 were grown as in (C), and localization of GFP-Vps27 was determined.

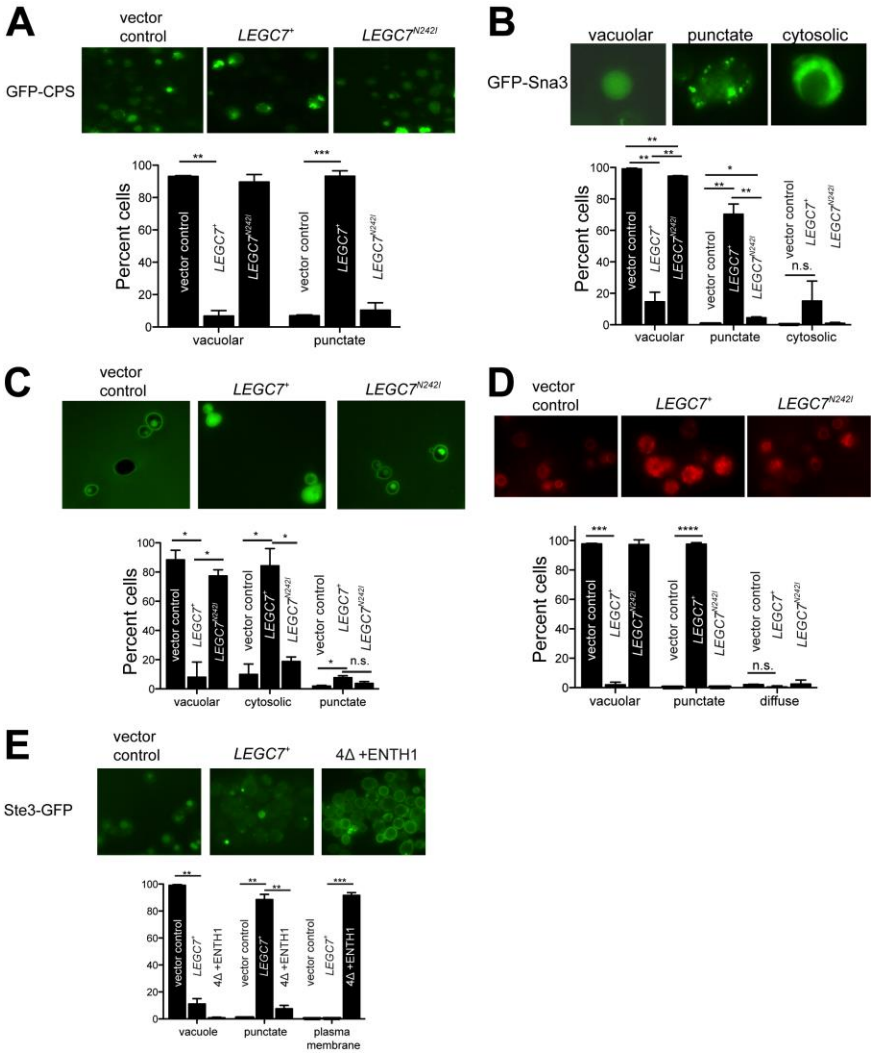

Figure 2.S1: Quantification of Figure 2.2 Microscopy
(A) BY4742 yeast strains harboring GFP-CPS and either the vector control, *LEGC7*⁺, or *LEGC7*^{N242I} plasmids were grown in selective media supplemented with 2% glucose at 30 °C, washed in ddH_2O, suspended in fresh CSM-uracil-lysine/2% galactose, incubated at 30°C for 16 h, then visualized. (B) BY4742 yeast strains containing GFP-Sna3 and either the vector control, *LEGC7*⁺, or *LEGC7*^{N242I} plasmids were grown as in (A), then visualized. (C) Cells containing the vector control, *LEGC7*⁺, or *LEGC7*^{N242I} plasmids were incubated with Lucifer Yellow (Materials and Methods), and then visualized. (D) Strains from (C) were grown in selective media supplemented with 2% glucose at 30 °C, washed in ddH_2O, suspended in fresh CSM-uracil/2% galactose, incubated at 30°C for 16 h, then stained with the yeast vacuolar marker FM4-64 [Vida 1992] and visualized. (E) Wild type SEY6210 or BWY3400 (Δ4+ENTH, Table 2.1) strains harboring Ste3-GFP and either the vector control or *LEGC7*⁺ plasmids were grown as in (A) and then visualized. Two separate trials, each consisting of a minimum of 222 individual cells were counted for each set, and images presented are lower magnification/larger fields of those presented in Figure 2.2. * *P*<.0261, ** *P* <.0051, *** *P*<.0008, **** *P*<.0001, unpaired two-tailed t Test.

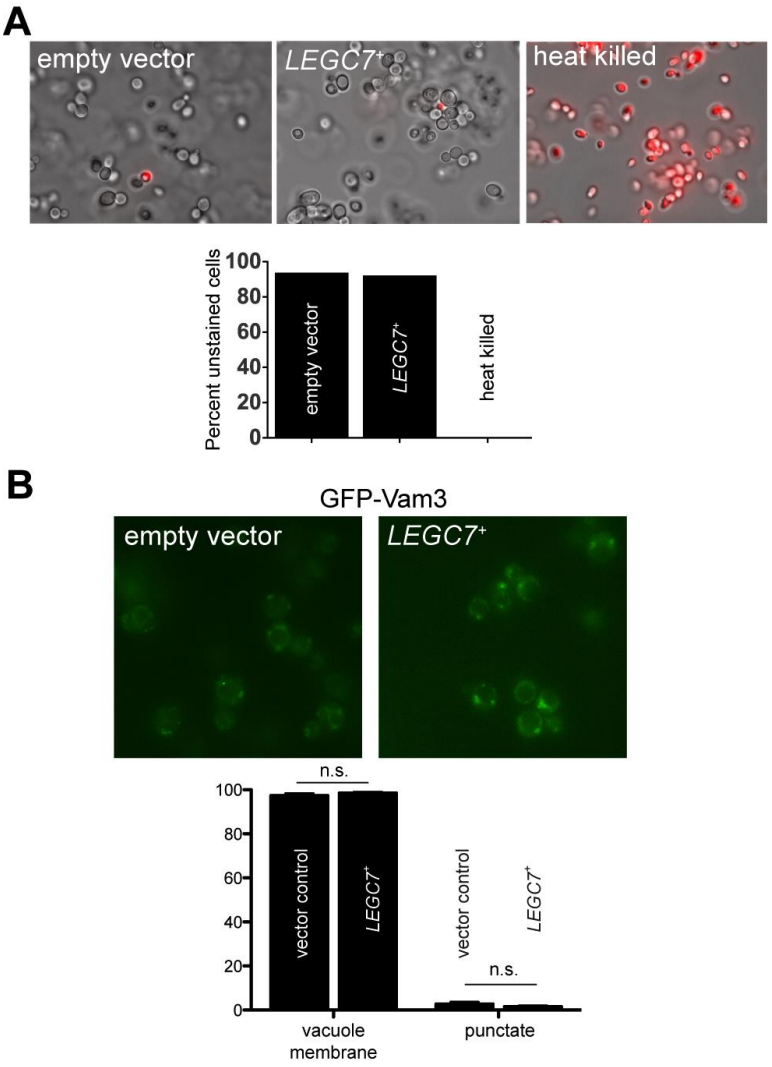

Figure 2.S2: LegC7 does not induce cell death during expression or alter GFP-Vam3 traffic**.** (A) BY4742 cells containing either a control or *LEGC7*+ plasmid were grown in selective media supplemented with 2% glucose at 30 °C, washed in ddH_2O, suspended in fresh CSM-uracil/2% galactose, and incubated at 30°C for 16 h. A sample of the BY4742 cells were incubated at 100°C for 10 min for a dead cell control, then 25 µM propidium iodide was added, incubated at 30°C for 30 minutes, washed, and visualized. At least 385 cells from each sample were scored for propidium iodide retention; representative micrographs for each condition are shown. (B) Wild type yeast strains expressing GFP-Vam3 [58] and expressing either *LEGC7*+ or *LEGC7*^{N242I} were grown in selective media supplemented with 2% glucose at 30 °C, washed in ddH_2O, suspended in fresh CSM-uracil-lysine/2% galactose, incubated at 30°C for 16 h, then visualized. Two separate trials, each consisting of a minimum of 300 individual cells were counted. n.s.; not significant, unpaired two-tailed t Test. Images presented are lower magnification/larger fields of those presented in Figure 2.3.

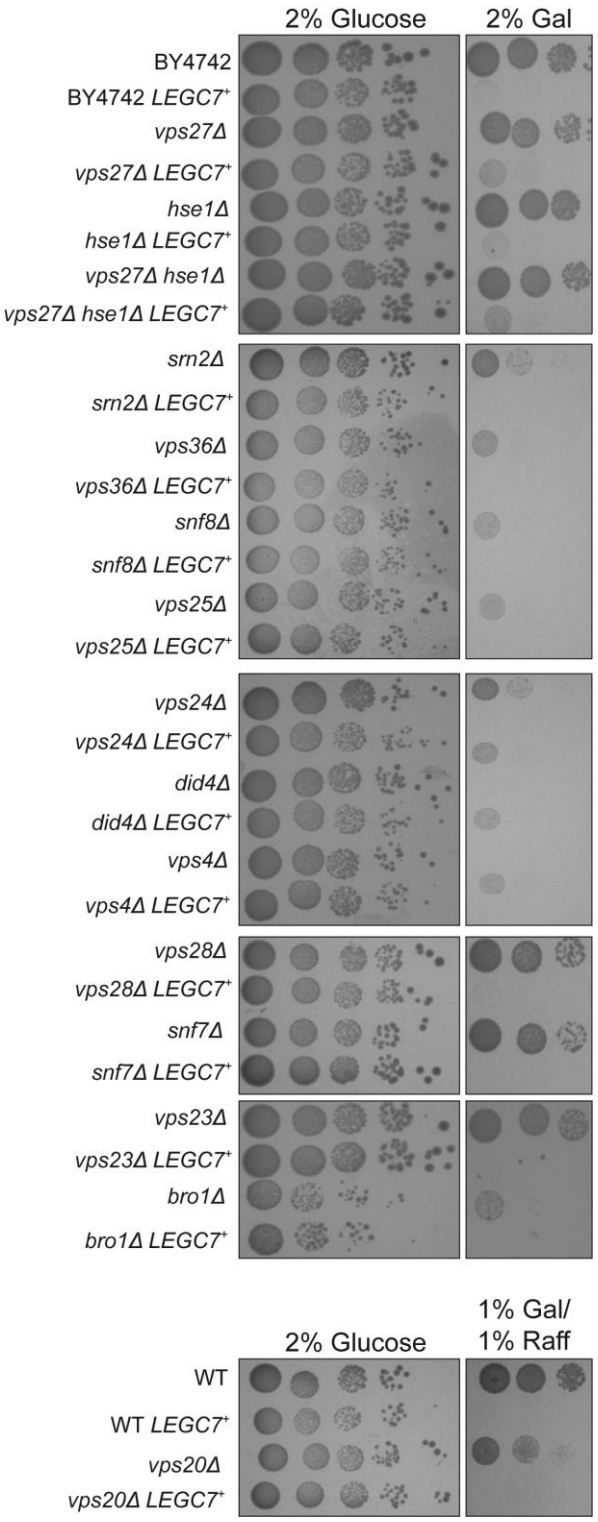

Figure 2.S3: Most Class E VPS mutants do not reverse LegC7 toxicity**.**
BY4742 or noted class E deletion strains harboring either the control or *LEGC7*+ plasmids were spotted onto CSM-Ura plates containing 2% glucose or 2% galactose in 10-fold serial dilutions (starting OD_{600} = 1.0) and grown at 30°C for 96 h.

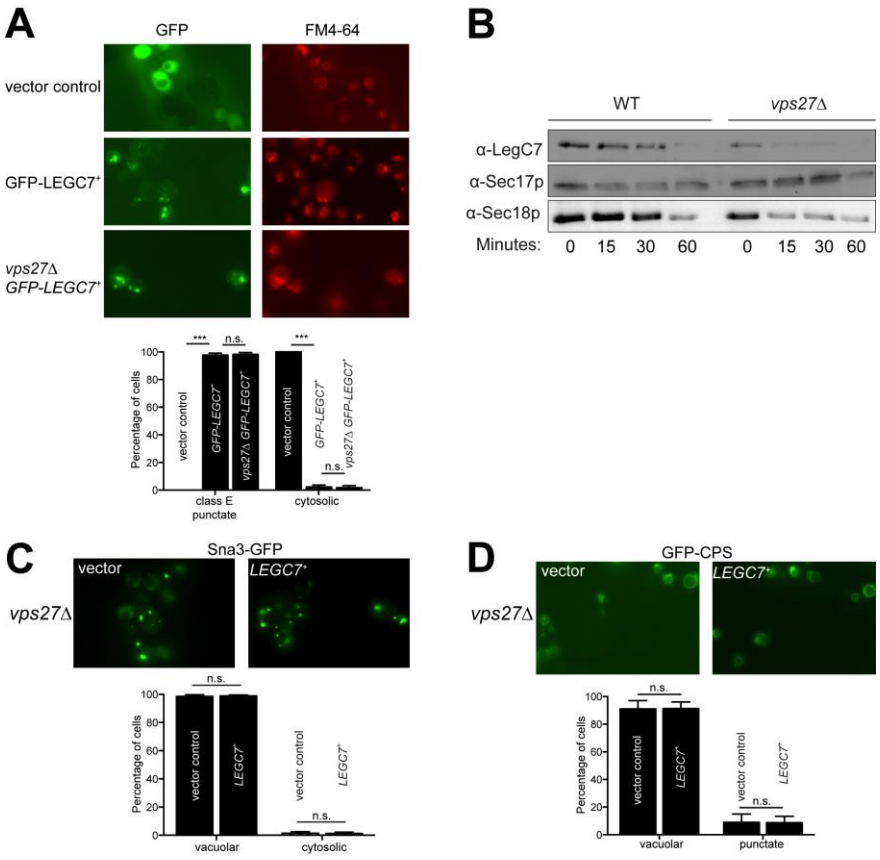

Figure 2.S4: Effects of *vps27Δ* on LegC7 function *in vivo*.
(A) BY4742 or *vps27Δ* strains expressing GFP or GFP-LegC7 were grown in selective media supplemented with 2% glucose at 30 °C, stained with FM4-64, and visualized for GFP and FM4-64 fluorescence. (B) BY4742 or *vps27Δ* strains harboring either the control or *LEGC7+* plasmids were grown in selective media containing 2% glucose at 30 °C, washed in ddH_2O, suspended in CSM-Ura 2% galactose, incubated at 30 °C for 16 h in order to induce LegC7 expression. Samples were diluted to OD_{600} = 1.0, and cycloheximide was added to a final concentration of 0.5 mg/ml. Cultures were incubated at 30°C and 1 OD of cells were withdrawn at the noted timepoints, processed to extract proteins [von der Haar 2007], and separated using SDS-PAGE and immunoblotted using LegC7 antiserum, Sec17 antiserum, or Sec18 (Rabbit 1:1000) serum[Kato 2001]. Yeast *vps27Δ* strains expressing either (C) GFP-CPS or (D) Sna3-GFP harboring the *LEGC7+* expression plasmid or vector control were grown in selective media supplemented with 2% glucose at 30 °C, washed in ddH_2O, suspended in fresh CSM-uracil-lysine/2% galactose, incubated at 30°C for 16 h, then visualized. Two separate trials, each consisting of a minimum of 214 individual cells were counted for microscopy. ***P<0.002, n.s.=not significant, unpaired two-tailed t Test. Images presented are lower magnification/larger fields of those presented in Figure 2.4.

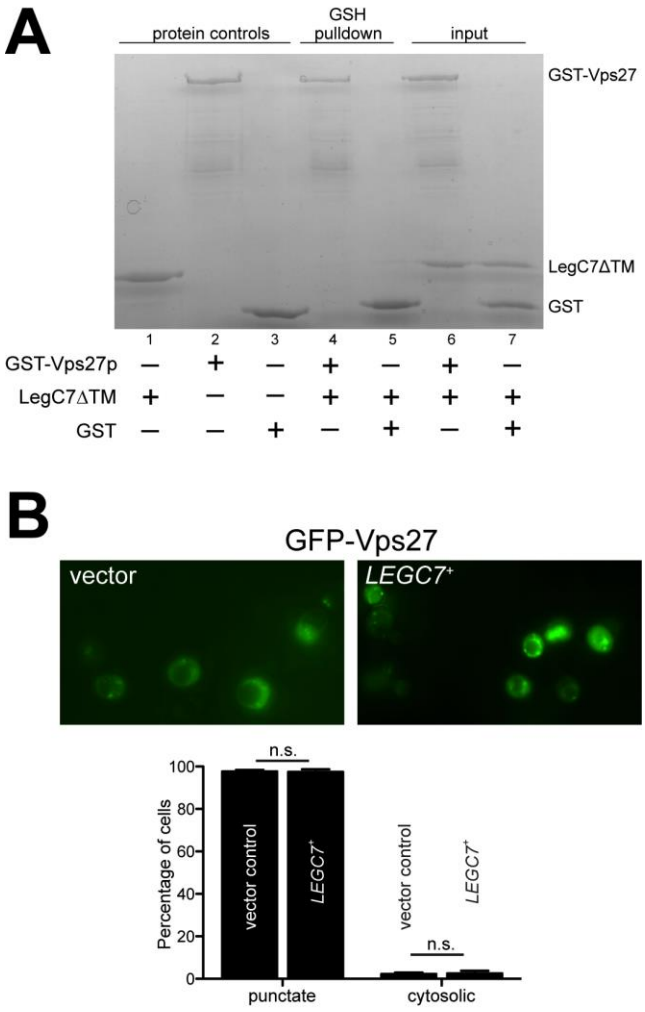

Figure 2.S5: LegC7ΔTM does not interact with GST-Vps27**.**
(A) 3μM LegC7ΔTM was mixed with equimolar concentrations of GST or GST-Vps27 in 20 mM HEPES-NaOH pH 8.0, 10% glycerol, 150mM NaCl, 2mM $MgCl_2$, 1 mM PMSF, and 1 x protease inhibitor cocktail (Pierce). Samples were incubated at 4°C with mixing for 1 hour and input controls were removed. 25μL of equilibrated glutathione resin was added and samples were incubated with mixing for 1 h at 4°C. Samples were washed 10 times with 1 ml of above buffer, suspended in 100μL SDS-PAGE buffer, boiled, and separated via SDS-PAGE. (B) Cells expressing GFP-Vps27 and *LEGC7+* were grown in selective media supplemented with 2% glucose at 30 °C, washed in ddH_2O, suspended in fresh CSM-uracil-lysine/2% galactose, incubated at 30°C for 16 h, then visualized. Two separate trials consisting of a minimum of 300 individual cells were counted; n.s.=not significant; unpaired two-tailed t Test. Images presented are lower magnification/larger fields of those presented in Figure 2.4.

CHAPTER 3

THE *LEGIONELLA PNEUMOPHILA* EFFECTOR PROTEIN, LEGC7, ALTERS THE LOCALIZATION OF THE CORVET COMPLEX

Kevin M. O'Brien, Chetan N. Hebbale, Margret Steward, and Vincent J. Starai. To be submitted to PLoS One.

ABSTRACT

The human pathogen *Legionella pneumophila,* which causes a severe form of pneumonia called Legionnaires' disease, invades alveolar macrophages and establishes a stable replicative niche within a highly specialized intracellular compartment, thus avoiding lysosomal degradation. *Legionella* utilizes a type IV secretion system to secrete around 300 effector proteins into host cells that manipulate a variety of host processes. Disruption of eukaryotic endosomal trafficking is a key pathway targeted by *Legionella* upon host cell entry in order to disrupt phagosome maturation. The *Legionella* effector protein LegC7 causes toxicity when expressed in yeast and we have previously demonstrated that LegC7 specifically disrupts the localization of cargos that traffic through the endosomal system while leaving other pathways unaltered. Here we expand upon this work by demonstrating that LegC7 toxicity is reduced or eliminated when a specific subset of early endosomal trafficking genes are deleted. We demonstrate that expression of LegC7 drastically disrupts the localization of Vps8p, a member of the early endosomal CORVET complex, and the normal distribution of the phosphoinositide essential for endosomal function, PI(3)P. Our results indicate that disruption of the CORVET complex assembly or functionality is the likely cause of the protein trafficking defects induced by LegC7 expression.

INTRODUCTION

Legionella pneumophila are gram-negative facultative intracellular pathogens that invade a diverse range of amoeba and protist hosts (Fields 1986, Fliermans 1981). Upon respiring water droplets contaminated with *Legionella,* human alveolar macrophages can also serve as a host cell for *Legionella* intracellular replication, which can cause a severe pneumonia termed Legionnaires' disease in susceptible individuals (Kaufmann 1981, McDade 1977). In order to direct its survival within the eukaryotic host, *Legionella* utilize a type IV secretion system (T4SS) to translocate approximately 300 predicted and confirmed effector proteins into the host cell (Horwitz 1983, Burnstein 2009, Luo 2004, Heidtman 2009, Lifshitza 2013). Once inside the host, these effector proteins disrupt the regulation of normal host pathways in order to create the membrane-bound replicative niche in which *Legionella* survives, the *Legionella*-containing vacuole (LCV).

Due to the large number of effectors and their suspected redundancy, however, discerning the activities of any single effector protein in the context of *Legionella* infection is often challenging. To enhance the identification and characterization of individual effector proteins from *Legionella*, researchers have turned to the budding yeast *Saccharomyces cerevisiae* as a surrogate eukaryotic host model system, which has proven instrumental in the characterization of effector protein activities from a number of pathogenic bacteria, including: *Shigella, Chlamydia,* and *Vibrio* (Sreelatha 2014, Hackstadt 1999). One such effector protein from *Legionella*, LegC7/YlfA, was initially characterized as inhibiting yeast growth upon expression (Campidonico 2005, de Felipe 2008). Further studies showed that LegC7 expression in yeast strongly disrupted the trafficking of

endosomal cargo to the vacuole (lysosome), suggesting that LegC7 may play a role in modulating endosome function in the eukaryotic host.

Endosomes are highly dynamic organelles in eukaryotic cells that function in protein trafficking, membrane protein degradation, and signaling (recent review Scott 2014). Endosomes receive cargo both from the Golgi as well as from the endocytic uptake of extracellular and plasma membrane material. These endosomes then undergo a maturation process from early to late compartments where compartment properties such as luminal pH is lowered and vesicle fusion machinery is exchanged. Rab GTPases play a central role in vesicle fusion serving as markers of intracellular compartments and recruiting further fusion factors such as tethering complexes; Vps21p functions as the Rab GTPase of early endosome compartments whereas Ypt7p functions on late endosomes and vacuoles (Singer-Kruger 1994, Horazdovsky 1994, Haas 1995). Loss of Vps21p and enrichment of Ypt7p, known as Rab conversion, is one of the hallmarks of endosome maturation. Mon1p and Ccz1p function to activate Ypt7p and are recruited to the early endosome in part by Vps21p thus functioning to activate and enrich Ypt7p on the maturing endosome (Nordmann 2010). Vps21p is inactivated through the action of Msb3p and Msb4p and is then is then removed from early endosome membranes (Albert 1999, Lachmann 2012). The net result of this process is the inactivation and removal of Vps21p and the activation and enrichment of Ypt7p.

The class C core vacuole/endosome tethering (CORVET) complex is a 6 membered multisubunit tethering complex that functions in early endosome fusion (Peplowska 2007, Balderhaar 2013). The CORVET complex is comprised of the subunits: Vps11p, Vps16p, Vps18p, Vps33p as well as Vps3p, and Vps8p; the latter two subunits being specific for the

CORVET complex and functioning in the binding of Vps21p (Markgraf 2009, Plemel 2011). The closely related and better studied homotypic fusion and protein sorting (HOPS) tethering complex contain the same four core subunits (Vps11, Vps16, Vps18, and Vps33) as well as two additional Rab binding subunits Vps39p and Vps41p which bind to Ypt7p (Seals 2000, Wurmser 2000, Nakamura 1997, Brett 2008, Plemel 2011).

Numerous other fusion factors are required for the functionality of endosome fusion. The lipid phosphatidylinositol-3-phosphate [PI(3)P] is enriched on early endosomes and serves to recruit various endosome specific proteins through specific PI(3)P binding domains such as the FYVE (Fab-1, YOTB, Vac1, and EEA-1) domain (Shin 2005, Odorizzi 1998, Gaullier 1998). PI(3)P is synthesized via the actions of Vps34p and associated complex members Vps15p, Vps30p and Vps38p (Auger 1989, Stack 1993, Kihara 2001). Vac1p is an early endosome fusion factor that is recruited in part by its FYVE domain and its interaction with Vps21p; Vac1p also binds to the early endosome Sec1-Munc18-like protein Vps45p (Weisman 1992, Peterson 1999, Tall 1999, Webb 1997). The exact role of Vac1p and Vps45p remains unclear though they function in early fusion reactions and ensure proper coordination between anterograde and retrograde endosome transport (Peterson 1999, Cabrera 2013).

Recently we demonstrated that upon LegC7 expression in the budding yeast *Saccharomyces cerevisiae*, cargos that transit through the endosomal system show profound mislocalization whereas cargos that traffic through alternative vacuole targeting pathways such as the AP3 and cytoplasm-to-vacuole targeting pathway are not disrupted (O'Brien 2015, Bennett 2013). Herein we expand upon the endosomal disruption caused by LegC7 expression in yeast by showing a tightly clustered web of specific genetic

interactions that focuses on the early endosome trafficking pathway. We demonstrate both the ability of LegC7 to prevent proper localization of Vac1p and Vps8p, a member of the CORVET complex, as well as a highly specific colocalization between LegC7- mRuby and Vps8-GFP. The high degree of Vps8p colocalization and loss of Vps8p localization upon LegC7 expression lead us to suggest that LegC7 induces endosomal sorting defects by targeting the functionality of the CORVET complex though it does not appear that disruption of the CORVET complex is the cause of toxicity.

MATERIALS AND METHODS

Plasmid and Strain Creation

In order to create a C-terminal mRuby tagged LegC7 plasmid we amplified the mRuby gene from the plasmid pFA6-link-yomRuby-SpHis5 using the primers YESC7RFP_F and YESC7RFP_R (Sheff 2004). The resulting PCR product was transformed into yeast with a singly cut pVJS52. Plasmids were isolated from resulting colonies and sequenced to determine a correct and in-frame insertion of mRuby.

In order to create N terminal GFP tagged constructs of endosome proteins we amplified the noted genes from BY4742 genomic DNA using the appropriate primer pairs (GFPVac1_F/GFPVac1_R, Vps21pGO_F/Vps21pGO_R, or Ypt7GFP_F/Ypt7GFP_R). PCR products were transformed into BY4742 strains along with pGO36 that had been cut with BglII (Odorizzi 1998). Plasmids from resulting colonies were isolated and transformed into new BY4742 for phenotypic analysis.

LegC7 lacking the first 44 amino acids was created by PCR using primer set LegC7d1-44_F and 3'LegC7Xba1 amplified from pVJS52. The resulting PCR product was

digested with EcoRI and Xba1 and ligated into pYES2NTc. Resulting plasmids were sequenced to confirm proper insertion.

Analysis of Colocalization

Yeast cells containing relevant plasmids or genomic insertions were grown in selective media containing 2% glucose for 16 hours. Cells were collected by centrifugation, washed with sterile water, and suspended in fresh selective media containing 2% galactose and grown for 16 hours at 30°. Cells were collected via centrifugation, suspended in an equal volume of 0.06% agar solution, and visualized. Resulting images were analyzed for colocalization by using FIJI by drawing a circular region of interest and using the coloc2 plugin (Schindelin 2012). Resulting Pearson's correlation coefficients above the threshold value were recorded for a minimum of 50 cells.

RESULTS

Deletions of genes involved in endosome trafficking reverse LegC7/YlfA-mediated lethality

We have previously shown that LegC7 expression specifically alters the delivery of endosomal cargo to the vacuole in *S. cerevisiae*; other cargo delivery pathways to the vacuole were unaltered by LegC7 expression (O'Brien 2015). Due to this apparent pathway specificity, we hypothesized that one or more genes related to endosomal traffic would be required for the toxicity of LegC7. Therefore, we undertook a directed genetic screen to identify non-essential genes that, when deleted, reduced the toxicity of LegC7 expression. For our screen, we selected 87 genes with known links to normal ER, Golgi, and endolysosomal traffic (Table 3.S1), and induced LegC7 expression in each of the individual deletion strains. Of the 87 strains screened, 23 showed some level of growth in the

presence of LegC7 expression, in contrast to the wild type yeast strain expressing LegC7 (Table 3.1, Figure 3.1, Figure 3.S1).

Strikingly, most of the genetic interactions observed centered on proteins involved in the trafficking of endosomes, including: CORVET/HOPS complex members (*VPS11, VPS16, VPS18, VPS33, VPS8, VPS41*), the early endosome Rab-family GTPase *VPS21*, the Rabenosyn-5 like protein *VAC1*, members of the early endosome SNARE complex (*PEP12, SYN8*), PI(3)P synthesis (*VPS30, VPS34, VPS38*), members of the retrograde endosome:Golgi SNARE complex (*SNC1*, *TLG2*), and the endosome:Golgi multisubunit tethering factor, the GARP complex (*VPS51, VPS52, VPS54*). An interaction network of these gene products is shown in Figure 3.1B. Reversals of LegC7 toxicity in strains with deletions in genes that were not closely related to early endosomal traffic, however, were relatively minor and comprised a small fraction of the total genetic interactions (Figure 3.SI1, Table 3.SI1). Therefore, some function of endosomal traffic appears to be required for LegC7-mediated toxicity in yeast.

Previous studies have shown GFP-LegC7 to localize to a pre-vacuolar compartment upon expression in yeast, suggesting that LegC7 may transit through endosomes to accumulate in this presumed "class E" compartment (de Felipe 2008). Therefore, we sought to visualize the localization of LegC7 in each of the mutant backgrounds that provided suppression of the LegC7 toxicity. Unfortunately, GFP-LegC7 constructs previously used for localization in yeast were not toxic to yeast, and low LegC7 expression levels were thought to be the cause (de Felipe 2008). In an attempt to generate a functional derivative of a fluorescently-tagged LegC7 protein, we chose to fuse mRuby protein (Sheff 2004) to the C-terminus of LegC7. This particular construct continued to be toxic to yeast upon

expression, in contrast to the N-terminal GFP-tagged constructs even though expression levels were equivalent (Figure 3.2A and B). Interestingly, localization of the toxic LegC7-mRuby was very different from the localization of the non-toxic GFP-LegC7 protein; LegC7-mRuby displayed a multi-punctate accumulation reminiscent of endosomal markers (Markgraf 2009), while GFP-LegC7 continued to accumulate in a single, "class E"-like structure (Figure 3.2C). Therefore, we continued to use LegC7-mRuby as a more representative marker of LegC7 localization and function in yeast.

Expression of LegC7-mRuby in each of the genetic reversal backgrounds did not appear to mislocalize LegC7-mRuby, when compared to wild type. Interestingly, we were completely unable to detect LegC7-mRuby accumulation in a *vps16Δ* background (Figure 3.SI3). These results suggest that the reversals of toxicity noted in the majority of these deletion strains may not be due to a gross mislocalization of LegC7, but rather the mislocalization of the actual LegC7 "target" in yeast. Furthermore, the lack of LegC7-mRuby mislocalization in many strains that are known to be defective in endosomal traffic (*vps21, vac1, vps8, vps11, vps16, vps18, vps33, vps41, ccz1, vps9, vps34, vps38, vps30, vps45, vps27, snc1, syn8, tlg2, gos1, pep12, vps52, vps51, vps54*) argues against the possibility of LegC7 as authentic cargo through this arm of the secretory pathway.

Identification and Localization of LegC7 Mutants

Previously we identified a point mutant in the second coiled coil domain of LegC7 (N242I) (O'Brien 2015). As LegC7 acts specifically on endosomal cargos we hypothesized that LegC7 may require a signal sequence for proper localization. To test this hypothesis we deleted the first 44 amino acids (Δ1-44) of LegC7 and examined overall toxicity. This deletion mutant suppressed toxicity to a minor degree but not as much as the previously

identified LegC7^{N242I} (Figure 3.3A). In order to ensure the loss of toxicity was not due to lowered expression levels of the protein we performed an immunoblot against LegC7 and detected that both of these constructs resulted in an increase of detectable LegC7 (Figure 3.3B). When we recapitulated these mutations in an mRuby tagged background we observed localization differences between WT and mutant versions of LegC7 (Figure 3.3C). Both the N242I and Δ1-44 mutants of LegC7 displayed roughly equal distributions of multipunctate and single punctate localization (Figure 3.3D). This single punctate localization is reminiscent of the non-toxic GFP-LegC7 construct. The fact that these non-toxic or less toxic derivatives of LegC7 alter localization in a similar way might point to a shared disruption in functionality or trafficking. The fact that some LegC7Δ1-44-mRuby still localized to a multi-punctate pattern argues against the existence of a true signal sequence on LegC7.

LegC7 expression alters localization of some endosome trafficking proteins

As the deletion of a subset of early endosome trafficking proteins reduces LegC7 toxicity, yet does not appear to alter LegC7-mRuby localization, we next sought to determine the effects of LegC7 expression on the localization these proteins. We chose 4 proteins representative of endosomal localization in yeast: Vps8p (CORVET complex), Vps21p (Early endosome Rab GTPase), Vac1p (Rabenosyn-5 like Rab effector), and Ypt7p (late endosome/vacuole Rab GTPase). Under normal growth conditions, Vps8-GFP tends to accumulate in a single punctum within most cells, consistent with previously published work (Figure 3.4A) (Markgraf 2009). Upon LegC7 expression, however, Vps8-GFP is no longer found in these punctae, but rather displays a diffuse cytosolic staining (Figure 3.4A).

We also observed a significant, though less drastic, alteration of GFP-Vac1 localization upon LegC7 expression. As seen with Vac8-GFP, GFP-Vac1 localizes to 1-3 punctae under normal growth conditions (Figure 3.4B). LegC7 expression, however, appears to reorganize some of the GFP-Vac1 punctae into large, multi-punctate aggregations (>3 punctae). We did not observe any significant quantifiable LegC7-dependent disruption in the localization of GFP-Vps21 or GFP-Ypt7 (Figures 3.4C and D). Taken together, this suggests that LegC7 may be able to disrupt the normal localization of some early endosomal Rab GTPase effector proteins, while not altering the localization of the Rab GTPase proteins themselves.

The localization of the important early endosome lipid PI(3)P can be visualized using a fluorescently tagged FYVE domain (Burd 1998). Expression of LegC7 results in an increase in the number of punctate accumulations of PI(3)P (Figure 3.4E).

Colocalization of LegC7 and Vps8

We next wondered if LegC7-mRuby colocalized with any of the above endosome proteins or GFP-Vps27 (O'Brien 2015). We observed a high degree of colocalization between LegC7-mRuby and Vps8-GFP with a Pearson's Correlation Coefficient (PCC) above 0.8 - significantly higher than the other tested proteins (Figure 3.5A, B, and C). LegC7-mRuby displayed an intermediate degree of colocalization with Vps21, Vac1, and Vps27. The PCC values for these proteins were not significantly different from one another but were statistically less than the PCC calculated between LegC7-mRuby and Vps8-GFP. Ypt7p, the late endosome and vacuole Rab GTPase displayed the lowest PCC, significantly less than all other measured values, which is consistent with the idea that LegC7 does not disrupt vacuole traffic or localize to the vacuole (Figure 3.5A and C).

Given the high degree of colocalization between LegC7-mRuby and Vps8-GFP we next wondered if this observed colocalization was disrupted in the context of our genetic interaction strains. The two gene deletions that resulted in the largest decrease in LegC7 toxicity were *vps16* and *vps33*. Interestingly when we measured the colocalization between Vps8-GFP and LegC7-mRuby in these backgrounds we did not observe any difference in PCC indicating that while deletion of core complex members does mislocalize Vps8-GFP it does not disrupt the ability of LegC7-mRuby to colocalize with this protein (Figure 3.5A). We also sought to test out our two mutant derivatives of LegC7 for their ability to colocalize with Vps8-GFP. Again we did not observe any significant lack of correlation between with of the mutants and Vps8-GFP. As an additional control the PCC of the LegC7^{N242I}-mRuby mutant was calculated against GFP-Vps21 and no difference was found compared to WT LegC7. This indicates that while LegC7-mRuby displays a high degree of colocalization with Vps8-GFP neither deletion of COREVT core complex member genes nor the mutants disrupt this effect indicating that both of these toxicity reversal effects are due to some alternate aspect of LegC7 activity.

DISCUSSION

We have previously shown that expression of LegC7 specifically disrupts cargos that traffic through the endosomal system, while leaving alternative trafficking pathways unaltered (O'Brien 2015). In order to determine host genes that are required for LegC7 toxicity we undertook a targeted genetic screen by which we looked for conditions when the toxicity of LegC7 was decreased upon gene deletion. We selected genes involved in endolysosomal trafficking as well as genes involved in other trafficking pathways. We identified 23 genes that, when deleted, resulted in decreases in LegC7 toxicity. Of the 23

identified genetic interactions we found 13 that showed a 50% or larger reduction of toxicity, all of these genes were endosome related. The genetic interactions were specific, as the majority of non-endosome genes did not show any toxicity reversal and those that did resulted in minor reductions in toxicity (Table 3.SI1). We found that deletion of CORVET/HOPS core complex members resulted in the strongest reversals of toxicity with deletion of *vps16* resulting in a complete reversal of toxicity. Outside of the core complex members the two remaining gene deletions that resulted in 75% toxicity reversal were the rabenyosin-5 like protein, *vac1,* and *pep12*, an early endosome SNARE. In the grouping of roughly 50% reversals we saw the early endosome Rab GTPase *vps21*, the CORVET complex member *vps8*, and a PI(3)P kinase *vps34*. We also saw a roughly 50% interaction with two members of the GARP complex, *vps51* and *vps54*. Deletion of the early endosome SNARE *syn8* and the SM-like protein *vps45* also resulted in greater than >50% reversal. Interestingly we only saw minor interactions with *vps9*, the Vps21p GEF and no interactions with *msb3* or *msb4*, which are GAPs that inactivate Vps21p (Nickerson 2012, Lachmann 2012).

As this was a directed screen that focused on endosome genes, it is possible that further interactions with LegC7 exist in pathways or genes we did not test. In order to determine if interacting genes reduced LegC7 toxicity simply by preventing proper trafficking of LegC7, we observed the localization of LegC7-mRuby in each of the backgrounds where toxicity was reduced. Deletion of these genes, with the exception of *vps16,* did not alter LegC7-mRuby localization, indicating that the toxicity reversals were not simply due to altered trafficking of LegC7. This also demonstrates that LegC7 does not rely on the early endosome trafficking machinery for localization. This observation means

that either LegC7 does not traffic to early endosomes or that LegC7 travels to the endosome though an undescribed alternative trafficking pathway. We cannot rule out the possibility that LegC7 traffics to the endosome in a fashion that is not dependent on Vps21p or the CORVET complex. Indeed recently, it was reported that a Vps21p independent early endosome pathway exists in yeast (Toshima 2013). This Vps21p independent pathway functions before the convergence of the biosynthetic and endocytic arms of the endosomal pathway. Given that LegC7 expression in yeast disrupts both arms of the endosomal pathway, we hypothesize that this is not the pathway utilized, or altered, by LegC7 (O'Brien 2015). The alternative explanation that LegC7 disrupts endosomal traffic indirectly is more probable. LegC7 colocalizes with ER proteins when expressed in mammalian cells providing evidence that LegC7 does not exist on endosomes, at least in mammalian cells (de Felipe 2008). We hypothesize that LegC7 acts early in the secretory pathway, perhaps in the ER or Golgi, and blocks the traffic of a certain protein(s) that is needed to recruit or activate endosomal-tethering complexes.

As LegC7 specifically targets the endosomal system, we tested if LegC7 contains an N terminal signal sequence by deleting the first 44 amino acids. We found that this deletion mutant reverses toxicity to a minor degree, arguing against the existence of a true signal sequence. When we observed the localization pattern of both the deletion mutant as well as LegC7^{N242I} we found the same pattern emerge with both constructs resulting in nearly equal distributions of a single punctate pattern and the multi-punctate, wild type, pattern. This similarity was surprising given that these mutations are in very different regions of LegC7. The single punctate pattern is also similar to the localization pattern of GFP-LegC7, which is non-toxic. Given that these constructs all show the single punctate localization

pattern, we propose that localization to this single compartment coincides with toxicity. It is unclear however, if this punctate structure is the cause, or result of, non-toxic derivatives of LegC7. Non-toxic derivatives of LegC7 may be degraded in a similar manner leading to the formation of this structure. Alternatively, mutations in LegC7 may induce similar patterns of improper trafficking resulting in the inability of LegC7 to induce toxicity.

In order to examine what effect LegC7 has on endosomal trafficking proteins we looked for mislocalization of representative endosomal proteins upon LegC7 expression. Expression of LegC7 results in a drastic loss of Vps8-GFP localization, either pointing to a failure of the CORVET complex to associate with the membrane, or a failure of the CORVET complex to functionally aggregate. We also observed a more minor, though significant, alteration of GFP-Vac1 localization. Unlike Vps8-GFP, which appears to lose punctate localization, the number of GFP-Vac1 punctae actually increase upon LegC7 expression. This increase in Vac1p punctae may be representative of a larger number, though less functional, groupings of early endosomal proteins. Consistent with this idea we see a disruption in the localization of PI(3)P as visualized through a fluorescently labeled FYVE motif. As Vac1p is recruited to endosomes partially due to an interaction with PI(3)P this may explain the partial mislocalization of Vac1p. It remains to be seen if the mislocalization of PI(3)P causes the other observed endosome phenotypes or if mislocalization of the lipid is simply another phenotype of LegC7 expression. We did not see an altered localization of GFP-Vps21, the early endosome Rab, indicating that the effects of LegC7 might occur downstream of Vps21p localization. Alternatively, if LegC7 acts indirectly on the endosome system the observed localization defects might represent differences in how these proteins localize to the early endosome membrane. Rab GTPases

are prenylated and inserted into appropriate membranes for functionality (Rocks 2005, Ali 2004). The exact targeting mechanism that explains Rab GTPase membrane specificity has yet to be determined but this process may not be inhibited by LegC7 activity. GFP-Ypt7 was not mislocalized which is consistent with the observation that cells expressing LegC7 still contain a morphologically intact vacuole and that LegC7 does not alter either AP3 or CVT cargos, both pathways that rely on Ypt7p (O'Brien 2015).

In order to further characterize the effects of LegC7 on endosomal proteins we sought to colocalize LegC7-mRuby with endosomal proteins. We found that LegC7-mRuby colocalizes to a high degree with Vps8-GFP. This colocalization is significantly higher than other tested proteins indicating a specificity of LegC7-mRuby for Vps8-GFP over other early endosome proteins. We observed PCCs between 0.5 and 0.6 for other known endosome proteins such as Vps21p, Vac1p, and Vps27p. While the PCC values for these three proteins are significantly higher than GFP-Ypt7 they are below the threshold for true colocalization. We did not observe any colocalization between LegC7-mRuby and GFP-Ypt7, which is again consistent with LegC7 not having an effect on Ypt7p or vacuole traffic. The lack of a high degree of colocalization between known endosome proteins and LegC7 suggests that LegC7 does not exist on endosomes, and may function to recruit Vps8p to alternative structures.

In order to determine what role the colocalization between LegC7-mRuby and Vps8-GFP played in toxicity we sought to measure colocalization in circumstances where LegC7 is non-toxic or less toxic. We wondered if LegC7-mRuby and Vps8-GFP would still colocalize in *vps16* or *vps33* null backgrounds. While deletion of *vps16* and deletion of *vps33* cause almost complete elimination of toxicity, we do not see a loss of colocalization between LegC7-mRuby and Vps8-GFP. We also do not see a loss in colocalization between

Vps8-GFP and the two LegC7 mutants. These data argue against the association between LegC7 and Vps8p as being the cause of toxicity.

Taken as a whole, LegC7 expression results in mislocalization of the CORVET complex which can explain the trafficking defects seen upon LegC7 expression. Disruption of endosomal trafficking through disruption of the CORVET complex also explains specificity, as this tethering factor is only known to function in the early endosome fusion pathway. Multiple lines of evidence support the idea that disruption of the CORVET complex is not responsible for the toxicity that is induced upon LegC7 expression. Deletion of *vps16* or *vps33* results in nearly no LegC7 toxicity yet does not disrupt the interaction between LegC7-mRuby and Vps8-GFP. Also the two identified mutant versions of LegC7 do not show an altered colocalization pattern reinforcing that colocalization of Vps8-GFP and toxicity are distinct events. In addition to these data, few endosome specific genes are essential meaning that disruption of endosome fusion is not lethal to cells. These data argue that the two major phenotypes of LegC7 expression, toxicity and endosome disruption, are distinct events. The endosomal disruption that occurs upon expression of LegC7 is due to mislocalization of the CORVET complex while the cause of toxicity has yet to be explained.

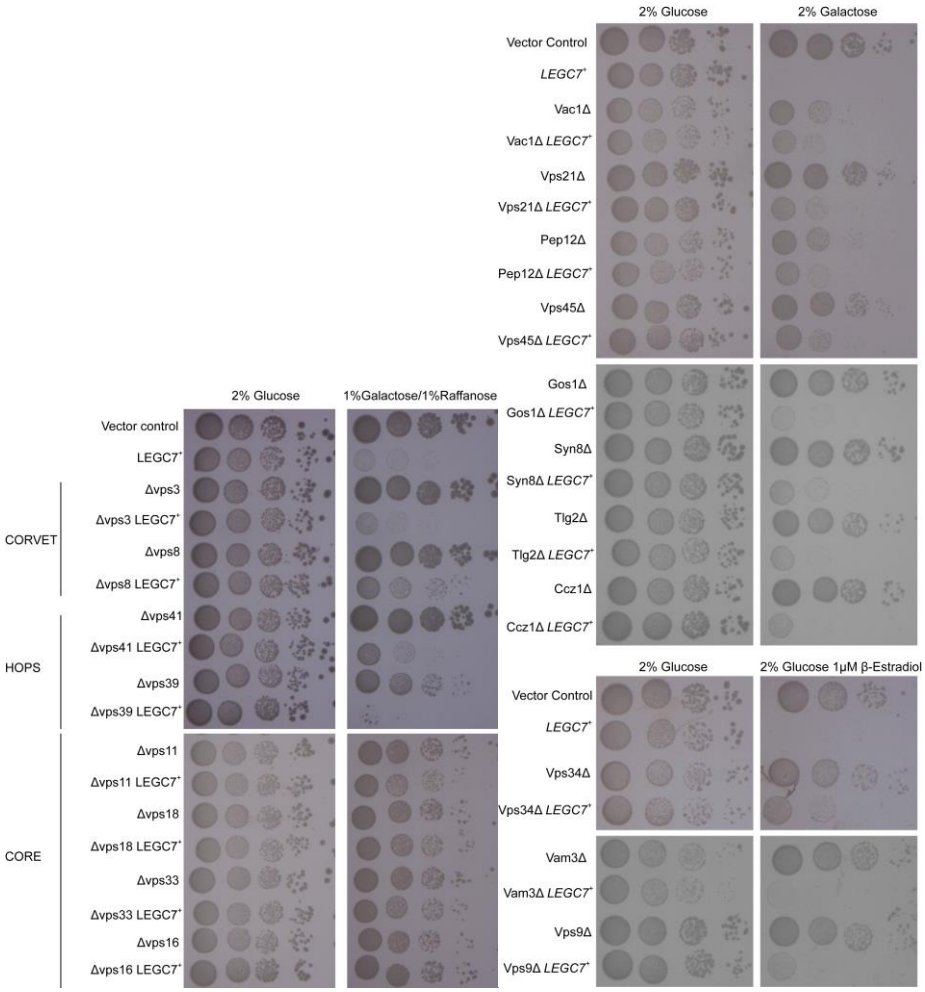

Figure 3.1: LegC7 toxicity is reduced upon deletion of a subset of endosomal trafficking genes.
A. Cells containing either pYES/2NTc or VJS52 in either a wildtype BY4742 background or noted deletion strains were grown for 16 hours in CSM-uracil containing 2% glucose. Strains were diluted to 1 OD unit/mL and 10 fold dilutions of these strains were spotted to CSM-uracil containing either 2% glucose or 2% galactose and incubated at 30° for 72 hours. Deletion of certain genes results in the inability of cells to grow using galactose as a carbon source. For these conditions cells were serially diluted onto media containing 2% glucose or 2% glucose and 1μM β-estradiol and grown for 72 hours at 30°.

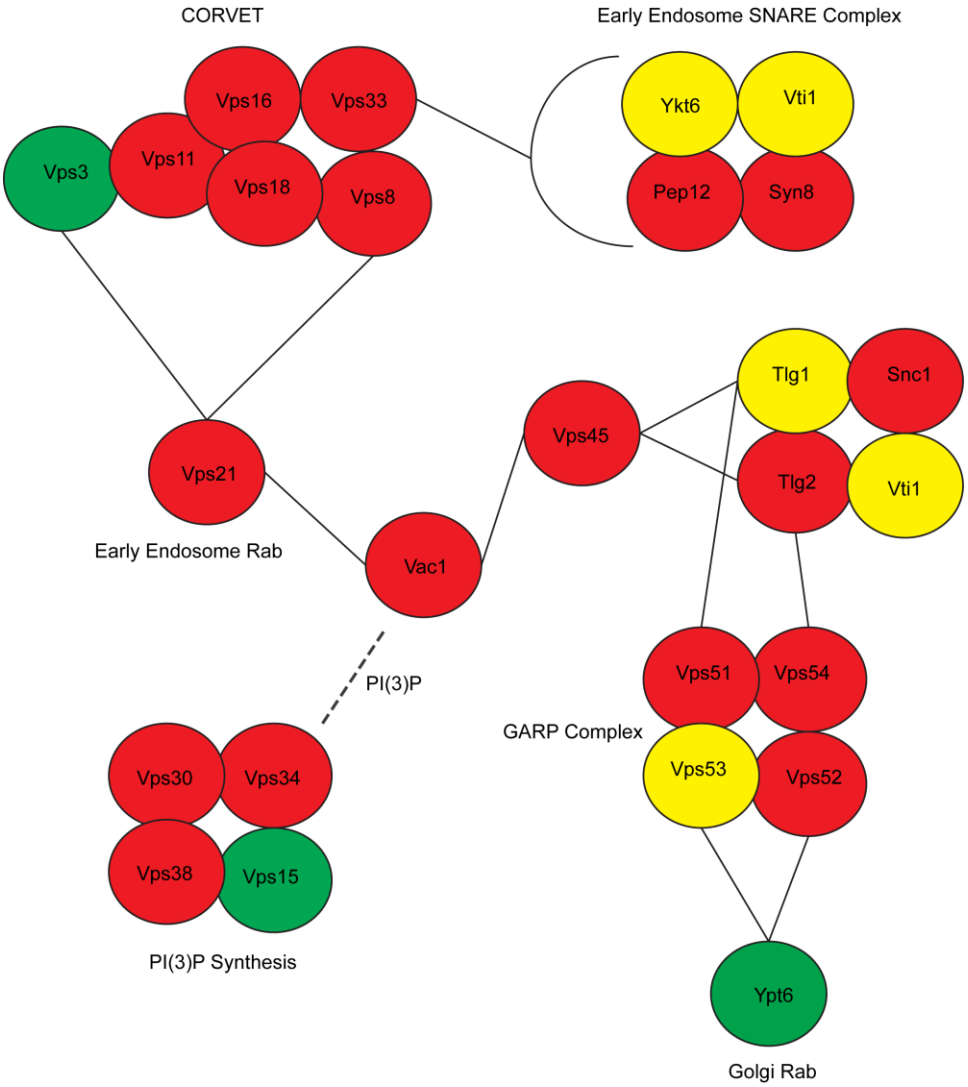

B. Interaction web of identified genes showing their close functional association. Solid lines indicate published physical interactions; dotted lines indicate published indirect interactions. Red=Genes that show genetic interaction with LegC7, Yellow=Essential genes, Green=Genes that do not show a genetic interaction with LegC7.

Table 3.1: Tabulation of genes that reverse LegC7 toxicity upon deletion.
Quantification of genetic interactions and gene functions from Figure 3.1 and 3.SI1.
++++ full reversal; +++ >75% reversal; ++ >50% reversal; + > 25% reversal; 0 no reversal.
* strain showed no or weak growth under galactose induction conditions and was thus tested using β-estradiol induction (Figure 3.SI2).

Gene(s)	Interaction
vps16	++++
vps33	+++
vps11	+++
vps18	+++
vac1	+++
pep12	+++
vps21	++
vps8	++
vps34	++*
vps45	++
vps51	++
vps54	++
syn8	++
tlg2	+
vps9	+*
vps52	+
vps30	+
vps38	+
snc1	+
vps27	+
ccz1	+
vps41	+
gos1	+

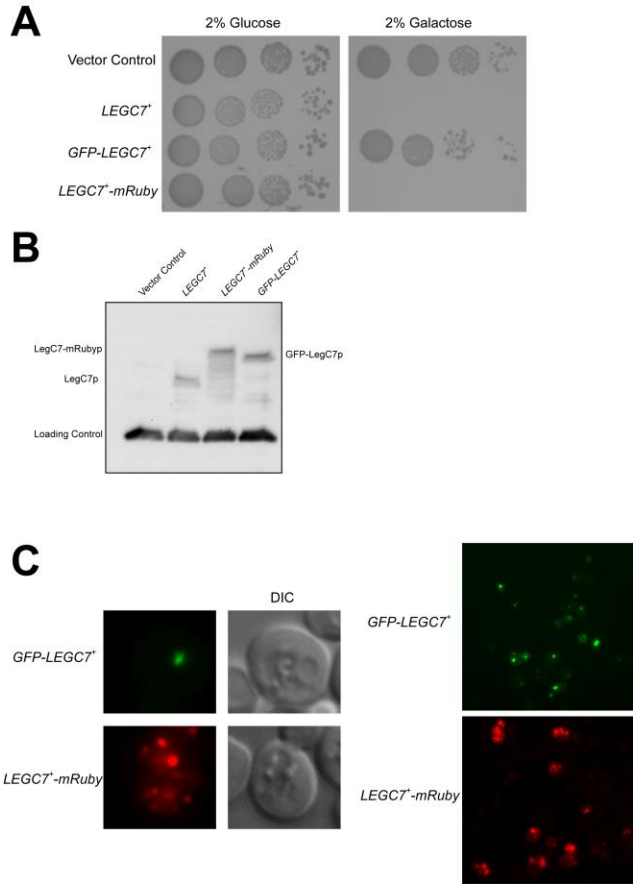

Figure 3.2: LegC7-mRuby forms a punctate pattern in the cytosol and is fully toxic
A. Dilution plating experiment comparing cells harboring the vector control, pVJS52, pVJS59, or pVJS60. Cells were grown for 16 hours at 30° in CSM-uracil containing 2% glucose before being serially diluted onto CSM-uracil media containing either 2% glucose or 2% galactose and incubated at 30° for 72 hours.
B. Western blot to compare expression levels of the 3 LegC7 constructs. Cells were grown in CSM-uracil containing 2% glucose for 16 hours at 30°. Cells were harvested by centrifugation and washed with sterile water before being suspended in CSM-uracil containing 2% galactose and growth at 30° for 18 hours. Total protein was extracted as described in (von der Haar 2007). Samples were immunoblotted for LegC7 (1:1000 Rabbit).
C. Comparison of the localization patterns of GFP-LegC7 and LegC7-mRuby. Cells were grown in CSM-uracil containing 2% glucose for 16 hours at 30°. Cells were collected by centrifugation, washed with sterile water, and suspended in CSM-uracil containing 2% galactose followed by growth at 30° for 18 hours. Cells were collected by centrifugation and suspended in 25 μL CSM-uracil mixed with an equal volume of 0.06% agar and visualized.

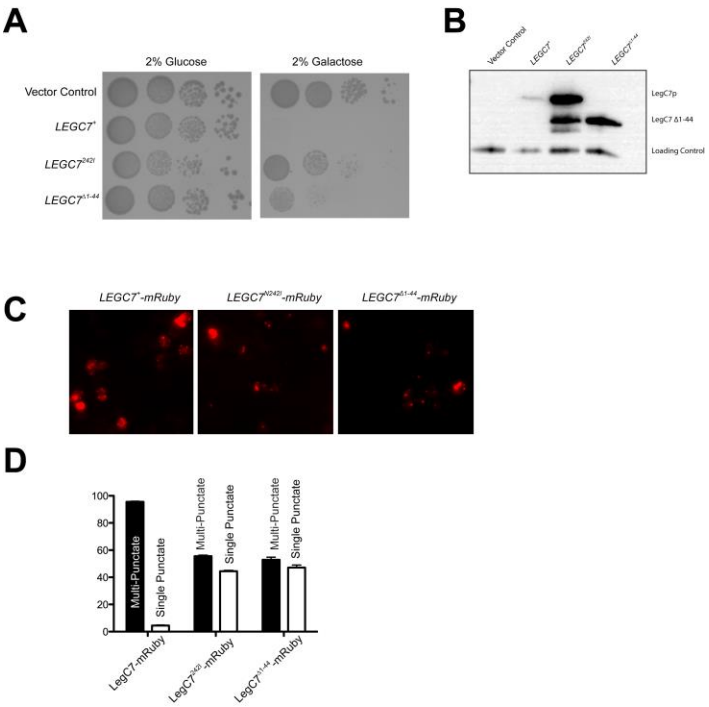

Figure 3.3: LegC7 does not contain an N terminal signal sequence

A. Deletion of the first 44 amino acids of LegC7 results in a minor reduction of toxicity. Cells harboring a vector control plasmid, pVJS52, pVJS54, or pVJS62 were grown for 16 hours at 30° in CSM-uracil containing 2% glucose before being serially diluted onto CSM-uracil media containing either 2% glucose or 2% galactose and incubated at 30° for 72 hours.

B. Western blot analysis of LegC7p, LegC7^{N242I}p, and LegC7$^{\Delta 1\text{-}44}$p. Cells harboring a vector control plasmid, pVJS52, pVJS54, or pVJS62 were grown for 16 hours at 30° in CSM-uracil containing 2% glucose. Cells were harvested by centrifugation and washed with sterile water before being suspended in CSM-uracil containing 2% galactose and grown at 30° for 18 hours. Total protein was extracted as described in (von der Haar 2007). Samples were immunoblotted for LegC7.

C. LegC7 mutants show altered localization patterns. Cells containing pVJS60, pVJS64, or pVJS67 were grown in CSM-uracil containing 2% glucose for 16 hours at 30°. Cells were collected by centrifugation, washed with sterile water, and suspended in CSM-uracil containing 2% galactose followed by growth at 30° for 18 hours. Cells were collected by centrifugation and suspended in 25 µL CSM-uracil mixed with an equal volume of 0.06% agar and visualized.

D. Quantification of localization phenotype between LegC7 and mutant derivatives.

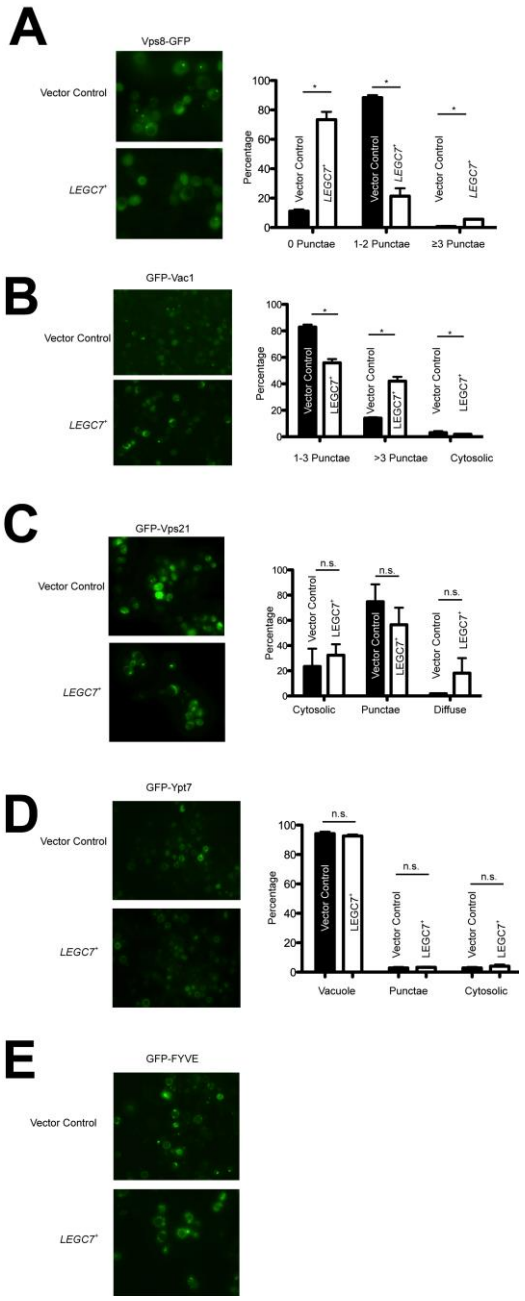

Figure 3.4: LegC7 disrupts the localization of Vps8-GFP and GFP-Vac1
A,B,C,D,E. Cells containing the noted GFP tagged endosome proteins and either the vector control or pVJS53 were grown in CSM-uracil-lysine containing 2% glucose for 16 hours at 30°. Cells were collected by centrifugation, washed with sterile water, and suspended in CSM-uracil-lysine containing 2% galactose followed by growth at 30° for 18 hours. Cells were collected by centrifugation and suspended in 25 µL CSM-uracil-lysine mixed with an equal volume of 0.06% agar and visualized. Phenotypes were quantified and significance was determined using unpaired two-tailed t-Test (n.s. not significant, * $P<0.05$).

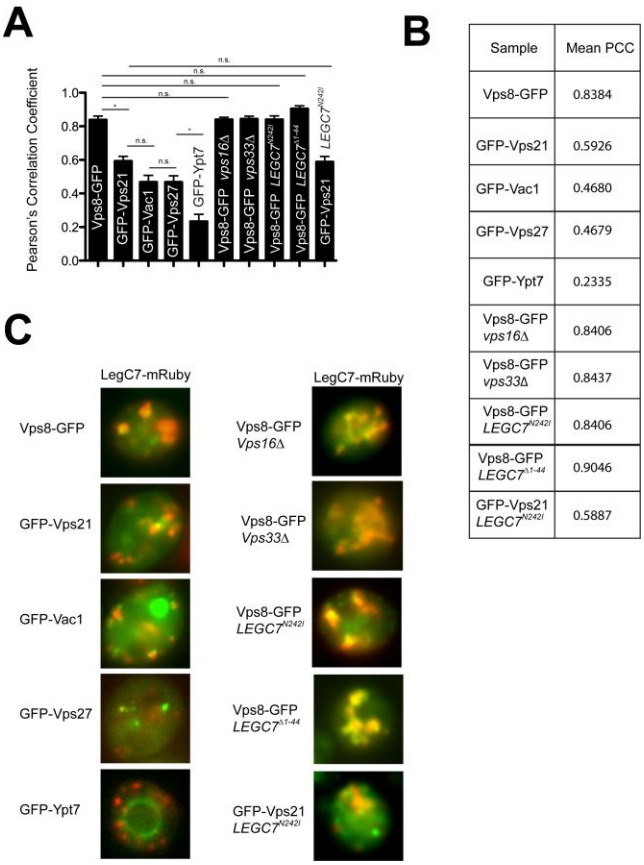

Sample	Mean PCC
Vps8-GFP	0.8384
GFP-Vps21	0.5926
GFP-Vac1	0.4680
GFP-Vps27	0.4679
GFP-Ypt7	0.2335
Vps8-GFP *vps16Δ*	0.8406
Vps8-GFP *vps33Δ*	0.8437
Vps8-GFP *LEGC7*^{N242I}	0.8406
Vps8-GFP *LEGC7*$^{\Delta 1-44}$	0.9046
GFP-Vps21 *LEGC7*^{N242I}	0.5887

Figure 3.5: LegC7 colocalizes with Vps8-GFP
A. A minimum of 50 cells that expressed both LegC7-mRuby and the noted GFP endosome protein were analyzed using the Coloc2 program in FIJI. Mean Pearson's correlation coefficients are displayed in the table. Phenotypes were quantified and significance was determined using 1 way ANOVA test (n.s. not significant, * $p<0.05$).
B. Mean PCC values from each condition in A.
C. Cells containing the noted GFP tagged endosomal protein and either the vector control or pVJS61 were grown in CSM-uracil-lysine containing 2% glucose for 16 hours at 30°. Cells were collected by centrifugation, washed with sterile water, and suspended in CSM-uracil-lysine containing 2% galactose followed by growth at 30° for 18 hours. Cells were collected by centrifugation and suspended in 25 µL CSM-uracil-lysine mixed with an equal volume of 0.06% agar and visualized.

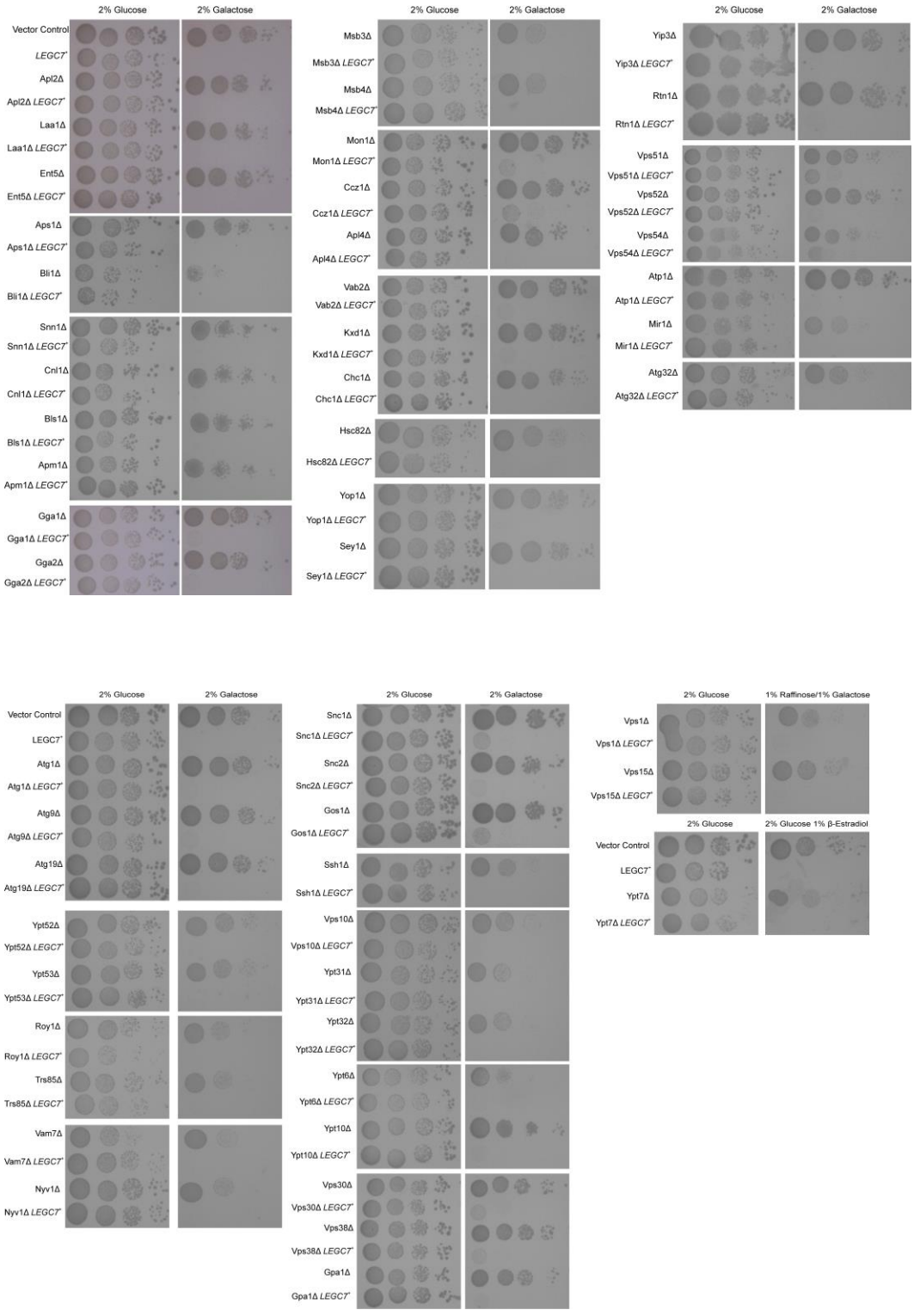

Figure 3.SI1: Representative dilution plating experiments showing degrees of reversal of LegC7 toxicity upon gene deletion.

SI Table 3.1: Full list of genetic interactions from Figure 3.3A and 3.SI1.
++++ full reversal; +++ >75% reversal; ++ >50% reversal; + > 25% reversal; 0 no reversal.
* strain showed no or weak growth under galactose induction conditions and was thus tested using β-estradiol induction.

Gene(s)	Interaction
vps11	+++
vps16	++++
vps18	+++
vps33	++++
vps39	0
vps41	+
vps3	0
vps8	++
vps21	++
ypt52	0
ypt53	0
ypt31	0
ypt32	0
ypt6	0
ypt10	0
ypt7	0*
mon1	0
ccz1	+
msb3	0
msb4	0
vps27	+
hse1	0
vps23	0
vps28	0
srn2	0
mvb12	0
vps36	0
snf8	0
vps25	0
vps20	0
snf7	0
vps24	0
did4	0
vps4	0
bro1	0
vam7	0

tlg2	+
syn8	+
vam3	0
nyv1	0
snc1	+
snc2	0
gos1	+
pep12	+++
trs85	0
roy1	0
atg1	0
atg9	0
atg19	0
ssh1	0
vps10	0
vps9	+*
vps34	++*
vps30	+
vps38	+
vps45	++
vac1	+++
vps15	0
gpa1	0
vps1	0
chc1	0
gga1	0
gga2	0
aps1	0
apm1	0
laa1	0
apl4	0
apl2	0
ent5	0
vab2	0
cnl1	0
kxd1	0
bli1	0
bls1	0
snn1	0
atp1	0
mir1	0

atg32	0
vps51	++
vps52	+
vps54	++
sey1	0
yop1	0
rtn1	0
yip3	0
hsc82	0

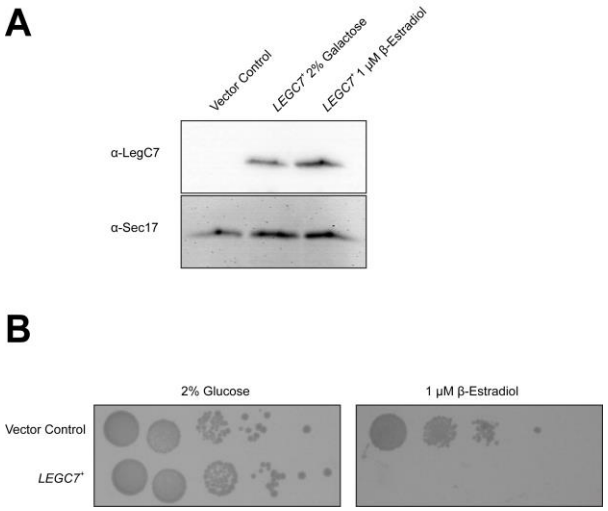

Figure 3.SI2

A. Induction of LegC7 by β-estradiol results in similar levels of protein expression. Cells were grown in CSM-uracil containing 2% glucose for 16 hours at 30°. Cells were harvested by centrifugation and washed with sterile water before being suspended in CSM-uracil containing 2% galactose or 2% glucose and 1μM β-estradiol and grown at 30° for 18 hours. Total protein was extracted as described in (von der Haar 2007). Samples were immunoblotted for LegC7.

B. Induction of LegC7 by β-estradiol results in full toxicity. Cells harboring a vector control plasmid, pVJS52, pVJS54, or pVJS62 were grown for 16 hours at 30° in CSM-uracil containing 2% glucose before being serially diluted onto CSM-uracil medai containing either 2% glucose or 2% glucose and 1μM β-estradiol and incubated at 30° for 72 hours.

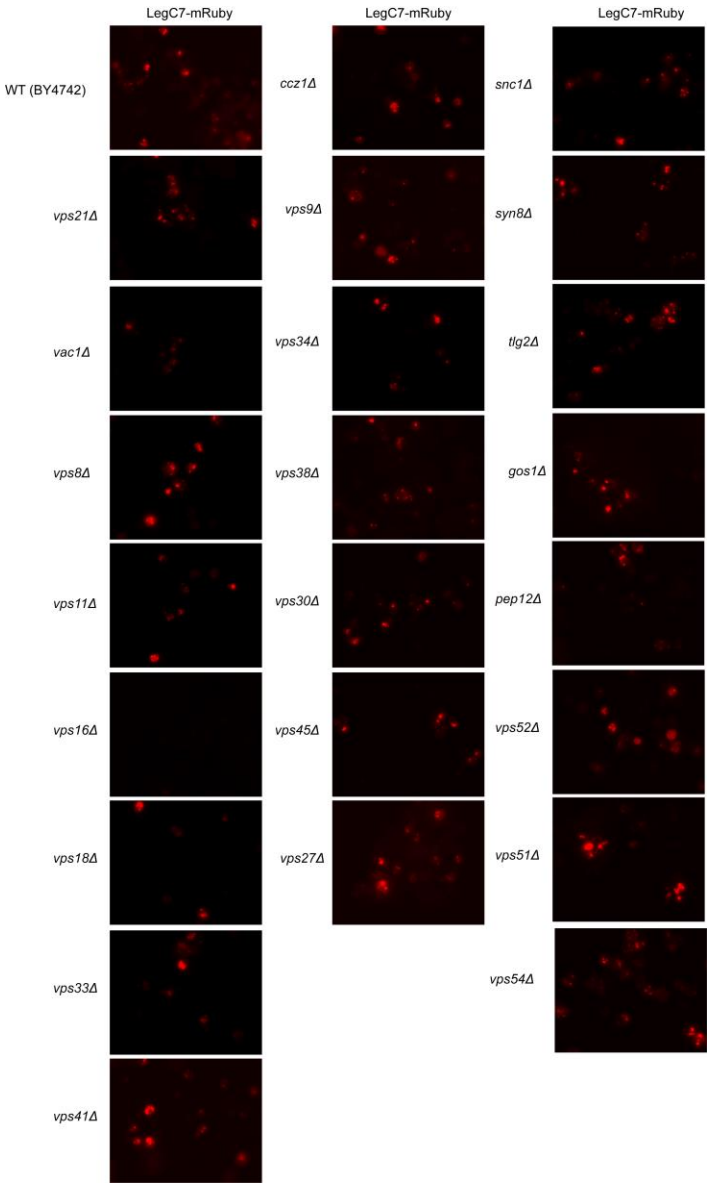

Figure 3.SI3: Genetic reversal strains do not mislocalize LegC7-mRuby.
Strains with noted deletions containing pVJS60 were grown in CSM-uracil containing 2% glucose for 16 hours at 30°. Cells were collected by centrifugation, washed with sterile water, and suspended in CSM-uracil containing 2% galactose followed by growth at 30° for 18 hours. Cells were collected by centrifugation and suspended in 25 µL CSM-uracil mixed with an equal volume of 0.06% agar and visualized.

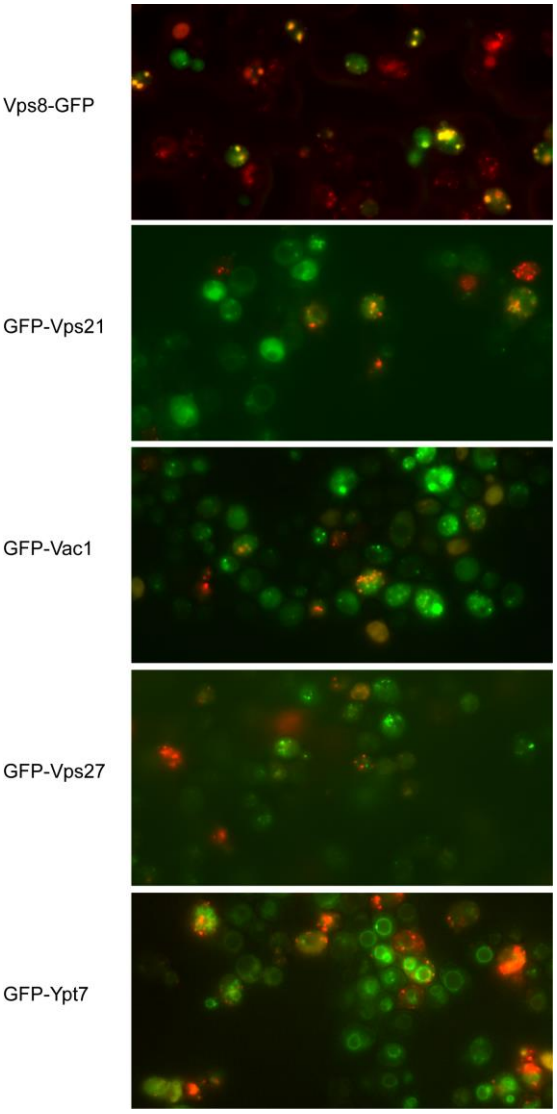

Figure 3.SI4: Representative field images from colocalization analyses as depicted in Figure 3.5.

Table 3.2 Strains, plasmids, and primers used in this study.

Plasmids		
Name	**Characteristics**	**Source**
pVJS52	pYES2/NT C, *legC7*, *ura3*	Bennett et al
pVJS53	pYES2/NT C, *legC7, lys2*	O'Brien et al 2015
pVJS54	pYES2/NT C, *legC7N242I*, *ura3*	O'Brien et al 2015
pVJS55	pYES2/NT C, *legC7N242I*, *lys2*	O'Brien et al 2015
pVJS59	GFP-LegC7 (pGO36)	O'Brien et al 2015
pVJS60	pYES2/NT C, *legC7-mRuby*, *ura3*	This Study
pVJS61	pYES2/NT C, *legC7-mRuby, lys2*	This Study
pVJS62	pYES2/NT C, *legC7Δ1-44*, *ura3*	This Study
pVJS63	pYES2/NT C, *legC7Δ1-44*, *lys2*	This Study
pVJS64	pYES2/NT C, *legC7Δ1-44-mRuby*, *ura3*	This Study
pVJS67	pYES2/NT C, *legC7N242I-mRuby*, *ura3*	This Study
pVJS68	GFP-Vps21 (pGO36)	This Study
pVJS69	GFP-Vac1 (pGO36)	This Study
pVJS70	GFP-Ypt7 (pGO36)	This Study
pACT1	pACT1-Gal4-EstrogenBD-VP16-NATMX	Veatch et al 2009
pFA6a	pFA6a-link-yomRuby-SpHis5	Sheff 2004, addgene
pGO36	pRS416, URA3	Odorizzi 1998

Strains		
Name	**Geneotype**	**Source**
BY4742	MATα *his3Δ1 leu2Δ0 lys2Δ0 ura3Δ0*	Brachmann 1998
SEY6210	MATα *his3-Δ200 trp1-Δ901 leu2-3,112 ura3-52 lys2-801 suc2-Δ9*	Robinson 1988
CUY2896	BY4733 MATα *his3Δ200 leu2Δ0 met15Δ0 trp1Δ63 ura3Δ0 vps8::HIS3-GAL1pr-GFP*	Markgraf 2009
BY4742 *vps11*Δ	BY4742 *vps11Δ::KANMX6*	GE Healthcare Dharmacon
BY4742 *vps16*Δ	BY4742 *vps16Δ::KANMX6*	GE Healthcare Dharmacon
BY4742 *vps18*Δ	BY4742 *vps18Δ::KANMX6*	GE Healthcare Dharmacon
BY4742 *vps33*Δ	BY4742 *vps33Δ::KANMX6*	GE Healthcare Dharmacon
BY4742 *vps3*Δ	BY4742 *vps3Δ::KANMX6*	GE Healthcare Dharmacon
BY4742 *vps8*Δ	BY4742 *vps8Δ::KANMX6*	GE Healthcare Dharmacon
BY4742 *vps39*Δ	BY4742 *vps39Δ::KANMX6*	GE Healthcare Dharmacon
VSY725	BY4742 *vps39Δ::KANMX6 leu2Δ0::pACT1-Gal4-EstrogenBD-VP16-NATMX*	This Study
BY4742 *vps41*Δ	BY4742 *vps41Δ::KANMX6*	GE Healthcare Dharmacon
BY4742 *vps21*Δ	BY4742 *vps21Δ::KANMX6*	GE Healthcare Dharmacon
BY4742 *ypt52*Δ	BY4742 *ypt52Δ::KANMX6*	GE Healthcare Dharmacon
BY4742 *ypt53*Δ	BY4742 *ypt53Δ::KANMX6*	GE Healthcare Dharmacon
BY4742 *ypt31*Δ	BY4742 *ypt31Δ::KANMX6*	GE Healthcare Dharmacon
BY4742 *ypt32*Δ	BY4742 *ypt32Δ::KANMX6*	GE Healthcare Dharmacon
BY4742 *ypt6*Δ	BY4742 *ypt6Δ::KANMX6*	GE Healthcare Dharmacon
BY4742 *ypt10*Δ	BY4742 *ypt10Δ::KANMX6*	GE Healthcare Dharmacon
BY4742 *ypt7*Δ	BY4742 *ypt7Δ::KANMX6*	GE Healthcare Dharmacon
VSY806	BY4742 *ypt7Δ::KANMX6 leu2Δ0::pACT1-Gal4-EstrogenBD-VP16-NATMX*	This Study
BY4742 *mon1*Δ	BY4742 *mon1Δ::KANMX6*	GE Healthcare Dharmacon
BY4742 *ccz1*Δ	BY4742 *ccz1Δ::KANMX6*	GE Healthcare Dharmacon
BY4742 *msb3Δ*	BY4742 *msb3Δ::KANMX6*	GE Healthcare Dharmacon
BY4742 *msb4Δ*	BY4742 *msb4Δ::KANMX6*	GE Healthcare Dharmacon
BY4742 *vam7Δ*	BY4742 *vam7Δ::KANMX6*	GE Healthcare Dharmacon
BY4742 *tlg2Δ*	BY4742 *tlg2Δ::KANMX6*	GE Healthcare Dharmacon
BY4742 *syn8Δ*	BY4742 *syn8Δ::KANMX6*	GE Healthcare Dharmacon
BY4742 *vam3Δ*	BY4742 *vam3Δ::KANMX6*	GE Healthcare Dharmacon

BY4742 *nyv1Δ*	BY4742 *nyv1Δ::KANMX6*	GE Healthcare Dharmacon
BY4742 *snc1Δ*	BY4742 *snc1Δ::KANMX6*	GE Healthcare Dharmacon
BY4742 *snc2Δ*	BY4742 *snc2Δ::KANMX6*	GE Healthcare Dharmacon
BY4742 *gos1Δ*	BY4742 *gos1Δ::KANMX6*	GE Healthcare Dharmacon
BY4742 *pep12Δ*	BY4742 *pep12Δ::KANMX6*	GE Healthcare Dharmacon
BY4742 *trs85Δ*	BY4742 *trs85Δ::KANMX6*	GE Healthcare Dharmacon
BY4742 *roy1Δ*	BY4742 *roy1Δ::KANMX6*	GE Healthcare Dharmacon
BY4742 *atg1Δ*	BY4742 *atg1Δ::KANMX6*	GE Healthcare Dharmacon
BY4742 *atg9Δ*	BY4742 *atg9Δ::KANMX6*	GE Healthcare Dharmacon
BY4742 *atg19Δ*	BY4742 *atg19Δ::KANMX6*	GE Healthcare Dharmacon
BY4742 *ssh1Δ*	BY4742 *ssh1Δ::KANMX6*	GE Healthcare Dharmacon
BY4742 *vps10Δ*	BY4742 *vps10Δ::KANMX6*	GE Healthcare Dharmacon
BY4742 *vps9Δ*	BY4742 *vps9Δ::KANMX6*	GE Healthcare Dharmacon
BY4742 *vps34Δ*	BY4742 *vps34Δ::KANMX6*	GE Healthcare Dharmacon
VSY701	BY4742 *vps34Δ::KANMX6 leu2Δ0::pACT1-Gal4-EstrogenBD-VP16-NATMX*	This Study
BY4742 *vps45Δ*	BY4742 *vps45Δ::KANMX6*	GE Healthcare Dharmacon
BY4742 *vac1Δ*	BY4742 *vac1Δ::KANMX6*	GE Healthcare Dharmacon
BY4742 *chc1Δ*	BY4742 *chc1Δ::KANMX6*	GE Healthcare Dharmacon
BY4742 *gga1Δ*	BY4742 *gga1Δ::KANMX6*	GE Healthcare Dharmacon
BY4742 *gga2Δ*	BY4742 *gga2Δ::KANMX6*	GE Healthcare Dharmacon
BY4742 *aps1Δ*	BY4742 *aps1Δ::KANMX6*	GE Healthcare Dharmacon
BY4742 *apm1Δ*	BY4742 *apm1Δ::KANMX6*	GE Healthcare Dharmacon
BY4742 *laa1Δ*	BY4742 *laa1Δ::KANMX6*	GE Healthcare Dharmacon
BY4742 *apl4Δ*	BY4742 *apl4Δ::KANMX6*	GE Healthcare Dharmacon
BY4742 *apl2Δ*	BY4742 *apl2Δ::KANMX6*	GE Healthcare Dharmacon
BY4742 *ent5Δ*	BY4742 *ent5Δ::KANMX6*	GE Healthcare Dharmacon
BY4742 *vab2Δ*	BY4742 *vab2Δ::KANMX6*	GE Healthcare Dharmacon
BY4742 *cnl1Δ*	BY4742 *cnl1Δ::KANMX6*	GE Healthcare Dharmacon
BY4742 *kxd1Δ*	BY4742 *kxd1Δ::KANMX6*	GE Healthcare Dharmacon
BY4742 *bli1Δ*	BY4742 *bli1Δ::KANMX6*	GE Healthcare Dharmacon
BY4742 *bls1Δ*	BY4742 *bls1Δ::KANMX6*	GE Healthcare Dharmacon
BY4742 *snn1Δ*	BY4742 *snn1Δ::KANMX6*	GE Healthcare Dharmacon
BY4742 *vps1Δ*	BY4742 *vps1Δ::KANMX6*	GE Healthcare Dharmacon
BY4742 *vps15Δ*	BY4742 *vps15Δ::KANMX6*	GE Healthcare Dharmacon
BY4742 *atp1Δ*	BY4742 *atp1Δ::KANMX6*	GE Healthcare Dharmacon
BY4742 *atp2Δ*	BY4742 *atp2Δ::KANMX6*	GE Healthcare Dharmacon
BY4742 *hsc82Δ*	BY4742 *hsc82Δ::KANMX6*	GE Healthcare Dharmacon
BY4742 *ggc1Δ*	BY4742 *ggc1Δ::KANMX6*	GE Healthcare Dharmacon
BY4742 *sey1Δ*	BY4742 *sey1Δ::KANMX6*	GE Healthcare Dharmacon
BY4742 *yop1Δ*	BY4742 *yop1Δ::KANMX6*	GE Healthcare Dharmacon

BY4742 *rtn1Δ*	BY4742 *rtn1Δ::KANMX6*	GE Healthcare Dharmacon
BY4742 *yip3Δ*	BY4742 *yip3Δ::KANMX6*	GE Healthcare Dharmacon
BY4742 *mir1Δ*	BY4742 *mir1Δ::KANMX6*	GE Healthcare Dharmacon
BY4742 *atg32Δ*	BY4742 *atg32Δ::KANMX6*	GE Healthcare Dharmacon
BY4742 *vps51Δ*	BY4742 *vps51Δ::KANMX6*	GE Healthcare Dharmacon
BY4742 *vps52Δ*	BY4742 *vps52Δ::KANMX6*	GE Healthcare Dharmacon
BY4742 *vps54Δ*	BY4742 *vps54Δ::KANMX6*	GE Healthcare Dharmacon
BY4742 *vps30Δ*	BY4742 *vps30Δ::KANMX6*	GE Healthcare Dharmacon
BY4742 *vps38Δ*	BY4742 *vps38Δ::KANMX6*	GE Healthcare Dharmacon
BY4742 *atg14*Δ	BY4742 *atg14*Δ::KANMX6	GE Healthcare Dharmacon
BY4742 *gpa1*Δ	BY4742 *gpa1*Δ::KANMX6	GE Healthcare Dharmacon
VSY550	BY4741 Vps18-TAP::His3	GE Healthcare Dharmacon
VSY1144	BY4733 MATα *his3Δ200 vps16Δ::NATMX4 leu2Δ0 met15Δ0 trp1Δ63 ura3Δ0 vps8::HIS3-GAL1pr-GFP*	This Study
VSY1107	BY4733 MATα *his3Δ200 vps33Δ::NATMX4 leu2Δ0 met15Δ0 trp1Δ63 ura3Δ0 vps8::HIS3-GAL1pr-GFP*	This Study

Primers	
Name	**Sequence**
GFPVac1_F	5'-ATGGATGAACTATACAAGTCCGGACTCAGATCTATGGATCTTGAAAATGTTTCATG-3'
GFPVac1_R	5'-GGGTGACCATGGGTTTAATTAAAGATCTCGAGCTCAAGCTTCGAATTCTGCAGTCGAC-3'
Vps21pGO_F	5'-ATGGATGAACTATACAAGTCCGGACTCAGATCTATGAACACATCAGTCACTTCC-3'
Vps21pGO_R	5'-CAAACAGTGCTTGCAGTTGTTAGAGATCTCGAGCTCAAGCTTCGAATTCTGCAGTCGAC-3'
Ypt7GFP_F	5'-ATGGATGAACTATACAAGTCCGGACTCAGATCTATGTCTTCTAGAAAAAAAAATATTTTG-3'
Ypt7GFP_R	5'-GATGGAGAAAATAATTCTTGTAGCTGTTGAAGATCTCGAGCTCAAGCTTCGAATTCTGCAGTCGAC-3'
LegC7d1-44_F	5'-GAAGAAGAATTCATGAGTCTTGCCCAAATCG-3'
YESC7RFP_F	5'-GATAGACAAACTATTGCTTTAGTCAATCAAGAGATGAACTCCTTGATTAAGGAAAATATGAGAATGAAAG-3'
YESC7RFP_R	5'-GCAAAATTTGCTGGCTTAGGTGGTGGGTAAGGCGCGGCCGCTCGAGTCTAGAGGGCCCTTCGAAG-3'
C7N242_F	5'-CTGATTTATTGGAAAAAATTCAAAAGGAATTGTCAAAA-3'
C7N242_R	5'-CTGATTTATTGGAAAAAATTCAAAAGGAATTGTCAAAA-3'

CHAPTER 4

THE *LEGIONELLA PNEUMOPHILA* EFFECTOR PROTEIN, LEGC7, REQUIRES THE GLYCOSYLATED PROTEIN CHAPERONE EMP47P FOR STABILITY AND TOXICITY IN YEAST

Kevin M. O'Brien and Vincent J. Starai. To be submitted to Molecular Biology of the Cell

ABSTRACT

Legionella pneumophila are facultative intracellular pathogens that can cause a severe pneumonia in susceptible individuals. LegC7, an effector protein secreted by *Legionella,* was previously shown to cause toxicity when expressed in yeast and expression of this effector in yeast specifically disrupts cargos that traffic through the endosomal system. In this work we immunoprecipitated LegC7 and identified Emp47p, the yeast homolog of the mammalian glycoprotein chaperone ERGIC-53, as a potential interaction partner based on mass spectrometry. Deletion of *emp47* results in the inability to detect LegC7 in cells. This lack of detection is not due to secretion of LegC7 or altered post-translational modification, detectability is restored upon deletion of *srn2* of a component of the ESCRT-1 system within the multivesicular body pathway (MVB) indicating that LegC7 is rapidly degraded upon *emp47* deletion. We also show that the interaction with Emp47p is responsible for LegC7 toxicity, as mutant derivatives of LegC7 do not require *emp47* for toxicity or stability. This work shows the important role of Emp47p in LegC7 stability suggesting that *Legionella* may manipulate the glycoprotein pathway in mammalian cells during infection. This work also demonstrates that Emp47p plays an important role in normal yeast endosomal trafficking.

INTRODUCTION

Legionella pneumophila are ubiquitous aquatic bacteria that can invade and colonize a wide variety of eukaryotic host organisms (Fliermans 1981). If contaminated water is aerosolized and inhaled by susceptible individuals a severe form of pneumonia termed Legionnaires' disease can result leading to community outbreaks and death amongst immunocompromised individuals (Fraiser 1977). In order to promote the remodeling and survival of the infected phagosome *Legionella* secretes around 300 effector proteins into the host through a type IVB secretion system termed the Dot/Icm system (Burnstein 2009, Heidtman 2009, Horwitz 1983). Host vesicle trafficking is a major target of these effectors; *Legionella* recruits ER derived vesicles to the infected phagosome membrane, *Legionella* must also disrupt endosomal maturation in order to prevent the

entry of the infected phagosome leading to eventual phagosome/lysosome fusion (Horwitz 1983, Shohdy 2005). The ER-to-Golgi trafficking pathway is highly manipulated by *Legionella,* explained in large part by the extensive targeting of the ER-to-Golgi Rab GTPase, Rab1 (Ingmundson 2007, Machner 2006). *Legionella* also targets the ER-to-Golgi trafficking pathway through manipulation of Arf1 as well as SNARE proteins pointing to this pathway as being the target of many *Legionella* effector proteins (Nagai 2002, King 2015, Arasaki 2012). The end result of these manipulations is the recruitment of ER derived vesicles to coat the infected phagosome membrane (Horwitz 1983). LegC7 is an effector protein that has previously been shown to cause toxicity when expressed in yeast (Campodonico 2005). Previously we demonstrated that LegC7 expression disrupts cargos that traffic through the yeast endosomal system and that LegC7 expression causes the disruption of key members of endosomal trafficking machinery (O'Brien 2015, O'Brien 2016).

Emp47p is suspected to act as a glycoprotein chaperone and was originally identified based on a di-lysine motif near the C-terminus and carbohydrate-binding domain (Schroder 1995). A second gene, *emp46*, was later identified that shared 45% identity with *emp47* and shown to have a similar localization pattern (Sato 2002). Overexpression of *emp46* could partially compensate for the deletion of *emp47* leading to the hypothesis that these two genes have similar, though distinct, functions. Deletion of one or both of these genes resulted in the aberrant secretion of glycoproteins (Sato 2002). It remains unclear exactly what the roles of Emp46p and Emp47p are though it appears that Emp47p may act as the receptor with Emp46p acting to select cargo or activating Emp47p. The mammalian homolog of *EMP47*, ERGIC-53, acts as a chaperone to a subset of N-linked glycoproteins (Kawasaki 2008). ERGIC-53 associates with COPII coated vesicles for anterograde transport and utilizes a dilysine motif for retrieval back to the ER (Nufer 2002, Itin 1995). A second protein, MCFD2, functions to increase the ability of ERGIC-53 to bind glycosylated proteins leading to the hypothesis that MCFD2 functions in cargo selection (Kawasaki 2008). Only a few known

cargos exist for ERGIC-53 including coagulation factors V and VIII, cathepsion C, and α1-antitrypsin (Zhang 2003, Nyfeler 2008, Vollenweider 1998).

Herein we describe that LegC7p interacts with Emp47p based on mass spectrometry and LegC7 requires *emp47* for detection in yeast cells due to the rapid degradation of LegC7 in the absence of *emp47.* We demonstrate that the interaction with *emp47* likely represents the toxic event induced by LegC7 expression as mutant versions of LegC7 that demonstrate toxicity reversals act differentially in regards to their dependence on *emp47* as well as a LegC7 mutant that gains toxicity upon deletion of *emp47.* ERGIC-53 might thus represent an important host pathway that is manipulated by *Legionella* during infection. Based on our previously described phenotypes of LegC7 expression we suspect that Emp47p may play a greater than appreciated role in normal endosome trafficking.

MATERIALS AND METHODS

Strain and Plasmid Preparation

Yeast strain BY4742 (MATα *his3Δ1 leu2Δ0 lys2Δ0 ura3Δ0*) was used for all experiments.

To create an N terminal Halo tagged LegC7 lacking the transmembrane domain we amplified LegC7 using the primers LegC7HaloF and LegC7dTMHaloF utilizing pVJS52 as a template. The resulting PCR product and pHis6-Halo were digested with Pvu1 and Not1 and ligated to create pVJS77 that was confirmed via sequencing (Georgia Genomics Facility, University of Georgia). In order to introduce the T122P mutation into LegC7 we performed site directed mutagenesis using the primer pair C7T122P_F/C7T122P_R and pVJS52 as a template. Resulting products were digested with Dpn1 and transformed into NEB 5α *E. coli,* plasmids were isolated and sequenced to ensure proper mutation. Creation of an mRuby tagged LegC7^{T122P} was accomplished by site directed mutagenesis of pVJS60 using the primers C7T122P_F/C7T122P_R. A full list of plasmids, primers, and strains can be found in Table 4.1.

To create a GST tagged Emp47p lacking the transmembrane domain *EMP47* lacking the last 33 amino acids (predicted transmembrane domain and cytosolic domains) the gene was amplified by PCR from BY4742 genomic DNA using the primer pair GSTEmp47_F and GSTEmp47_R. The resulting PCR product and the vector pET42a were digested with Kpn1 and EcoR1 and ligated to create pVJS79.

Preparation of LegC7 conjugated resin.

Rosetta 2 pLysS cells containing pVJS77 were grown in Terrific Broth (TB) to an OD of 1.5-2. Expression of LegC7ΔTM-Halo was induced by addition of 1mM IPTG, cells were then grown at 18° for 18 hours. Cells were harvested by centrifugation and cell pellets were disrupted by a single pass through the One Shot cell disruption system at 20,000 psi. Lysates were centrifuged for 20 minutes at 20,000 xg at 4° after the addition of 1mM PMSF and DNAse. The resulting supernatant was applied to 500µL Halo resin and incubated for 1 hour at 4 degrees. The resin was washed with 30mL of Halo buffer (50mM HEPES pH6.5, 300mM NaCl, and 0.5mM EDTA) before a 30 minute incubation at 22° with Halo buffer containing 1mM ATP and 10mM $MgCl_2$. The column was then washed with 30mL of Halo buffer containing 1% Triton before a final wash of 30mL Halo buffer. Antiserum raised against LegC7 was then passed over the column and the column was washed with 10mL of IgG binding buffer (100mM Sodium Phosphate, 150mM NaCl) (O'Brien 2015). Bound antibodies were then eluted using 1mL of elution buffer (0.2M Glycine pH2.0). Eluted antibodies were then conjugated to IgG resin using the Pierce Protein A IgG Plus Orientation Kit according to manufacturer's instructions. Briefly, the purified antibody solution was added to a Protein A column in batches and washed with IgG binding buffer. The bound antibodies were cross-linked using disuccinimidyl suberate (DSS) and any additional DSS sites were blocked with 0.1M ethanolamine. This resin was used for immunoprecipitations of LegC7.

Mass Spectrometry

BY4742 pACT1 cells containing VJS52 or vector control were grown at 30° for 16 hours in CSM-uracil before addition of 1μM β-estradiol. Cells were grown for an additional three hours at 30°. Cells were then collected by centrifugation, suspended in 15mL pulldown buffer (50mM PIPEs pH6.8, 300mM NaCl, 1.5 mM $MgCl_2$, 1% Triton-X100) and flash frozen in liquid nitrogen. Frozen cells were processed in a Warring blender to a fine powder, roughly 3-1minute blending cycles. Cells were allowed to thaw at room temperature and pulldown buffer was added along with 1x protease inhibitor tablet (Pierce Protease Inhibitor Mini Tablets, EDTA Free) and 1mM PMSF. Cell lysates were dounce homogenized and incubated for 90 minutes at 4°. Lysates were centrifuged at 20,000 xg for 20 minutes at 4° and the supernatant was added to 400μL LegC7 conjugated resin and incubated for 16 hours at 4°. The resin was collected by passing the material over a column and washing with 10 mL of pulldown buffer. The resin was removed from the column and washed using 3x1mL washes of pulldown buffer. The resin was suspended in 250 μL of pulldown buffer and SDS-PAGE loading buffer lacking β-mercaptoethanol was added to 1.5x. The sample was then boiled and loaded onto a pre-cast SDS-PAGE gel and run for 10 minutes. The gel was stained with Coomassie Brilliant Blue stain and the total protein band was excised and sent to the University of Georgia Mass Spectrometry Core facility for analysis.

In order to identify if LegC7 contained any N- or O-linked glycosylation, LegC7 was purified as described as above and sent to the Complex Carbohydrate Research Center at the University of Georgia. Full methods for glyocopeptide mass spectrometry analysis are contained in Figure 4.SI2.

Purification of GST-Emp47ΔTM

Purification of LegC7ΔTM was performed as described in (O'Brien 2015). GST-Emp47ΔTM was purified by transforming pVJS79 into Rosetta 2 pLysS *E. coli* cells which were grown in Terrific Broth (TB) broth to an OD of 1.5-2. Expression of GST-Emp47ΔTM was induced by addition of 1mM IPTG, cells were then grown at 18° for 18 hours. Cells were harvested by centrifugation, suspended

in GST Lysis/Binding buffer (100mM Tris pH8.0, 400mM NaCl, 1mM EDTA, 2mM EGTA) and disrupted by a single pass through the One Shot cell disruption system at 20,000 psi. Lysates were centrifuged for 20 minutes at 20,000 xg at 4° after the addition of 1mM PMSF and DNAse. The resulting supernatant was added to glutathione resin and nutated for 1 hour at 4°. The resin was collected by passing it over a column and was washed with 20 column volumes of GST Lysis/Binding buffer + 1mM DTT, 5mM ATP, and 20mM $MgCl_2$. Protein was eluted by incubation of the resin with GST Lysis/Binding buffer +1mM reduced glutathione. Protein was dialyzed into PS buffer (20mM PIPES-KOH pH6.8, 200mM Sorbitol, 150mM KCl).

RESULTS

Identification of Emp47p as a Potential Interaction Partner of LegC7

In order to identify the biochemical target(s) of LegC7 we immunoprecipitated LegC7 from yeast cells using anti-LegC7 conjugated resin and identified any interacting proteins via mass spectrometry. An equivalent pulldown from cells containing the vector control was used to account for proteins that non-specifically bound to the resin. The protein with the highest confidence score, apart from LegC7, was Emp47p (Accession number 1169517) followed by its paralog, and known binding partner, Emp46p (Accession number 74676594) (Table 4.2). We also noted that the protein with the 6th highest confidence score was Ssp120p (Accession number 730698) that was recently described as an Emp47 interaction protein (Margulis 2015). Emp47p, Emp46p, or Ssp120p were not identified in the control immunoprecipitation (Full list of identified proteins is found in Table 4.SI1). We repeated the immunoprecipitation and again detected the presence of Emp47p, Emp46p, and Ssp120p (Table 4.3, LegC7 section). Considering that Emp47p was identified in two independent experiments, the high confidence scores, and the presence of known interacting proteins, we chose to further characterize a potential interaction between LegC7 and Emp47p.

LegC7 is degraded via the ESCRT pathway upon *emp47* deletion

In order to ascertain any genetic interactions between LegC7 and the identified genes we transformed pVJS52 into *emp46*, *emp47*, or *ssp120* null yeast strains. No reversal of toxicity was noted for LegC7 upon deletion of *emp46* or *ssp120,* however, deletion of *emp47* resulted in a complete elimination of LegC7 toxicity (Figure 4.1A). We next immunoblotted for LegC7 in these backgrounds but we were unable to detect any LegC7 in *emp47* null cells (Figure 4.1B). Interestingly while deletion of *emp46* does not reverse LegC7 toxicity we noticed a reproducible decrease in the level of LegC7 that was detected in this background, roughly 20% of WT levels as quantified using densitometry (Figure 4.1B).

If LegC7 relies on Emp47p for ER export we wondered if deletion of *emp47* might lead to ER retention of LegC7 resulting in hyper-posttranslational modification, such as hyperglycosylation, leading to an inability of our antibody to detect the protein. We performed a Western blot against the N-terminal His tag and were still unable to detect LegC7 leading us to conclude that the lack of detection is not due to aberrant post-translational modification (Figure 4.1C).

In order to confirm these results we next sought to visualize LegC7-mRuby in the various deletion backgrounds to observe any localization defects that might exist. In confirmation of our inability to detect LegC7 in an *emp47* null background we were also unable to detect any LegC7-mRuby via Western blot or fluorescence microscopy in an *emp47* background (Figure 4.2A, B). In the *emp46* and *ssp120* background we detected normal levels of LegC7-mRuby and noted apparently normal localization patterns (Figure 4.2A). Interestingly when we visualized the localization pattern of GFP-LegC7, a previously characterized non-toxic derivative of LegC7, we were able to detect normal localization indicating that non-toxic varieties of LegC7 do not rely on *emp47* (Figure 4.2C).

We next sought to test for an *in vitro* interaction between LegC7ΔTM (aa 282-486) and Emp47ΔTM (aa 1-413). We did not observe an interaction between these two proteins (Figure 4.SI1). It is possible that the interaction requires one or both of the membrane domains or that the interaction depends on other proteins such as Emp46p or Ssp120p.

Given that LegC7 does not appear to be present in these cells we next sought to discern why we were unable to detect LegC7 in an *emp47* null background. Recently it was demonstrated that Ssp120p interacts with Emp47p, the authors noted a similar inability to detect Ssp120p when *emp47* was deleted (Margulis 2015). The report identified that Ssp120p was aberrantly secreted from the cell in these circumstances. In order to determine if LegC7 is also secreted upon *emp47* deletion we induced LegC7 expression in wild type or *emp47* null cells and TCA precipitated the media before immunoblotting for LegC7. We were unable to detect any band that cross-reacted with our LegC7 antisera indicating that LegC7 is likely not secreted in the same manner of Ssp120p, this is unsurprising given that LegC7 is a membrane protein while Ssp120 is a soluble protein. We surmised that if LegC7 was acting similarly to Ssp120p the equivalent sorting defect might mean that LegC7 would be sent to the plasma membrane where it could then be endocytosed and degraded via the multivesicular body pathway. In order to test this hypothesis we created a double *emp47 srn2* double knockout that would hopefully prevent or delay degradation of LegC7 by this pathway. Indeed we were able to detect LegC7 again in this background indicating that in the absence of *emp47,* LegC7 is rapidly degraded through the multivesicular body pathway, the cell's canonical membrane protein degradation pathway (Figure 4.1D). The toxicity of LegC7 is restored upon deletion of *srn2* in an *emp47* null background (Figure 4.1E).

<u>LegC7 is not a glycosylated *in vivo*</u>

As Emp47p is thought to act as a receptor of a subset of glycoproteins we sought to test the hypothesis that LegC7 is glycosylated *in vivo*. BY4742 cells expressing LegC7 from pVJS52 were collected, lysed, and subjected to digestion with either EndoH or PNGaseF; no size shift in LegC7

was detected (Figure 4.3). This argues against this potential N-linked glycosylation site being relevant to the Emp47p interaction but leaves open the possibility of less common glycosylation linkage unable to be processed by these two enzymes, or the possibility that only a small percentage of LegC7 is glycosylated *in vivo* leading to an inability to visualize the removal of the sugar moiety. In order to determine if LegC7 is glycosylated in any manner we immunoprecipitated LegC7 from yeast cells and sent this sample to the University of Georgia Complex Carbohydrate Research Center for glycopeptide mass spectrometry analysis. No evidence of either N- or O-linked glycosylation was discovered leading us to conclude that LegC7 is not glycosylated *in vivo* and ruling out the possibility that LegC7 interacts with Emp47p through a glycosylation-based interaction (Figure 4.SI3).

Carboxypeptidase S requires Emp47p for proper trafficking

We have previously observed the disruption of endosomal cargos upon expression of LegC7 (O'Brien 2015). We noted that deletion of genes involved in endosome traffic such as the early endosome Rab GTPase *vps21* and members of the CORVET complex do not cause a mislocalization effect of LegC7-mRuby leading us to conclude that either LegC7 traffics to the endosome through an unknown pathway or that LegC7 can induce endosomal trafficking defects indirectly (O'Brien 2016). Given our identification of the genetic dependence of LegC7 on *emp47* we sought to test the hypothesis that LegC7 acts indirectly to inhibit endosome fusion. If LegC7 directly inhibited some aspect of endosome fusion we would expect to see a high degree of colocalization between LegC7-RFP and disrupted cargos such as carboxypeptidase S (CPS). However, when we co-expressed GFP-CPS and LegC7-RFP we found limited overlap of the two proteins leading us to surmise that LegC7 does not inhibit endosome fusion directly (Figure 4.4A). We next wondered if deletion of *emp46, emp47,* or *ssp120* would display any defects in the trafficking of GFP-CPS, a cargo that we have previously shown to be disrupted upon LegC7 expression (O'Brien 2015). Interestingly we found that deletion of *emp46* or *ssp120* does in fact result in a defect of GFP-CPS localization (Figure 4.4B,

C). Interestingly we were only able to visualize GFP-CPS in a small percentage of *emp47* null cells, indicating that this protein, like Ssp120p and LegC7, may depend on *emp47* for normal localization in cells (Figure 4.4B, C). The GFP-CPS that was observed appeared to be disrupted in localization. Interestingly this effect is specific for GFP-CPS as we did not notice any disruption of Sna3-GFP, another cargo that is disrupted upon LegC7 expression.

EMP47 is required for LegC7 toxicity

Previously, we have defined two mutants of LegC7 (N242I, and a deletion of the first 44 amino acids [Δ1-44]) (O'Brien 2015, O'Brien 2016). While the mutants do not cause the same endosomal sorting defects and are less toxic than WT LegC7, we were unable to determine functional differences between the mutants and WT LegC7 in that the mutants show the same co-localization pattern with endosome proteins as LegC7 (O'Brien 2016). Through a random mutagenic screen as described in O'Brien 2015, we have identified a third mutant LegC7^{T122P}, a mutation immediately following the predicted transmembrane domain of LegC7. In order to determine if the mutants act differently than wild type LegC7 in the context of a possible Emp47p interaction we transformed in plasmids bearing each of the mutant versions of LegC7 into *emp47* null backgrounds and performed a dilution plating assay (Figure 4.5A). While LegC7 shows no toxicity upon *emp47* deletion, we noted that LegC7^{N242I} and LegC7$^{\Delta 1\text{-}44}$ mutant versions of LegC7 showed no difference in toxicity in WT or *emp47* null backgrounds (Figure 4.5A). Interestingly the LegC7^{T122P} mutation, which displays the strongest reversal of toxicity in WT backgrounds, became fully toxic when *emp47* was deleted. This effect is specific, as deletion of *emp46* or *ssp120* did not increase the toxicity of LegC7^{T122P}. In confirmation of these results, we next examined each mutant version of LegC7 by Western blot (Figure 4.5B). In wild type cells, we have previously noted that the LegC7 mutants are found at increased concentrations compared to WT LegC7. We were able to detect each of the mutants in the *emp47* null background and expression levels of LegC7^{N242I} and LegC7$^{\Delta 1\text{-}44}$ were indistinguishable from expression levels in WT yeast. Interestingly we noted that

the amount of detectable LegC7^{T122P} was reduced in the context of *emp47* null cells and the level of expression was concomitant with the level of WT LegC7 expression in WT yeast cells when LegC7 is toxic. These results show that the broad interaction between LegC7 and *emp47* is likely the toxic event as demonstrated by the mutant versions of LegC7 having different dependences on *emp47* compared to wild-type LegC7 as well as the gain of toxicity demonstrated by LegC7^{T122P}. Upon examination of mRuby tagged versions of these mutant strains we saw no difference in localization between WT and *emp47* null backgrounds (Figure 4.5C). All these results argue that these very different mutants in different locations of LegC7 all share a common lack of dependence on *emp47* showing the true root of these mutants' decrease in toxicity. When we performed immunoprecipitations on LegC7^{N242I} or LegC7^{T122P} we discovered that both resulted in detection of Emp47p and Ssp120p (Table 4.3, full list in Table 4.SI2). Interestingly we found Emp46p associated with LegC7^{N242I} but not LegC7^{T122P}. Ssp120p was identified in the LegC7^{T122P} immunoprecipitation albeit at a lower confidence score.

DISCUSSION

Emp47p was identified as a potential biochemical interaction protein of LegC7 based on mass spectrometry results in two independent experiments. In confirmation of this interaction we also identified two known Emp47p interaction proteins in our mass spectrometry results: Emp46p and Ssp120p. In order to validate these results we chose to perform a genetic screen to see if deletion of *emp47* had any effect on LegC7 toxicity. We discovered that deletion of *emp47* resulted in a complete elimination of LegC7 toxicity while deletion of *emp46* or *ssp120* did not have an effect on LegC7 toxicity. When we performed Western blots for LegC7 in *emp47* null backgrounds we were unable to detect LegC7. We noted that deletion of *emp46* resulted in roughly 20% of LegC7 detection compared to wild-type cells even though there was no reduction in toxicity. We were also unable to detect LegC7-mRuby in *emp47* null backgrounds either visually or by immunoblot but could detect normal localization and expression in *emp46* and *ssp120* null backgrounds. We were

unable to recapitulate a binding interaction *in vitro* between LegC7ΔTM and Emp47ΔTM leading us to hypothesize that an interaction may depend on either the binding of either Emp46p or Ssp120p or might require either the LegC7 N-terminal domain or Emp47p C-terminal domain.

We next wondered why we were unable to detect LegC7 upon deletion of *emp47*. We wondered if LegC7 was being secreted from the cell, as is the case with Ssp120p upon *emp47* deletion. We induced LegC7 expression and TCA precipitated the media but were unable to detect LegC7 in this manner, leading us to conclude that LegC7 is not secreted from the cell. One important difference between Ssp120p and LegC7 is that LegC7 is predicted to be a membrane protein, which would prevent typical secretion from the cell. If deletion of *emp47* results in the secretion of luminal proteins, we reasoned that the equivalent event for membrane proteins would involve traffic of the protein to the plasma membrane, followed by ESCRT-mediated degradation. When we deleted *srn2*, a component of the ESCRT-I complex, in the context of an *emp47* null strain we restored the ability to detect LegC7. This indicates that LegC7 is degraded via the ESCRT pathway upon deletion of *emp47.* The ESCRT pathway represents the main degradative pathway for membrane proteins in the cell. Based on the phenotypic similarity between LegC7 and Ssp120p we suspect that LegC7 is directed to the plasma membrane in *emp47* null cells before degradation through the MVB pathway. Interestingly in the *emp47 srn2* double knockout LegC7 was fully toxic indicating that perhaps localization is not crucial for LegC7 toxicity.

Given that LegC7 depends on the presence of a glycosylated cargo receptor for stability in cells, we next tested to see if LegC7 was glycosylated *in vivo*. Based on *in silico* analysis LegC7 only contains one canonical N-linked glycosylation site in the form of NXT/S found at the forth amino acid. Previously we have characterized a deletion mutant lacking the first 44 amino acids of LegC7 and found only a minor reduction in toxicity (O'Brien 2016). The minor reduction of toxicity of this construct combined with the complete dependence of LegC7 on *emp47* for cellular stability argues that this site is not relevant for this interaction. Though *in silico* predictions paired with previous

toxicity observations make N-glycosylation unlikely we treated lysates with EndoH and PNGase F but observed no evidence that LegC7 was modified in any of these conditions. We next performed glycopeptide mass spectrometry analysis on LegC7 that had been immunoprecipitated from yeast cells but did not detect any evidence for glycosylation. Taken together these data argue against LegC7 containing N- or O-linked glycosylation ruling out the possibility that the Emp47p-LegC7 interaction depends on a glycosylation event. It remains possible that only a small percentage of LegC7 is glycosylated *in vivo* rendering us unable to detect this modification in either of our experiments. However, due to the drastic genetic dependence of LegC7 on *emp47* we propose that this possibility is unlikely.

LegC7 expression in yeast disrupts the localization of cargos that traffic though the endosome system while leaving cargos that traffic in non-endosome dependent pathways unaffected (O'Brien 2015). We also noted strong reductions in LegC7 toxicity when early endosome trafficking genes were deleted (O'Brien 2016). Interestingly we noted that deletions in early endosome trafficking machinery did not alter the localization pattern of LegC7-mRuby, leading us to hypothesize that either LegC7 acts indirectly to inhibit endosome fusion, or traffics to the endosome in a non-canonical fashion. Given that LegC7-mRuby demonstrates limited colocalization with GFP-CPS we propose that LegC7 does not directly inhibit endosome fusion. An indirect effect on endosome trafficking would also fit with our newly discovered dependence of LegC7 on *emp47*. LegC7 may act while in the ER resulting in downstream endosomal trafficking defects. The idea that LegC7 functions in the ER also fits with a previous observation that LegC7 localizes to the ER when expressed in mammalian cells (de Felipe 2008). We noted that deletion of *emp46, emp47,* or *ssp120* results in mislocalization of GFP-CPS. We cannot say if this disruption is due to the inability of GFP-CPS to leave the ER or if the disruption occurs later in the secretory pathway. In either case however, this is the first evidence to our knowledge, that Emp47p functions

in the localization of a normally endosomal trafficked protein. This indicates that either CPS, or an adaptor required for the trafficking of CPS, is likely an Emp47p cargo protein.

We next examined mutant versions of LegC7 and their dependence on Emp47p. Two of our characterized mutants, LegC7^{N242I} and LegC7$^{\Delta 1\text{-}44}$, showed no differences in toxicity between wild type and *emp47* null cells. These results demonstrate that the mutant versions of LegC7, which are less toxic, do not show the same dependence on *emp47.* LegC7^{T122P}, which in wild type cells provided nearly a full toxicity reversal; became fully toxic in *emp47* null cells. The Western blot results further confirmed these results as both LegC7^{N242I} and LegC7$^{\Delta 1\text{-}44}$ displayed equal expression levels between wild type and *emp47* null cells. In *emp47* null strains, the amount of LegC7^{T122P} decreased to match the expression levels of wild-type LegC7 in wild-type backgrounds, consistent with toxicity. We were able to detect each of the mRuby tagged mutants in the *emp47* null background as well as the non-toxic GFP-LegC7. These data taken together indicate that LegC7 toxicity depends on *emp47*. When we performed immunoprecipitations on LegC7^{N242I} and LegC7^{T122P} we noted that both proteins showed an interaction with Emp47p. The results for LegC7^{N242I} were very similar to WT LegC7. Interestingly Emp46p was not identified in the LegC7^{T122P} immunoprecipitation indicating that LegC7 might be modulating activity or interaction with these proteins to exert its effect.

Importantly our previous work defined two important phenotypes of LegC7 expression, namely toxicity and endosome disruption. Previously we have demonstrated identical colocalization patterns between LegC7-mRuby, LegC7^{N242I}-mRuby, and LegC7$^{\Delta 1\text{-}44}$-mRuby, constructs which show differences in overall toxicity, which suggested that endosomal disruption was not the toxic event. Here we have demonstrated that it is the dependence on *emp47* that differentiates LegC7 from the mutant derivatives. These data, coupled with the gain of toxic function of LegC7^{T122P}, demonstrates that it is the *emp47* related event that is important for toxicity.

Disruption of the localization of GFP-CPS upon deletion of *emp46, emp47,* and *ssp120* demonstrates that these genes play an important role in proper endosome trafficking.

Legionella is well established to target ER trafficking such as manipulation of the ER to Golgi Rab GTPase Rab1 by effectors SidM, SidD, and AnkX among others (Machner 2006, Tan 2011, Campanacci 2013). *Legionella* has never been shown to directly manipulate host glyocoproteins but targeting or manipulating ERGIC-53 through an ER based mechanism would be consistent with the pattern of *Legionella* infections. As such, the manipulation of ERGIC-53 may prove to be an important pathway that is targeted by *Legionella* during infection. This work may also help to define the cargo proteins and functions of Emp47p or ERGIC-53 in eukaryotic cell biology.

ACKNOWLEDGEMENTS

This research was supported in part by the National Institutes of Health grants 1S10OD018530 and P41GM10349010 to the Complex Carbohydrate Research Center.

Table 4.1: Plasmids, strains, and primers used in this study

Plasmids

Name	Characteristics	Source
pVJS52	pYES2/NT C, *legC7*, *ura3*	Bennett et al
pVJS54	pYES2/NT C, *legC7N242I*, *ura3*	O'Brien et al 2015
pVJS60	pYES2/NT C, *legC7-mRuby*, *ura3*	O'Brien et al 2016
pVJS64	pYES2/NT C, *legC7Δ1-44-mRuby*, *ura3*	O'Brien et al 2016
pVJS67	pYES2/NT C, *legC7N242I-mRuby*, *ura3*	O'Brien et al 2016
pVJS61	pYES2/NT C, *legC7-mRuby, lys2*	O'Brien 2016
pVJS62	pYES2/NT C, *legC7Δ1-44*, *ura3*	O'Brien et al 2016
pAGL	pACT1-Gal4-EstrogenBD-VP16-NATMX	Veatch et al 2009
pCDNA4/V5-HisA	pcDNA4, PCMV, Zeocin	ThermoFisher Scientific
pVJS76	pCDNA4/V5-HisA, *legc7*	This Study
pVJS77	pHis6-HaloTag Halo-LegC7ΔTM	This Study
pVJS78	pYES2/NT C, *legC7T122P*, *ura3*	This Study
pVJS78	pYES2/NT C, *legC7T122P-mRuby*, *ura3*	This Study
YCPlac33-sGFP-VRG4	YCPlac33, *URA3,* sGFP-Vrg4	Losev 2006
pPS1622	pRS316, *sec63-sGFP, ura3*	Prinz 2000
pVJS79	pET42a, *emp47ΔTM*	This study
pVJS80	2μ, *URA3,* LegC7-SUC2-HIS4c	This study
pGO45	pRS416, GFP-CPS	Odorizzi 1998

Strains

Name	Geneotype	Source
BY4742	MATα *his3Δ1 leu2Δ0 lys2Δ0 ura3Δ0*	Brachmann 1998
BY4742 pACT1	MATα *his3Δ1 lys2Δ0 ura3Δ0 leu2Δ*0::pACT1-Gal4-EstrogenBD-VP16-NATMX	This Study
BY4742 e*mp46*Δ	BY4742 *emp46Δ::KANMX6*	GE Healthcare Dharmacon
BY4742 e*mp47*Δ	BY4742 *emp47Δ::KANMX6*	GE Healthcare Dharmacon
BY4742 s*sp120*Δ	BY4742 *ssp120Δ::KANMX6*	GE Healthcare Dharmacon
BY4742 *ire1*Δ	BY4742 *ire1Δ::KANMX6*	GE Healthcare Dharmacon
VSY1288	BY4742 *emp47Δ::KANMX6 srn2Δ::NATMX4*	This Study

Plasmids

Name	Sequence
C7T122P_F	5'-CACATTGGCGTCTTATTAGTAATAGGGGGAGTTCCAGGACTAACCTATACCGCAG-3'
C7T122P_R	5'-CACATTGGCGTCTTATTAGTAATAGGGGGAGTTCCAGGACTAACCTATACCGCAG-3'
LegC7HaloR	5'-CTTTAGTCAATTAAGAGAAGGCGGCCGCGGAGGA-3'
LegC7dTMHaloF	5'-GGAGGACGATCGCCAAACGATTAAAAGAAGG-3'
GSTEmp47_F	5'-GGAGGAGGTACCATGATGATGTTAATTACTATGAAAAGTAC-3'
GSTEmp47_R	5'-GGTCCTCAGGTCGACGAAATTGCCAGAAAATAAGAATTCGGAGGA-3'
LegC7_477_F	5'-TGACAGGTGGTTTGTTACGCATGCAAGCTTGATATCGAAATGGCTACTAATGAAACAGAG-3'
LegC7_477_R	5'-CAAACTATTGCTTTAGTCAATCAACCTAAGAACTCAAGTGGTTACACCTCTAGACCATC-3'
Srn2pr29	5'GGCGTTCTGAAAAGAAGGAAATATGCACATACGATTTAGGTGACAC-3'
Srn2pr32	5'-CTCCCTATAGTGAGTCGTATTTAGTTCAGCAGCTACCGCCATTATC-3'

Table 4.2 :List of the top 6 proteins with the highest confidence scores identified by mass spectrometry from the LegC7 immunoprecipitation.

ORF	**Accession Number**	**Score**	**Number of Peptides**
Emp47	1169517	3050.32	31
Emp46	74676594	1277.74	21
Sro9	93204604	923.29	9
Atp2	84028178	821.02	9
Hsc82	1708315	737.75	8
Ssp120	730698	481.79	7

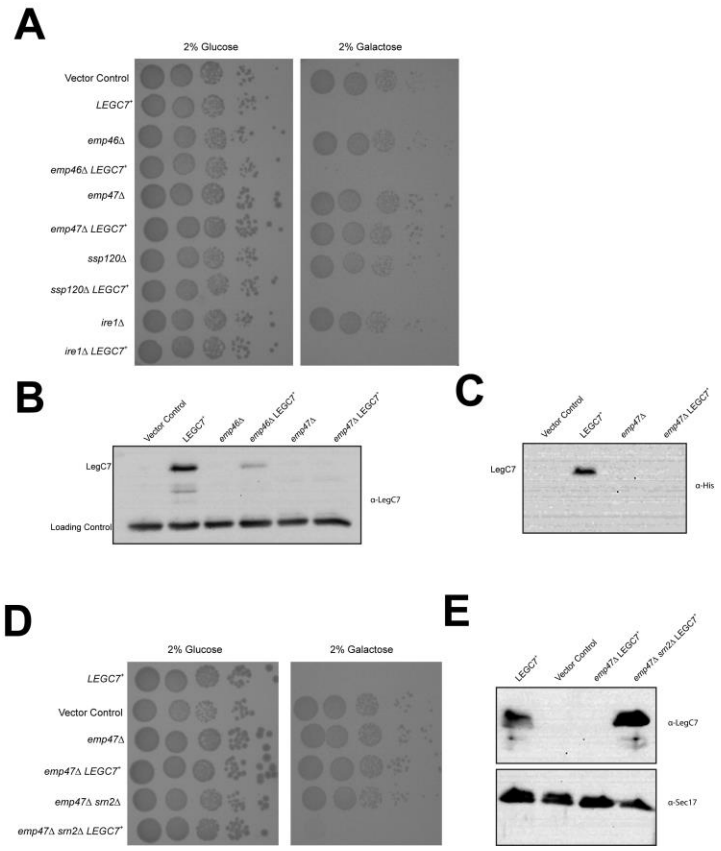

Figure 4.1: LegC7 is degraded upon *emp47* deletion
A. BY4742 cells or noted deletions containing either pVJS52 or pYES2/NTc were grown in CSM-uracil media containing 2% glucose for 16 hours at 30°. Cells were grown for 16 hours at 30° in CSM-uracil containing 2% glucose before being serially diluted onto CSM-uracil media containing either 2% glucose or 2% galactose and incubated at 30° for 72 hours.
B. BY4742 cells or noted gene deletions containing either pVJS52 or pYES2/NTc were grown in CSM-uracil containing 2% glucose for 16 hours at 30°. Cells were harvested by centrifugation and washed with sterile water before being suspended in CSM-uracil containing 2% galactose and growth at 30° for 18 hours. Total protein was extracted as described in (von der Haar 2007). Samples were immunoblotted for LegC7 (1:1000 Rabbit).
C. BY4742 cells or BY4742 *emp47Δ* containing either pVJS52 or pYES2/NTc were grown in CSM-uracil containing 2% glucose for 16 hours at 30°. Cells were harvested by centrifugation and washed with sterile water before being suspended in CSM-uracil containing 2% galactose and growth at 30° for 18 hours. Total protein was extracted as described in (von der Haar 2007). Samples were immunoblotted for 6xHis (1:1000 Mouse).
D. BY4742 cells or noted gene deletions containing either pVJS52 or pYES2/NTc were grown in CSM-uracil containing 2% glucose for 16 hours at 30°. Cells were harvested by centrifugation and washed with sterile water before being suspended in CSM-uracil containing 2% galactose and growth at 30° for 18 hours. Total protein was extracted as described in (von der Haar 2007). Samples were immunoblotted for LegC7 (1:1000 Rabbit) or Sec17 (1:1000 Rabbit).
E. BY4742 cells or noted deletions containing either pVJS52 or pYES2/NTc were grown in CSM-uracil media containing 2% glucose for 16 hours at 30°. Cells were grown for 16 hours at 30° in CSM-uracil containing 2% glucose before being serially diluted onto CSM-uracil media containing either 2% glucose or 2% galactose and incubated at 30° for 72 hours.

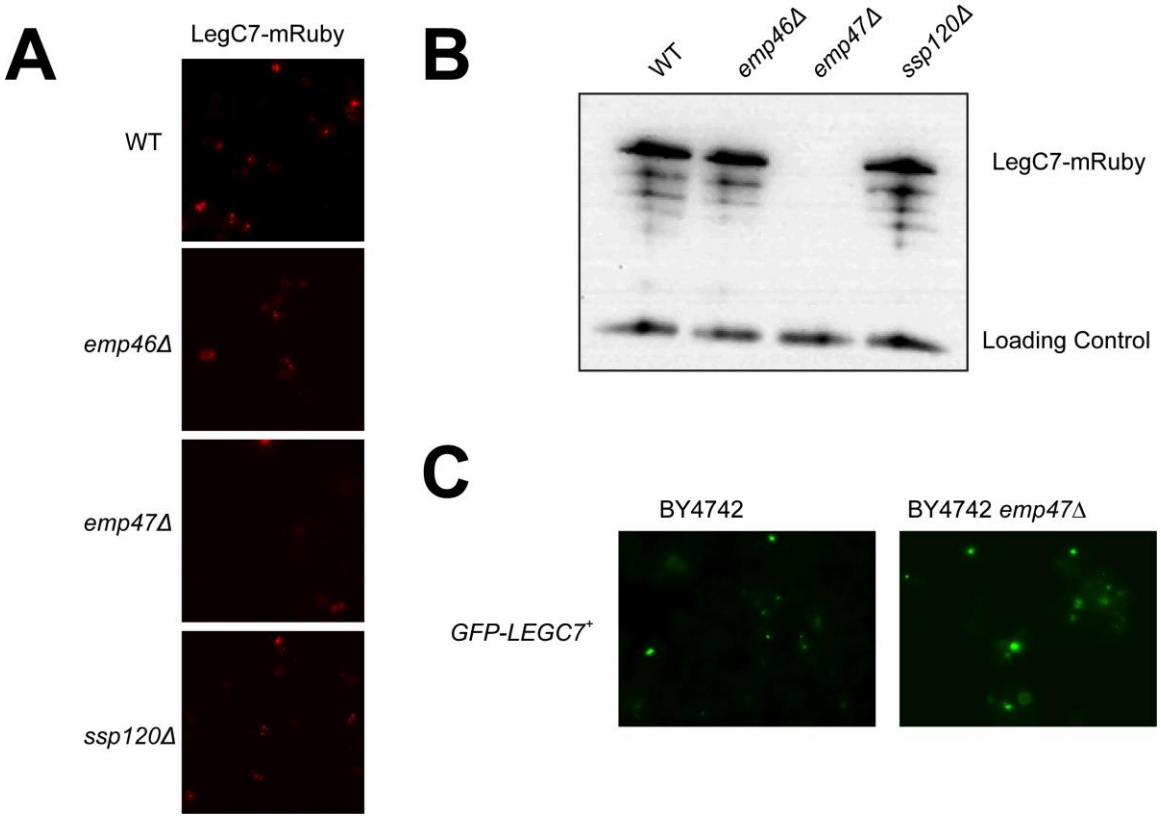

Figure 4.2: LegC7-mRuby cannot be detected upon *emp47* deletion
A. BY4742 cells or noted gene deletions containing pVJS60 were grown in CSM-uracil containing 2% glucose for 16 hours at 30°. Cells were harvested by centrifugation and washed with sterile water before being suspended in CSM-uracil containing 2% galactose and growth at 30° for 18 hours. Cells were collected by centrifugation and suspended in 25 µL CSM-uracil mixed with an equal volume of 0.06% agar and visualized.
B. BY4742 cells or noted gene deletions containing pVJS60 were grown in CSM-uracil containing 2% glucose for 16 hours at 30°. Cells were harvested by centrifugation and washed with sterile water before being suspended in CSM-uracil containing 2% galactose and growth at 30° for 18 hours. Total protein was extracted as described in (von der Haar 2007). Samples were immunoblotted for LegC7 (1:1000 Rabbit).
C. BY4742 cells or *emp47* null cells containing pVJS59 were grown in CSM-uracil containing 2% glucose for 16 hours at 30°. Cells were collected by centrifugation and suspended in 25 µL CSM-uracil mixed with an equal volume of 0.06% agar and visualized.

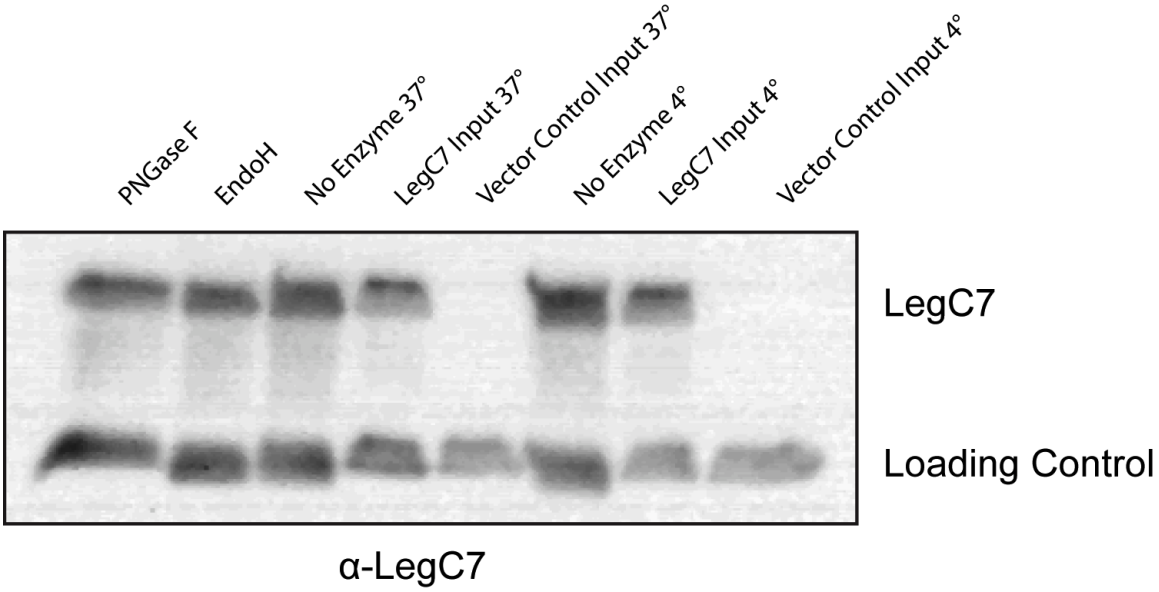

Figure 4.3: LegC7 is not glycosylated *in vivo.*
A. BY4742 cells containing pVJS52 were grown in CSM-uracil containing 2% glucose for 16 hours at 30°. Cells were harvested by centrifugation and washed with sterile water before being suspended in CSM-uracil containing 2% galactose and growth at 30° for 18 hours. 1 optical density (OD) unit of cells were collected and total protein was extracted using the quantitative protein extraction method described in (Von der Haar 2007) for input controls. For the deglycosylation assay 1OD unit of cells were collected and suspended in 100 µL denaturation buffer (0.1M NaOH, 0.05M EDTA, 0.5% SDS, and 40mM DTT). Cells were incubated at 100° for 10 minutes. 1.5µL of 4M acetic acid was then added and the tubes were vortexed for 30 seconds before a second incubation at 100° for 10minutes. The samples were split and incubated for 4 hours at 37° with the either EndoH and G5 buffer (0.05 Sodium citrate) or PNGase F and G7 buffer (50mM Sodium Phosphate pH 7.5). Samples were then analyzed via SDS-PAGE and immunodetected for LegC7 (1:1000 Rabbit).

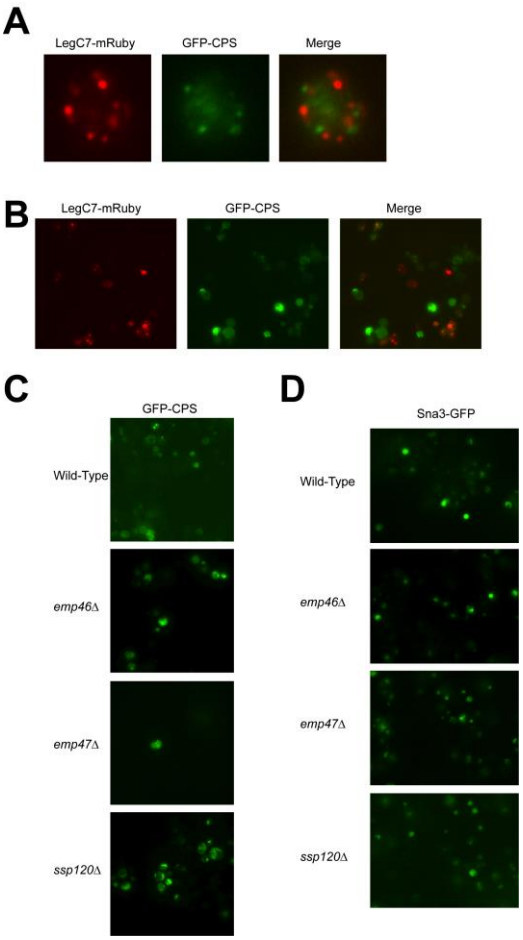

Figure 4.4: LegC7 Disrupts Endosomal Trafficking Indirectly
A and B Cells containing pVJS61 and pGO45 were grown in CSM-uracil-lysine media containing 2% glucose for 16 hours at 30°. Cells were collected by centrifugation and suspended in CSM-uracil-lysine containing 2% galactose for 18 hours at 30°. Cells were collected by centrifugation and suspended in 25 µL CSM-uracil-lysine mixed with an equal volume of 0.06% agar and visualized. A. Representative single cell image. B. Field image of colocalization.
C. BY4742 cells or noted deletion strains containing pGO45 were grown in CSM-uracil containing 2% glucose for 16 hours at 30°. Cells were harvested by centrifugation and washed with sterile water before being suspended in CSM-uracil containing 2% galactose and growth at 30° for 18 hours. Cells were collected by centrifugation and suspended in 25 µL CSM-uracil mixed with an equal volume of 0.06% agar and visualized.
D. BY4742 cells or noted deletion strains containing pMM134 were grown in CSM-uracil containing 2% glucose for 16 hours at 30°. Cells were harvested by centrifugation and washed with sterile water before being suspended in CSM-uracil containing 2% galactose and growth at 30° for 18 hours. Cells were collected by centrifugation and suspended in 25 µL CSM-uracil mixed with an equal volume of 0.06% agar and visualized.

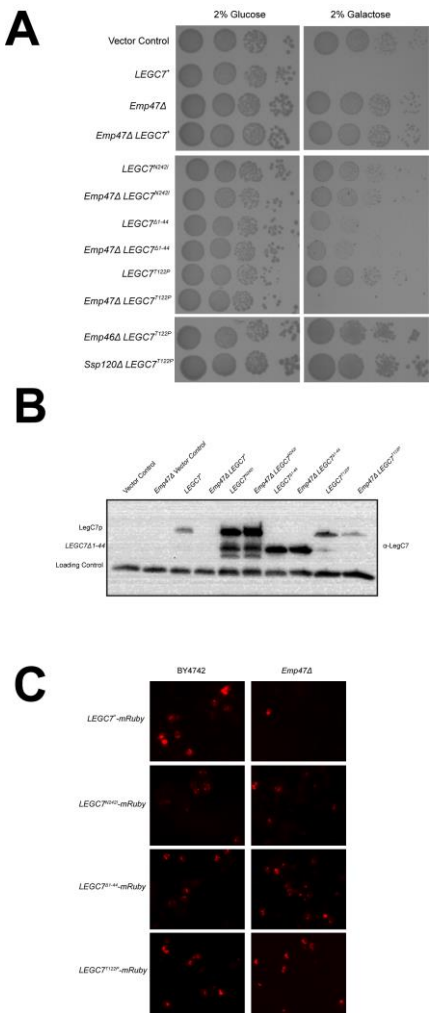

Figure 4.5: LegC7 Mutants Respond Differentially to Deletion of *emp47*
A. BY4742 cells or noted deletions containing either pVJS52, pVJS54, pVJS62, pVJS77 or pYES2/NTc were grown in CSM-uracil media containing 2% glucose for 16 hours at 30°. Cells were grown for 16 hours at 30° in CSM-uracil containing 2% glucose before being serially diluted onto CSM-uracil media containing either 2% glucose or 2% galactose and incubated at 30° for 72 hours.
B. BY4742 cells or noted gene deletions containing either pVJS52, pVJS54, pVJS62, pVJS77 or pYES2/NTc were grown in CSM-uracil containing 2% glucose for 16 hours at 30°. Cells were harvested by centrifugation and washed with sterile water before being suspended in CSM-uracil containing 2% galactose and growth at 30° for 18 hours. Total protein was extracted as described in (von der Haar 2007). Samples were immunoblotted for LegC7 (1:1000 Rabbit).
C. BY4742 cells or BY4742 *emp47Δ* containing either pVJS52, pVJS54, pVJS62, pVJS77 or pYES2/NTc were grown in CSM-uracil containing 2% glucose for 16 hours at 30°. Cells were harvested by centrifugation and washed with sterile water before being suspended in CSM-uracil containing 2% galactose and growth at 30° for 18 hours. Cells were collected by centrifugation and suspended in 25 µL CSM-uracil mixed with an equal volume of 0.06% agar and visualized.

Table 4.3: List of the proteins with the highest confidence scores identified by mass spectrometry from the LegC7, LegC7^{N242I}, and LegC7^{T122P} immunoprecipitations.

LegC7

ORF	Accession Number	Score	Number of Peptides
Emp47	1169517	1871.74	22
Kar2	121575	581.57	9
Ssp120	730698	554.04	5
Emp46	74676594	537.61	11
Bmh1	728968	274	3
Pma1	1168544	266.63	3

LegC7^{N242I}

ORF	Accession Number	Score	Number of Peptides
Emp47	1169517	2009.91	23
Emp46	74676594	625.42	6
Ssp120	730698	466.74	9
Bmh1	728968	461.24	2
Met6	730018	271.75	4
Ahp1	1709682	259.72	4

LegC7^{T122P}

ORF	Accession Number	Score	Number of Peptides
Ssa4	123634	1789.34	16
Emp47	1169517	1440.95	20
Hsp60	123579	887.43	7
Vma2	586211	707.96	9
Met6	730018	698.11	12
Kar2	121575	571.6	1
Hsp104	1346246	434.06	6
Atp1	341940649	418.67	9
Tma19	549064	410.91	7
Bmh1	728968	340.98	6
Vma1	137464	316.41	9
Ahp1	1709682	307.36	5
Sro9	93204604	297.95	3
Ipp1	158515407	261.01	5
Ssp120	730698	244.93	5

A

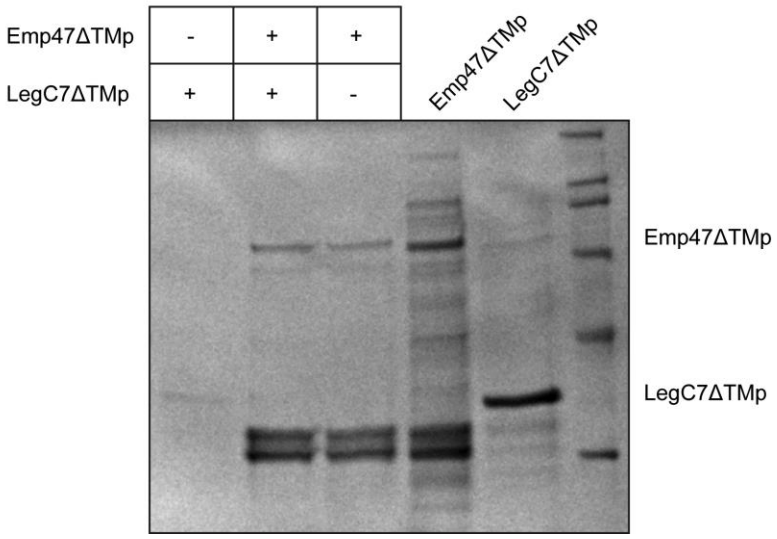

Figure 4.SI1: LegC7ΔTM does not interact with Emp47ΔTM**.**
A. LegC7ΔTM and Emp47ΔTM or each protein individually was incubated at 1.9 μM in pulldown buffer (20mM PIPES pH 6.8, 200mM Sorbitol, 300mM NaCl) with 25 μL glutathione resin. Samples were mixed end over end for 1 hour at 4°. Resin was collected by centrifugation and washed 6 times with 200 μL of pulldown buffer. Samples were then suspended in 100μL pulldown buffer and incubated for 10 minutes at 100°. Samples were analyzed via SDS-PAGE gel that was stained with Coomassie Brilliant Blue for visualization.

Supplemental Table 4.1 : Full list of identified interacting proteins from LegC7 or control immunoprecipitation.

Vector Control:

Accession	Description	Score	# Peptides
417149	RecName: Full=Heat shock protein SSA1; AltName: Full=Heat shock protein YG100	2120.09	3
123624	RecName: Full=Heat shock protein SSA2	2113.22	3
1169787	RecName: Full=Glyceraldehyde-3-phosphate dehydrogenase 3; Short=GAPDH 3	1769.27	6
125609	RecName: Full=Pyruvate kinase 1; Short=PK 1; AltName: Full=cell division cycle protein 19	1383.99	20
120645	RecName: Full=Glyceraldehyde-3-phosphate dehydrogenase 2; Short=GAPDH 2	1144.03	2
1169786	RecName: Full=Glyceraldehyde-3-phosphate dehydrogenase 1; Short=GAPDH 1	902.16	4
364509011	inclusion membrane protein A [Legionella pneumophila subsp. pneumophila ATCC 43290]	790.56	13
129930	RecName: Full=Phosphoglycerate kinase	627.01	9
119161	RecName: Full=Elongation factor 1-alpha; Short=EF-1-alpha; AltName: Full=Eukaryotic elongation factor 1A; Short=eEF1A; AltName: Full=Translation elongation factor 1A	472.76	7
548880	RecName: Full=Uncharacterized protein MRP8	456.71	8
119337	RecName: Full=Enolase 2; AltName: Full=2-phospho-D-glycerate hydro-lyase 2; AltName: Full=2-phosphoglycerate dehydratase 2	386.53	5
137083	RecName: Full=Transcriptional regulator URE2; AltName: Full=Disulfide reductase; AltName: Full=Glutathione peroxidase	381.15	5
1709086	RecName: Full=Mannose-1-phosphate guanyltransferase; AltName: Full=ATP-mannose-1-phosphate guanylyltransferase; AltName: Full=GDP-mannose pyrophosphorylase; AltName: Full=NDP-hexose pyrophosphorylase	306.25	5

391359302	RecName: Full=Heat shock protein SSC1, mitochondrial; AltName: Full=Endonuclease SceI 75 kDa subunit; Short=Endo.SceI 75 kDa subunit; AltName: Full=mtHSP70; Flags: Precursor	295.68	4
586211	RecName: Full=V-type proton ATPase subunit B; Short=V-ATPase subunit B; AltName: Full=V-ATPase 57 kDa subunit; AltName: Full=Vacuolar proton pump subunit B	268.27	5
1730231	RecName: Full=Guanine nucleotide-binding protein subunit beta-like protein; AltName: Full=Receptor for activated C kinase; AltName: Full=Receptor of activated protein kinase C 1; Short=RACK1	256.59	3
136373	RecName: Full=Tryptophan synthase	213.94	3
548534	RecName: Full=Phosphoglycerate mutase 1; Short=PGAM 1; AltName: Full=BPG-dependent PGAM 1; AltName: Full=MPGM 1; AltName: Full=Phosphoglyceromutase 1	174.33	3
30923172	RecName: Full=Pyruvate decarboxylase isozyme 1	171.03	4
137464	RecName: Full=V-type proton ATPase catalytic subunit A; Short=V-ATPase subunit A; AltName: Full=Vacuolar proton pump subunit A; Contains: RecName: Full=Endonuclease PI-SceI; AltName: Full=Sce VMA intein; AltName: Full=VMA1-derived endonuclease; Short=VDE	157.20	2
1350714	RecName: Full=60S ribosomal protein L4-B; AltName: Full=L2; AltName: Full=RP2; AltName: Full=YL2	155.14	3
113626	RecName: Full=Fructose-bisphosphate aldolase; Short=FBP aldolase; Short=FBPA; AltName: Full=Fructose-1,6-bisphosphate aldolase	136.78	2
2500359	RecName: Full=60S ribosomal protein L13-A	132.59	1
122107	RecName: Full=Histone H4	115.45	2
364508367	aconitate hydratase [Legionella pneumophila subsp. pneumophila ATCC 43290]	114.79	1
2497124	RecName: Full=Eisosome protein 1	113.49	2
10383762	prion domain-containing protein RNQ1 [Saccharomyces cerevisiae	111.62	1

	S288c]		
395129625	succinyl-CoA synthetase, beta subunit [Legionella pneumophila subsp. pneumophila]	111.48	1
308153683	RecName: Full=Alcohol dehydrogenase 1; AltName: Full=Alcohol dehydrogenase I; AltName: Full=YADH-1	103.49	1
364509682	H+-transporting two-sector ATPase, ATP synthase F1 subunit beta [Legionella pneumophila subsp. pneumophila ATCC 43290]	98.62	2
38372623	RecName: Full=Actin	84.94	3
364509684	F0F1-ATPase subunit alpha, ATP synthase alpha chain [Legionella pneumophila subsp. pneumophila ATCC 43290]	84.73	1
134393	RecName: Full=Rab guanine nucleotide exchange factor SEC2; AltName: Full=GDP-GTP exchange factor SEC2	78.27	2
129060	RecName: Full=Dihydrolipoyllysine-residue acetyltransferase component of pyruvate dehydrogenase complex, mitochondrial; AltName: Full=Dihydrolipoamide acetyltransferase component of pyruvate dehydrogenase complex; AltName: Full=Pyruvate dehydrogenase complex component E2; Short=PDC-E2; Short=PDCE2; Flags: Precursor	77.91	2
469493155	DNA-directed RNA polymerase beta' subunit [Legionella pneumophila subsp. pneumophila LPE509]	77.36	1
302595956	RecName: Full=Polyubiquitin; Contains: RecName: Full=Ubiquitin; Flags: Precursor	76.14	3
395130537	pyruvate dehydrogenase, decarboxylase component E1, thiamin-binding [Legionella pneumophila subsp. pneumophila]	74.33	1
1723685	RecName: Full=Sphingolipid long chain base-responsive protein PIL1	61.31	1
347595828	RecName: Full=Protein URA2; Includes: RecName: Full=Glutamine-dependent carbamoyl-phosphate synthase; Includes: RecName: Full=Aspartate carbamoyltransferase	57.68	1

364507152	50S ribosomal protein L19 [Legionella pneumophila subsp. pneumophila ATCC 43290]	47.08	1
119857	RecName: Full=rRNA 2'-O-methyltransferase fibrillarin; AltName: Full=Histone-glutamine methyltransferase; AltName: Full=U3 small nucleolar RNA-associated protein NOP1; Short=Nucleolar protein 1; Short=U3 snoRNA-associated protein NOP1	46.06	1
469492647	Isocitrate dehydrogenase [NADP] [Legionella pneumophila subsp. pneumophila LPE509]	45.88	1
364507081	translation elongation factor G (EF-G) [Legionella pneumophila subsp. pneumophila ATCC 43290]	44.94	1
1707995	RecName: Full=Serine hydroxymethyltransferase, cytosolic; Short=SHMT; AltName: Full=Glycine hydroxymethyltransferase; AltName: Full=Serine methylase	43.92	1
364507291	dihydrolipoamide succinyltransferase [Legionella pneumophila subsp. pneumophila ATCC 43290]	42.61	1
338819293	RecName: Full=60S ribosomal protein L2-B; AltName: Full=L5; AltName: Full=RP8; AltName: Full=YL6	41.27	2

LegC7

Accession	Description	Score	# Peptides
364509011	inclusion membrane protein A [Legionella pneumophila subsp. pneumophila ATCC 43290]	9684.45	46
1169517	RecName: Full=Protein EMP47; AltName: Full=47 kDa endomembrane protein; AltName: Full=Endosomal P44 protein; Flags: Precursor	3050.32	31
1169787	RecName: Full=Glyceraldehyde-3-phosphate dehydrogenase 3; Short=GAPDH 3	2758.32	7
120645	RecName: Full=Glyceraldehyde-3-phosphate dehydrogenase 2; Short=GAPDH 2	2429.94	3
417149	RecName: Full=Heat shock protein SSA1; AltName: Full=Heat shock protein YG100	2144.35	4
123624	RecName: Full=Heat shock protein SSA2	2088.89	3
1169786	RecName: Full=Glyceraldehyde-3-phosphate	2057.76	13

	dehydrogenase 1; Short=GAPDH 1		
125609	RecName: Full=Pyruvate kinase 1; Short=PK 1; AltName: Full=cell division cycle protein 19	1346.43	22
74676594	RecName: Full=Protein EMP46; AltName: Full=46 kDa endomembrane protein; Flags: Precursor	1277.74	21
30923172	RecName: Full=Pyruvate decarboxylase isozyme 1	1150.67	18
586211	RecName: Full=V-type proton ATPase subunit B; Short=V-ATPase subunit B; AltName: Full=V-ATPase 57 kDa subunit; AltName: Full=Vacuolar proton pump subunit B	1044.63	17
137464	RecName: Full=V-type proton ATPase catalytic subunit A; Short=V-ATPase subunit A; AltName: Full=Vacuolar proton pump subunit A; Contains: RecName: Full=Endonuclease PI-SceI; AltName: Full=Sce VMA intein; AltName: Full=VMA1-derived endonuclease; Short=VDE	956.75	14
93204604	RecName: Full=RNA-binding protein SRO9; AltName: Full=Suppressor of RHO3 protein 9	923.29	9
84028178	RecName: Full=ATP synthase subunit beta, mitochondrial; Flags: Precursor	821.02	9
330443451	glycine--tRNA ligase [Saccharomyces cerevisiae S288c]	800.08	13
1708315	RecName: Full=ATP-dependent molecular chaperone HSC82; AltName: Full=82 kDa heat shock cognate protein; AltName: Full=Heat shock protein Hsp90 constitutive isoform	737.75	8
119161	RecName: Full=Elongation factor 1-alpha; Short=EF-1-alpha; AltName: Full=Eukaryotic elongation factor 1A; Short=eEF1A; AltName: Full=Translation elongation factor 1A	731.97	14
391359302	RecName: Full=Heat shock protein SSC1, mitochondrial; AltName: Full=Endonuclease SceI 75 kDa subunit; Short=Endo.SceI 75 kDa subunit; AltName: Full=mtHSP70; Flags: Precursor	715.77	8
135134	RecName: Full=Isoleucine--tRNA ligase, cytoplasmic; AltName: Full=Isoleucyl-tRNA synthetase; Short=IleRS	666.45	13
347595828	RecName: Full=Protein URA2; Includes: RecName: Full=Glutamine-dependent carbamoyl-phosphate synthase; Includes: RecName: Full=Aspartate carbamoyltransferase	659.70	10
308153683	RecName: Full=Alcohol dehydrogenase 1; AltName: Full=Alcohol dehydrogenase I; AltName: Full=YADH-1	567.36	10
1709086	RecName: Full=Mannose-1-phosphate guanyltransferase; AltName: Full=ATP-mannose-1-phosphate guanylyltransferase; AltName: Full=GDP-mannose pyrophosphorylase; AltName: Full=NDP-hexose pyrophosphorylase	561.09	10

119337	RecName: Full=Enolase 2; AltName: Full=2-phospho-D-glycerate hydro-lyase 2; AltName: Full=2-phosphoglycerate dehydratase 2	559.32	6
129930	RecName: Full=Phosphoglycerate kinase	545.97	13
730698	RecName: Full=Protein SSP120; Flags: Precursor	481.79	7
124159	RecName: Full=Isocitrate dehydrogenase [NAD] subunit 2, mitochondrial; AltName: Full=Isocitric dehydrogenase; AltName: Full=NAD(+)-specific ICDH; Flags: Precursor	474.07	6
127277	RecName: Full=Mitochondrial phosphate carrier protein; AltName: Full=Mitochondrial import receptor; AltName: Full=Phosphate transport protein; Short=PTP; AltName: Full=mPic 1; AltName: Full=p32; Contains: RecName: Full=Mitochondrial phosphate carrier protein, N-terminally processed	403.57	6
3121873	RecName: Full=Coronin-like protein	389.80	9
124376	RecName: Full=Acetolactate synthase catalytic subunit, mitochondrial; AltName: Full=Acetohydroxy-acid synthase catalytic subunit; Short=AHAS; Short=ALS; Flags: Precursor	381.30	6
584738	RecName: Full=ADP,ATP carrier protein 2; AltName: Full=ADP/ATP translocase 2; AltName: Full=Adenine nucleotide translocator 2; Short=ANT 2; AltName: Full=Petite colonies protein 9	362.39	5
731640	RecName: Full=Putative proline--tRNA ligase YHR020W; AltName: Full=Prolyl-tRNA synthetase; Short=ProRS	317.44	7
59799591	RecName: Full=Serine/threonine-protein kinase HRK1; AltName: Full=Hygromycin resistance kinase 1	298.80	8
1730231	RecName: Full=Guanine nucleotide-binding protein subunit beta-like protein; AltName: Full=Receptor for activated C kinase; AltName: Full=Receptor of activated protein kinase C 1; Short=RACK1	291.04	4
1174608	RecName: Full=Tubulin beta chain; AltName: Full=Beta-tubulin	270.01	4
133146	RecName: Full=Ran GTPase-activating protein 1; AltName: Full=Protein involved in RNA production/processing	223.91	5
1346525	RecName: Full=S-adenosylmethionine synthase 1; Short=AdoMet synthase 1; AltName: Full=Methionine adenosyltransferase 1; Short=MAT 1	207.93	2
302595956	RecName: Full=Polyubiquitin; Contains: RecName: Full=Ubiquitin; Flags: Precursor	200.54	5
1168544	RecName: Full=Plasma membrane ATPase 1; AltName: Full=Proton pump 1	194.12	4
548976	RecName: Full=Suppressor protein SRP40	190.52	4

113626	RecName: Full=Fructose-bisphosphate aldolase; Short=FBP aldolase; Short=FBPA; AltName: Full=Fructose-1,6-bisphosphate aldolase	179.11	2
114152884	RecName: Full=Glutamate--tRNA ligase, cytoplasmic; AltName: Full=Glutamyl-tRNA synthetase; Short=(c)ERS; Short=GluRS; AltName: Full=P85	174.56	2
1174622	RecName: Full=T-complex protein 1 subunit theta; Short=TCP-1-theta; AltName: Full=CCT-theta	170.66	3
1350714	RecName: Full=60S ribosomal protein L4-B; AltName: Full=L2; AltName: Full=RP2; AltName: Full=YL2	167.56	4
2507307	RecName: Full=60S ribosomal protein L3; AltName: Full=Maintenance of killer protein 8; AltName: Full=RP1; AltName: Full=Trichodermin resistance protein; AltName: Full=YL1	166.36	2
38372623	RecName: Full=Actin	156.94	3
584850	RecName: Full=Protein BOB1; AltName: Full=BEM1-binding protein; AltName: Full=Growth inhibitory protein 7	148.85	3
341940649	RecName: Full=ATP synthase subunit alpha, mitochondrial; Flags: Precursor	148.04	1
10383762	prion domain-containing protein RNQ1 [Saccharomyces cerevisiae S288c]	138.65	1
731845	RecName: Full=Homoisocitrate dehydrogenase, mitochondrial; Short=HIcDH; Flags: Precursor	134.47	3
266448	RecName: Full=Long-chain-fatty-acid--CoA ligase 1; AltName: Full=Fatty acid activator 1; AltName: Full=Long-chain acyl-CoA synthetase 1	132.03	2
730687	RecName: Full=40S ribosomal protein S20	119.97	2
462072	RecName: Full=Fatty acid synthase subunit beta; Includes: RecName: Full=3-hydroxyacyl-[acyl-carrier-protein] dehydratase; Includes: RecName: Full=Enoyl-[acyl-carrier-protein] reductase [NADH]; Includes: RecName: Full=[Acyl-carrier-protein] acetyltransferase; Includes: RecName: Full=[Acyl-carrier-protein] malonyltransferase; Includes: RecName: Full=S-acyl fatty acid synthase thioesterase	113.02	1
395129777	Cpn60 chaperonin GroEL, large subunit of GroESL [Legionella pneumophila subsp. pneumophila]	109.51	2
2507038	RecName: Full=Glycerol-1-phosphate phosphohydrolase 1; AltName: Full=(DL)-glycerol-3-phosphatase 1; AltName: Full=Related to HOR2 protein 2	108.84	1
1729835	RecName: Full=Tubulin alpha-1 chain	100.28	2
160380616	RecName: Full=ATP-dependent RNA helicase DBP3; AltName: Full=DEAD box protein 3; AltName: Full=Helicase CA3	88.61	2

364507081	translation elongation factor G (EF-G) [Legionella pneumophila subsp. pneumophila ATCC 43290]	85.32	1
137083	RecName: Full=Transcriptional regulator URE2; AltName: Full=Disulfide reductase; AltName: Full=Glutathione peroxidase	80.53	1
462173	RecName: Full=Glutamine--fructose-6-phosphate aminotransferase [isomerizing]; Short=GFAT; AltName: Full=D-fructose-6-phosphate amidotransferase; AltName: Full=Hexosephosphate aminotransferase	79.46	2
731502	RecName: Full=Importin subunit beta-4; AltName: Full=Importin-123; AltName: Full=Karyopherin subunit beta-4; AltName: Full=Karyopherin-123; AltName: Full=Ran-binding protein YRB4	78.26	1
128576	RecName: Full=Nuclear localization sequence-binding protein; AltName: Full=p67	75.33	1
229891574	RecName: Full=40S ribosomal protein S0-A; AltName: Full=Nucleic acid-binding protein NAB1A	74.93	1
131619	RecName: Full=Bifunctional purine biosynthetic protein ADE5,7; Includes: RecName: Full=Phosphoribosylamine--glycine ligase; AltName: Full=Glycinamide ribonucleotide synthetase; Short=GARS; AltName: Full=Phosphoribosylglycinamide synthetase; Includes: RecName: Full=Phosphoribosylformylglycinamidine cyclo-ligase; AltName: Full=AIR synthase; Short=AIRS; AltName: Full=Phosphoribosyl-aminoimidazole synthetase	73.31	2
206558283	RecName: Full=Nucleolar protein 58; AltName: Full=Nucleolar protein 5	70.61	1
338819315	RecName: Full=40S ribosomal protein S11-B; AltName: Full=RP41; AltName: Full=S18; AltName: Full=YS12	62.67	1
6323863	acetyl-CoA carboxylase HFA1 [Saccharomyces cerevisiae S288c]	62.53	1
3915530	RecName: Full=Uncharacterized protein YOL098C	55.40	2
364508474	hypothetical protein lp12_1736 [Legionella pneumophila subsp. pneumophila ATCC 43290]	53.54	1
2500369	RecName: Full=60S ribosomal protein L21-B	48.80	1
1707995	RecName: Full=Serine hydroxymethyltransferase, cytosolic; Short=SHMT; AltName: Full=Glycine hydroxymethyltransferase; AltName: Full=Serine methylase	48.24	3
730741	RecName: Full=Mitochondrial GTP/GDP carrier protein 1	44.62	1
1168802	RecName: Full=Carboxypeptidase S; AltName: Full=GLY-X carboxypeptidase; AltName: Full=YSCS	44.59	2
544232	RecName: Full=Elongation factor 1-gamma 2;	43.64	1

	Short=EF-1-gamma 2; AltName: Full=Eukaryotic elongation factor 1Bgamma 2; Short=eEF1Bgamma 2; AltName: Full=Translation elongation factor 1B gamma 2		
548880	RecName: Full=Uncharacterized protein MRP8	40.82	1

Supplemental Table 4.2: Full list of identified interacting proteins from LegC7, LegC7^{N242I}, LegC7^{T122P}, or control immunoprecipitation.

Vector Control

Accession	Description	Score	# Peptides
417149	RecName: Full=Heat shock protein SSA1; AltName: Full=Heat shock protein YG100	1405.76	1
123624	RecName: Full=Heat shock protein SSA2	1357.62	1
119337	RecName: Full=Enolase 2; AltName: Full=2-phospho-D-glycerate hydro-lyase 2; AltName: Full=2-phosphoglycerate dehydratase 2	697.14	1
137083	RecName: Full=Transcriptional regulator URE2; AltName: Full=Disulfide reductase; AltName: Full=Glutathione peroxidase	679.16	12
391359302	RecName: Full=Heat shock protein SSC1, mitochondrial; AltName: Full=Endonuclease SceI 75 kDa subunit; Short=Endo.SceI 75 kDa subunit; AltName: Full=mtHSP70; Flags: Precursor	676.18	11
308153602	RecName: Full=Enolase 1; AltName: Full=2-phospho-D-glycerate hydro-lyase 1; AltName: Full=2-phosphoglycerate dehydratase 1	558.85	1
125609	RecName: Full=Pyruvate kinase 1; Short=PK 1; AltName: Full=cell division cycle protein 19	450.09	8
1169787	RecName: Full=Glyceraldehyde-3-phosphate dehydrogenase 3; Short=GAPDH 3	432.49	1
120645	RecName: Full=Glyceraldehyde-3-phosphate dehydrogenase 2; Short=GAPDH 2	387.75	1
119161	RecName: Full=Elongation factor 1-alpha; Short=EF-1-alpha; AltName: Full=Eukaryotic elongation factor 1A; Short=eEF1A; AltName: Full=Translation elongation factor 1A	351.10	6
30923172	RecName: Full=Pyruvate decarboxylase isozyme 1	287.31	7
133017	RecName: Full=60S ribosomal protein L8-A; AltName: Full=L4; AltName: Full=L4-2; AltName: Full=L7a-1; AltName: Full=Maintenance of killer protein 7; AltName: Full=RP6; AltName: Full=YL5	243.65	4
136069	RecName: Full=Triosephosphate isomerase; Short=TIM; AltName: Full=Triose-phosphate isomerase	233.33	3
338819274	RecName: Full=60S ribosomal protein L12-B; AltName: Full=L15; AltName: Full=YL23	213.34	2
2500359	RecName: Full=60S ribosomal protein L13-A	204.29	2

129930	RecName: Full=Phosphoglycerate kinase	196.34	4
1710524	RecName: Full=60S ribosomal protein L25; AltName: Full=RP16L; AltName: Full=YL25; AltName: Full=YP42'	168.36	1
1173063	RecName: Full=60S ribosomal protein L17-B; AltName: Full=L20; AltName: Full=YL17	162.68	2
132935	RecName: Full=60S ribosomal protein L33-A; AltName: Full=L37; AltName: Full=RP47; AltName: Full=YL37	157.74	3
1350714	RecName: Full=60S ribosomal protein L4-B; AltName: Full=L2; AltName: Full=RP2; AltName: Full=YL2	154.59	4
1350934	RecName: Full=40S ribosomal protein S13; AltName: Full=S27a; AltName: Full=YS15	152.35	1
229891574	RecName: Full=40S ribosomal protein S0-A; AltName: Full=Nucleic acid-binding protein NAB1A	152.26	2
133026	RecName: Full=60S ribosomal protein L7-A; AltName: Full=L6; AltName: Full=RP11; AltName: Full=YL8	152.18	3
308153666	RecName: Full=60S ribosomal protein L5; AltName: Full=L1; AltName: Full=L1a; AltName: Full=Ribosomal 5S RNA-binding protein; AltName: Full=YL3	146.47	3
338819348	RecName: Full=40S ribosomal protein S24-B; AltName: Full=RP50	135.05	1
1172812	RecName: Full=60S ribosomal protein L10; AltName: Full=L9; AltName: Full=Ubiquinol-cytochrome C reductase complex subunit VI-requiring protein	134.12	1
338819356	RecName: Full=40S ribosomal protein S6-B; AltName: Full=RP9; AltName: Full=S10; AltName: Full=YS4	126.75	1
113380	RecName: Full=Alcohol dehydrogenase 2; AltName: Full=Alcohol dehydrogenase II; AltName: Full=YADH-2	123.93	2
123635	RecName: Full=Heat shock protein SSB1; AltName: Full=Cold-inducible protein YG101	123.81	2
2500369	RecName: Full=60S ribosomal protein L21-B	120.97	2
113626	RecName: Full=Fructose-bisphosphate aldolase; Short=FBP aldolase; Short=FBPA; AltName: Full=Fructose-1,6-bisphosphate aldolase	120.79	3
2507307	RecName: Full=60S ribosomal protein L3; AltName: Full=Maintenance of killer protein 8; AltName: Full=RP1; AltName: Full=Trichodermin resistance protein; AltName: Full=YL1	120.17	2
1173269	RecName: Full=40S ribosomal protein S5;	101.96	1

	AltName: Full=RP14; AltName: Full=S2; AltName: Full=YS8		
1710642	RecName: Full=60S ribosomal protein L16-B; AltName: Full=L21; AltName: Full=RP23; AltName: Full=YL15	97.67	2
338819293	RecName: Full=60S ribosomal protein L2-B; AltName: Full=L5; AltName: Full=RP8; AltName: Full=YL6	96.94	3
269969549	RecName: Full=40S ribosomal protein S1-B	96.01	1
338819315	RecName: Full=40S ribosomal protein S11-B; AltName: Full=RP41; AltName: Full=S18; AltName: Full=YS12	93.73	1
6174938	RecName: Full=60S ribosomal protein L34-A	89.34	2
1352907	RecName: Full=Adenosine kinase	81.87	1
135747	RecName: Full=Thioredoxin-1; AltName: Full=Thioredoxin I; Short=TR-I; AltName: Full=Thioredoxin-2	81.67	1
338819354	RecName: Full=40S ribosomal protein S4-B; AltName: Full=RP5; AltName: Full=S7; AltName: Full=YS6	79.71	2
118110	RecName: Full=Peptidyl-prolyl cis-trans isomerase; Short=PPIase; AltName: Full=Cyclophilin; Short=CPH; AltName: Full=Cyclosporin A-binding protein; AltName: Full=PPI-II; AltName: Full=Rotamase	79.43	2
338819278	RecName: Full=60S ribosomal protein L19-B; AltName: Full=L23; AltName: Full=RP15L; AltName: Full=RP33; AltName: Full=YL14	77.83	1
585935	RecName: Full=40S ribosomal protein S9-B; AltName: Full=RP21; AltName: Full=S13; AltName: Full=YP28; AltName: Full=YS11	73.78	1
1709086	RecName: Full=Mannose-1-phosphate guanyltransferase; AltName: Full=ATP-mannose-1-phosphate guanylyltransferase; AltName: Full=GDP-mannose pyrophosphorylase; AltName: Full=NDP-hexose pyrophosphorylase	71.73	1
308153499	RecName: Full=60S acidic ribosomal protein P0; Short=A0; AltName: Full=L10E	71.11	1
308153561	RecName: Full=60S ribosomal protein L28; AltName: Full=L27a; AltName: Full=L29; AltName: Full=RP44; AltName: Full=RP62; AltName: Full=YL24	71.04	1
1710574	RecName: Full=60S ribosomal protein L26-A; AltName: Full=L33; AltName: Full=YL33	68.70	2
132948	RecName: Full=60S ribosomal protein L30; AltName: Full=L32; AltName: Full=RP73;	68.03	1

	AltName: Full=YL38		
1708315	RecName: Full=ATP-dependent molecular chaperone HSC82; AltName: Full=82 kDa heat shock cognate protein; AltName: Full=Heat shock protein Hsp90 constitutive isoform	67.86	1
85681890	RecName: Full=60S ribosomal protein L11-B; AltName: Full=L16; AltName: Full=RP39; AltName: Full=YL22	67.39	1
85681892	RecName: Full=40S ribosomal protein S28-A; AltName: Full=S33; AltName: Full=YS27	66.76	1
730458	RecName: Full=40S ribosomal protein S26-A	66.12	1
1709978	RecName: Full=60S ribosomal protein L15-B; AltName: Full=L13; AltName: Full=RP15R; AltName: Full=YL10; AltName: Full=YP18	60.49	1
1173255	RecName: Full=40S ribosomal protein S3; AltName: Full=RP13; AltName: Full=YS3	56.85	1
133961	RecName: Full=40S ribosomal protein S2; AltName: Full=Omnipotent suppressor protein SUP44; AltName: Full=RP12; AltName: Full=S4; AltName: Full=YS5	56.85	1
132943	RecName: Full=60S ribosomal protein L24-A; AltName: Full=L30; AltName: Full=RP29; AltName: Full=YL21	45.96	1
338819319	RecName: Full=40S ribosomal protein S16-B; AltName: Full=RP61R	45.22	1
585169	RecName: Full=Bifunctional protein GAL10; Includes: RecName: Full=UDP-glucose 4-epimerase; AltName: Full=Galactowaldenase; Includes: RecName: Full=Aldose 1-epimerase; AltName: Full=Galactose mutarotase	45.03	1
46397814	RecName: Full=40S ribosomal protein S14-A; AltName: Full=RP59A	45.00	1
133036	RecName: Full=60S ribosomal protein L9-A; AltName: Full=L8; AltName: Full=RP24; AltName: Full=YL11	43.57	1
464970	RecName: Full=Peroxiredoxin TSA1; AltName: Full=Cytoplasmic thiol peroxidase 1; Short=cTPx 1; AltName: Full=PRP; AltName: Full=Thiol-specific antioxidant protein 1; AltName: Full=Thioredoxin peroxidase	42.23	1

LegC7

Accession	Description	Score	# Peptides
123624	RecName: Full=Heat shock protein SSA2	4216.88	5
417149	RecName: Full=Heat shock protein SSA1; AltName: Full=Heat shock protein YG100	4132.81	4
1169787	RecName: Full=Glyceraldehyde-3-phosphate dehydrogenase 3; Short=GAPDH 3	2413.25	5
120645	RecName: Full=Glyceraldehyde-3-phosphate dehydrogenase 2; Short=GAPDH 2	1957.78	1
1169517	RecName: Full=Protein EMP47; AltName: Full=47 kDa endomembrane protein; AltName: Full=Endosomal P44 protein; Flags: Precursor	1871.74	22
119337	RecName: Full=Enolase 2; AltName: Full=2-phospho-D-glycerate hydro-lyase 2; AltName: Full=2-phosphoglycerate dehydratase 2	1785.31	4
308153602	RecName: Full=Enolase 1; AltName: Full=2-phospho-D-glycerate hydro-lyase 1; AltName: Full=2-phosphoglycerate dehydratase 1	1572.79	3
129930	RecName: Full=Phosphoglycerate kinase	1220.91	15
391359302	RecName: Full=Heat shock protein SSC1, mitochondrial; AltName: Full=Endonuclease SceI 75 kDa subunit; Short=Endo.SceI 75 kDa subunit; AltName: Full=mtHSP70; Flags: Precursor	1140.26	16
125609	RecName: Full=Pyruvate kinase 1; Short=PK 1; AltName: Full=cell division cycle protein 19	1090.09	18
137083	RecName: Full=Transcriptional regulator URE2; AltName: Full=Disulfide reductase; AltName: Full=Glutathione peroxidase	796.86	11
30923172	RecName: Full=Pyruvate decarboxylase isozyme 1	790.20	12
1169786	RecName: Full=Glyceraldehyde-3-phosphate dehydrogenase 1; Short=GAPDH 1	764.72	2
123635	RecName: Full=Heat shock protein SSB1; AltName: Full=Cold-inducible protein YG101	721.76	10
1350714	RecName: Full=60S ribosomal protein L4-B; AltName: Full=L2; AltName: Full=RP2; AltName: Full=YL2	678.89	8
121575	RecName: Full=78 kDa glucose-regulated protein homolog; Short=GRP-78; AltName: Full=Immunoglobulin heavy chain-binding protein homolog; Short=BiP; Flags: Precursor	581.57	5
730698	RecName: Full=Protein SSP120; Flags: Precursor	554.04	5
119161	RecName: Full=Elongation factor 1-alpha; Short=EF-1-alpha; AltName: Full=Eukaryotic elongation factor 1A; Short=eEF1A; AltName: Full=Translation elongation factor 1A	545.78	10
74676594	RecName: Full=Protein EMP46; AltName: Full=46 kDa endomembrane protein; Flags: Precursor	537.61	11
1708315	RecName: Full=ATP-dependent molecular chaperone	507.71	8

	HSC82; AltName: Full=82 kDa heat shock cognate protein; AltName: Full=Heat shock protein Hsp90 constitutive isoform		
308153683	RecName: Full=Alcohol dehydrogenase 1; AltName: Full=Alcohol dehydrogenase I; AltName: Full=YADH-1	500.71	6
113626	RecName: Full=Fructose-bisphosphate aldolase; Short=FBP aldolase; Short=FBPA; AltName: Full=Fructose-1,6-bisphosphate aldolase	438.96	5
136069	RecName: Full=Triosephosphate isomerase; Short=TIM; AltName: Full=Triose-phosphate isomerase	399.59	6
269969549	RecName: Full=40S ribosomal protein S1-B	369.90	2
417670	RecName: Full=60S ribosomal protein L8-B; AltName: Full=L4; AltName: Full=L4-1; AltName: Full=RP6; AltName: Full=YL5	338.95	6
2500359	RecName: Full=60S ribosomal protein L13-A	333.71	5
118110	RecName: Full=Peptidyl-prolyl cis-trans isomerase; Short=PPIase; AltName: Full=Cyclophilin; Short=CPH; AltName: Full=Cyclosporin A-binding protein; AltName: Full=PPI-II; AltName: Full=Rotamase	311.66	6
59799591	RecName: Full=Serine/threonine-protein kinase HRK1; AltName: Full=Hygromycin resistance kinase 1	306.87	5
585935	RecName: Full=40S ribosomal protein S9-B; AltName: Full=RP21; AltName: Full=S13; AltName: Full=YP28; AltName: Full=YS11	299.07	5
308153499	RecName: Full=60S acidic ribosomal protein P0; Short=A0; AltName: Full=L10E	298.11	3
1350934	RecName: Full=40S ribosomal protein S13; AltName: Full=S27a; AltName: Full=YS15	291.66	5
338819274	RecName: Full=60S ribosomal protein L12-B; AltName: Full=L15; AltName: Full=YL23	284.35	4
1173063	RecName: Full=60S ribosomal protein L17-B; AltName: Full=L20; AltName: Full=YL17	281.85	3
229891577	RecName: Full=40S ribosomal protein S0-B; AltName: Full=Nucleic acid-binding protein NAB1B	278.55	3
728968	RecName: Full=Protein BMH1	274.00	3
269969543	RecName: Full=40S ribosomal protein S1-A	273.83	1
46397814	RecName: Full=40S ribosomal protein S14-A; AltName: Full=RP59A	266.94	4
1168544	RecName: Full=Plasma membrane ATPase 1; AltName: Full=Proton pump 1	266.63	3
93204604	RecName: Full=RNA-binding protein SRO9; AltName: Full=Suppressor of RHO3 protein 9	247.38	4
338819278	RecName: Full=60S ribosomal protein L19-B; AltName: Full=L23; AltName: Full=RP15L; AltName: Full=RP33; AltName: Full=YL14	247.19	3
347595828	RecName: Full=Protein URA2; Includes: RecName: Full=Glutamine-dependent carbamoyl-phosphate synthase; Includes: RecName: Full=Aspartate	228.60	4

	carbamoyltransferase		
338819356	RecName: Full=40S ribosomal protein S6-B; AltName: Full=RP9; AltName: Full=S10; AltName: Full=YS4	225.73	4
1710524	RecName: Full=60S ribosomal protein L25; AltName: Full=RP16L; AltName: Full=YL25; AltName: Full=YP42'	218.47	2
338819354	RecName: Full=40S ribosomal protein S4-B; AltName: Full=RP5; AltName: Full=S7; AltName: Full=YS6	217.82	6
1709086	RecName: Full=Mannose-1-phosphate guanyltransferase; AltName: Full=ATP-mannose-1-phosphate guanylyltransferase; AltName: Full=GDP-mannose pyrophosphorylase; AltName: Full=NDP-hexose pyrophosphorylase	216.80	4
549656	RecName: Full=60S ribosomal protein L14-A	216.43	2
338819348	RecName: Full=40S ribosomal protein S24-B; AltName: Full=RP50	215.31	4
338819346	RecName: Full=40S ribosomal protein S23-B; AltName: Full=RP37; AltName: Full=S28; AltName: Full=YS14	214.89	4
416935	RecName: Full=Elongation factor 2; Short=EF-2; AltName: Full=Eukaryotic elongation factor 2; Short=eEF2; AltName: Full=Ribosomal translocase; AltName: Full=Translation elongation factor 2	209.65	4
730687	RecName: Full=40S ribosomal protein S20	205.07	4
338819276	RecName: Full=60S ribosomal protein L18-B; AltName: Full=RP28	197.33	2
85681891	RecName: Full=40S ribosomal protein S22-B; AltName: Full=RP50; AltName: Full=S24; AltName: Full=YP58; AltName: Full=YS22	194.10	1
1709682	RecName: Full=Peroxiredoxin type-2; AltName: Full=AHPC1; AltName: Full=Cytoplasmic thiol peroxidase 3; Short=cTPx 3; AltName: Full=Peroxiredoxin type II; AltName: Full=Peroxisomal alkyl hydroperoxide reductase; AltName: Full=TPx type II; AltName: Full=Thiol-specific antioxidant II; Short=TSA II; AltName: Full=Thioredoxin peroxidase type II; AltName: Full=Thioredoxin reductase type II	183.24	2
548854	RecName: Full=40S ribosomal protein S27-A; AltName: Full=RP61; AltName: Full=YS20	176.55	3
1710642	RecName: Full=60S ribosomal protein L16-B; AltName: Full=L21; AltName: Full=RP23; AltName: Full=YL15	174.19	1
548534	RecName: Full=Phosphoglycerate mutase 1; Short=PGAM 1; AltName: Full=BPG-dependent PGAM 1; AltName: Full=MPGM 1; AltName: Full=Phosphoglyceromutase 1	173.65	2
160395531	RecName: Full=ATP-dependent RNA helicase eIF4A; AltName: Full=Eukaryotic initiation factor 4A; Short=eIF-4A; AltName: Full=Stimulator factor I 37 kDa component; AltName: Full=Translation initiation factor 1/2; AltName: Full=p37	172.96	4
585167	RecName: Full=Galactose-1-phosphate	167.95	2

	uridylyltransferase; Short=Gal-1-P uridylyltransferase; AltName: Full=UDP-glucose--hexose-1-phosphate uridylyltransferase		
120227	RecName: Full=FK506-binding protein 1; Short=FKBP; AltName: Full=Peptidyl-prolyl cis-trans isomerase; Short=PPIase; AltName: Full=Rapamycin-binding protein	166.11	3
85681890	RecName: Full=60S ribosomal protein L11-B; AltName: Full=L16; AltName: Full=RP39; AltName: Full=YL22	154.07	1
730458	RecName: Full=40S ribosomal protein S26-A	153.88	2
338819322	RecName: Full=40S ribosomal protein S18-B	152.67	2
338819319	RecName: Full=40S ribosomal protein S16-B; AltName: Full=RP61R	152.52	2
308153666	RecName: Full=60S ribosomal protein L5; AltName: Full=L1; AltName: Full=L1a; AltName: Full=Ribosomal 5S RNA-binding protein; AltName: Full=YL3	152.00	4
730452	RecName: Full=60S ribosomal protein L16-A; AltName: Full=L13a; AltName: Full=L21; AltName: Full=RP22; AltName: Full=YL15	148.26	1
1173255	RecName: Full=40S ribosomal protein S3; AltName: Full=RP13; AltName: Full=YS3	148.20	3
1346942	RecName: Full=60S ribosomal protein L6-B; AltName: Full=L17; AltName: Full=RP18; AltName: Full=YL16	147.42	2
133026	RecName: Full=60S ribosomal protein L7-A; AltName: Full=L6; AltName: Full=RP11; AltName: Full=YL8	144.92	3
338819289	RecName: Full=60S ribosomal protein L20-B; AltName: Full=L18a	139.27	3
308153561	RecName: Full=60S ribosomal protein L28; AltName: Full=L27a; AltName: Full=L29; AltName: Full=RP44; AltName: Full=RP62; AltName: Full=YL24	133.21	1
1352907	RecName: Full=Adenosine kinase	132.51	1
1710574	RecName: Full=60S ribosomal protein L26-A; AltName: Full=L33; AltName: Full=YL33	129.84	3
2507307	RecName: Full=60S ribosomal protein L3; AltName: Full=Maintenance of killer protein 8; AltName: Full=RP1; AltName: Full=Trichodermin resistance protein; AltName: Full=YL1	126.93	3
132935	RecName: Full=60S ribosomal protein L33-A; AltName: Full=L37; AltName: Full=RP47; AltName: Full=YL37	126.90	2
2507329	RecName: Full=40S ribosomal protein S7-A; AltName: Full=RP30; AltName: Full=RP40	125.32	3
68846657	RecName: Full=Mitochondrial outer membrane protein porin 1; AltName: Full=Voltage-dependent anion-selective channel protein 1; Short=VDAC-1	124.87	2
1172812	RecName: Full=60S ribosomal protein L10; AltName: Full=L9; AltName: Full=Ubiquinol-cytochrome C reductase complex subunit VI-requiring protein	122.81	2
6174938	RecName: Full=60S ribosomal protein L34-A	121.89	2
585166	RecName: Full=Galactokinase; AltName:	118.12	3

	Full=Galactose kinase		
134039184	RecName: Full=Transposon Ty1-LR4 Gag polyprotein; AltName: Full=Gag-p49; AltName: Full=Transposon Ty1 protein A; Short=TY1A; Short=TYA; AltName: Full=p58; Contains: RecName: Full=Capsid protein; Short=CA; AltName: Full=Gag-p45; AltName: Full=p54; Contains: RecName: Full=Gag-p4	117.77	2
20981689	RecName: Full=Magnesium-activated aldehyde dehydrogenase, cytosolic; AltName: Full=Mg(2+)-activated acetaldehyde dehydrogenase; Short=Mg(2+)-ACDH	114.96	1
132948	RecName: Full=60S ribosomal protein L30; AltName: Full=L32; AltName: Full=RP73; AltName: Full=YL38	114.17	1
302595956	RecName: Full=Polyubiquitin; Contains: RecName: Full=Ubiquitin; Flags: Precursor	113.68	4
338819293	RecName: Full=60S ribosomal protein L2-B; AltName: Full=L5; AltName: Full=RP8; AltName: Full=YL6	113.50	2
133066	RecName: Full=60S acidic ribosomal protein P2-alpha; Short=P2A; AltName: Full=A2; AltName: Full=L12EIB; AltName: Full=L44; AltName: Full=YP2alpha	104.75	1
585169	RecName: Full=Bifunctional protein GAL10; Includes: RecName: Full=UDP-glucose 4-epimerase; AltName: Full=Galactowaldenase; Includes: RecName: Full=Aldose 1-epimerase; AltName: Full=Galactose mutarotase	102.97	1
120745	RecName: Full=Glucose-6-phosphate isomerase; Short=GPI; AltName: Full=Phosphoglucose isomerase; Short=PGI; AltName: Full=Phosphohexose isomerase; Short=PHI	101.40	3
123054	RecName: Full=Ferrochelatase, mitochondrial; AltName: Full=Heme synthase; AltName: Full=Protoheme ferro-lyase; Flags: Precursor	100.53	3
730018	RecName: Full=5-methyltetrahydropteroyltriglutamate--homocysteine methyltransferase; AltName: Full=Cobalamin-independent methionine synthase; AltName: Full=Delta-P8 protein; AltName: Full=Methionine synthase, vitamin-B12 independent isozyme	94.82	1
85681892	RecName: Full=40S ribosomal protein S28-A; AltName: Full=S33; AltName: Full=YS27	94.62	2
133858	RecName: Full=40S ribosomal protein S19-B; AltName: Full=RP55B; AltName: Full=S16a; AltName: Full=YS16B	92.32	2
134633	RecName: Full=Superoxide dismutase [Cu-Zn]	83.18	1
338819295	RecName: Full=60S ribosomal protein L35-B	81.65	1
134039200	RecName: Full=60S ribosomal protein L27-A	81.39	2
1723685	RecName: Full=Sphingolipid long chain base-responsive protein PIL1	80.96	1
464970	RecName: Full=Peroxiredoxin TSA1; AltName:	80.84	2

	Full=Cytoplasmic thiol peroxidase 1; Short=cTPx 1; AltName: Full=PRP; AltName: Full=Thiol-specific antioxidant protein 1; AltName: Full=Thioredoxin peroxidase		
338819315	RecName: Full=40S ribosomal protein S11-B; AltName: Full=RP41; AltName: Full=S18; AltName: Full=YS12	79.03	2
38372623	RecName: Full=Actin	76.36	2
119857	RecName: Full=rRNA 2'-O-methyltransferase fibrillarin; AltName: Full=Histone-glutamine methyltransferase; AltName: Full=U3 small nucleolar RNA-associated protein NOP1; Short=Nucleolar protein 1; Short=U3 snoRNA-associated protein NOP1	74.88	1
224493074	RecName: Full=Adenylate kinase; AltName: Full=ATP-AMP transphosphorylase; AltName: Full=ATP:AMP phosphotransferase; AltName: Full=Adenylate kinase cytosolic and mitochondrial; AltName: Full=Adenylate monophosphate kinase; Flags: Precursor	72.55	1
2500369	RecName: Full=60S ribosomal protein L21-B	72.38	1
132943	RecName: Full=60S ribosomal protein L24-A; AltName: Full=L30; AltName: Full=RP29; AltName: Full=YL21	71.83	2
1350929	RecName: Full=40S ribosomal protein S12	68.63	1
1173269	RecName: Full=40S ribosomal protein S5; AltName: Full=RP14; AltName: Full=S2; AltName: Full=YS8	67.20	3
1730231	RecName: Full=Guanine nucleotide-binding protein subunit beta-like protein; AltName: Full=Receptor for activated C kinase; AltName: Full=Receptor of activated protein kinase C 1; Short=RACK1	66.71	1
347595816	RecName: Full=Glutamine synthetase; Short=GS; AltName: Full=Glutamate--ammonia ligase	65.28	1
417090	RecName: Full=GTP-binding nuclear protein GSP1/CNR1; AltName: Full=Chromosome stability protein 17; AltName: Full=GTPase Ran homolog; AltName: Full=Genetic suppressor of PRP20-1	65.28	1
548976	RecName: Full=Suppressor protein SRP40	65.13	2
120479	RecName: Full=Farnesyl pyrophosphate synthase; Short=FPP synthase; Short=FPS; AltName: Full=(2E,6E)-farnesyl diphosphate synthase; AltName: Full=Dimethylallyltranstransferase; AltName: Full=Farnesyl diphosphate synthase; AltName: Full=Geranyltranstransferase	62.07	1
1346525	RecName: Full=S-adenosylmethionine synthase 1; Short=AdoMet synthase 1; AltName: Full=Methionine adenosyltransferase 1; Short=MAT 1	59.84	1
83288131	RecName: Full=40S ribosomal protein S25-B; AltName: Full=RP45; AltName: Full=S31; AltName: Full=YS23	59.25	1
133961	RecName: Full=40S ribosomal protein S2; AltName: Full=Omnipotent suppressor protein SUP44; AltName: Full=RP12; AltName: Full=S4; AltName: Full=YS5	58.52	2
1706591	RecName: Full=Elongation factor 3B; Short=EF-3B;	58.27	2

	AltName: Full=Homolog of EF-3; AltName: Full=Translation elongation factor 3B		
134034935	RecName: Full=60S ribosomal protein L31-A; AltName: Full=L34; AltName: Full=YL28	54.20	2
84028178	RecName: Full=ATP synthase subunit beta, mitochondrial; Flags: Precursor	54.19	1
1730165	RecName: Full=tRNA-aminoacylation cofactor ARC1; AltName: Full=Acyl-RNA-complex protein 1; AltName: Full=GU4 nucleic-binding protein 1; Short=G4p1 protein; AltName: Full=P42; AltName: Full=tRNA-interacting factor ARC1	54.18	1
462072	RecName: Full=Fatty acid synthase subunit beta; Includes: RecName: Full=3-hydroxyacyl-[acyl-carrier-protein] dehydratase; Includes: RecName: Full=Enoyl-[acyl-carrier-protein] reductase [NADH]; Includes: RecName: Full=[Acyl-carrier-protein] acetyltransferase; Includes: RecName: Full=[Acyl-carrier-protein] malonyltransferase; Includes: RecName: Full=S-acyl fatty acid synthase thioesterase	53.09	1
266966	RecName: Full=40S ribosomal protein S15; AltName: Full=RIG protein; AltName: Full=RP52; AltName: Full=S21; AltName: Full=YS21	50.78	1
338819342	RecName: Full=60S ribosomal protein L43-A; AltName: Full=L37a; AltName: Full=YL35	48.36	1
130806	RecName: Full=Pre-mRNA-processing ATP-dependent RNA helicase PRP5	47.34	1
1350741	RecName: Full=60S ribosomal protein L36-A; AltName: Full=L39; AltName: Full=YL39	46.75	1
133036	RecName: Full=60S ribosomal protein L9-A; AltName: Full=L8; AltName: Full=RP24; AltName: Full=YL11	46.52	2
1176558	RecName: Full=40S ribosomal protein S10-B	45.58	1
585885	RecName: Full=60S ribosomal protein L32	44.50	2
1168802	RecName: Full=Carboxypeptidase S; AltName: Full=GLY-X carboxypeptidase; AltName: Full=YSCS	44.44	1
137464	RecName: Full=V-type proton ATPase catalytic subunit A; Short=V-ATPase subunit A; AltName: Full=Vacuolar proton pump subunit A; Contains: RecName: Full=Endonuclease PI-SceI; AltName: Full=Sce VMA intein; AltName: Full=VMA1-derived endonuclease; Short=VDE	43.42	3
74583435	RecName: Full=Protein dopey	41.43	1
135747	RecName: Full=Thioredoxin-1; AltName: Full=Thioredoxin I; Short=TR-I; AltName: Full=Thioredoxin-2	40.35	1

LegC7^{N242I}

Accession	Description	Score	# Peptides
1169787	RecName: Full=Glyceraldehyde-3-phosphate dehydrogenase 3; Short=GAPDH 3	3464.52	6
417149	RecName: Full=Heat shock protein SSA1; AltName: Full=Heat shock protein YG100	2712.04	2
123624	RecName: Full=Heat shock protein SSA2	2695.97	2
119337	RecName: Full=Enolase 2; AltName: Full=2-phospho-D-glycerate hydro-lyase 2; AltName: Full=2-phosphoglycerate dehydratase 2	2671.19	6
120645	RecName: Full=Glyceraldehyde-3-phosphate dehydrogenase 2; Short=GAPDH 2	2606.30	1
129930	RecName: Full=Phosphoglycerate kinase	2244.09	27
1169517	RecName: Full=Protein EMP47; AltName: Full=47 kDa endomembrane protein; AltName: Full=Endosomal P44 protein; Flags: Precursor	2009.91	23
308153602	RecName: Full=Enolase 1; AltName: Full=2-phospho-D-glycerate hydro-lyase 1; AltName: Full=2-phosphoglycerate dehydratase 1	1978.35	5
125609	RecName: Full=Pyruvate kinase 1; Short=PK 1; AltName: Full=cell division cycle protein 19	1614.98	24
1169786	RecName: Full=Glyceraldehyde-3-phosphate dehydrogenase 1; Short=GAPDH 1	1409.85	6
136069	RecName: Full=Triosephosphate isomerase; Short=TIM; AltName: Full=Triose-phosphate isomerase	1229.45	10
1708315	RecName: Full=ATP-dependent molecular chaperone HSC82; AltName: Full=82 kDa heat shock cognate protein; AltName: Full=Heat shock protein Hsp90 constitutive isoform	789.17	12
308153683	RecName: Full=Alcohol dehydrogenase 1; AltName: Full=Alcohol dehydrogenase I; AltName: Full=YADH-1	726.90	10
391359302	RecName: Full=Heat shock protein SSC1, mitochondrial; AltName: Full=Endonuclease SceI 75 kDa subunit; Short=Endo.SceI 75 kDa subunit; AltName: Full=mtHSP70; Flags: Precursor	691.80	9
30923172	RecName: Full=Pyruvate decarboxylase isozyme 1	672.89	14
113626	RecName: Full=Fructose-bisphosphate aldolase; Short=FBP aldolase; Short=FBPA; AltName: Full=Fructose-1,6-bisphosphate aldolase	646.50	9
123635	RecName: Full=Heat shock protein SSB1; AltName: Full=Cold-inducible protein YG101	629.37	1
730698	RecName: Full=Protein SSP120; Flags: Precursor	625.42	6
119161	RecName: Full=Elongation factor 1-alpha; Short=EF-1-alpha; AltName: Full=Eukaryotic elongation factor 1A; Short=eEF1A; AltName: Full=Translation elongation factor 1A	625.38	11

729768	RecName: Full=Heat shock protein SSB2	621.68	1
1350714	RecName: Full=60S ribosomal protein L4-B; AltName: Full=L2; AltName: Full=RP2; AltName: Full=YL2	604.61	7
548534	RecName: Full=Phosphoglycerate mutase 1; Short=PGAM 1; AltName: Full=BPG-dependent PGAM 1; AltName: Full=MPGM 1; AltName: Full=Phosphoglyceromutase 1	588.87	10
118110	RecName: Full=Peptidyl-prolyl cis-trans isomerase; Short=PPIase; AltName: Full=Cyclophilin; Short=CPH; AltName: Full=Cyclosporin A-binding protein; AltName: Full=PPI-II; AltName: Full=Rotamase	580.83	9
416935	RecName: Full=Elongation factor 2; Short=EF-2; AltName: Full=Eukaryotic elongation factor 2; Short=eEF2; AltName: Full=Ribosomal translocase; AltName: Full=Translation elongation factor 2	503.44	8
417670	RecName: Full=60S ribosomal protein L8-B; AltName: Full=L4; AltName: Full=L4-1; AltName: Full=RP6; AltName: Full=YL5	491.16	8
74676594	RecName: Full=Protein EMP46; AltName: Full=46 kDa endomembrane protein; Flags: Precursor	466.74	9
728968	RecName: Full=Protein BMH1	461.24	2
137083	RecName: Full=Transcriptional regulator URE2; AltName: Full=Disulfide reductase; AltName: Full=Glutathione peroxidase	457.95	8
1350934	RecName: Full=40S ribosomal protein S13; AltName: Full=S27a; AltName: Full=YS15	431.10	5
1173269	RecName: Full=40S ribosomal protein S5; AltName: Full=RP14; AltName: Full=S2; AltName: Full=YS8	419.60	3
308153499	RecName: Full=60S acidic ribosomal protein P0; Short=A0; AltName: Full=L10E	382.55	4
269969543	RecName: Full=40S ribosomal protein S1-A	378.54	1
338819278	RecName: Full=60S ribosomal protein L19-B; AltName: Full=L23; AltName: Full=RP15L; AltName: Full=RP33; AltName: Full=YL14	372.51	4
2500359	RecName: Full=60S ribosomal protein L13-A	356.01	6
730701	RecName: Full=Adenosylhomocysteinase; Short=AdoHcyase; AltName: Full=S-adenosyl-L-homocysteine hydrolase	354.12	6
1710642	RecName: Full=60S ribosomal protein L16-B; AltName: Full=L21; AltName: Full=RP23; AltName: Full=YL15	350.48	2
120745	RecName: Full=Glucose-6-phosphate isomerase; Short=GPI; AltName: Full=Phosphoglucose isomerase; Short=PGI; AltName: Full=Phosphohexose isomerase; Short=PHI	345.32	5
160395531	RecName: Full=ATP-dependent RNA helicase eIF4A; AltName: Full=Eukaryotic initiation factor 4A; Short=eIF-4A; AltName: Full=Stimulator factor I 37 kDa component; AltName: Full=Translation initiation factor 1/2; AltName: Full=p37	343.09	4

133026	RecName: Full=60S ribosomal protein L7-A; AltName: Full=L6; AltName: Full=RP11; AltName: Full=YL8	342.42	5
269969549	RecName: Full=40S ribosomal protein S1-B	341.26	2
46397814	RecName: Full=40S ribosomal protein S14-A; AltName: Full=RP59A	318.19	4
308153666	RecName: Full=60S ribosomal protein L5; AltName: Full=L1; AltName: Full=L1a; AltName: Full=Ribosomal 5S RNA-binding protein; AltName: Full=YL3	285.32	4
730018	RecName: Full=5-methyltetrahydropteroyltriglutamate--homocysteine methyltransferase; AltName: Full=Cobalamin-independent methionine synthase; AltName: Full=Delta-P8 protein; AltName: Full=Methionine synthase, vitamin-B12 independent isozyme	271.75	4
338819274	RecName: Full=60S ribosomal protein L12-B; AltName: Full=L15; AltName: Full=YL23	260.47	4
1709682	RecName: Full=Peroxiredoxin type-2; AltName: Full=AHPC1; AltName: Full=Cytoplasmic thiol peroxidase 3; Short=cTPx 3; AltName: Full=Peroxiredoxin type II; AltName: Full=Peroxisomal alkyl hydroperoxide reductase; AltName: Full=TPx type II; AltName: Full=Thiol-specific antioxidant II; Short=TSA II; AltName: Full=Thioredoxin peroxidase type II; AltName: Full=Thioredoxin reductase type II	259.72	4
548854	RecName: Full=40S ribosomal protein S27-A; AltName: Full=RP61; AltName: Full=YS20	254.47	3
585935	RecName: Full=40S ribosomal protein S9-B; AltName: Full=RP21; AltName: Full=S13; AltName: Full=YP28; AltName: Full=YS11	251.60	6
461631	RecName: Full=Protein BMH2	249.49	1
88984204	RecName: Full=Glutaredoxin-2, mitochondrial; AltName: Full=Glutathione-dependent oxidoreductase 2; AltName: Full=Thioltransferase; Flags: Precursor	240.93	2
229891577	RecName: Full=40S ribosomal protein S0-B; AltName: Full=Nucleic acid-binding protein NAB1B	235.94	1
302595956	RecName: Full=Polyubiquitin; Contains: RecName: Full=Ubiquitin; Flags: Precursor	234.67	6
20981689	RecName: Full=Magnesium-activated aldehyde dehydrogenase, cytosolic; AltName: Full=Mg(2+)-activated acetaldehyde dehydrogenase; Short=Mg(2+)-ACDH	233.52	3
338819348	RecName: Full=40S ribosomal protein S24-B; AltName: Full=RP50	224.78	3
338819276	RecName: Full=60S ribosomal protein L18-B; AltName: Full=RP28	224.08	4
1346942	RecName: Full=60S ribosomal protein L6-B; AltName: Full=L17; AltName: Full=RP18; AltName: Full=YL16	221.80	3
338819293	RecName: Full=60S ribosomal protein L2-B; AltName: Full=L5; AltName: Full=RP8; AltName: Full=YL6	221.01	6

1168544	RecName: Full=Plasma membrane ATPase 1; AltName: Full=Proton pump 1	215.19	2
338819346	RecName: Full=40S ribosomal protein S23-B; AltName: Full=RP37; AltName: Full=S28; AltName: Full=YS14	213.95	3
338819322	RecName: Full=40S ribosomal protein S18-B	213.62	3
1710524	RecName: Full=60S ribosomal protein L25; AltName: Full=RP16L; AltName: Full=YL25; AltName: Full=YP42'	210.05	2
549656	RecName: Full=60S ribosomal protein L14-A	205.82	3
2507038	RecName: Full=Glycerol-1-phosphate phosphohydrolase 1; AltName: Full=(DL)-glycerol-3-phosphatase 1; AltName: Full=Related to HOR2 protein 2	204.05	3
308153652	RecName: Full=Elongation factor 3A; Short=EF-3; Short=EF-3A; AltName: Full=Eukaryotic elongation factor 3; Short=eEF3; AltName: Full=Translation elongation factor 3A; AltName: Full=Yeast elongation factor 3	203.15	3
338819289	RecName: Full=60S ribosomal protein L20-B; AltName: Full=L18a	200.68	5
1173063	RecName: Full=60S ribosomal protein L17-B; AltName: Full=L20; AltName: Full=YL17	198.75	2
132935	RecName: Full=60S ribosomal protein L33-A; AltName: Full=L37; AltName: Full=RP47; AltName: Full=YL37	194.74	4
338819319	RecName: Full=40S ribosomal protein S16-B; AltName: Full=RP61R	194.44	4
730452	RecName: Full=60S ribosomal protein L16-A; AltName: Full=L13a; AltName: Full=L21; AltName: Full=RP22; AltName: Full=YL15	188.06	1
120227	RecName: Full=FK506-binding protein 1; Short=FKBP; AltName: Full=Peptidyl-prolyl cis-trans isomerase; Short=PPIase; AltName: Full=Rapamycin-binding protein	185.89	3
338819354	RecName: Full=40S ribosomal protein S4-B; AltName: Full=RP5; AltName: Full=S7; AltName: Full=YS6	179.63	6
135743	RecName: Full=Thioredoxin-2; AltName: Full=Thioredoxin II; Short=TR-II; AltName: Full=Thioredoxin-1	177.54	1
730687	RecName: Full=40S ribosomal protein S20	176.92	4
586211	RecName: Full=V-type proton ATPase subunit B; Short=V-ATPase subunit B; AltName: Full=V-ATPase 57 kDa subunit; AltName: Full=Vacuolar proton pump subunit B	175.58	3
85681891	RecName: Full=40S ribosomal protein S22-B; AltName: Full=RP50; AltName: Full=S24; AltName: Full=YP58; AltName: Full=YS22	174.15	2
135747	RecName: Full=Thioredoxin-1; AltName: Full=Thioredoxin I; Short=TR-I; AltName: Full=Thioredoxin-2	172.78	1
229891574	RecName: Full=40S ribosomal protein S0-A; AltName:	171.59	1

	Full=Nucleic acid-binding protein NAB1A		
85681892	RecName: Full=40S ribosomal protein S28-A; AltName: Full=S33; AltName: Full=YS27	169.76	2
308153561	RecName: Full=60S ribosomal protein L28; AltName: Full=L27a; AltName: Full=L29; AltName: Full=RP44; AltName: Full=RP62; AltName: Full=YL24	169.60	3
124159	RecName: Full=Isocitrate dehydrogenase [NAD] subunit 2, mitochondrial; AltName: Full=Isocitric dehydrogenase; AltName: Full=NAD(+)-specific ICDH; Flags: Precursor	169.29	3
224493074	RecName: Full=Adenylate kinase; AltName: Full=ATP-AMP transphosphorylase; AltName: Full=ATP:AMP phosphotransferase; AltName: Full=Adenylate kinase cytosolic and mitochondrial; AltName: Full=Adenylate monophosphate kinase; Flags: Precursor	165.81	4
85681890	RecName: Full=60S ribosomal protein L11-B; AltName: Full=L16; AltName: Full=RP39; AltName: Full=YL22	162.42	2
1352907	RecName: Full=Adenosine kinase	155.20	2
1709086	RecName: Full=Mannose-1-phosphate guanyltransferase; AltName: Full=ATP-mannose-1-phosphate guanylyltransferase; AltName: Full=GDP-mannose pyrophosphorylase; AltName: Full=NDP-hexose pyrophosphorylase	153.24	3
2507307	RecName: Full=60S ribosomal protein L3; AltName: Full=Maintenance of killer protein 8; AltName: Full=RP1; AltName: Full=Trichodermin resistance protein; AltName: Full=YL1	148.42	5
132943	RecName: Full=60S ribosomal protein L24-A; AltName: Full=L30; AltName: Full=RP29; AltName: Full=YL21	145.06	3
123579	RecName: Full=Heat shock protein 60, mitochondrial; AltName: Full=CPN60; AltName: Full=P66; AltName: Full=Stimulator factor I 66 kDa component; Flags: Precursor	137.87	3
1346525	RecName: Full=S-adenosylmethionine synthase 1; Short=AdoMet synthase 1; AltName: Full=Methionine adenosyltransferase 1; Short=MAT 1	137.69	1
1346246	RecName: Full=Heat shock protein 104; AltName: Full=Protein aggregation-remodeling factor HSP104	137.23	3
1172812	RecName: Full=60S ribosomal protein L10; AltName: Full=L9; AltName: Full=Ubiquinol-cytochrome C reductase complex subunit VI-requiring protein	135.56	2
1708310	RecName: Full=Heat shock protein homolog SSE1; AltName: Full=Chaperone protein MSI3	135.42	3
338819356	RecName: Full=40S ribosomal protein S6-B; AltName: Full=RP9; AltName: Full=S10; AltName: Full=YS4	132.77	2
133962	RecName: Full=40S ribosomal protein S17-A; AltName: Full=RP51A	132.29	2
118513	RecName: Full=Aspartate-semialdehyde dehydrogenase; Short=ASA dehydrogenase;	130.05	1

	Short=ASADH; AltName: Full=Aspartate-beta-semialdehyde dehydrogenase		
1173255	RecName: Full=40S ribosomal protein S3; AltName: Full=RP13; AltName: Full=YS3	129.06	3
127027	RecName: Full=Protein MET17; Includes: RecName: Full=O-acetylhomoserine sulfhydrylase; Short=OAH sulfhydrylase; AltName: Full=Homocysteine synthase; Includes: RecName: Full=O-acetylserine sulfhydrylase; Short=OAS sulfhydrylase	128.34	1
68846657	RecName: Full=Mitochondrial outer membrane protein porin 1; AltName: Full=Voltage-dependent anion-selective channel protein 1; Short=VDAC-1	123.93	3
549064	RecName: Full=Translationally-controlled tumor protein homolog; Short=TCTP; AltName: Full=Microtubule and mitochondria-interacting protein 1; AltName: Full=Translation machinery-associated protein 19	123.32	5
133858	RecName: Full=40S ribosomal protein S19-B; AltName: Full=RP55B; AltName: Full=S16a; AltName: Full=YS16B	122.85	3
132948	RecName: Full=60S ribosomal protein L30; AltName: Full=L32; AltName: Full=RP73; AltName: Full=YL38	122.27	3
134039200	RecName: Full=60S ribosomal protein L27-A	120.62	3
1350929	RecName: Full=40S ribosomal protein S12	120.15	2
728743	RecName: Full=6-phosphogluconate dehydrogenase, decarboxylating 1	115.11	1
2500369	RecName: Full=60S ribosomal protein L21-B	114.30	3
38372623	RecName: Full=Actin	106.15	3
133066	RecName: Full=60S acidic ribosomal protein P2-alpha; Short=P2A; AltName: Full=A2; AltName: Full=L12EIB; AltName: Full=L44; AltName: Full=YP2alpha	105.31	1
1707995	RecName: Full=Serine hydroxymethyltransferase, cytosolic; Short=SHMT; AltName: Full=Glycine hydroxymethyltransferase; AltName: Full=Serine methylase	102.96	3
134633	RecName: Full=Superoxide dismutase [Cu-Zn]	102.23	1
130240	RecName: Full=CDP-diacylglycerol--inositol 3-phosphatidyltransferase; AltName: Full=Phosphatidylinositol synthase; Short=PI synthase; Short=PtdIns synthase	101.20	2
1351010	RecName: Full=40S ribosomal protein S7-B	95.75	1
137464	RecName: Full=V-type proton ATPase catalytic subunit A; Short=V-ATPase subunit A; AltName: Full=Vacuolar proton pump subunit A; Contains: RecName: Full=Endonuclease PI-SceI; AltName: Full=Sce VMA intein; AltName: Full=VMA1-derived endonuclease; Short=VDE	94.99	3
347595816	RecName: Full=Glutamine synthetase; Short=GS; AltName: Full=Glutamate--ammonia ligase	93.53	1

417090	RecName: Full=GTP-binding nuclear protein GSP1/CNR1; AltName: Full=Chromosome stability protein 17; AltName: Full=GTPase Ran homolog; AltName: Full=Genetic suppressor of PRP20-1	90.41	2
73921293	RecName: Full=Protein ZEO1; AltName: Full=Zeocin resistance protein 1	88.21	1
2507329	RecName: Full=40S ribosomal protein S7-A; AltName: Full=RP30; AltName: Full=RP40	86.42	2
730458	RecName: Full=40S ribosomal protein S26-A	86.08	2
1350741	RecName: Full=60S ribosomal protein L36-A; AltName: Full=L39; AltName: Full=YL39	84.60	2
1723685	RecName: Full=Sphingolipid long chain base-responsive protein PIL1	80.27	1
135816	RecName: Full=Threonine synthase; Short=TS	80.20	1
338819315	RecName: Full=40S ribosomal protein S11-B; AltName: Full=RP41; AltName: Full=S18; AltName: Full=YS12	78.96	2
1705679	RecName: Full=Cell division control protein 48; AltName: Full=Cell division cycle protein 48	76.05	2
1710574	RecName: Full=60S ribosomal protein L26-A; AltName: Full=L33; AltName: Full=YL33	75.31	3
338819295	RecName: Full=60S ribosomal protein L35-B	70.27	1
133036	RecName: Full=60S ribosomal protein L9-A; AltName: Full=L8; AltName: Full=RP24; AltName: Full=YL11	69.58	2
464970	RecName: Full=Peroxiredoxin TSA1; AltName: Full=Cytoplasmic thiol peroxidase 1; Short=cTPx 1; AltName: Full=PRP; AltName: Full=Thiol-specific antioxidant protein 1; AltName: Full=Thioredoxin peroxidase	69.19	3
121087	RecName: Full=Glycerol 2-dehydrogenase (NADP(+)); AltName: Full=Galactose-inducible crystallin-like protein 1	69.07	1
1176558	RecName: Full=40S ribosomal protein S10-B	66.60	1
1710538	RecName: Full=60S ribosomal protein L22-A; AltName: Full=L1c; AltName: Full=RP4; AltName: Full=YL31	66.58	1
84028178	RecName: Full=ATP synthase subunit beta, mitochondrial; Flags: Precursor	62.79	1
83288131	RecName: Full=40S ribosomal protein S25-B; AltName: Full=RP45; AltName: Full=S31; AltName: Full=YS23	61.62	1
134039184	RecName: Full=Transposon Ty1-LR4 Gag polyprotein; AltName: Full=Gag-p49; AltName: Full=Transposon Ty1 protein A; Short=TY1A; Short=TYA; AltName: Full=p58; Contains: RecName: Full=Capsid protein; Short=CA; AltName: Full=Gag-p45; AltName: Full=p54; Contains: RecName: Full=Gag-p4	59.81	1
585166	RecName: Full=Galactokinase; AltName: Full=Galactose kinase	58.94	3
417441	RecName: Full=Polyadenylate-binding protein, cytoplasmic and nuclear; Short=PABP; Short=Poly(A)-binding protein; AltName: Full=ARS consensus-binding	58.48	1

	protein ACBP-67; AltName: Full=Polyadenylate tail-binding protein		
330443451	glycine--tRNA ligase [Saccharomyces cerevisiae S288c]	52.34	1
239977091	RecName: Full=Cell wall mannoprotein CIS3; AltName: Full=Covalently-linked cell wall protein 5/11; AltName: Full=Protein with internal repeats 4; AltName: Full=Soluble cell wall protein 8; Flags: Precursor	50.34	1
6137243	RecName: Full=Uncharacterized protein YLR179C	48.32	1
341940649	RecName: Full=ATP synthase subunit alpha, mitochondrial; Flags: Precursor	47.33	2
399368	RecName: Full=Homoserine dehydrogenase; Short=HDH	47.33	1
158515407	RecName: Full=Inorganic pyrophosphatase; AltName: Full=Pyrophosphate phospho-hydrolase; Short=PPase	45.57	2
417810	RecName: Full=Single-stranded nucleic acid-binding protein	43.45	1
730570	RecName: Full=Ribosome biogenesis protein RLP7; AltName: Full=Ribosomal protein L7-like	42.79	1
544232	RecName: Full=Elongation factor 1-gamma 2; Short=EF-1-gamma 2; AltName: Full=Eukaryotic elongation factor 1Bgamma 2; Short=eEF1Bgamma 2; AltName: Full=Translation elongation factor 1B gamma 2	40.09	2

LegC7^{T122P}

Accession	Description	Score	# Peptides
129930	RecName: Full=Phosphoglycerate kinase	3836.30	35
123624	RecName: Full=Heat shock protein SSA2	3761.43	3
417149	RecName: Full=Heat shock protein SSA1; AltName: Full=Heat shock protein YG100	3734.11	2
119337	RecName: Full=Enolase 2; AltName: Full=2-phospho-D-glycerate hydro-lyase 2; AltName: Full=2-phosphoglycerate dehydratase 2	3210.23	6
1169787	RecName: Full=Glyceraldehyde-3-phosphate dehydrogenase 3; Short=GAPDH 3	2657.83	7
308153602	RecName: Full=Enolase 1; AltName: Full=2-phospho-D-glycerate hydro-lyase 1; AltName: Full=2-phosphoglycerate dehydratase 1	2170.20	4
120645	RecName: Full=Glyceraldehyde-3-phosphate dehydrogenase 2; Short=GAPDH 2	2119.43	1
123634	RecName: Full=Heat shock protein SSA4	1789.34	1
1708315	RecName: Full=ATP-dependent molecular chaperone HSC82; AltName: Full=82 kDa heat shock cognate protein; AltName: Full=Heat shock protein Hsp90 constitutive isoform	1680.96	3
125609	RecName: Full=Pyruvate kinase 1; Short=PK 1; AltName: Full=cell division cycle protein 19	1661.98	25

123677	RecName: Full=ATP-dependent molecular chaperone HSP82; AltName: Full=82 kDa heat shock protein; AltName: Full=Heat shock protein Hsp90 heat-inducible isoform	1566.57	2
1169517	RecName: Full=Protein EMP47; AltName: Full=47 kDa endomembrane protein; AltName: Full=Endosomal P44 protein; Flags: Precursor	1440.95	20
391359302	RecName: Full=Heat shock protein SSC1, mitochondrial; AltName: Full=Endonuclease SceI 75 kDa subunit; Short=Endo.SceI 75 kDa subunit; AltName: Full=mtHSP70; Flags: Precursor	1095.10	14
136069	RecName: Full=Triosephosphate isomerase; Short=TIM; AltName: Full=Triose-phosphate isomerase	1059.72	12
1169786	RecName: Full=Glyceraldehyde-3-phosphate dehydrogenase 1; Short=GAPDH 1	1040.06	3
123635	RecName: Full=Heat shock protein SSB1; AltName: Full=Cold-inducible protein YG101	1021.99	1
729768	RecName: Full=Heat shock protein SSB2	1013.56	1
30923172	RecName: Full=Pyruvate decarboxylase isozyme 1	981.50	14
119161	RecName: Full=Elongation factor 1-alpha; Short=EF-1-alpha; AltName: Full=Eukaryotic elongation factor 1A; Short=eEF1A; AltName: Full=Translation elongation factor 1A	943.60	17
548534	RecName: Full=Phosphoglycerate mutase 1; Short=PGAM 1; AltName: Full=BPG-dependent PGAM 1; AltName: Full=MPGM 1; AltName: Full=Phosphoglyceromutase 1	917.48	13
123579	RecName: Full=Heat shock protein 60, mitochondrial; AltName: Full=CPN60; AltName: Full=P66; AltName: Full=Stimulator factor I 66 kDa component; Flags: Precursor	887.43	7
416935	RecName: Full=Elongation factor 2; Short=EF-2; AltName: Full=Eukaryotic elongation factor 2; Short=eEF2; AltName: Full=Ribosomal translocase; AltName: Full=Translation elongation factor 2	794.21	14
113626	RecName: Full=Fructose-bisphosphate aldolase; Short=FBP aldolase; Short=FBPA; AltName: Full=Fructose-1,6-bisphosphate aldolase	767.26	9
586211	RecName: Full=V-type proton ATPase subunit B; Short=V-ATPase subunit B; AltName: Full=V-ATPase 57 kDa subunit; AltName: Full=Vacuolar proton pump subunit B	707.96	9
730018	RecName: Full=5-methyltetrahydropteroyltriglutamate--	698.11	12

	homocysteine methyltransferase; AltName: Full=Cobalamin-independent methionine synthase; AltName: Full=Delta-P8 protein; AltName: Full=Methionine synthase, vitamin-B12 independent isozyme		
308153683	RecName: Full=Alcohol dehydrogenase 1; AltName: Full=Alcohol dehydrogenase I; AltName: Full=YADH-1	683.87	8
121087	RecName: Full=Glycerol 2-dehydrogenase (NADP(+)); AltName: Full=Galactose-inducible crystallin-like protein 1	649.70	8
585880	RecName: Full=60S ribosomal protein L4-A; AltName: Full=L2; AltName: Full=RP2; AltName: Full=YL2	644.53	10
120745	RecName: Full=Glucose-6-phosphate isomerase; Short=GPI; AltName: Full=Phosphoglucose isomerase; Short=PGI; AltName: Full=Phosphohexose isomerase; Short=PHI	621.51	9
1709086	RecName: Full=Mannose-1-phosphate guanyltransferase; AltName: Full=ATP-mannose-1-phosphate guanylyltransferase; AltName: Full=GDP-mannose pyrophosphorylase; AltName: Full=NDP-hexose pyrophosphorylase	577.44	9
121575	RecName: Full=78 kDa glucose-regulated protein homolog; Short=GRP-78; AltName: Full=Immunoglobulin heavy chain-binding protein homolog; Short=BiP; Flags: Precursor	571.60	1
1168544	RecName: Full=Plasma membrane ATPase 1; AltName: Full=Proton pump 1	534.51	9
417670	RecName: Full=60S ribosomal protein L8-B; AltName: Full=L4; AltName: Full=L4-1; AltName: Full=RP6; AltName: Full=YL5	514.53	10
118110	RecName: Full=Peptidyl-prolyl cis-trans isomerase; Short=PPIase; AltName: Full=Cyclophilin; Short=CPH; AltName: Full=Cyclosporin A-binding protein; AltName: Full=PPI-II; AltName: Full=Rotamase	508.90	6
585166	RecName: Full=Galactokinase; AltName: Full=Galactose kinase	476.87	8
585169	RecName: Full=Bifunctional protein GAL10; Includes: RecName: Full=UDP-glucose 4-epimerase; AltName: Full=Galactowaldenase; Includes: RecName: Full=Aldose 1-epimerase; AltName: Full=Galactose mutarotase	473.84	8
1350934	RecName: Full=40S ribosomal protein S13; AltName: Full=S27a; AltName: Full=YS15	456.60	7
730701	RecName: Full=Adenosylhomocysteinase;	440.31	6

	Short=AdoHcyase; AltName: Full=S-adenosyl-L-homocysteine hydrolase		
1346246	RecName: Full=Heat shock protein 104; AltName: Full=Protein aggregation-remodeling factor HSP104	434.06	6
160395531	RecName: Full=ATP-dependent RNA helicase eIF4A; AltName: Full=Eukaryotic initiation factor 4A; Short=eIF-4A; AltName: Full=Stimulator factor I 37 kDa component; AltName: Full=Translation initiation factor 1/2; AltName: Full=p37	430.94	6
20981695	RecName: Full=Fatty acid synthase subunit alpha; Includes: RecName: Full=Acyl carrier; Includes: RecName: Full=3-oxoacyl-[acyl-carrier-protein] reductase; AltName: Full=Beta-ketoacyl reductase; Includes: RecName: Full=3-oxoacyl-[acyl-carrier-protein] synthase; AltName: Full=Beta-ketoacyl synthase	421.33	8
341940649	RecName: Full=ATP synthase subunit alpha, mitochondrial; Flags: Precursor	418.67	9
1173269	RecName: Full=40S ribosomal protein S5; AltName: Full=RP14; AltName: Full=S2; AltName: Full=YS8	417.23	5
549064	RecName: Full=Translationally-controlled tumor protein homolog; Short=TCTP; AltName: Full=Microtubule and mitochondria-interacting protein 1; AltName: Full=Translation machinery-associated protein 19	410.91	7
269969549	RecName: Full=40S ribosomal protein S1-B	409.49	3
229891577	RecName: Full=40S ribosomal protein S0-B; AltName: Full=Nucleic acid-binding protein NAB1B	406.59	1
2500359	RecName: Full=60S ribosomal protein L13-A	402.95	6
347595828	RecName: Full=Protein URA2; Includes: RecName: Full=Glutamine-dependent carbamoyl-phosphate synthase; Includes: RecName: Full=Aspartate carbamoyltransferase	399.02	5
224493074	RecName: Full=Adenylate kinase; AltName: Full=ATP-AMP transphosphorylase; AltName: Full=ATP:AMP phosphotransferase; AltName: Full=Adenylate kinase cytosolic and mitochondrial; AltName: Full=Adenylate monophosphate kinase; Flags: Precursor	391.13	8
338819278	RecName: Full=60S ribosomal protein L19-B; AltName: Full=L23; AltName: Full=RP15L; AltName: Full=RP33; AltName: Full=YL14	391.09	5

133962	RecName: Full=40S ribosomal protein S17-A; AltName: Full=RP51A	385.66	6
229891574	RecName: Full=40S ribosomal protein S0-A; AltName: Full=Nucleic acid-binding protein NAB1A	383.56	1
2507038	RecName: Full=Glycerol-1-phosphate phosphohydrolase 1; AltName: Full=(DL)-glycerol-3-phosphatase 1; AltName: Full=Related to HOR2 protein 2	380.63	5
1729825	RecName: Full=Transaldolase	377.34	5
133026	RecName: Full=60S ribosomal protein L7-A; AltName: Full=L6; AltName: Full=RP11; AltName: Full=YL8	376.52	7
59799591	RecName: Full=Serine/threonine-protein kinase HRK1; AltName: Full=Hygromycin resistance kinase 1	374.93	9
308153652	RecName: Full=Elongation factor 3A; Short=EF-3; Short=EF-3A; AltName: Full=Eukaryotic elongation factor 3; Short=eEF3; AltName: Full=Translation elongation factor 3A; AltName: Full=Yeast elongation factor 3	364.93	5
27808714	bleomycin hydrolase [Saccharomyces cerevisiae S288c]	360.30	4
548494	RecName: Full=Phosphoglucomutase 2; Short=PGM 2; AltName: Full=D-glucose-1,6-diphosphate:D-glucose-1-phosphate phosphotransferase; AltName: Full=Glucose phosphomutase 2	346.57	7
728968	RecName: Full=Protein BMH1	340.98	6
46397814	RecName: Full=40S ribosomal protein S14-A; AltName: Full=RP59A	331.61	5
308153499	RecName: Full=60S acidic ribosomal protein P0; Short=A0; AltName: Full=L10E	327.72	5
1710642	RecName: Full=60S ribosomal protein L16-B; AltName: Full=L21; AltName: Full=RP23; AltName: Full=YL15	327.52	3
137464	RecName: Full=V-type proton ATPase catalytic subunit A; Short=V-ATPase subunit A; AltName: Full=Vacuolar proton pump subunit A; Contains: RecName: Full=Endonuclease PI-SceI; AltName: Full=Sce VMA intein; AltName: Full=VMA1-derived endonuclease; Short=VDE	316.41	9
303308545	RecName: Full=Ubiquitin-40S ribosomal protein S31; Contains: RecName: Full=Ubiquitin; Contains: RecName: Full=40S ribosomal protein S31; AltName: Full=CEP76; AltName: Full=S37; AltName: Full=YS24; Flags: Precursor	311.34	8

1709682	RecName: Full=Peroxiredoxin type-2; AltName: Full=AHPC1; AltName: Full=Cytoplasmic thiol peroxidase 3; Short=cTPx 3; AltName: Full=Peroxiredoxin type II; AltName: Full=Peroxisomal alkyl hydroperoxide reductase; AltName: Full=TPx type II; AltName: Full=Thiol-specific antioxidant II; Short=TSA II; AltName: Full=Thioredoxin peroxidase type II; AltName: Full=Thioredoxin reductase type II	307.36	5
93204604	RecName: Full=RNA-binding protein SRO9; AltName: Full=Suppressor of RHO3 protein 9	297.95	3
137083	RecName: Full=Transcriptional regulator URE2; AltName: Full=Disulfide reductase; AltName: Full=Glutathione peroxidase	297.22	8
338819276	RecName: Full=60S ribosomal protein L18-B; AltName: Full=RP28	292.13	5
124159	RecName: Full=Isocitrate dehydrogenase [NAD] subunit 2, mitochondrial; AltName: Full=Isocitric dehydrogenase; AltName: Full=NAD(+)-specific ICDH; Flags: Precursor	288.63	4
1173063	RecName: Full=60S ribosomal protein L17-B; AltName: Full=L20; AltName: Full=YL17	288.08	4
464970	RecName: Full=Peroxiredoxin TSA1; AltName: Full=Cytoplasmic thiol peroxidase 1; Short=cTPx 1; AltName: Full=PRP; AltName: Full=Thiol-specific antioxidant protein 1; AltName: Full=Thioredoxin peroxidase	267.93	4
338819354	RecName: Full=40S ribosomal protein S4-B; AltName: Full=RP5; AltName: Full=S7; AltName: Full=YS6	264.79	8
158515407	RecName: Full=Inorganic pyrophosphatase; AltName: Full=Pyrophosphate phospho-hydrolase; Short=PPase	261.01	5
127049	RecName: Full=S-adenosylmethionine synthase 2; Short=AdoMet synthase 2; AltName: Full=Methionine adenosyltransferase 2; Short=MAT 2	259.51	1
85681891	RecName: Full=40S ribosomal protein S22-B; AltName: Full=RP50; AltName: Full=S24; AltName: Full=YP58; AltName: Full=YS22	255.75	2
338819322	RecName: Full=40S ribosomal protein S18-B	254.95	4
731845	RecName: Full=Homoisocitrate dehydrogenase, mitochondrial; Short=HIcDH; Flags: Precursor	251.87	3
585935	RecName: Full=40S ribosomal protein S9-B; AltName: Full=RP21; AltName: Full=S13; AltName: Full=YP28; AltName: Full=YS11	251.51	4
132935	RecName: Full=60S ribosomal protein L33-A; AltName: Full=L37; AltName: Full=RP47;	247.98	4

	AltName: Full=YL37		
338819346	RecName: Full=40S ribosomal protein S23-B; AltName: Full=RP37; AltName: Full=S28; AltName: Full=YS14	245.82	4
730698	RecName: Full=Protein SSP120; Flags: Precursor	244.93	5
85681890	RecName: Full=60S ribosomal protein L11-B; AltName: Full=L16; AltName: Full=RP39; AltName: Full=YL22	236.86	3
120227	RecName: Full=FK506-binding protein 1; Short=FKBP; AltName: Full=Peptidyl-prolyl cis-trans isomerase; Short=PPIase; AltName: Full=Rapamycin-binding protein	234.77	4
1168802	RecName: Full=Carboxypeptidase S; AltName: Full=GLY-X carboxypeptidase; AltName: Full=YSCS	228.73	5
548976	RecName: Full=Suppressor protein SRP40	228.70	4
730452	RecName: Full=60S ribosomal protein L16-A; AltName: Full=L13a; AltName: Full=L21; AltName: Full=RP22; AltName: Full=YL15	226.94	2
338819348	RecName: Full=40S ribosomal protein S24-B; AltName: Full=RP50	225.41	5
131619	RecName: Full=Bifunctional purine biosynthetic protein ADE5,7; Includes: RecName: Full=Phosphoribosylamine--glycine ligase; AltName: Full=Glycinamide ribonucleotide synthetase; Short=GARS; AltName: Full=Phosphoribosylglycinamide synthetase; Includes: RecName: Full=Phosphoribosylformylglycinamidine cyclo-ligase; AltName: Full=AIR synthase; Short=AIRS; AltName: Full=Phosphoribosyl-aminoimidazole synthetase	224.84	3
338819274	RecName: Full=60S ribosomal protein L12-B; AltName: Full=L15; AltName: Full=YL23	221.36	4
1352907	RecName: Full=Adenosine kinase	220.04	3
38372623	RecName: Full=Actin	217.23	4
88984204	RecName: Full=Glutaredoxin-2, mitochondrial; AltName: Full=Glutathione-dependent oxidoreductase 2; AltName: Full=Thioltransferase; Flags: Precursor	216.88	2
462072	RecName: Full=Fatty acid synthase subunit beta; Includes: RecName: Full=3-hydroxyacyl-[acyl-carrier-protein] dehydratase; Includes: RecName: Full=Enoyl-[acyl-carrier-protein] reductase [NADH]; Includes: RecName: Full=[Acyl-carrier-protein] acetyltransferase; Includes: RecName: Full=[Acyl-carrier-protein] malonyltransferase; Includes: RecName:	216.27	5

	Full=S-acyl fatty acid synthase thioesterase		
338819360	RecName: Full=40S ribosomal protein S8-B; AltName: Full=RP19; AltName: Full=S14; AltName: Full=YS9	211.86	2
127027	RecName: Full=Protein MET17; Includes: RecName: Full=O-acetylhomoserine sulfhydrylase; Short=OAH sulfhydrylase; AltName: Full=Homocysteine synthase; Includes: RecName: Full=O-acetylserine sulfhydrylase; Short=OAS sulfhydrylase	210.70	2
1346525	RecName: Full=S-adenosylmethionine synthase 1; Short=AdoMet synthase 1; AltName: Full=Methionine adenosyltransferase 1; Short=MAT 1	207.42	1
2500369	RecName: Full=60S ribosomal protein L21-B	207.04	4
728743	RecName: Full=6-phosphogluconate dehydrogenase, decarboxylating 1	206.67	4
730687	RecName: Full=40S ribosomal protein S20	199.51	3
20981689	RecName: Full=Magnesium-activated aldehyde dehydrogenase, cytosolic; AltName: Full=Mg(2+)-activated acetaldehyde dehydrogenase; Short=Mg(2+)-ACDH	199.10	4
330443451	glycine--tRNA ligase [Saccharomyces cerevisiae S288c]	195.09	4
308153666	RecName: Full=60S ribosomal protein L5; AltName: Full=L1; AltName: Full=L1a; AltName: Full=Ribosomal 5S RNA-binding protein; AltName: Full=YL3	194.56	4
338819319	RecName: Full=40S ribosomal protein S16-B; AltName: Full=RP61R	192.42	4
1710524	RecName: Full=60S ribosomal protein L25; AltName: Full=RP16L; AltName: Full=YL25; AltName: Full=YP42'	191.82	1
134221	RecName: Full=Small COPII coat GTPase SAR1; AltName: Full=GTP-binding protein SAR1; AltName: Full=Secretion-associated RAS-related protein 1	189.08	2
548854	RecName: Full=40S ribosomal protein S27-A; AltName: Full=RP61; AltName: Full=YS20	186.59	3
269969543	RecName: Full=40S ribosomal protein S1-A	186.15	1
338819289	RecName: Full=60S ribosomal protein L20-B; AltName: Full=L18a	180.17	3
731323	RecName: Full=Putative inosine-5'-monophosphate dehydrogenase 1; Short=IMP dehydrogenase 1; Short=IMPD 1; Short=IMPDH 1	178.40	1
338819356	RecName: Full=40S ribosomal protein S6-B; AltName: Full=RP9; AltName: Full=S10; AltName: Full=YS4	175.96	3

1350929	RecName: Full=40S ribosomal protein S12	174.61	3
1707995	RecName: Full=Serine hydroxymethyltransferase, cytosolic; Short=SHMT; AltName: Full=Glycine hydroxymethyltransferase; AltName: Full=Serine methylase	172.98	7
1173255	RecName: Full=40S ribosomal protein S3; AltName: Full=RP13; AltName: Full=YS3	171.62	4
125121	RecName: Full=ATP-dependent 6-phosphofructokinase subunit alpha; AltName: Full=ATP-dependent 6-phosphofructokinase; Short=ATP-PFK; Short=Phosphofructokinase 1; AltName: Full=Phosphohexokinase	171.30	3
1172812	RecName: Full=60S ribosomal protein L10; AltName: Full=L9; AltName: Full=Ubiquinol-cytochrome C reductase complex subunit VI-requiring protein	170.81	2
135747	RecName: Full=Thioredoxin-1; AltName: Full=Thioredoxin I; Short=TR-I; AltName: Full=Thioredoxin-2	167.39	1
338819293	RecName: Full=60S ribosomal protein L2-B; AltName: Full=L5; AltName: Full=RP8; AltName: Full=YL6	164.81	3
585609	RecName: Full=Pyruvate dehydrogenase E1 component subunit beta, mitochondrial; AltName: Full=Pyruvate dehydrogenase complex component E1 beta; Short=PDHE1-B; Flags: Precursor	164.74	3
2492777	RecName: Full=NADP-dependent alcohol dehydrogenase 6; AltName: Full=NADP-dependent alcohol dehydrogenase VI; AltName: Full=ScADHVI	162.19	3
134633	RecName: Full=Superoxide dismutase [Cu-Zn]	161.59	3
399275	RecName: Full=Cofilin; AltName: Full=Actin-depolymerizing factor 1	160.45	1
1705679	RecName: Full=Cell division control protein 48; AltName: Full=Cell division cycle protein 48	157.43	4
135743	RecName: Full=Thioredoxin-2; AltName: Full=Thioredoxin II; Short=TR-II; AltName: Full=Thioredoxin-1	156.46	1
74627231	RecName: Full=NADPH-dependent alpha-keto amide reductase; Short=AKR-E; AltName: Full=YKAR	154.76	2
128576	RecName: Full=Nuclear localization sequence-binding protein; AltName: Full=p67	150.89	2
133858	RecName: Full=40S ribosomal protein S19-B; AltName: Full=RP55B; AltName: Full=S16a; AltName: Full=YS16B	146.15	3
1708310	RecName: Full=Heat shock protein homolog	145.36	4

	SSE1; AltName: Full=Chaperone protein MSI3		
549656	RecName: Full=60S ribosomal protein L14-A	142.55	2
308153480	RecName: Full=Phosphoribosylaminoimidazole-succinocarboxamide synthase; AltName: Full=SAICAR synthetase	141.42	2
68846657	RecName: Full=Mitochondrial outer membrane protein porin 1; AltName: Full=Voltage-dependent anion-selective channel protein 1; Short=VDAC-1	141.31	3
1723783	RecName: Full=Probable family 17 glucosidase SCW4; AltName: Full=Soluble cell wall protein 4; Flags: Precursor	140.98	1
585376	RecName: Full=Probable mannosyltransferase KTR3	140.38	2
118094	RecName: Full=Peptidyl-prolyl cis-trans isomerase C, mitochondrial; Short=PPIase C; AltName: Full=Cyclophilin C; AltName: Full=PPI-III; AltName: Full=Rotamase C; Flags: Precursor	140.26	2
1730231	RecName: Full=Guanine nucleotide-binding protein subunit beta-like protein; AltName: Full=Receptor for activated C kinase; AltName: Full=Receptor of activated protein kinase C 1; Short=RACK1	138.96	2
124376	RecName: Full=Acetolactate synthase catalytic subunit, mitochondrial; AltName: Full=Acetohydroxy-acid synthase catalytic subunit; Short=AHAS; Short=ALS; Flags: Precursor	132.36	1
115208	RecName: Full=C-1-tetrahydrofolate synthase, cytoplasmic; Short=C1-THF synthase; Includes: RecName: Full=Methylenetetrahydrofolate dehydrogenase; Includes: RecName: Full=Methenyltetrahydrofolate cyclohydrolase; Includes: RecName: Full=Formyltetrahydrofolate synthetase	131.26	4
308153561	RecName: Full=60S ribosomal protein L28; AltName: Full=L27a; AltName: Full=L29; AltName: Full=RP44; AltName: Full=RP62; AltName: Full=YL24	130.62	1
399368	RecName: Full=Homoserine dehydrogenase; Short=HDH	130.11	2
1350741	RecName: Full=60S ribosomal protein L36-A; AltName: Full=L39; AltName: Full=YL39	127.48	2
68845631	RecName: Full=Elongation factor 1-beta; Short=EF-1-beta; AltName: Full=Eukaryotic elongation factor 1Balpha; Short=eEF1Balpha; AltName: Full=Translation elongation factor 1B	125.78	3

	alpha		
206558283	RecName: Full=Nucleolar protein 58; AltName: Full=Nucleolar protein 5	124.84	1
1709978	RecName: Full=60S ribosomal protein L15-B; AltName: Full=L13; AltName: Full=RP15R; AltName: Full=YL10; AltName: Full=YP18	122.71	1
1346942	RecName: Full=60S ribosomal protein L6-B; AltName: Full=L17; AltName: Full=RP18; AltName: Full=YL16	122.69	3
3121873	RecName: Full=Coronin-like protein	122.61	2
585167	RecName: Full=Galactose-1-phosphate uridylyltransferase; Short=Gal-1-P uridylyltransferase; AltName: Full=UDP-glucose--hexose-1-phosphate uridylyltransferase	121.66	3
84028178	RecName: Full=ATP synthase subunit beta, mitochondrial; Flags: Precursor	119.92	4
83303932	RecName: Full=Inositol-3-phosphate synthase; Short=MIP synthase; AltName: Full=Myo-inositol 1-phosphate synthase; Short=IPS; Short=MI-1-P synthase	119.25	3
2507307	RecName: Full=60S ribosomal protein L3; AltName: Full=Maintenance of killer protein 8; AltName: Full=RP1; AltName: Full=Trichodermin resistance protein; AltName: Full=YL1	118.35	4
1730165	RecName: Full=tRNA-aminoacylation cofactor ARC1; AltName: Full=Acyl-RNA-complex protein 1; AltName: Full=GU4 nucleic-binding protein 1; Short=G4p1 protein; AltName: Full=P42; AltName: Full=tRNA-interacting factor ARC1	116.91	1
730458	RecName: Full=40S ribosomal protein S26-A	111.38	2
133069	RecName: Full=60S acidic ribosomal protein P1-beta; Short=P1B; AltName: Full=Ax; AltName: Full=L12EIIB; AltName: Full=L44'; AltName: Full=YP1beta	108.30	1
135816	RecName: Full=Threonine synthase; Short=TS	106.23	3
1351010	RecName: Full=40S ribosomal protein S7-B	103.75	1
2507329	RecName: Full=40S ribosomal protein S7-A; AltName: Full=RP30; AltName: Full=RP40	102.41	3
1351256	RecName: Full=Transketolase 1; Short=TK 1	102.27	2
417090	RecName: Full=GTP-binding nuclear protein GSP1/CNR1; AltName: Full=Chromosome stability protein 17; AltName: Full=GTPase Ran homolog; AltName: Full=Genetic suppressor of PRP20-1	100.95	3
461745	RecName: Full=Citrate synthase, mitochondrial; Flags: Precursor	99.84	1

120479	RecName: Full=Farnesyl pyrophosphate synthase; Short=FPP synthase; Short=FPS; AltName: Full=(2E,6E)-farnesyl diphosphate synthase; AltName: Full=Dimethylallyltranstransferase; AltName: Full=Farnesyl diphosphate synthase; AltName: Full=Geranyltranstransferase	96.07	1
417541	RecName: Full=Pyrroline-5-carboxylate reductase; Short=P5C reductase; Short=P5CR	95.61	2
417432	RecName: Full=NADPH dehydrogenase 2; AltName: Full=Old yellow enzyme 2	91.58	4
136373	RecName: Full=Tryptophan synthase	90.32	1
418423	RecName: Full=Fumarate reductase 1; Short=FRDS1; AltName: Full=FAD-dependent oxidoreductase; AltName: Full=NADH-dependent fumarate reductase; AltName: Full=Soluble fumarate reductase, cytoplasmic isozyme	88.30	1
1710574	RecName: Full=60S ribosomal protein L26-A; AltName: Full=L33; AltName: Full=YL33	87.15	3
2498945	RecName: Full=Spermidine synthase; Short=SPDSY; AltName: Full=Putrescine aminopropyltransferase	86.00	1
134285	RecName: Full=Phosphomannomutase; Short=PMM	83.50	3
83288131	RecName: Full=40S ribosomal protein S25-B; AltName: Full=RP45; AltName: Full=S31; AltName: Full=YS23	79.13	2
73921293	RecName: Full=Protein ZEO1; AltName: Full=Zeocin resistance protein 1	79.12	1
132948	RecName: Full=60S ribosomal protein L30; AltName: Full=L32; AltName: Full=RP73; AltName: Full=YL38	78.66	3
462098	RecName: Full=Fimbrin; AltName: Full=ABP67	78.33	1
85681892	RecName: Full=40S ribosomal protein S28-A; AltName: Full=S33; AltName: Full=YS27	74.99	3
239977091	RecName: Full=Cell wall mannoprotein CIS3; AltName: Full=Covalently-linked cell wall protein 5/11; AltName: Full=Protein with internal repeats 4; AltName: Full=Soluble cell wall protein 8; Flags: Precursor	74.97	1
134039200	RecName: Full=60S ribosomal protein L27-A	74.90	1
1176558	RecName: Full=40S ribosomal protein S10-B	74.15	1
1723933	RecName: Full=NADPH-dependent aldehyde reductase ARI1	73.87	1
132943	RecName: Full=60S ribosomal protein L24-A; AltName: Full=L30; AltName: Full=RP29; AltName: Full=YL21	73.74	3
1174608	RecName: Full=Tubulin beta chain; AltName:	72.29	1

	Full=Beta-tubulin		
133066	RecName: Full=60S acidic ribosomal protein P2-alpha; Short=P2A; AltName: Full=A2; AltName: Full=L12EIB; AltName: Full=L44; AltName: Full=YP2alpha	71.66	1
544232	RecName: Full=Elongation factor 1-gamma 2; Short=EF-1-gamma 2; AltName: Full=Eukaryotic elongation factor 1Bgamma 2; Short=eEF1Bgamma 2; AltName: Full=Translation elongation factor 1B gamma 2	71.56	2
1706252	RecName: Full=Peptidyl-prolyl cis-trans isomerase CPR6; Short=PPIase CPR6; AltName: Full=Rotamase CPR6	69.64	1
73621199	RecName: Full=Multiprotein-bridging factor 1; AltName: Full=Suppressor of frameshift mutations protein 13	69.47	2
114121	RecName: Full=ADP-ribosylation factor 1	68.93	2
18266826	RecName: Full=Protein APA1; Includes: RecName: Full=Diadenosine 5',5'''-P1,P4-tetraphosphate phosphorylase 1; Short=Ap4A phosphorylase 1; AltName: Full=ADP-sulfurylase; AltName: Full=ATP adenylyltransferase; AltName: Full=Diadenosine tetraphosphate alpha,beta-phosphorylase (ADP-forming)	66.27	2
338819315	RecName: Full=40S ribosomal protein S11-B; AltName: Full=RP41; AltName: Full=S18; AltName: Full=YS12	63.98	1
549796	RecName: Full=GTP-binding protein YPT52	62.74	1
150421629	RecName: Full=Protein phosphatase 2C homolog 7, mitochondrial; Short=PP2C-7; Flags: Precursor	60.50	2
338819350	RecName: Full=40S ribosomal protein S30-B	58.76	1
1703099	RecName: Full=Acetyl-coenzyme A synthetase 2; AltName: Full=Acetate--CoA ligase 2; AltName: Full=Acyl-activating enzyme 2	58.63	2
2833223	RecName: Full=Nucleolar protein 56; AltName: Full=Ribosome biosynthesis protein SIK1; AltName: Full=Suppressor of I kappa b protein 1	58.48	1
1705966	RecName: Full=Acetyl-CoA carboxylase; Short=ACC; AltName: Full=Fatty acid synthetase 3; AltName: Full=mRNA transport-defective protein 7; Includes: RecName: Full=Biotin carboxylase	58.47	1
731427	RecName: Full=D-lactate dehydrogenase [cytochrome] 3; AltName: Full=D-lactate ferricytochrome C oxidoreductase; Short=D-LCR	58.33	1

130806	RecName: Full=Pre-mRNA-processing ATP-dependent RNA helicase PRP5	56.86	1
88983982	RecName: Full=Adenine phosphoribosyltransferase 1; Short=APRT 1	56.60	1
134039184	RecName: Full=Transposon Ty1-LR4 Gag polyprotein; AltName: Full=Gag-p49; AltName: Full=Transposon Ty1 protein A; Short=TY1A; Short=TYA; AltName: Full=p58; Contains: RecName: Full=Capsid protein; Short=CA; AltName: Full=Gag-p45; AltName: Full=p54; Contains: RecName: Full=Gag-p4	56.57	1
51704292	RecName: Full=Vacuolar transporter chaperone 4; AltName: Full=Phosphate metabolism protein 3	56.36	1
133036	RecName: Full=60S ribosomal protein L9-A; AltName: Full=L8; AltName: Full=RP24; AltName: Full=YL11	54.21	1
74627280	RecName: Full=Polyamine N-acetyltransferase 1; AltName: Full=Arylalkylamine N-acetyltransferase homolog; Short=scAANAT	52.29	1
121967	RecName: Full=Histone H2A.1	49.97	1
118823	RecName: Full=Dolichol-phosphate mannosyltransferase; AltName: Full=Dolichol-phosphate mannose synthase; Short=DPM synthase; AltName: Full=Dolichyl-phosphate beta-D-mannosyltransferase; AltName: Full=Mannose-P-dolichol synthase; Short=MPD synthase	48.71	1
285814101	TPA: glucose-6-phosphate 1-epimerase [Saccharomyces cerevisiae S288c]	47.73	1
418391	RecName: Full=Zinc-regulated transporter 1; AltName: Full=High-affinity zinc transport protein ZRT1	46.73	1
114152884	RecName: Full=Glutamate--tRNA ligase, cytoplasmic; AltName: Full=Glutamyl-tRNA synthetase; Short=(c)ERS; Short=GluRS; AltName: Full=P85	43.66	1
134265	RecName: Full=SEC14 cytosolic factor; AltName: Full=Phosphatidylinositol/phosphatidylcholine transfer protein; Short=PI/PC TP	42.87	1
110283007	RecName: Full=Ribosome-associated complex subunit SSZ1; AltName: Full=DnaK-related protein SSZ1; AltName: Full=Heat shock protein 70 homolog SSZ1; AltName: Full=Pleiotropic drug resistance protein 13	42.07	1
119857	RecName: Full=rRNA 2'-O-methyltransferase fibrillarin; AltName: Full=Histone-glutamine methyltransferase; AltName: Full=U3 small	41.19	1

	nucleolar RNA-associated protein NOP1; Short=Nucleolar protein 1; Short=U3 snoRNA-associated protein NOP1		
585885	RecName: Full=60S ribosomal protein L32	40.93	2
338819295	RecName: Full=60S ribosomal protein L35-B	40.28	1
731484	RecName: Full=D-3-phosphoglycerate dehydrogenase 1; Short=3-PGDH 1	40.12	1

Supplemental Methods:

Protease digestion and LC-MS/MS analysis of Leg C7 sample.

Precipitation of protein from SDS buffer and reduction/carbamidomethylation: Cold acetone was added to the protein mixture in SDS buffer and incubated overnight at -20 °C. The precipitate obtained was recovered by centrifugation and washed with cold acetone. Protein precipitate was redissolved in digestion buffer (50 mM aq. NH_4CO_3), reduced by DTT (25 mM for 45 min), carbamidomethylated by Iodoacetamide (90 mM for 45 min) and dialyzed against ddH_2O.

Trypsin digestion: 25 µL of digestion buffer (50 mM aq. NH_4CO_3) was added to 20 µL of Sample (~ 20.0 µg) protein solution. The protein sample was digested by adding 5 µL sequencing-grade trypsin (Promega, 0.5 µg/µL) and incubated at 37 ºC for 24 h. The digests were desalted by C18 centrifuge cartridges. The digests in elution buffer (80 % acetonitrile and 0.1 % formic acid) were dried under speed vac. The peptides and glycopeptides were subsequently re-dissolved in solvent A (0.1% formic acid in water) and stored at - 30 ºC until analysis by nano-LC-MS/MS.

Data acquisition of protein digest samples using nano-LC-MS/MS: Desalted peptides were analyzed on an Orbitrap Fusion instrument (Thermo Scientific) equipped with a nanospray ion source with CID, HCD and ETD fragmentation options and connected to a Dionex binary solvent system. Pre-packed nano-LC columns of 15 cm length with 75 µm internal diameter (id), filled with 2 µm C18 material (reverse phase) were used for chromatographic separation of samples. After the precursor ion scan at 120000 resolution in Orbitrap analyzer, precursors at a time frame of 3 sec were selected for subsequent fragmentation using HCD at normalized collision energy of 28. Another acquisition with a program HCD product triggered ETD, where ETD fragmentation occurs based on the presence of glycan oxonium ions in the HCD fragmentation of the same peptide, was also employed. The threshold for triggering an MS/MS event on ion-trap was set to 500 counts. Charge state screening was enabled, and precursors with unknown charge state or a charge state of +1 were excluded (positive ion mode). Dynamic exclusion was enabled (exclusion duration of 60 s). The fragment ions were analyzed on orbitrap for HCD at 30000 resolution.

Peptides and glycopeptide analysis: The .raw files of the LC-MS/MS acquisition were analyzed through Byonic v2.6 and Proteome Discoverer 1.4 software against the .fasta sequence of LegC7 sample. Search was conducted with modifications such as oxidation of methionine, carbamidomethylation of cysteine and possible *N*-glycans from the corresponding expression species. A precursor ion tolerance of 10 ppm and fragment ion tolerance of 0.1 Da was set for the search with up to two missed cleavage for the target enzyme trypsin. Based on the identifications of the software and manual validation of spectra, sequences of amino acids on the peptides were validated. The HCD MS^2 spectra of glycopeptides were evaluated for the glycan neutral loss pattern, oxonium ions and the glycopeptide fragmentations to assign the sequence and the presence of glycans in the glycopeptides.

A

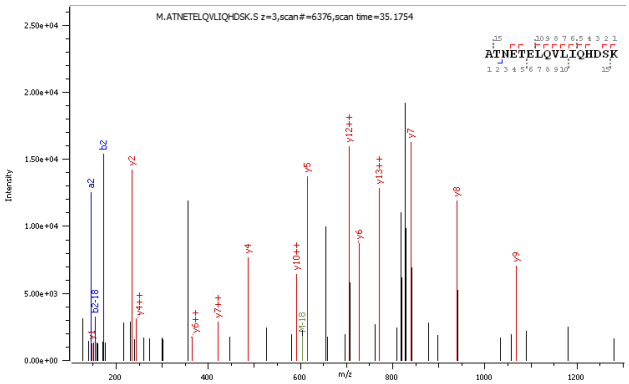
M.ATNETELQVLIQHDSK.S z=3,scan#=6376,scan time=35.1754
ATNETELQVLIQHDSK
Intensity
m/z

B

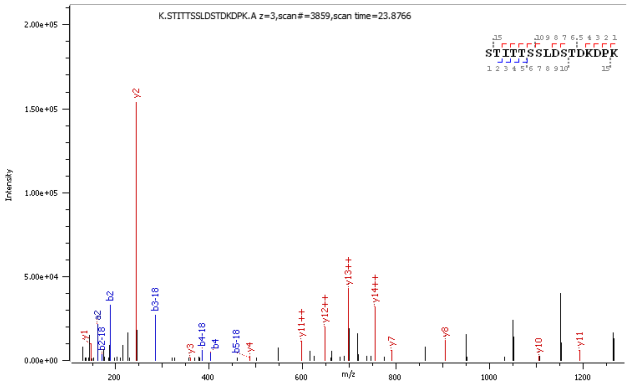
K.STITTSSLDSTDKDPK.A z=3,scan#=3859,scan time=23.8766
STITTSSLDSTDKDPK
Intensity
m/z

C

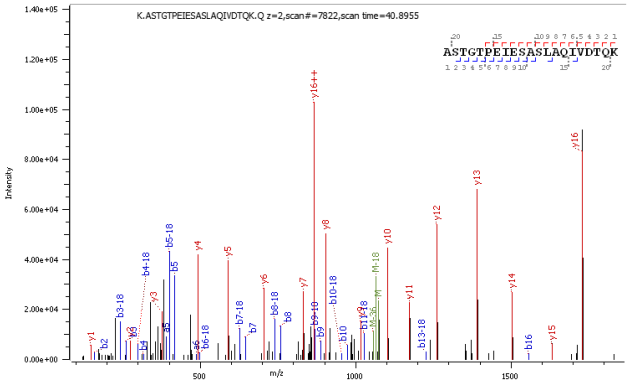
K.ASTGTPEIESASLAQIVDTQK.Q z=2,scan#=7822,scan time=40.8955
ASTGTPEIESASLAQIVDTQK
Intensity
m/z

D

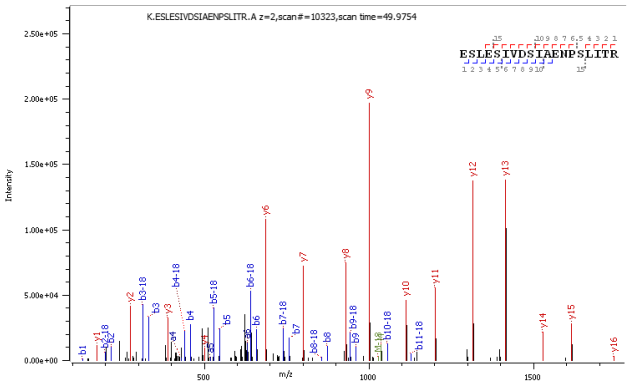
K.ESLESIVDSIAENPSLITR.A z=2,scan#=10323,scan time=49.9754
ESLESIVDSIAENPSLITR
Intensity
m/z

E

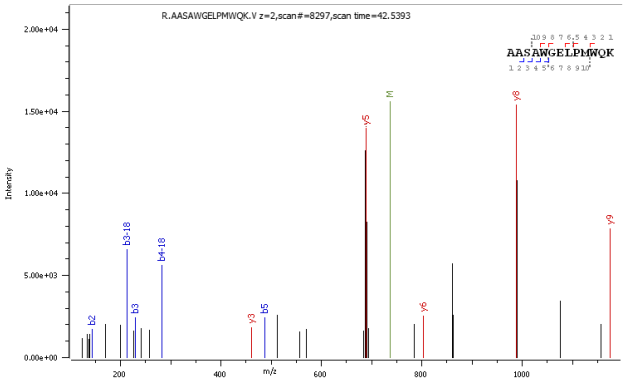
R.AASAWGELPMWQK.V z=2,scan#=8297,scan time=42.5393
AASAWGELPMWQK
Intensity
m/z

F

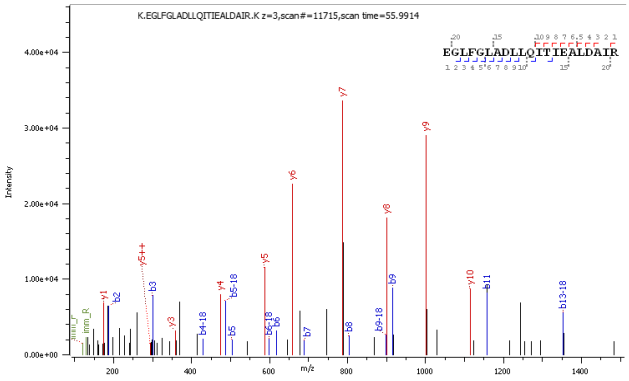
K.EGLFGLADLLQITTIEALDAIR.K z=3,scan#=11715,scan time=55.9914
EGLFGLADLLQITTIEALDAIR
Intensity
m/z

G

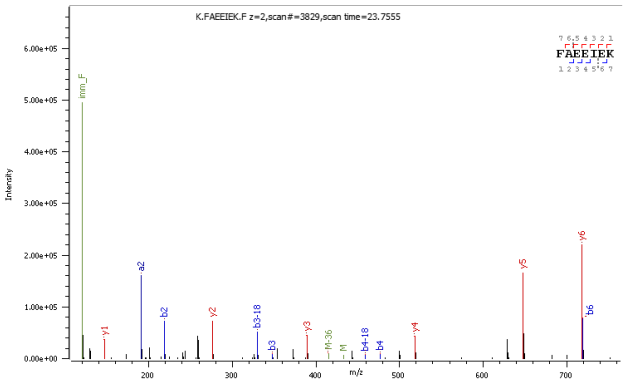
K.FAEEIEK.F z=2,scan#=3829,scan time=23.7555
FAEEIEK
Intensity
m/z
imm_F
a2
b2
y1
y2
b3-18
b3
y3
M-36
M
b4-18
b4
y4
y5
y6
b6

H

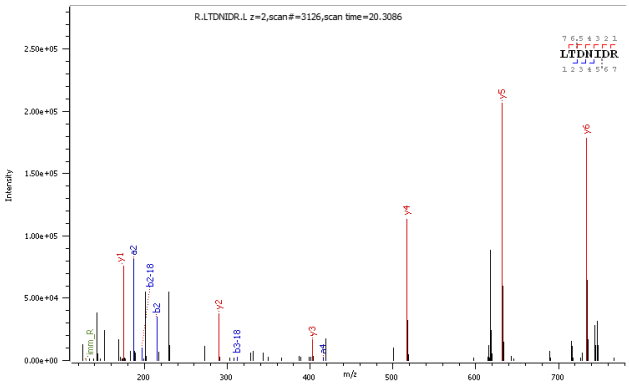
R.LTDNIDR.L z=2,scan#=3126,scan time=20.3086
LTDNIDR
Intensity
m/z
imm_R
y1
a2
b2-18
b2
y2
b3-18
y3
a4
y4
y5
y6

I

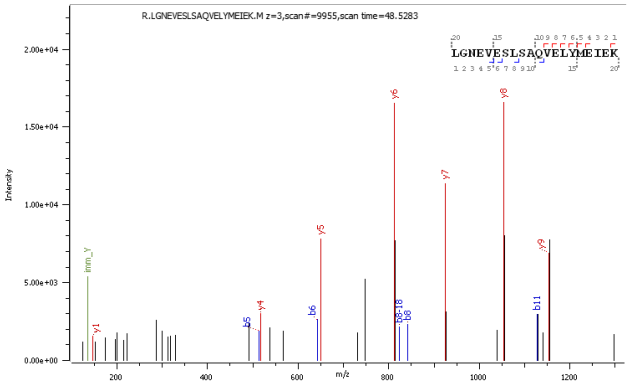
R.LGNEVESLSAQVELYMEIEK.M z=3,scan#=9955,scan time=48.5283
LGNEVESLSAQVELYMEIEK
Intensity
m/z
imm_Y
y1
b5
y4
b6
y5
y6
b8-18
b8
y7
y8
y9
b11

J

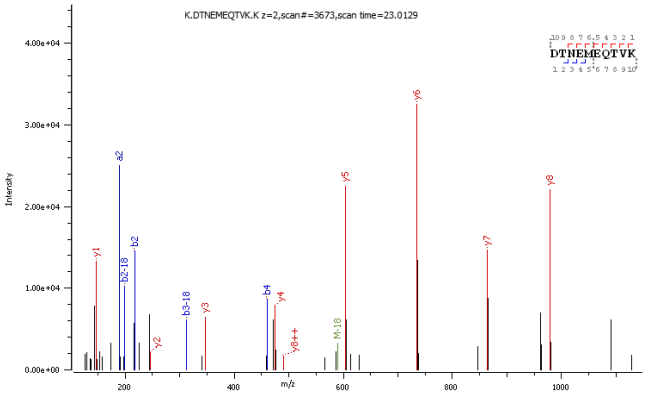
K.DTNEMEQTVK.K z=2,scan#=3673,scan time=23.0129
DTNEMEQTVK
Intensity
m/z
y1
a2
b2
b2-18
b3-18
y3
y2
b4
y4
y8++
M-18
y5
y6
y7
y8

K

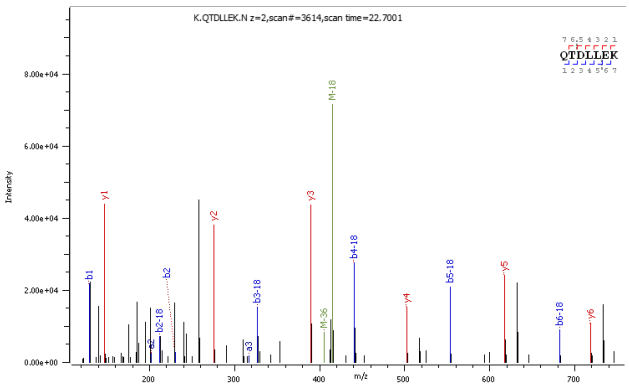
K.QTDLLEK.N z=2,scan#=3614,scan time=22.7001
QTDLLEK
Intensity
m/z
b1
y1
b2
y2
a2
b2-18
b3-18
a3
y3
M-36
M-18
b4-18
y4
b5-18
y5
b6-18
y6

L

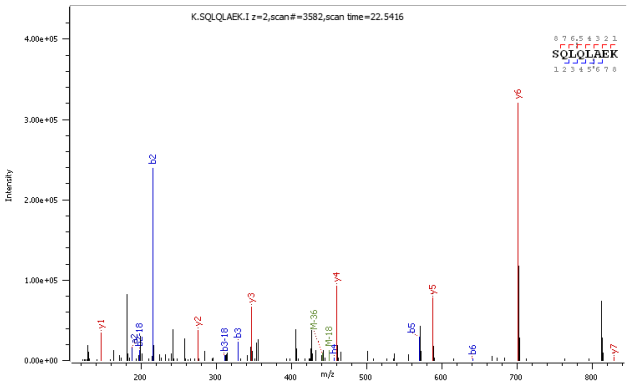
K.SQLQLAEK.I z=2,scan#=3582,scan time=22.5416
SQLQLAEK
Intensity
m/z
y1
b2
b2-18
y2
b3-18
b3
y3
M-36
M-18
y4
b5
y5
b6
y6
y7

M

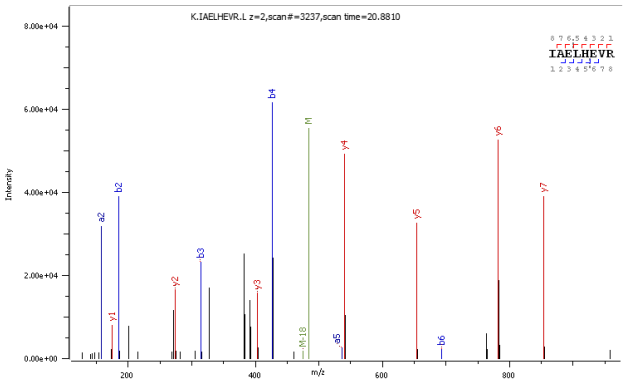
K.IAELHEVR.L z=2,scan#=3237,scan time=20.8810
IAELHEVR
Intensity
m/z

N

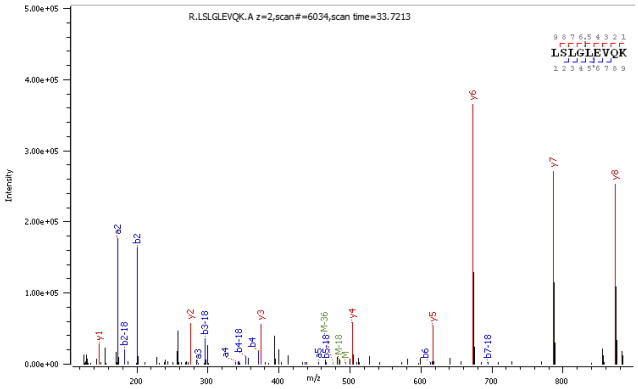
R.LSLGLEVQK.A z=2,scan#=6034,scan time=33.7213
LSLGLEVQK
Intensity
m/z

O

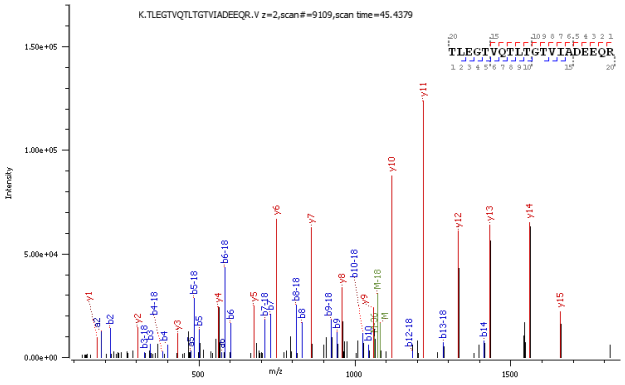
K.TLEGTVQTLTGTVIADEEQR.V z=2,scan#=9109,scan time=45.4379
TLEGTVQTLTGTVIADEEQR
Intensity
m/z

P

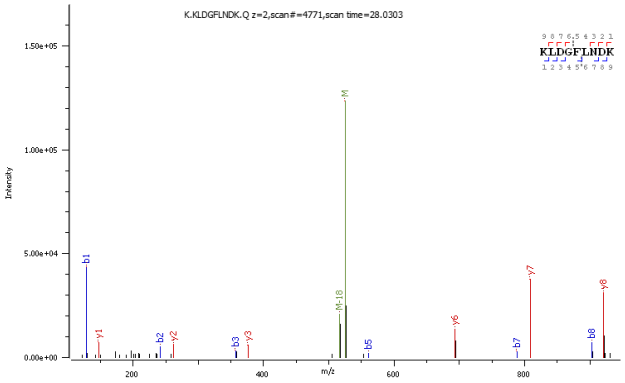

Q

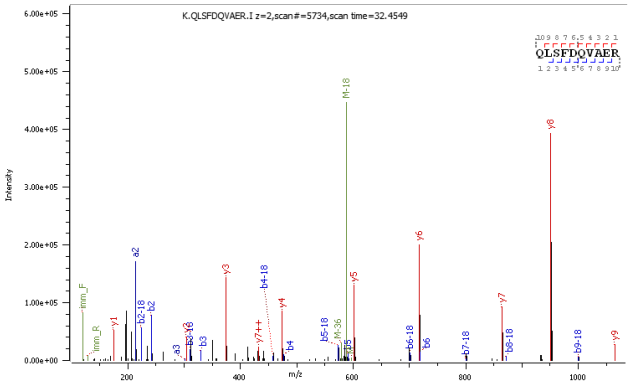

R

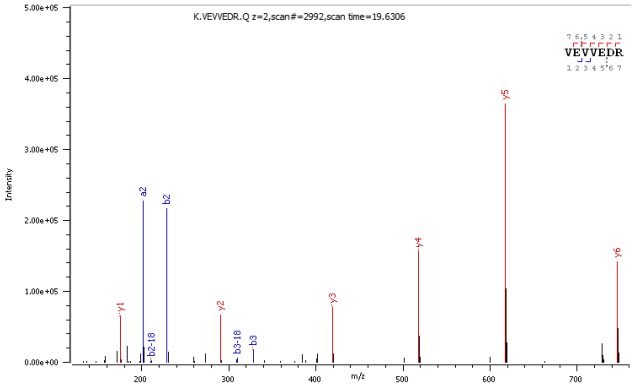

Figure 4.SI2: LegC7 is not glycosylated *in vivo.*
Full glycopeptide mass spectrometry results and supplemental methods.

CHAPTER 5

CONCLUSIONS

Legionella pneumophila utilizes effector proteins to manipulate host trafficking pathways in order to ensure its survival. Two important pathways that *Legionella* manipulates are the ER-to-Golgi trafficking pathway and the endosome maturation pathway. In order to avoid fusion of the lysosome with the LCV, *Legionella* must manipulate the endosome pathway, in order to maintain the LCV as a stable niche (Toulabi 2013, Gaspar 2014). LegC7 is a verified effector protein of *Legionella* that is translocated into host cells in a Dot/Icm dependent manner (Campodonico 2005). Initial work on LegC7, as well as our preliminary investigations, identified two major phenotypes of LegC7 expression in yeast: toxicity and vesicle trafficking defects (Campodonico 2005, de Felipe 2009, O'Brien 2015).

LegC7 was originally identified, in part, due to the aberrant secretion of CPY-Invertase, a normally vacuolar-directed protein, which demonstrated that LegC7 expression induced a general trafficking defect (de Felipe 2008). In order to better understand the trafficking defects that are induced upon LegC7 expression, we chose to observe the localization of model cargos that transit through all three biosynthetic pathways to the yeast vacuole. GFP-CPS and Sna3-GFP, two cargos that are known to traffic from the Golgi through the endosomes before final vacuolar delivery, were disrupted upon LegC7 expression (Odorizzi 1998, MacDonald 2012, O'Brien 2015). Both of these cargos localized to punctate structures throughout the cell. Interestingly these disrupted vesicles

appear to retain some proteolytic functionality as measured by partial GFP-CPS processing. Endocytic cargos such as the lipid soluble dye, FM4-64, were also disrupted upon LegC7 expression, though LegC7 does not prevent endocytosis. LegC7 does not appear to disrupt alternative trafficking pathways to the yeast vacuole. Vam3-GFP, a vacuolar SNARE, traffics to the vacuole directly from the Golgi, and the localization of this protein was unaffected by LegC7 expression (Cowles 1997). A third pathway to the vacuole known as the cytoplasm to vacuole targeting pathway (CVT), was not disrupted by LegC7 expression as measured by the proper proteolytic processing of the CVT cargo, Ape1p (Suzuki 2002). In total, these data show that LegC7 specifically disrupts the endosomal pathway while leaving alternative trafficking pathways unaltered. Given that many endosome fusion factors are utilized for other trafficking pathways to the vacuole, the specific disruption of endosomal system indicated that LegC7 targets some factor that was unique to this pathway pointing towards a defect in the early endosome maturation.

Given that LegC7 specifically disrupts endosomal traffic, we suspected that one or more endosome genes would be important for LegC7 toxicity and that when deleted, would reverse LegC7 toxicity. Ultimately we identified that deletion of the CORVET and HOPS core complex members: *VPS11, VPS16, VPS18,* and *VPS33* gave the strongest reversals of LegC7 toxicity. We also found a number of endosomal genes that gave strong (50%+) reversals: *VPS21, VPS8, VAC1, VPS34, PEP12, SYN8,* and *VPS45.* A small number of weaker interactions were discovered, centered on early endosome genes. The small number of genetic interactions that we identified, coupled with their specificity to early endosome trafficking, provides further evidence that LegC7 alters some aspect of early endosome traffic. In order to be sure that the reversal effects of these endosome genes were not simply due to a

mislocalization of LegC7, we expressed LegC7-mRuby in each of these backgrounds to look for any altered localization. We did not observe any mislocalization of LegC7-mRuby in any of these backgrounds with the exception of the *vps16* null background, indicating that the reversal effects of these deletions were more specific than simply mislocalizing LegC7. The observation that LegC7-mRuby is not mislocalized in these backgrounds provides evidence that LegC7 may not actually exist on endosomes and may impart the endosomal trafficking defects indirectly. Indeed, when we attempted to colocalize LegC7-mRuby with GFP-CPS, a disrupted cargo, we found limited overlap demonstrating that LegC7 is largely not found on the disrupted vesicles. Based on electron microscopy we noted that expression of LegC7 induces altered multivesicular body phenotypes and results in fewer intraluminal vesicles. These two phenotypes point to defects in the ESCRT pathway.

Expression of LegC7 results in the specific disruption of Vps8-GFP, a member of the early endosome trafficking complex, CORVET. Expression of LegC7 also alters the localization of GFP-Vac1 to a lesser degree. Interestingly we did not see a disruption of GFP-Vps21, the early endosome Rab GTPase. We suspect that this is due to the different mechanisms of localizations of these proteins. Vac1p is recruited to endosome membranes through a combination of interactions with Vps21p and a FYVE domain which binds to the early endosomal lipid, PI(3)P (Peterson 1999). Since Vps21p localization is not altered, we suspect that this observation explains why the Vac1p mislocalization is not more dramatic. Vps21p, like many Rab GTPases, is posttranslationally modified with a prenyl group leading to membrane association (Andres 1993). While this hydrophobic moiety explains membrane association, it does not explain localization specificity, which is still largely not understood. The fact that Vps21p is localized to the endosome membrane via an alternate

mechanism to Vac1p might point to a distinction in how LegC7 alters endosomal trafficking. LegC7-mRuby shows a high degree of colocalization with Vps8-GFP, further pointing to an effect of LegC7 on the CORVET complex. The disruption of endosomal trafficking is likely due to the fact that LegC7 appears to disrupt the localization or functionality of the CORVET complex, which is required for early endosome fusion. Consistent with this hypothesis, overexpression of *VAC1* partially suppresses LegC7 toxicity; overexpression of *VAC1* is also known to partially compensate for endosomal trafficking defects caused by deletion of members of the CORVET complex (Cabrera 2013).

In order to detect interactions between LegC7 and host proteins, we performed an immunoprecipitation of LegC7 and identified any interacting proteins via mass spectrometry. In two independent experiments we identified the glycosylated protein chaperone Emp47p, and its two known binding partners: Emp46p and Ssp120p. *EMP47* shows sequence similarly with the mammalian gene ERGIC-53. To our surprise deletion of E*MP47* resulted in the complete elimination of LegC7 toxicity which is explained by the observation that we cannot detect LegC7 in this background. The inability to detect LegC7 is likely not due to aberrant post-translational modification, as we were also unable to detect LegC7 by immunoblotting for an N-terminal His tag. Recently it was reported that upon deletion of *EMP47,* Ssp120p was also undetectable by immunoblot, drawing a parallel to LegC7 (Margulis 2015). Ssp120p is aberrantly secreted from the cells under these conditions; however, we were unable to detect LegC7 in the media, likely because LegC7 is a membrane protein. When we deleted *SRN2,* a component of the ESCRT pathway, in the context of an *emp47* null strain we restored our ability to detect LegC7. This indicates that LegC7 is degraded via the multivesicular body pathway upon deletion of *EMP47.*

In total, we have defined two general phenotypes of LegC7 expression: toxicity and endosome disruption. We propose that specific endosome disruption by LegC7 is the result of disruption of the CORVET complex. Expression of LegC7 results in a drastic mislocalization of Vps8p, a phenotype that is specific even amongst other early endosome fusion factors. The CORVET complex is only known to function in early endosome fusion events, matching the observed specificity of the LegC7 induced trafficking disruption. No members of the CORVET complex are essential genes, demonstrating that a disruption of this complex is likely not responsible for toxicity. We next wondered if LegC7 was directly or indirectly inhibiting endosome fusion. Under a direct model of inhibition, LegC7 would traffic to the endosome before having its effect on the CORVET complex, ultimately inhibiting endosome fusion. In an indirect model, LegC7 would target an upstream pathway that would result in the inability of the CORVET complex to promote endosome fusion. Two pieces of data suggest that LegC7 acts indirectly. First, deletion of early endosome trafficking genes does not result in a mislocalization of LegC7-mRuby, suggesting that LegC7 does not actually localize to endosomes. In addition to these data, we noticed limited colocalization between LegC7-mRuby and the disrupted cargo GFP-CPS. A direct inhibition effect suggests that LegC7 would be found on the disrupted compartments, so a limited overlap suggests an indirect effect. These data indicate that LegC7 likely acts earlier in the secretory pathway, preventing the trafficking of a secondary protein required for CORVET recruitment or function. In support of an indirect effect on endosome fusion, we identified the ER protein, Emp47p, as a potential interaction protein of LegC7.

Emp47p was identified as a potential interaction partner of LegC7 in two independent immunoprecipitation experiments. Deletion of *EMP47* results in the rapid and complete ESCRT dependent degradation of LegC7. Ssp120p, a known binding partner of Emp47p, also requires Emp47p for normal cellular stability, being secreted from the cell upon *EMP47* deletion (Margulis 2015). Interestingly we noted that all three identified LegC7 mutants acted differently in regards to their reliance on *EMP47.* LegC7^{N242I} and LegC7$^{\Delta 1\text{-}44}$ were in no way altered upon *emp47* deletion in terms of overall toxicity or expression levels. LegC7^{T122P}, which displays the least toxicity in wild-type cells, becomes completely toxic upon *emp47* deletion with concomitant decrease in the amount of detectable protein. These data strongly suggest that the association between Emp47p and LegC7 is responsible for the toxic event. In order to obtain a mechanistic understanding of these phenotypes we performed immunoprecipitations using LegC7^{N242I} and LegC7^{T122P}. LegC7^{N242I} immunoprecipitated with Emp47p, Emp46p, and Ssp120p suggesting that a simple binding interaction between LegC7 and Emp47p is not sufficient for phenotype induction. This matches with the fact the *EMP47* is not an essential gene eliminating a model where LegC7 simply binds to, and blocks the functionally of, Emp47p. LegC7^{T122P} immunoprecipitated with Emp47p and Ssp120p but not Emp46p. Our data rule out the possibility that LegC7 is acting as a canonical cargo protein of Emp47p because LegC7 is not glycosylated *in vivo.* Further work will be needed to more specifically define the binding interaction between LegC7 and Emp47p as well as the role of the other Emp47p subunits: Emp46p and Ssp120p. Expression of EMP47 from a plasmid will allow for both specific and random mutagenesis of EMP47 to determine which domains of EMP47 are required for the interaction with LegC7. We are seeking to mutate the di-lysine and di-

leucine motifs that are important for Emp47p trafficking in yeast cells. We also seek to mutate key residues within the carbohydrate recognition domain of EMP47. A putative coiled coil-binding domain on the luminal end of Emp47p also represents a potentially important domain for modulating LegC7 interaction.

Like the Emp47p accessory subunit, Ssp120, LegC7 cannot be detected upon deletion of *emp47.* This similarity, coupled with the differential immunoprecipitation of Emp46p with LegC7^{T122P} suggests that proper recruitment of Emp47p accessory proteins might be key in understanding the effects of LegC7. This model posits that LegC7 disrupts the functionality of Emp47p and prevents the trafficking of some number of glycosylated proteins including at least one that is involved in endosome trafficking and at least one protein that is essential for cell viability. Without any idea of Emp47p cargos, it remains speculation what the identities of these two proteins might be. A previous study utilized concanavalin A coupled resin to immunopercipitate glycoproteins that were aberrantly secreted in *emp47* null cells (Sato 2002). Repetition of this experiment coupled with mass spectrometry would identify numerous potential cargos of Emp47p and lend insight into what effects that Emp47p has on cells.

Which endosomal protein might be disrupted by deletion of *EMP47*? Vps38p of the Vps34p PI(3)P kinase complex is an appealing target. Vps38p is the only membrane protein of the 4-member complex and contains numerous canonical N-glycosylation motifs that could indicate that Vps38p is glycosylated *in vivo* and thus may be a cargo of Emp47. PI(3)P is an important marker for early endosomes and defects in PI(3)P could have wide reaching effects on the endosome system. Vac1p, which we note is mislocalized upon LegC7 expression, is localized to endosomes due in part an interaction with PI(3)P

(Weisman 1992). Vac1p binds to GTP-bound Vps21p and is thought to stabilize this active form of the Rab GTPase (Tall 1999). In turn, active Vps21p serves to recruit Vps8p to the membrane. If Vps21p were not activated or not stabilized in an active form, we would expect a defect in Vps8p recruitment to the membrane, which we observe upon LegC7 expression. PI(3)P is also required to recruit early members of the ESCRT pathway (Bilodeau 2003). Inefficient recruitment of the ESCRT components would lead to the accumulation of Class E compartments and defects in ILV formation, both of which occur in cells expressing LegC7. Thus the endosomal defects that result from LegC7 expression can be explained by a defect in the regulation of PI(3)P kinase activity. We do indeed note that PI(3)P is mislocalized upon LegC7 expression. These data alone do not prove if the PI(3)P disruption is the cause of the downstream effects, we need to confirm whether or not PI(3)P is disrupted in *emp47* null cells. Direct observation via microscopy and immunoprecipitation of Vps38p would be necessary to provide evidence for the hypothesis that Emp47p has an effect on endosomes through the trafficking of this particular protein.

Though a disruption of PI(3)P may explain the ability of LegC7 to impart endosomal trafficking defects it does not explain toxicity. No individual members of the PI(3)P kinase complex are essential genes. How then does a disruption of Emp47p activity lead to toxicity, and why do deletions in early endosomal genes reduce toxicity? There are only two essential genes in the early endosome trafficking machinery, the SNARE proteins *YKT6* and *VTI1*. These two SNARE proteins are members of the early endosome SNARE complex that is bound by the CORVET complex through its Vps33p and Vps16p subunits (Lobingier 2012, Lurick 2015, Kramer 2011). If bound CORVET/SNARE complexes were unable to be recycled due to the endosome trafficking defects induced by LegC7 than this sequestering

could result in toxicity. This hypothesis would explain why deletion of non-essential early endosome trafficking genes results in the suppression of toxicity. Our two strongest genetic suppression phenotypes are due to the deletion of *VPS16* and *VPS33,* the two SNARE binding subunits of the core complex. Indeed deletion of any of the core complex members results in strong reversals of toxicity. Disruption of earlier acting endosome fusion factors would prevent the proper assembly of the CORVET complex which in turn would lead to decreased SNARE binding. This hypothesis could be tested by purification of the CORVET complex to test for SNARE binding in the presence and absence of LegC7. Additionally, immunoprecipitations of Ykt6p or Vti1p upon LegC7 expression may provide critical clues as to the validity of this hypothesis.

Assuming our described phenotypes of LegC7 expression are similar in macrophages how do the effects of LegC7 fit with the known lifecycle of *Legionella* within host cells? The LCV does not progress far into the phagosome/endosome maturation pathway and ultimately does not fuse with the lysosome. The disruption of endosome fusion by LegC7 would act to stall host endosome maturation providing a temporal block, allowing other effector proteins to remodel the LCV membrane into an ER-like structure. Many *Legionella* effectors target ER proteins and processes so the hypothesis that LegC7 manipulates endosomal maturation through the ER protein ERGIC-53 would be consistent with the known *Legionella* lifecycle. The ERGIC-53 pathway might represent an uncharacterized host pathway that is manipulated by other *Legionella* effectors. Disruption of a protein chaperone could have far reaching implications in mammalian hosts due to the potential wide range of cargos. Using siRNA to knockdown the expression of ERGIC-53 we will test to see if LegC7 is degraded or mislocalized in mammalian cells. If this phenotype

holds true we will perform infections of macrophages with *Legionella* with and without silencing of ERGIC-53. These experiments will inform the field if *Legionella* manipulates the ERGIC-53 pathway during normal infections. We cannot rule out the possibility that LegC7 acts in concert with other effector proteins. Immunoprecipitations of LegC7 from host macrophages during infections would provide information about the binding targets of LegC7 in mammalian cells or if LegC7 acts directly with other *Legionella* effectors.

In total, this work has defined that the *Legionella pneumophila* effector protein, LegC7, specifically disrupts cargos that traffic through the endosomal system through a disruption of the CORVET complex. Based on numerous lines of evidence it appears that this disruption occurs indirectly, earlier in the secretory pathway. In support of the indirect action hypothesis, we have also shown that LegC7 requires the ER glycoprotein chaperone, Emp47p, for stability in yeast cells. The interaction between LegC7 and Emp47p likely results in the toxic event, suggesting a more important role of Emp47p in both endosomal trafficking and overall cell viability. We suggest that further work with LegC7 may help define the role of Emp47p/ERGIC-53 in both normal eukaryotic cell biology and in regards to *Legionella* infections.

REFERENCES

Akbar MA, Ray S, Krämer H. The SM protein Car/Vps33A regulates SNARE-mediated trafficking to lysosomes and lysosome-related organelles. Molecular Biology of the Cell. 2009;*20*:1705-1714.

Alexandrov K, Horiuchi H, Steele-Mortimer O, Seabra MC, Zerial M. (1994). Rab escort protein-1 is a multifunctional protein that accompanies newly prenylated rab proteins to their target membranes. The EMBO journal. 1994;*13*:5262.

Altman E, Segal G. The response regulator CpxR directly regulates expression of several *Legionella pneumophila* icm/dot components as well as new translocated substrates. Journal of Bacteriology. 2008:190:1985-96.

Andres DA, Seabra MC, Brown MS, Armstrong SA, Smeland TE, Cremers FP, Goldstein JL. cDNA cloning of component A of Rab geranylgeranyl transferase and demonstration of its role as a Rab escort protein. Cell. 1993;73:1091-9.

Angers CG, Merz AJ. HOPS interacts with Apl5 at the vacuole membrane and is required for consumption of AP-3 transport vesicles. Mol Biol Cell. 2009;20:4563-74.

Aragon V, Rossier O, Cianciotto NP. *Legionella pneumophila* genes that encode lipase and phospholipase C activitiesa. Microbiology. 2002;148:2223-31.

Arasaki K, Toomre DK, Roy CR. The *Legionella pneumophila* effector DrrA is sufficient to stimulate SNARE-dependent membrane fusion. Cell host & microbe. 2012;11:46-57.

Auffarth K, Arlt H, Lachmann J, Cabrera M, Ungermann C. Tracking of the dynamic localization of the Rab-specific HOPS subunits reveal their distinct interaction with Ypt7 and vacuoles. Cellular logistics. 2014;4:e29191.

Aurass P, Gerlach T, Becher D, Voigt B, Karste S, Bernhardt J, Riedel K, Hecker M, Flieger A. Life stage-specific proteomes of *Legionella pneumophila* reveal a highly differential abundance of virulence-associated Dot/Icm effectors. Molecular & Cellular Proteomics. 2015;15:177-200.

Aurell H, Etienne J, Forey F, Reyrolle M, Girardo P, Farge P, Decludt B, Campese C, Vandenesch F, Jarraud S. *Legionella pneumophila* serogroup 1 strain Paris: endemic distribution throughout France. Journal of clinical microbiology. 2003;41:3320-2.

Baba M, Osumi M, Scott SV, Klionsky DJ, Ohsumi Y. Two distinct pathways for targeting proteins from the cytoplasm to the vacuole/lysosome. The Journal of cell biology. 1997;139:1687-95.

Babst M, Katzmann DJ, Estepa-Sabal EJ, Meerloo T, Emr SD. Escrt-III: an endosome-associated heterooligomeric protein complex required for mvb sorting. Developmental cell. 2002;3:271-82.

Babst M, Wendland B, Estepa EJ, Emr SD. The Vps4p AAA ATPase regulates membrane association of a Vps protein complex required for normal endosome function. The EMBO journal. 1998;17:2982-93.

Bache KG, Raiborg C, Mehlum A, Stenmark H. STAM and Hrs are subunits of a multivalent ubiquitin-binding complex on early endosomes. Journal of Biological Chemistry. 2003;278:12513-21.

Baker RW, Jeffrey PD, Zick M, Phillips BP, Wickner WT, Hughson FM. A direct role for the Sec1/Munc18-family protein Vps33 as a template for SNARE assembly. Science. 2015;349:1111-4.

Balderhaar HJ, Ungermann C. CORVET and HOPS tethering complexes–coordinators of endosome and lysosome fusion. Journal of cell science. 2013a;126:1307-16.

Balderhaar HJ, Lachmann J, Yavavli E, Bröcker C, Lürick A, Ungermann C. The CORVET complex promotes tethering and fusion of Rab5/Vps21-positive membranes. Proceedings of the National Academy of Sciences. 2013b;110:3823-8.

Bandyopadhyay P, Liu S, Gabbai CB, Venitelli Z, Steinman HM. Environmental mimics and the Lvh type IVA secretion system contribute to virulence-related phenotypes of *Legionella pneumophila*. Infection and immunity. 2007;75:723-35.

Bellinger-Kawahara C, Horwitz MA. Complement component C3 fixes selectively to the major outer membrane protein (MOMP) of *Legionella pneumophila* and mediates phagocytosis of liposome-MOMP complexes by human monocytes. The Journal of experimental medicine. 1990;172:1201-10.

Bennett TL, Kraft SM, Reaves BJ, Mima J, O'Brien KM, Starai VJ. LegC3, an effector protein from *Legionella pneumophila*, inhibits homotypic yeast vacuole fusion in vivo and in vitro. PloS one. 2013;8:e56798.

Benson RF, Fields BS. Classification of the genus *Legionella*. In Seminars in respiratory infections 1998 Jun (Vol. 13, No. 2, pp. 90-99).

Belle A, Tanay A, Bitincka L, Shamir R, O'Shea EK. Quantification of protein half-lives in the budding yeast proteome. Proceedings of the National Academy of Sciences. 2006;103:13004-9.

Berger KH, Merriam JJ, Isberg RR. Altered intracellular targeting properties associated with mutations in the *Legionella pneumophila dotA* gene. Molecular microbiology. 1994;14:809-22.

Bilodeau PS, Winistorfer SC, Kearney WR, Robertson AD, Piper RC. Vps27-Hse1 and ESCRT-I complexes cooperate to increase efficiency of sorting ubiquitinated proteins at the endosome. The Journal of cell biology. 2003;163:237-43.

Block MR, Glick BS, Wilcox CA, Wieland FT, Rothman JE. Purification of an N-ethylmaleimide-sensitive protein catalyzing vesicular transport. Proceedings of the national academy of sciences. 1988;85:7852-6.

Bonifacino JS, Glick BS. The mechanisms of vesicle budding and fusion. Cell. 2004;116:153-66.

Bowers K, Lottridge J, Helliwell SB, Goldthwaite LM, Luzio JP, Stevens TH. Protein–protein interactions of ESCRT complexes in the yeast *Saccharomyces cerevisiae*. Traffic. 2004;5:194-210.

Bowers K, Stevens TH. Protein transport from the late Golgi to the vacuole in the yeast *Saccharomyces cerevisiae*. Biochimica et Biophysica Acta (BBA)-Molecular Cell Research. 2005;1744:438-54.

Brachmann CB, Davies A, Cost GJ, Caputo E, Li J, Hieter P, Boeke JD. Designer deletion strains derived from *Saccharomyces cerevisiae* S288C: a useful set of strains and plasmids for PCR-mediated gene disruption and other applications. YEAST.1998;14:115-32.

Brandhorst D, Zwilling D, Rizzoli SO, Lippert U, Lang T, Jahn R. Homotypic fusion of early endosomes: SNAREs do not determine fusion specificity. Proceedings of the National Academy of Sciences of the United States of America. 2006;103:2701-6.

Brassinga AK, Sifri CD. The *Caenorhabditis elegans* model of *Legionella* infection. In Legionella 2013 (pp. 439-461). Humana Press.

Brenner DJ, Steigerwalt AG, McDade JE. Classification of the Legionnaires' disease bacterium: *Legionella pneumophila*, genus novum, species nova, of the family *Legionellaceae*, familia nova. Annals of Internal Medicine. 1979;90:656-8.

Brett CL, Plemel RL, Lobingier BT, Vignali M, Fields S, Merz AJ. Efficient termination of vacuolar Rab GTPase signaling requires coordinated action by a GAP and a protein kinase. The Journal of cell biology. 2008;182:1141-51.

Bröcker C, Engelbrecht-Vandré S, Ungermann C. Multisubunit tethering complexes and their role in membrane fusion. Current biology. 2010;20:R943-52.

Bröcker C, Kuhlee A, Gatsogiannis C, kleine Balderhaar HJ, Hönscher C, Engelbrecht-Vandré S, Ungermann C, Raunser S. Molecular architecture of the multisubunit homotypic fusion and vacuole protein sorting (HOPS) tethering complex. Proceedings of the National Academy of Sciences. 2012;109:1991-6.

Bucci C, Lütcke A, Steele-Mortimer O, Olkkonen VM, Dupree P, Chiariello M, Bruni CB, Simons K, Zerial M. Co-operative regulation of endocytosis by three Rab5 isoforms. FEBS letters. 1995;366:65-71.

Burd CG, Emr SD. Phosphatidylinositol (3)-phosphate signaling mediated by specific binding to RING FYVE domains. Molecular cell. 1998;2:157-62.

Burd CG, Mustol PA, Schu PV, Emr SD. A yeast protein related to a mammalian Ras-binding protein, Vps9p, is required for localization of vacuolar proteins. Molecular and cellular biology. 1996;16:2369-77.

Burstein D, Zusman T, Degtyar E, Viner R, Segal G, Pupko T. Genome-scale identification of *Legionella pneumophila* effectors using a machine learning approach. PLoS Pathog. 2009;5:e1000508.

Butler JC, Breiman RF. Legionellosis. In Bacterial Infections of Humans 1998 (pp. 355-375). Springer US.

Burkhardt P, Hattendorf DA, Weis WI, Fasshauer D. Munc18a controls SNARE assembly through its interaction with the syntaxin N-peptide. The EMBO journal. 2008;27:923-33.

Burstein D, Zusman T, Degtyar E, Viner R, Segal G, Pupko T. Genome-scale identification of *Legionella pneumophila* effectors using a machine learning approach. PLoS Pathog. 2009;5:e1000508.

Burstein D, Amaro F, Zusman T, Lifshitz Z, Cohen O, Gilbert JA, Pupko T, Shuman HA, Segal G. Genomic analysis of 38 Legionella species identifies large and diverse effector repertoires. Nature genetics. 2016.

Cabezas A, Pattni K, Stenmark H. Cloning and subcellular localization of a human phosphatidylinositol 3-phosphate 5-kinase, PIKfyve/Fab1. Gene. 2006;371:34-41.

Cabrera M, Ostrowicz CW, Mari M, LaGrassa TJ, Reggiori F, Ungermann C. Vps41 phosphorylation and the Rab Ypt7 control the targeting of the HOPS complex to endosome–vacuole fusion sites. Molecular biology of the cell. 2009;20:1937-48.

Cabrera M, Langemeyer L, Mari M, Rethmeier R, Orban I, Perz A, Bröcker C, Griffith J, Klose D, Steinhoff HJ, Reggiori F. Phosphorylation of a membrane curvature–sensing motif switches function of the HOPS subunit Vps41 in membrane tethering. The Journal of cell biology. 2010;191:845-59.

Cai H, Reinisch K, Ferro-Novick S. Coats, tethers, Rabs, and SNAREs work together to mediate the intracellular destination of a transport vesicle. Developmental cell. 2007;12:671-82.

Campanacci V, Mukherjee S, Roy CR, Cherfils J. Structure of the *Legionella* effector AnkX reveals the mechanism of phosphocholine transfer by the FIC domain. The EMBO journal. 2013;32:1469-77.

Campodonico EM, Chesnel L, Roy CR. A yeast genetic system for the identification and characterization of substrate proteins transferred into host cells by the *Legionella pneumophila* Dot/Icm system. Molecular microbiology. 2005;56:918-33.

Cantalupo G, Alifano P, Roberti V, Bruni CB, Bucci C. Rab-interacting lysosomal protein (RILP): the Rab7 effector required for transport to lysosomes. The EMBO Journal. 2001;20:683-93.

Carlton JG, Martin-Serrano J. Parallels between cytokinesis and retroviral budding: a role for the ESCRT machinery. Science. 2007;316:1908-12.

Carr CM, Grote E, Munson M, Hughson FM, Novick PJ. Sec1p binds to SNARE complexes and concentrates at sites of secretion. The Journal of cell biology. 1999;146:333-44.

Cascales E, Christie PJ. The versatile bacterial type IV secretion systems. Nature Reviews Microbiology. 2003;1:137-49.

Chen J, de Felipe KS, Clarke M, Lu H, Anderson OR, Segal G, Shuman HA. *Legionella* effectors that promote nonlytic release from protozoa. Science. 2004;303:1358-61.

Chen YG, Wang Z, Ma J, Zhang L, Lu Z. Endofin, a FYVE domain protein, interacts with Smad4 and facilitates transforming growth factor-β signaling. Journal of Biological Chemistry. 2007;282:9688-95.

Chen PI, Kong C, Su X, Stahl PD. Rab5 isoforms differentially regulate the trafficking and degradation of epidermal growth factor receptors. Journal of Biological Chemistry. 2009;284:30328-38.

Chen Y, Machner MP. Targeting of the Small GTPase Rab6A′ by the *Legionella pneumophila* Effector LidA. Infection and immunity. 2013;81:2226-35.

Chien M, Morozova I, Shi S, Sheng H, Chen J, Gomez SM, Asamani G, Hill K, Nuara J, Feder M, Rineer J. The genomic sequence of the accidental pathogen *Legionella pneumophila*. Science. 2004;305:1966-8.

Choy A, Dancourt J, Mugo B, O'Connor TJ, Isberg RR, Melia TJ, Roy CR. The *Legionella* effector RavZ inhibits host autophagy through irreversible Atg8 deconjugation. Science. 2012;338:1072-6.

Chu T, Sun J, Saksena S, Emr SD. New component of ESCRT-I regulates endosomal sorting complex assembly. The Journal of cell biology. 2006;175:815-23.

Cirillo SL, Yan L, Littman M, Samrakandi MM, Cirillo JD. Role of the *Legionella pneumophila rtxA* gene in amoebae. Microbiology. 2002;148:1667-77.

Conibear E, Stevens TH. Vps52p, Vps53p, and Vps54p form a novel multisubunit complex required for protein sorting at the yeast late Golgi. Molecular biology of the cell. 2000;11:305-23.

Conibear E, Cleck JN, Stevens TH. Vps51p mediates the association of the GARP (Vps52/53/54) complex with the late Golgi t-SNARE Tlg1p. Molecular biology of the cell. 2003;14:1610-23.

Cooke FT, Dove SK, McEwen RK, Painter G, Holmes AB, Hall MN, Michell RH, Parker PJ. The stress-activated phosphatidylinositol 3-phosphate 5-kinase Fab1p is essential for vacuole function in *S. cerevisiae*. Current biology. 1998;8:1219-S2.

Cowles CR, Snyder WB, Burd CG, Emr SD. Novel Golgi to vacuole delivery pathway in yeast: identification of a sorting determinant and required transport component. The EMBO Journal. 1997;16:2769-82.

Costa J, Teixeira PG, d'Avó AF, Júnior CS, Veríssimo A. Intragenic Recombination Has a Critical Role on the Evolution of *Legionella pneumophila* Virulence-Related Effector *sidJ*. PloS one. 2014;9:e109840.

Creasey EA, Isberg RR. The protein SdhA maintains the integrity of the *Legionella*-containing vacuole. Proceedings of the National Academy of Sciences. 2012;109:3481-6.

Darsow T, Burd CG, Emr SD. Acidic di-leucine motif essential for AP-3–dependent sorting and restriction of the functional specificity of the Vam3p vacuolar t-SNARE. The Journal of cell biology. 1998;142:913-22.

D'Auria G, Jiménez-Hernández N, Peris-Bondia F, Moya A, Latorre A. *Legionella pneumophila* pangenome reveals strain-specific virulence factors. BMC genomics. 2010;11:181.

Deák F, Xu Y, Chang WP, Dulubova I, Khvotchev M, Liu X, Südhof TC, Rizo J. Munc18-1 binding to the neuronal SNARE complex controls synaptic vesicle priming. The Journal of cell biology. 2009;184:751-64.

DebRoy S, Dao J, Söderberg M, Rossier O, Cianciotto NP. *Legionella pneumophila* type II secretome reveals unique exoproteins and a chitinase that promotes bacterial persistence in the lung. Proceedings of the National Academy of Sciences. 2006;103:19146-51.

De Buck E, Lebeau I, Maes L, Geukens N, Meyen E, Van Mellaert L, Anné J, Lammertyn E. A putative twin-arginine translocation pathway in *Legionella pneumophila*. Biochemical and biophysical research communications. 2004;317:654-61.

de Felipe KS, Pampou S, Jovanovic OS, Pericone CD, Senna FY, Kalachikov S, Shuman HA. Evidence for acquisition of *Legionella* type IV secretion substrates via interdomain horizontal gene transfer. Journal of bacteriology. 2005;187:7716-26.

de Felipe KS, Glover RT, Charpentier X, Anderson OR, Reyes M, Pericone CD, Shuman HA. *Legionella* eukaryotic-like type IV substrates interfere with organelle trafficking. PLoS Pathog. 2008;4:e1000117.

Del Campo CM, Mishra AK, Wang YH, Roy CR, Janmey PA, Lambright DG. Structural basis for PI (4) P-specific membrane recruitment of the *Legionella pneumophila* effector DrrA/SidM. Structure. 2014;22:397-408.

De Renzis S, Sönnichsen B, Zerial M. Divalent Rab effectors regulate the sub-compartmental organization and sorting of early endosomes. Nature cell biology. 2002;4:124-33.

Derré I, Isberg RR. *Legionella pneumophila* replication vacuole formation involves rapid recruitment of proteins of the early secretory system. Infection and immunity. 2004 May 1;72(5):3048-53.

Demircioglu FE, Burkhardt P, Fasshauer D. The SM protein Sly1 accelerates assembly of the ER–Golgi SNARE complex. Proceedings of the National Academy of Sciences. 2014;111:13828-33.

Di Paolo G, De Camilli P. Phosphoinositides in cell regulation and membrane dynamics. Nature. 2006;443:651-7.

Dolinsky S, Haneburger I, Cichy A, Hannemann M, Itzen A, Hilbi H. The *Legionella longbeachae* Icm/Dot substrate SidC selectively binds PtdIns (4) P with nanomolar affinity and promotes pathogen vacuole-ER interactions. Infection and Immunity. 2014:IAI-01685.

Dolezal P, Aili M, Tong J, Jiang JH, Marobbio CM, fung Lee S, Schuelein R, Belluzzo S, Binova E, Mousnier A, Frankel G. *Legionella pneumophila* secretes a mitochondrial carrier protein during infection. PLoS Pathog. 2012;8:e1002459.

Dorer MS, Kirton D, Bader JS, Isberg RR. RNA interference analysis of *Legionella* in Drosophila cells: exploitation of early secretory apparatus dynamics. PLoS Pathog. 2006;2:e34.

Elliott JA, Winn WC. Treatment of alveolar macrophages with cytochalasin D inhibits uptake and subsequent growth of *Legionella pneumophila*. Infection and immunity. 1986;51:31-6.

Ellson CD, Andrews S, Stephens LR, Hawkins PT. The PX domain: a new phosphoinositide-binding module. Journal of Cell Science. 2002;115:1099-105.

Ensminger AW, Isberg RR. E3 ubiquitin ligase activity and targeting of BAT3 by multiple *Legionella pneumophila* translocated substrates. Infection and immunity. 2010;78:3905-19.

Falcón-Pérez JM, Dell'Angelica EC. The pallidin (Pldn) gene and the role of SNARE proteins in melanosome biogenesis. Pigment cell research. 2002;15:82-6.

Feyder S, De Craene JO, Bär S, Bertazzi DL, Friant S. Membrane trafficking in the yeast *Saccharomyces cerevisiae* model. International journal of molecular sciences. 2015;16:1509-25.

Fields BS, Barbaree JM, Shotts EB, Feeley JC, Morrill WE, Sanden GN, Dykstra MJ. Comparison of guinea pig and protozoan models for determining virulence of *Legionella* species. Infection and Immunity. 1986;53:553-9.

Fields BS, Benson RF, Besser RE. *Legionella* and Legionnaires' disease: 25 years of investigation. Clinical microbiology reviews. 2002;15:506-26.

Fliermans CB, Cherry WB, Orrison LH, Smith SJ, Tison DL, Pope DH. Ecological distribution of *Legionella pneumophila*. Applied and Environmental Microbiology. 1981;41:9-16.

Flores-Rodriguez N, Kenwright DA, Chung PH, Harrison AW, Stefani F, Waigh TA, Allan VJ, Woodman PG. ESCRT-0 marks an APPL1-independent transit route for EGFR between the cell surface and the EEA1-positive early endosome. Journal of cell science. 2015;128:755-67.

Finsel I, Ragaz C, Hoffmann C, Harrison CF, Weber S, van Rahden VA, Johannes L, Hilbi H. The *Legionella* effector RidL inhibits retrograde trafficking to promote intracellular replication. Cell host & microbe. 2013;14:38-50.

Finsel I, Hilbi H. Formation of a pathogen vacuole according to *Legionella pneumophila*: how to kill one bird with many stones. Cellular microbiology. 2015;17:935-50.

Fitzgeorge RB, Baskerville A, Broster M, Hambleton P, Dennis PJ. Aerosol infection of animals with strains of *Legionella pneumophila* of different virulence: comparison with intraperitoneal and intranasal routes of infection. Epidemiology and Infection. 1983;90:81-9.

Fraser DW, Tsai TR, Orenstein W, Parkin WE, Beecham HJ, Sharrar RG, Harris J, Mallison GF, Martin SM, McDade JE, Shepard CC. Legionnaires' disease: description of an epidemic of pneumonia. New England Journal of Medicine. 1977;297:1189-97.

Fuche F, Vianney A, Andrea C, Doublet P, Gilbert C. Functional type 1 secretion system involved in *Legionella pneumophila* virulence. Journal of bacteriology. 2015;197:563-71.

Fujio H, Yoshida SI, Miyamoto H, Mitsuyama M, Mizuguchi Y. Investigation of the role of macrophages and endogenous interferon-γ in natural resistance of mice against *Legionella pneumophila* infection. FEMS Microbiology Letters. 1992;89:183-91.

Fukasawa M, Varlamov O, Eng WS, Söllner TH, Rothman JE. Localization and activity of the SNARE Ykt6 determined by its regulatory domain and palmitoylation. Proceedings of the National Academy of Sciences of the United States of America. 2004;101:4815-20.

Gary JD, Wurmser AE, Bonangelino CJ, Weisman LS, Emr SD. Fab1p is essential for PtdIns (3) P 5-kinase activity and the maintenance of vacuolar size and membrane homeostasis. The Journal of cell biology. 1998;143:65-79.

Gaspar AH, Machner MP. VipD is a Rab5-activated phospholipase A1 that protects *Legionella pneumophila* from endosomal fusion. Proceedings of the National Academy of Sciences. 2014;111:4560-5.

Gerrard SR, Bryant NJ, Stevens TH. VPS21 controls entry of endocytosed and biosynthetic proteins into the yeast prevacuolar compartment. Molecular Biology of the Cell. 2000;11:613-26.

Gerrard SR, Mecklem AB, Stevens TH. The yeast endosomal t-SNARE, Pep12p, functions in the absence of its transmembrane domain. Traffic. 2000;1:45-55.

Gibson III FC, Tzianabos AO, Rodgers FG. Adherence of *Legionella pneumophila* to U-937 cells, guinea-pig alveolar macrophages, and MRC-5 cells by a novel, complement-independent binding mechanism. Canadian journal of microbiology. 1994;40:865-72.

Gillooly DJ, Morrow IC, Lindsay M, Gould R, Bryant NJ, Gaullier JM, Parton RG, Stenmark H. Localization of phosphatidylinositol 3-phosphate in yeast and mammalian cells. The EMBO journal. 2000;19:4577-88.

Glick TH, Gregg MB, Berman B, Mallison G, Rhodes WW, Kassanoff I. Pontiac fever an epidemic of unknown etiology in a health department: I. Clinical and epidemiologic aspects. American Journal of Epidemiology. 1978;107:149-60.

Glöckner G, Albert-Weissenberger C, Weinmann E, Jacobi S, Schunder E, Steinert M, Hacker J, Heuner K. Identification and characterization of a new conjugation/type IVA secretion system (*trb/tra*) of *Legionella pneumophila* Corby localized on two mobile genomic islands. International Journal of Medical Microbiology. 2008;298:411-28.

Goldstein JL, Brown MS, Anderson RG, Russell DW, Schneider WJ. Receptor-mediated endocytosis: concepts emerging from the LDL receptor system. Annual review of cell biology. 1985;1:1-39.

Goody RS, Rak A, Alexandrov K. The structural and mechanistic basis for recycling of Rab proteins between membrane compartments. Cellular and Molecular Life Sciences CMLS. 2005;62:1657-70.

Goody PR, Heller K, Oesterlin LK, Müller MP, Itzen A, Goody RS. Reversible phosphocholination of Rab proteins by *Legionella pneumophila* effector proteins. The EMBO journal. 2012;31:1774-84.

Gorvel JP, Chavrier P, Zerial M, Gruenberg J. Rab5 controls early endosome fusion in vitro. Cell. 1991;64:915-25.

Graham SC, Wartosch L, Gray SR, Scourfield EJ, Deane JE, Luzio JP, Owen DJ. Structural basis of Vps33A recruitment to the human HOPS complex by Vps16. Proceedings of the National Academy of Sciences. 2013;110:13345-50.

Gruenberg J, Griffiths G, Howell KE. Characterization of the early endosome and putative endocytic carrier vesicles in vivo and with an assay of vesicle fusion *in vitro*. The Journal of Cell Biology. 1989;108:1301-16.

Gruenberg J. The endocytic pathway: a mosaic of domains. Nature reviews Molecular cell biology. 2001;2:721-30.

Haas A, Scheglmann D, Lazar T, Gallwitz D, Wickner W. The GTPase Ypt7p of *Saccharomyces cerevisiae* is required on both partner vacuoles for the homotypic fusion step of vacuole inheritance. The EMBO Journal. 1995;14:5258.

Hackstadt T, Scidmore-Carlson MA, Shaw EI, Fischer ER. The *Chlamydia trachomatis* IncA protein is required for homotypic vesicle fusion. Cellular microbiology. 1999;1:119-30.

Hägele S, Köhler R, Merkert H, Schleicher M, Hacker J, Steinert M. *Dictyostelium discoideum*: a new host model system for intracellular pathogens of the genus *Legionella*. Cellular microbiology. 2000;2:165-71.

Haglund K, Di Fiore PP, Dikic I. Distinct monoubiquitin signals in receptor endocytosis. Trends in biochemical sciences. 2003;28:598-604.

Hales LM, Shuman HA. The *Legionella pneumophila rpoS* gene is required for growth within Acanthamoeba castellanii. Journal of bacteriology. 1999;181:4879-89.

Hama H, Tall GG, Horazdovsky BF. Vps9p is a guanine nucleotide exchange factor involved in vesicle-mediated vacuolar protein transport. Journal of Biological Chemistry. 1999;274:15284-91.

Harb OS, Venkataraman C, Haack BJ, Gao LY, Kwaik YA. Heterogeneity in the attachment and uptake mechanisms of the Legionnaires' disease bacterium, *Legionella pneumophila*, by protozoan hosts. Applied and environmental microbiology. 1998;64:126-32.

Hardiman CA, Roy CR. AMPylation is critical for Rab1 localization to vacuoles containing *Legionella pneumophila*. MBio. 2014;5:e01035-13.

Harding CR, Schroeder GN, Reynolds S, Kosta A, Collins JW, Mousnier A, Frankel G. *Legionella pneumophila* pathogenesis in the *Galleria mellonella* infection model. Infection and immunity. 2012;80:2780-90.

Hayashi T, Nakamichi M, Naitou H, Ohashi N, Imai Y, Miyake M. Proteomic analysis of growth phase-dependent expression of *Legionella pneumophila* proteins which involves regulation of bacterial virulence traits. PloS one. 2010;5:e11718.

Hayes MJ, Bryon K, Satkurunathan J, Levine TP. Yeast Homologues of Three BLOC-1 Subunits Highlight KxDL Proteins As Conserved Interactors of BLOC-1. Traffic. 2011;12:260-8.

Heidtman M, Chen EJ, Moy MY, Isberg RR. Large-scale identification of *Legionella pneumophila* Dot/Icm substrates that modulate host cell vesicle trafficking pathways. Cellular microbiology. 2009;11:230-48.

Henne WM, Buchkovich NJ, Zhao Y, Emr SD. The endosomal sorting complex ESCRT-II mediates the assembly and architecture of ESCRT-III helices. Cell. 2012;151:356-71.

Hickey CM, Stroupe C, Wickner W. The major role of the Rab Ypt7p in vacuole fusion is supporting HOPS membrane association. Journal of Biological Chemistry. 2009;284:16118-25.

Hierro A, Sun J, Rusnak AS, Kim J, Prag G, Emr SD, Hurley JH. Structure of the ESCRT-II endosomal trafficking complex. Nature. 2004;431:221-5.

Hilbi H, Weber S, Finsel I. Anchors for effectors: subversion of phosphoinositide lipids by *Legionella*. *Legionella*: from protozoa to humans. 2011:64.

Hirano S, Suzuki N, Slagsvold T, Kawasaki M, Trambaiolo D, Kato R, Stenmark H, Wakatsuki S. Structural basis of ubiquitin recognition by mammalian Eap45 GLUE domain. Nature structural & molecular biology. 2006;13:1031-2.

Hoffmann C, Finsel I, Otto A, Pfaffinger G, Rothmeier E, Hecker M, Becher D, Hilbi H. Functional analysis of novel Rab GTPases identified in the proteome of purified *Legionella*-containing vacuoles from macrophages. Cellular microbiology. 2014;16:1034-52.

Horazdovsky BF, Busch GR, Emr SD. VPS21 encodes a rab5-like GTP binding protein that is required for the sorting of yeast vacuolar proteins. The EMBO Journal. 1994;13:1297.

Horenkamp FA, Kauffman KJ, Kohler LJ, Sherwood RK, Krueger KP, Shteyn V, Roy CR, Melia TJ, Reinisch KM. The *Legionella* Anti-autophagy Effector RavZ Targets the Autophagosome via PI3P-and Curvature-Sensing Motifs. Developmental cell. 2015;34:569-76.

Horwitz MA. The Legionnaires' disease bacterium (*Legionella pneumophila*) inhibits phagosome-lysosome fusion in human monocytes. The Journal of experimental medicine. 1983;158:2108-26.

Horwitz MA, Maxfield FR. *Legionella pneumophila* inhibits acidification of its phagosome in human monocytes. The Journal of cell biology. 1984;99:1936-43.

Horwitz MA. Characterization of avirulent mutant *Legionella pneumophila* that survive but do not multiply within human monocytes. The Journal of experimental medicine. 1987;166:1310-28.

Hsu F, Zhu W, Brennan L, Tao L, Luo ZQ, Mao Y. Structural basis for substrate recognition by a unique *Legionella* phosphoinositide phosphatase. Proceedings of the National Academy of Sciences. 2012;109:13567-72.

Huotari J, Helenius A. Endosome maturation. The EMBO journal. 2011;30:3481-500.

Hutchins MU, Klionsky DJ. Vacuolar localization of oligomeric α-mannosidase requires the cytoplasm to vacuole targeting and autophagy pathway components in *Saccharomyces cerevisiae*. Journal of Biological Chemistry. 2001;276:20491-8.

Ingmundson A, Delprato A, Lambright DG, Roy CR. *Legionella pneumophila* proteins that regulate Rab1 membrane cycling. Nature. 2007;450:365-9.

Isaac DT, Laguna RK, Valtz N, Isberg RR. MavN is a *Legionella pneumophila* vacuole-associated protein required for efficient iron acquisition during intracellular growth. Proceedings of the National Academy of Sciences. 2015;112:E5208-17.

Ishii K, Enda H, Noda M, Kajino M, Kim A, Kurimoto E, Sato K, Nakano A, Kobayashi Y, Yagi H, Uchiyama S. pH-Dependent Assembly and Segregation of the Coiled-Coil Segments of Yeast Putative Cargo Receptors Emp46p and Emp47p. PloS one. 2015 Oct 8;10(10):e0140287.

Itin C, Schindler R, Hauri HP. Targeting of protein ERGIC-53 to the ER/ERGIC/cis-Golgi recycling pathway. The Journal of cell biology. 1995;131:57-67.

Ivanov SS, Charron G, Hang HC, Roy CR. Lipidation by the host prenyltransferase machinery facilitates membrane localization of *Legionella pneumophila* effector proteins. Journal of Biological Chemistry. 2010;285:34686-98.

Jacobi S, Heuner K. Description of a putative type I secretion system in *Legionella pneumophila*. International journal of medical microbiology. 2003;293:349-58.

Jeong KC, Sexton JA, Vogel JP. Spatiotemporal regulation of a *Legionella pneumophila* T4SS substrate by the metaeffector SidJ. PLoS Pathog. 2015;11:e1004695.

Kagan JC, Roy CR. *Legionella* phagosomes intercept vesicular traffic from endoplasmic reticulum exit sites. Nature cell biology. 2002;4:945-54.

Kagan JC, Stein MP, Pypaert M, Roy CR. *Legionella* subvert the functions of Rab1 and Sec22b to create a replicative organelle. The Journal of experimental medicine. 2004;199:1201-11.

Kalaidzidis I, Miaczynska M, Brewińska-Olchowik M, Hupalowska A, Ferguson C, Parton RG, Kalaidzidis Y, Zerial M. APPL endosomes are not obligatory endocytic intermediates but act as stable cargo-sorting compartments. The Journal of cell biology. 2015;211:123-44.

Kato M, Wickner W. Ergosterol is required for the Sec18/ATP-dependent priming step of homotypic vacuole fusion. The EMBO Journal. 2001;20:4035-40.

Katzmann DJ, Babst M, Emr SD. Ubiquitin-dependent sorting into the multivesicular body pathway requires the function of a conserved endosomal protein sorting complex, ESCRT-I. Cell. 2001;106:145-55.

Katzmann DJ, Stefan CJ, Babst M, Emr SD. Vps27 recruits ESCRT machinery to endosomes during MVB sorting. The Journal of cell biology. 2003;162:413-23.

Kawamata T, Kamada Y, Suzuki K, Kuboshima N, Akimatsu H, Ota S, Ohsumi M, Ohsumi Y. Characterization of a novel autophagy-specific gene, ATG29. Biochemical and biophysical research communications. 2005;338:1884-9.

Kawasaki N, Ichikawa Y, Matsuo I, Totani K, Matsumoto N, Ito Y, Yamamoto K. The sugar-binding ability of ERGIC-53 is enhanced by its interaction with MCFD2. Blood. 2008;111:1972-9.

Kaufmann AF, McDade JE, Patton CM, Bennett JV, Skaliy P, Feeley JC, Anderson DC, Potter ME, Newhouse VF, Gregg MB, Brachman PS. Pontiac fever: isolation of the etiologic agent (*Legionella pneumophila*) and demonstration of its mode of transmission. American journal of epidemiology. 1981;114:337-47.

Kihara A, Noda T, Ishihara N, Ohsumi Y. Two Distinct Vps34 Phosphatidylinositol 3–Kinase Complexes Function in Autophagy and Carboxypeptidase Y Sorting in *Saccharomyces cerevisiae*. The Journal of cell biology. 2001;152:519-30.

Kirisako T, Baba M, Ishihara N, Miyazawa K, Ohsumi M, Yoshimori T, Noda T, Ohsumi Y. Formation process of autophagosome is traced with Apg8/Aut7p in yeast. The Journal of cell biology. 1999;147:435-46.

Kim BY, Ueda M, Kominami E, Akagawa K, Kohsaka S, Akazawa C. Identification of mouse Vps16 and biochemical characterization of mammalian class C Vps complex. Biochemical and biophysical research communications. 2003;311:577-82.

Kim J, Scott SV, Oda MN, Klionsky DJ. Transport of a large oligomeric protein by the cytoplasm to vacuole protein targeting pathway. The Journal of cell biology. 1997;137:609-18.

King NP, Newton P, Schuelein R, Brown DL, Petru M, Zarsky V, Dolezal P, Luo L, Bugarcic A, Stanley AC, Murray RZ. Soluble NSF attachment protein receptor molecular mimicry by a *Legionella pneumophila* Dot/Icm effector. Cellular microbiology. 2015;17:767-84.

Klionsky DJ, Emr SD. Membrane protein sorting: biosynthesis, transport and processing of yeast vacuolar alkaline phosphatase. The EMBO Journal. 1989;8:2241.

Kölling R, Hollenberg CP. The ABC-transporter Ste6 accumulates in the plasma membrane in a ubiquitinated form in endocytosis mutants. The EMBO journal. 1994;13:3261.

Klionsky DJ, Cueva R, Yaver DS. Aminopeptidase I of *Saccharomyces cerevisiae* is localized to the vacuole independent of the secretory pathway. The Journal of Cell Biology. 1992;119:287-99.

Kostelansky MS, Sun J, Lee S, Kim J, Ghirlando R, Hierro A, Emr SD, Hurley JH. Structural and functional organization of the ESCRT-I trafficking complex. Cell. 2006;125:113-26.

Krämer L, Ungermann C. HOPS drives vacuole fusion by binding the vacuolar SNARE complex and the Vam7 PX domain via two distinct sites. Molecular biology of the cell. 2011;22:2601-11.

Krishan A. Rapid flow cytofluorometric analysis of mammalian cell cycle by propidium iodide staining. The Journal of cell biology. 1975;66:188-93.

Ku B, Lee KH, Park WS, Yang CS, Ge J, Lee SG, Cha SS, Shao F, Do Heo W, Jung JU, Oh BH. VipD of *Legionella pneumophila* targets activated Rab5 and Rab22 to interfere with endosomal trafficking in macrophages. PLoS Pathog. 2012;8:e1003082.

Kubori T, Shinzawa N, Kanuka H, Nagai H. *Legionella* metaeffector exploits host proteasome to temporally regulate cognate effector. PLoS Pathog. 2010;6:e1001216.

Kubori T, Koike M, Bui XT, Higaki S, Aizawa SI, Nagai H. Native structure of a type IV secretion system core complex essential for *Legionella* pathogenesis. Proceedings of the National Academy of Sciences. 2014;111:11804-9.

Kweon DH, Kim CS, Shin YK. Regulation of neuronal SNARE assembly by the membrane. Nature Structural & Molecular Biology. 2003;10:440-7.

Lachmann J, Barr FA, Ungermann C. The Msb3/Gyp3 GAP controls the activity of the Rab GTPases Vps21 and Ypt7 at endosomes and vacuoles. Molecular biology of the cell. 2012;23:2516-26.

LaGrassa TJ, Ungermann C. The vacuolar kinase Yck3 maintains organelle fragmentation by regulating the HOPS tethering complex. The Journal of cell biology. 2005;168:401-14.

Lata S, Schoehn G, Jain A, Pires R, Piehler J, Gőttlinger HG, Weissenhorn W. Helical structures of ESCRT-III are disassembled by VPS4. Science. 2008;321:1354-7.

Leber R, Silles E, Sandoval IV, Mazón MJ. Yol082p, a novel CVT protein involved in the selective targeting of aminopeptidase I to the yeast vacuole. Journal of Biological Chemistry. 2001;276:29210-7.

Lemmon MA. Membrane recognition by phospholipid-binding domains. Nature reviews Molecular cell biology. 2008;9:99-111.

Lewis MJ, Pelham HR. A new yeast endosomal SNARE related to mammalian syntaxin 8. Traffic. 2002;3:922-9.

Li SC, Kane PM. The yeast lysosome-like vacuole: endpoint and crossroads. Biochimica et Biophysica Acta (BBA)-Molecular Cell Research. 2009;1793:650-63.

Lifshitz Z, Burstein D, Peeri M, Zusman T, Schwartz K, Shuman HA, Pupko T, Segal G. Computational modeling and experimental validation of the *Legionella* and *Coxiella* virulence-related type-IVB secretion signal. Proceedings of the National Academy of Sciences. 2013;110:E707-15.

Lin YH, Doms AG, Cheng E, Kim B, Evans TR, Machner MP. Host cell-catalyzed S-palmitoylation mediates Golgi targeting of the *Legionella* ubiquitin ligase GobX. Journal of Biological Chemistry. 2015;290:25766-81.

Liu Y, Nakatsukasa K, Kotera M, Kanada A, Nishimura T, Kishi T, Mimura S, Kamura T. Non–SCF-type F-box protein Roy1/Ymr258c interacts with a Rab5-like GTPase Ypt52 and inhibits Ypt52 function. Molecular biology of the cell. 2011;22:1575-84.

Liu K, Jian Y, Sun X, Yang C, Gao Z, Zhang Z, Liu X, Li Y, Xu J, Jing Y, Mitani S. Negative regulation of phosphatidylinositol 3-phosphate levels in early-to-late endosome conversion. The Journal of cell biology. 2016;212:181-98.

Lo B, Li L, Gissen P, Christensen H, McKiernan PJ, Ye C, Abdelhaleem M, Hayes JA, Williams MD, Chitayat D, Kahr WH. Requirement of VPS33B, a member of the Sec1/Munc18 protein family, in megakaryocyte and platelet α-granule biogenesis. Blood. 2005;106:4159-66.

Lobingier BT, Merz AJ. Sec1/Munc18 protein Vps33 binds to SNARE domains and the quaternary SNARE complex. Molecular biology of the cell. 2012;23:4611-22.

Losev E, Reinke CA, Jellen J, Strongin DE, Bevis BJ, Glick BS. Golgi maturation visualized in living yeast. Nature. 2006;441:1002-6.

Lu Q, Hope LW, Brasch M, Reinhard C, Cohen SN. TSG101 interaction with HRS mediates endosomal trafficking and receptor down-regulation. Proceedings of the National Academy of Sciences. 2003;100:7626-31.

Lu H, Clarke M. Dynamic properties of *Legionella*-containing phagosomes in *Dictyostelium* amoebae. Cellular microbiology. 2005 Jul 1;7(7):995-1007.

Lürick A, Kuhlee A, Bröcker C, Kümmel D, Raunser S, Ungermann C. The HABC domain of the snare vam3 interacts with the hops tethering complex to facilitate vacuole fusion. Journal of Biological Chemistry. 2015;290:5405-13.

Luo ZQ, Isberg RR. Multiple substrates of the *Legionella pneumophila* Dot/Icm system identified by interbacterial protein transfer. Proceedings of the National Academy of Sciences of the United States of America. 2004;101:841-6.

Lupashin V, Sztul E. Golgi tethering factors. Biochimica et Biophysica Acta (BBA)-Molecular Cell Research. 2005;1744:325-39.

MacDonald C, Stringer DK, Piper RC. Sna3 is an Rsp5 adaptor protein that relies on ubiquitination for its MVB sorting. Traffic. 2012;13:586-98.

Machner MP, Isberg RR. Targeting of host Rab GTPase function by the intravacuolar pathogen *Legionella pneumophila*. Developmental cell. 2006;11:47-56.

Machner MP, Isberg RR. A bifunctional bacterial protein links GDI displacement to Rab1 activation. Science. 2007;318:974-7.

Maldonado-Báez L, Dores MR, Perkins EM, Drivas TG, Hicke L, Wendland B. Interaction between Epsin/Yap180 adaptors and the scaffolds Ede1/Pan1 is required for endocytosis. Molecular biology of the cell. 2008;19:2936-48.

Malsam J, Kreye S, Sollner TH. Membrane fusion: SNAREs and regulation. Cell Molecular Life Sciences. 2008;65:2814-32.

Manske C, Hilbi H. Metabolism of the vacuolar pathogen *Legionella* and implications for virulence. Frontiers in cellular and infection microbiology. 2013;4:125.

Margulis NG, Wilson JD, Bentivoglio CM, Dhungel N, Gitler AD, Barlowe C. Analysis of COPII Vesicles Indicates a Role for the Emp47–Ssp120 Complex in Transport of Cell Surface Glycoproteins. Traffic. 2016.

Marra A, Blander SJ, Horwitz MA, Shuman HA. Identification of a *Legionella pneumophila* locus required for intracellular multiplication in human macrophages. Proceedings of the National Academy of Sciences. 1992;89:9607-11.

Marston BJ, Lipman HB, Breiman RF. Surveillance for Legionnaires' disease: risk factors for morbidity and mortality. Archives of Internal Medicine. 1994;154:2417-22.

Matanis T, Akhmanova A, Wulf P, Del Nery E, Weide T, Stepanova T, Galjart N, Grosveld F, Goud B, De Zeeuw CI, Barnekow A. Bicaudal-D regulates COPI-independent Golgi–ER transport by recruiting the dynein–dynactin motor complex. Nature Cell Biology. 2002;4:986-92.

Matthews M, Roy CR. Identification and subcellular localization of the *Legionella pneumophila* IcmX protein: a factor essential for establishment of a replicative organelle in eukaryotic host cells. Infection and immunity. 2000;68:3971-82.

Matsuo H, Chevallier J, Mayran N, Le Blanc I, Ferguson C, Fauré J, Blanc NS, Matile S, Dubochet J, Sadoul R, Parton RG. Role of LBPA and Alix in multivesicular liposome formation and endosome organization. Science. 2004;303:531-4.

Marcusson EG, Horazdovsky BF, Cereghino JL, Gharakhanian E, Emr SD. The sorting receptor for yeast vacuolar carboxypeptidase Y is encoded by the VPS10 gene. Cell. 1994;77:579-86.

Markgraf DF, Ahnert F, Arlt H, Mari M, Peplowska K, Epp N, Griffith J, Reggiori F, Ungermann C. The CORVET subunit Vps8 cooperates with the Rab5 homolog Vps21 to induce clustering of late endosomal compartments. Molecular biology of the cell. 2009;20:5276-89.

Masui S, Sasaki T, Ishikawa H. Genes for the type IV secretion system in an intracellular symbiont, *Wolbachia*, a causative agent of various sexual alterations in arthropods. Journal of bacteriology. 2000;182:6529-31.

Maxfield FR, Yamashiro DJ. Endosome acidification and the pathways of receptor-mediated endocytosis. InImmunobiology of Proteins and Peptides IV 1987 (pp. 189-198). Springer US.

Mayer A, Wickner W, Haas A. Sec18p (NSF)-driven release of Sec17p (α-SNAP) can precede docking and fusion of yeast vacuoles. Cell. 1996;85:83-94.

Mayers JR, Wang L, Pramanik J, Johnson A, Sarkeshik A, Wang Y, Saengsawang W, Yates JR, Audhya A. Regulation of ubiquitin-dependent cargo sorting by multiple endocytic adaptors at the plasma membrane. Proceedings of the National Academy of Sciences. 2013;110:11857-62.

McDade JE, Shepard CC, Fraser DW, Tsai TR, Redus MA, Dowdle WR. Legionnaires' disease: isolation of a bacterium and demonstration of its role in other respiratory disease. New England Journal of Medicine. 1977;297:1197-203.

McNatt MW, McKittrick I, West M, Odorizzi G. Direct binding to Rsp5 mediates ubiquitin-independent sorting of Sna3 via the multivesicular body pathway. Molecular biology of the cell. 2007;18:697-706.

McEwan DG, Popovic D, Gubas A, Terawaki S, Suzuki H, Stadel D, Coxon FP, de Stegmann DM, Bhogaraju S, Maddi K, Kirchof A. PLEKHM1 regulates autophagosome-lysosome fusion through HOPS complex and LC3/GABARAP proteins. Molecular cell. 2015;57:39-54.

Miaczynska M, Pelkmans L, Zerial M. Not just a sink: endosomes in control of signal transduction. Current opinion in cell biology. 2004;16:400-6.

Misra S, Hurley JH. Crystal structure of a phosphatidylinositol 3-phosphate-specific membrane-targeting motif, the FYVE domain of Vps27p. Cell. 1999;97:657-66.

Misura KM, Scheller RH, Weis WI. Three-dimensional structure of the neuronal-Sec1–syntaxin 1a complex. Nature. 2000;404:355-62.

Morita E, Sandrin V, Chung HY, Morham SG, Gygi SP, Rodesch CK, Sundquist WI. Human ESCRT and ALIX proteins interact with proteins of the midbody and function in cytokinesis. The EMBO journal. 2007;26:4215-27.

Morrison HA, Dionne H, Rusten TE, Brech A, Fisher WW, Pfeiffer BD, Celniker SE, Stenmark H, Bilder D. Regulation of early endosomal entry by the Drosophila tumor suppressors Rabenosyn and Vps45. Molecular biology of the cell. 2008;19:4167-76.

Mousnier A, Schroeder GN, Stoneham CA, So EC, Garnett JA, Yu L, Matthews SJ, Choudhary JS, Hartland EL, Frankel G. A new method to determine in vivo interactomes reveals binding of the *Legionella pneumophila* effector PieE to multiple rab GTPases. MBio. 2014;5:e01148-14.

Munson M, Chen X, Cocina AE, Schultz SM, Hughson FM. Interactions within the yeast t-SNARE Sso1p that control SNARE complex assembly. Nature Structural & Molecular Biology. 2000;7:894-902.

Murata T, Delprato A, Ingmundson A, Toomre DK, Lambright DG, Roy CR. The *Legionella pneumophila* effector protein DrrA is a Rab1 guanine nucleotide-exchange factor. Nature cell biology. 2006;8:971-7.

Nagai H, Kagan JC, Zhu X, Kahn RA, Roy CR. A bacterial guanine nucleotide exchange factor activates ARF on *Legionella* phagosomes. Science. 2002;295:679-82.

Nagai H, Cambronne ED, Kagan JC, Amor JC, Kahn RA, Roy CR. A C-terminal translocation signal required for Dot/Icm-dependent delivery of the *Legionella* RalF protein to host cells. Proceedings of the National Academy of Sciences of the United States of America. 2005;102:826-31.

Nakatsukasa K, Kanada A, Matsuzaki M, Byrne SD, Okumura F, Kamura T. The Nutrient Stress-induced Small GTPase Rab5 Contributes to the Activation of Vesicle Trafficking and Vacuolar Activity. Journal of Biological Chemistry. 2014;289:20970-8.

Nazarian R, Falcón-Pérez JM, Dell'Angelica EC. Biogenesis of lysosome-related organelles complex 3 (BLOC-3): a complex containing the Hermansky–Pudlak syndrome (HPS) proteins HPS1 and HPS4. Proceedings of the National Academy of Sciences. 2003;100:8770-5.

Neunuebel MR, Chen Y, Gaspar AH, Backlund PS, Yergey A, Machner MP. De-AMPylation of the small GTPase Rab1 by the pathogen *Legionella pneumophila*. Science. 2011;333:453-6.

Neunuebel MR, Mohammadi S, Jarnik M, Machner MP. *Legionella pneumophila* LidA affects nucleotide binding and activity of the host GTPase Rab1. Journal of bacteriology. 2012;194:1389-400.

Nevo O, Zusman T, Rasis M, Lifshitz Z, Segal G. Identification of *Legionella pneumophila* effectors regulated by the LetAS-RsmYZ-CsrA regulatory cascade, many of which modulate vesicular trafficking. Journal of bacteriology. 2014;196:681-92.

Newton HJ, Sansom FM, Dao J, Cazalet C, Bruggemann H, Albert-Weissenberger C, Buchrieser C, Cianciotto NP, Hartland EL. Significant role for ladC in initiation of *Legionella pneumophila* infection. Infection and immunity. 2008;76:3075-85.

Nickerson DP, West M, Odorizzi G. Did2 coordinates Vps4-mediated dissociation of ESCRT-III from endosomes. The Journal of cell biology. 2006;175:715-20.

Nickerson DP, Russell MR, Lo SY, Chapin HC, Milnes JM, Merz AJ. Termination of Isoform-Selective Vps21/Rab5 Signaling at Endolysosomal Organelles by Msb3/Gyp3. Traffic. 2012;13:1411-28.

Nielsen E, Severin F, Backer JM, Hyman AA, Zerial M. Rab5 regulates motility of early endosomes on microtubules. Nature Cell Biology. 1999;1:376-82.

Nielsen E, Christoforidis S, Uttenweiler-Joseph S, Miaczynska M, Dewitte F, Wilm M, Hoflack B, Zerial M. Rabenosyn-5, a novel Rab5 effector, is complexed with hVPS45 and recruited to endosomes through a FYVE finger domain. The Journal of cell biology. 2000;151:601-12.

Ninio S, Celli J, Roy CR. A *Legionella pneumophila* effector protein encoded in a region of genomic plasticity binds to Dot/Icm-modified vacuoles. PLoS Pathog. 2009;5:e1000278.

Nordmann M, Cabrera M, Perz A, Bröcker C, Ostrowicz C, Engelbrecht-Vandré S, Ungermann C. The Mon1-Ccz1 complex is the GEF of the late endosomal Rab7 homolog Ypt7. Current Biology. 2010;20:1654-9.

Nufer O, Guldbrandsen S, Degen M, Kappeler F, Paccaud JP, Tani K, Hauri HP. Role of cytoplasmic C-terminal amino acids of membrane proteins in ER export. Journal of Cell Science. 2002;115:619-28.

Nyfeler B, Zhang B, Ginsburg D, Kaufman RJ, Hauri HP. Cargo selectivity of the ERGIC-53/MCFD2 transport receptor complex. Traffic. 2006;7:1473-81.

Nyfeler B, Reiterer V, Wendeler MW, Stefan E, Zhang B, Michnick SW, Hauri HP. Identification of ERGIC-53 as an intracellular transport receptor of α1-antitrypsin. The Journal of cell biology. 2008;180:705-12.

O'Brien KM, Lindsay EL, Starai VJ. The Legionella pneumophila effector protein, LegC7, alters yeast endosomal trafficking. PloS one. 2015;10(2).

O'Connor TJ, Boyd D, Dorer MS, Isberg RR. Aggravating genetic interactions allow a solution to redundancy in a bacterial pathogen. Science. 2012;338:1440-4.

Odorizzi G, Babst M, Emr SD. Fab1p PtdIns (3) P 5-kinase function essential for protein sorting in the multivesicular body. Cell. 1998;95:847-58.

Odorizzi G, Babst M, Emr SD. Phosphoinositide signaling and the regulation of membrane trafficking in yeast. Trends in biochemical sciences. 2000;25:229-35.

Ostrowicz CW, Bröcker C, Ahnert F, Nordmann M, Lachmann J, Peplowska K, Perz A, Auffarth K, Engelbrecht-Vandré S, Ungermann C. Defined subunit arrangement and rab interactions are required for functionality of the HOPS tethering complex. Traffic. 2010;11:1334-46.

Padrón D, Wang YJ, Yamamoto M, Yin H, Roth MG. Phosphatidylinositol phosphate 5-kinase Iβ recruits AP-2 to the plasma membrane and regulates rates of constitutive endocytosis. The Journal of cell biology. 2003;162:693-701.

Pan X, Lührmann A, Satoh A, Laskowski-Arce MA, Roy CR. Ankyrin repeat proteins comprise a diverse family of bacterial type IV effectors. Science. 2008;320:1651-4.

Paulsel AL, Merz AJ, Nickerson DP. Vps9 family protein Muk1 is the second Rab5 guanosine nucleotide exchange factor in budding yeast. Journal of Biological Chemistry. 2013;288:18162-71.

Paumet F, Rahimian V, Di Liberto M, Rothman JE. Concerted auto-regulation in yeast endosomal t-SNAREs. Journal of Biological Chemistry. 2005;280:21137-43.

Paumet F, Wesolowski J, Garcia-Diaz A, Delevoye C, Aulner N, Shuman HA, Subtil A, Rothman JE. Intracellular bacteria encode inhibitory SNARE-like proteins. PloS one. 2009;4:e7375.

Peracino B, Balest A, Bozzaro S. Phosphoinositides differentially regulate bacterial uptake and Nramp1-induced resistance to *Legionella* infection in *Dictyostelium*. Journal of cell science. 2010;123:4039-51.

Peplowska K, Markgraf DF, Ostrowicz CW, Bange G, Ungermann C. The CORVET tethering complex interacts with the yeast Rab5 homolog Vps21 and is involved in endo-lysosomal biogenesis. Developmental cell. 2007;12:739-50.

Perini ED, Schaefer R, Stöter M, Kalaidzidis Y, Zerial M. Mammalian CORVET is required for fusion and conversion of distinct early endosome subpopulations. Traffic. 2014;15:1366-89.

Peter AT, Lachmann J, Rana M, Bunge M, Cabrera M, Ungermann C. The BLOC-1 complex promotes endosomal maturation by recruiting the Rab5 GTPase-activating protein Msb3. The Journal of cell biology. 2013;201:97-111.

Peterson MR, Burd CG, Emr SD. Vac1p coordinates Rab and phosphatidylinositol 3-kinase signaling in Vps45p-dependent vesicle docking/fusion at the endosome. Current biology. 1999;9:159-S1.

Peterson MR, Emr SD. The class C Vps complex functions at multiple stages of the vacuolar transport pathway. Traffic. 2001;2:476-86.

Perini ED, Schaefer R, Stöter M, Kalaidzidis Y, Zerial M. Mammalian CORVET is required for fusion and conversion of distinct early endosome subpopulations. Traffic. 2014;15:1366-89.

Pine L, George JR, Reeves MW, Harrell WK. Development of a chemically defined liquid medium for growth of *Legionella pneumophila*. Journal of Clinical Microbiology. 1979;9:615-26.

Poteryaev D, Datta S, Ackema K, Zerial M, Spang A. Identification of the switch in early-to-late endosome transition. Cell. 2010;141:497-508.

Prag G, Watson H, Kim YC, Beach BM, Ghirlando R, Hummer G, Bonifacino JS, Hurley JH. The Vps27/Hse1 complex is a GAT domain-based scaffold for ubiquitin-dependent sorting. Developmental cell. 2007;12:973-86.

Price CT, Al-Quadan T, Santic M, Jones SC, Kwaik YA. Exploitation of conserved eukaryotic host cell farnesylation machinery by an F-box effector of *Legionella pneumophila*. The Journal of experimental medicine. 2010;207:1713-26.

Price CT, Al-Quadan T, Santic M, Rosenshine I, Kwaik YA. Host proteasomal degradation generates amino acids essential for intracellular bacterial growth. Science. 2011;334:1553-7.

Prinz WA, Grzyb L, Veenhuis M, Kahana JA, Silver PA, Rapoport TA. Mutants affecting the structure of the cortical endoplasmic reticulum in *Saccharomyces cerevisiae*. The Journal of cell biology. 2000;150:461-74.

Progida C, Malerød L, Stuffers S, Brech A, Bucci C, Stenmark H. RILP is required for the proper morphology and function of late endosomes. Journal of cell science. 2007;120:3729-37.

Prosser DC, Whitworth K, Wendland B. Quantitative analysis of endocytosis with cytoplasmic pHluorin chimeras. Traffic. 2010;11:1141-50.

Raiborg C, Bremnes B, Mehlum A, Gillooly DJ, D'Arrigo A, Stang E, Stenmark H. FYVE and coiled-coil domains determine the specific localisation of Hrs to early endosomes. Journal of cell science. 2001;114:2255-63.

Raiborg C, Bache KG, Gillooly DJ, Madshus IH, Stang E, Stenmark H. Hrs sorts ubiquitinated proteins into clathrin-coated microdomains of early endosomes. Nature cell biology. 2002;4:394-8.

Rak A, Pylypenko O, Durek T, Watzke A, Kushnir S, Brunsveld L, Waldmann H, Goody RS, Alexandrov K. Structure of Rab GDP-dissociation inhibitor in complex with prenylated YPT1 GTPase. Science. 2003;302:646-50.

Rana M, Lachmann J, Ungermann C. Identification of a Rab GTPase-activating protein cascade that controls recycling of the Rab5 GTPase Vps21 from the vacuole. Molecular biology of the cell. 2015;26:2535-49.

Rasis M, Segal G. The LetA-RsmYZ-CsrA regulatory cascade, together with RpoS and PmrA, post-transcriptionally regulates stationary phase activation of *Legionella pneumophila* Icm/Dot effectors. Molecular microbiology. 2009;72:995-1010.

Raymond CK, Howald-Stevenson I, Vater CA, Stevens TH. Morphological classification of the yeast vacuolar protein sorting mutants: evidence for a prevacuolar compartment in class E vps mutants. Molecular biology of the cell. 1992;3:1389-402.

Rechnitzer C, Blom J. Engulfment of the Philadelphia strain of *Legionella pneumophila* within pseudopod coils in human phagocytes. Apmis. 1989;97:105-14.

Reggiori F, Klionsky DJ. Autophagic processes in yeast: mechanism, machinery and regulation. Genetics. 2013;194:341-61.

Ren X, Kloer DP, Kim YC, Ghirlando R, Saidi LF, Hummer G, Hurley JH. Hybrid structural model of the complete human ESCRT-0 complex. Structure. 2009;17:406-16.

Richardson SC, Winistorfer SC, Poupon V, Luzio JP, Piper RC. Mammalian late vacuole protein sorting orthologues participate in early endosomal fusion and interact with the cytoskeleton. Molecular biology of the cell. 2004;15:1197-210.

Riezman H. Endocytosis in yeast: several of the yeast secretory mutants are defective in endocytosis. Cell. 1985;40:1001-9.

Rink J, Ghigo E, Kalaidzidis Y, Zerial M. Rab conversion as a mechanism of progression from early to late endosomes. Cell. 2005;122:735-49.

Robinson JS, Klionsky DJ, Banta LM, Emr SD. Protein sorting in *Saccharomyces cerevisiae*: isolation of mutants defective in the delivery and processing of multiple vacuolar hydrolases. Molecular and cellular biology. 1988;8:4936-48.

Rodkey TL, Liu S, Barry M, McNew JA. Munc18a scaffolds SNARE assembly to promote membrane fusion. Molecular biology of the cell. 2008;19:5422-34.

Rohde G, Wenzel D, Haucke V. A phosphatidylinositol (4, 5)-bisphosphate binding site within μ2-adaptin regulates clathrin-mediated endocytosis. The Journal of cell biology. 2002;158:209-14.

Rolando M, Escoll P, Nora T, Botti J, Boitez V, Bedia C, Daniels C, Abraham G, Stogios PJ, Skarina T, Christophe C. *Legionella pneumophila* S1P-lyase targets host sphingolipid metabolism and restrains autophagy. Proceedings of the National Academy of Sciences. 2016:201522067.

Rossi V, Banfield DK, Vacca M, Dietrich LE, Ungermann C, D'Esposito M, Galli T, Filippini F. Longins and their longin domains: regulated SNAREs and multifunctional SNARE regulators. Trends in biochemical sciences. 2004;29:682-8.

Rossier O, Cianciotto NP. Type II Protein Secretion Is a Subset of the PilD-Dependent Processes That Facilitate Intracellular Infection by *Legionella pneumophila*. Infection and immunity. 2001;69:2092-8.

Rossier O, Starkenburg SR, Cianciotto NP. *Legionella pneumophila* type II protein secretion promotes virulence in the A/J mouse model of Legionnaires' disease pneumonia. Infection and immunity. 2004;72:310-21.

Rossier O, Cianciotto NP. The *Legionella pneumophila tatB* gene facilitates secretion of phospholipase C, growth under iron-limiting conditions, and intracellular infection. Infection and immunity. 2005;73:2020-32.

Roth AF, Sullivan DM, Davis NG. A large PEST-like sequence directs the ubiquitination, endocytosis, and vacuolar degradation of the yeast a-factor receptor. The Journal of cell biology. 1998 Aug 24;142(4):949-61.

Rothman JH, Howald I, Stevens TH. Characterization of genes required for protein sorting and vacuolar function in the yeast *Saccharomyces cerevisiae*. The EMBO Journal. 1989;8:2057.

Saksena S, Wahlman J, Teis D, Johnson AE, Emr SD. Functional reconstitution of ESCRT-III assembly and disassembly. Cell. 2009;136:97-109.

Sato K, Nakano A. Emp47p and its close homolog Emp46p have a tyrosine-containing endoplasmic reticulum exit signal and function in glycoprotein secretion in *Saccharomyces cerevisiae*. Molecular biology of the cell. 2002;13:2518-32.

Sato K, Nakano A. Oligomerization of a cargo receptor directs protein sorting into COPII-coated transport vesicles. Molecular biology of the cell. 2003;14:3055-63.

Scheffzek K, Klebe C, Fritz-Wolf K, Kabsch W, Wittinghofer A. Crystal structure of the nuclear Ras-related protein Ran in its GDP-bound form. Nature. 1995;374:378-81.

Scheffzek K, Ahmadian MR, Kabsch W, Wiesmüller L, Lautwein A, Schmitz F, Wittinghofer A. The Ras-RasGAP complex: structural basis for GTPase activation and its loss in oncogenic Ras mutants. Science. 1997;277:333-9.

Schimmoller F, Riezman H. Involvement of Ypt7p, a small GTPase, in traffic from late endosome to the vacuole in yeast. Journal of Cell Science. 1993;106:823-30.

Schindler C, Chen Y, Pu J, Guo X, Bonifacino JS. EARP is a multisubunit tethering complex involved in endocytic recycling. Nature cell biology. 2015;17:639-50.

Schoebel S, Cichy AL, Goody RS, Itzen A. Protein LidA from *Legionella* is a Rab GTPase supereffector. Proceedings of the National Academy of Sciences. 2011;108:17945-50.

Schröder S, Schimmöller F, Singer-Krüger B, Riezman H. The Golgi-localization of yeast Emp47p depends on its di-lysine motif but is not affected by the ret1-1 mutation in alpha-COP. The Journal of Cell Biology. 1995;131:895-912.

Schroeder GN, Petty NK, Mousnier A, Harding CR, Vogrin AJ, Wee B, Fry NK, Harrison TG, Newton HJ, Thomson NR, Beatson SA. *Legionella pneumophila* strain 130b possesses a unique combination of type IV secretion systems and novel Dot/Icm secretion system effector proteins. Journal of bacteriology. 2010;192:6001-16.

Schu PV, Takegawa K, Fry MJ, Stack JH, Waterfield MD, Emr SD. Phosphatidylinositol 3-kinase encoded by yeast VPS34 gene essential for protein sorting. Science. 1993;260:88-91.

Schuh AL, Audhya A. The ESCRT machinery: from the plasma membrane to endosomes and back again. Critical reviews in biochemistry and molecular biology. 2014;49:242-61.

Scott SV, Hefner-Gravink A, Morano KA, Noda T, Ohsumi Y, Klionsky DJ. Cytoplasm-to-vacuole targeting and autophagy employ the same machinery to deliver proteins to the yeast vacuole. Proceedings of the national academy of sciences. 1996;93:12304-8.

Scott SV, Guan J, Hutchins MU, Kim J, Klionsky DJ. Cvt19 is a receptor for the cytoplasm-to-vacuole targeting pathway. Molecular cell. 2001;7:1131-41.

Scott BL, Van Komen JS, Irshad H, Liu S, Wilson KA, McNew JA. Sec1p directly stimulates SNARE-mediated membrane fusion in vitro. The Journal of cell biology. 2004;167:75-85.

Scott A, Gaspar J, Stuchell-Brereton MD, Alam SL, Skalicky JJ, Sundquist WI. Structure and ESCRT-III protein interactions of the MIT domain of human VPS4A. Proceedings of the National Academy of Sciences of the United States of America. 2005;102:13813-8.

Seabra MC, Goldstein JL, Südhof TC, Brown MS. Rab geranylgeranyl transferase. A multisubunit enzyme that prenylates GTP-binding proteins terminating in Cys-X-Cys or Cys-Cys. Journal of Biological Chemistry. 1992;267:14497-503.

Seals DF, Eitzen G, Margolis N, Wickner WT, Price A. A Ypt/Rab effector complex containing the Sec1 homolog Vps33p is required for homotypic vacuole fusion. Proceedings of the national academy of sciences. 2000;97:9402-7.

Seeley ES, Kato M, Margolis N, Wickner W, Eitzen G. Genomic analysis of homotypic vacuole fusion. Molecular biology of the cell. 2002;13:782-94.

Segal G, Purcell M, Shuman HA. Host cell killing and bacterial conjugation require overlapping sets of genes within a 22-kb region of the *Legionella pneumophila* genome. Proceedings of the National Academy of Sciences. 1998;95:1669-74.

Shanks SG, Carpp LN, Struthers MS, McCann RK, Bryant NJ. The Sec1/Munc18 protein Vps45 regulates cellular levels of its SNARE binding partners Tlg2 and Snc2 in *Saccharomyces cerevisiae*. PloS one. 2012;7:e49628.

Shin S. 3 Innate Immunity to Intracellular Pathogens: Lessons Learned from *Legionella pneumophila*. Advances in applied microbiology. 2012 Jan 1;79:43.

Shohdy N, Efe JA, Emr SD, Shuman HA. Pathogen effector protein screening in yeast identifies *Legionella* factors that interfere with membrane trafficking. Proceedings of the National Academy of Sciences of the United States of America. 2005;102:4866-71.

Singer-Krüger B, Stenmark H, Düsterhöft A, Philippsen P, Yoo JS, Gallwitz D, Zerial M. Role of three rab5-like GTPases, Ypt51p, Ypt52p, and Ypt53p, in the endocytic and vacuolar protein sorting pathways of yeast. The Journal of cell biology. 1994;125:283-98.

Siniossoglou S, Pelham HR. An effector of Ypt6p binds the SNARE Tlg1p and mediates selective fusion of vesicles with late Golgi membranes. The EMBO Journal. 2001;20:5991-8.

Slagsvold T, Aasland R, Hirano S, Bache KG, Raiborg C, Trambaiolo D, Wakatsuki S, Stenmark H. Eap45 in mammalian ESCRT-II binds ubiquitin via a phosphoinositide-interacting GLUE domain. Journal of Biological Chemistry. 2005;280:19600-6.

Söderberg MA, Rossier O, Cianciotto NP. The type II protein secretion system of Legionella pneumophila promotes growth at low temperatures. Journal of bacteriology. 2004;186:3712-20.

Söderberg MA, Dao J, Starkenburg SR, Cianciotto NP. Importance of type II secretion for survival of *Legionella pneumophila* in tap water and in amoebae at low temperatures. Applied and environmental microbiology. 2008;74:5583-8.

Soldati T, Riederer MA, Pfeffer SR. Rab GDI: a solubilizing and recycling factor for rab9 protein. Molecular Biology of the Cell. 1993;4:425-34.

Solinger JA, Spang A. Tethering complexes in the endocytic pathway: CORVET and HOPS. FEBS Journal. 2013;280:2743-57.

Söllner T, Bennett MK, Whiteheart SW, Scheller RH, Rothman JE. A protein assembly-disassembly pathway in vitro that may correspond to sequential steps of synaptic vesicle docking, activation, and fusion. Cell. 1993;75:409-18.

Sorkin A, von Zastrow M. Endocytosis and signalling: intertwining molecular networks. Nature reviews Molecular cell biology. 2009;10:609-22.

Sreelatha A, Bennett TL, Carpinone EM, O'Brien KM, Jordan KD, Burdette DL, Orth K, Starai VJ. *Vibrio* effector protein VopQ inhibits fusion of V-ATPase–containing membranes. Proceedings of the National Academy of Sciences. 2015;112:100-5.

Stack JH, DeWald DB, Takegawa K, Emr SD. Vesicle-mediated protein transport: regulatory interactions between the Vps15 protein kinase and the Vps34 PtdIns 3-kinase essential for protein sorting to the vacuole in yeast. The Journal of cell biology. 1995;129:321-34.

Starai VJ, Hickey CM, Wickner W. HOPS proofreads the trans-SNARE complex for yeast vacuole fusion. Molecular biology of the cell. 2008;19:2500-8.

Steele TW. Legionnaires' disease in South Australia, 1979-1988. The Medical journal of Australia. 1989;151:322-5.

Stenmark H. Rab GTPases as coordinators of vesicle traffic. Nature reviews Molecular cell biology. 2009;10:513-25.

Stewart CR, Rossier O, Cianciotto NP. Surface translocation by *Legionella pneumophila*: a form of sliding motility that is dependent upon type II protein secretion. Journal of bacteriology. 2009;191:1537-46.

Strom MS, Lory S. Structure-function and biogenesis of the type IV pili. Annual Reviews in Microbiology. 1993;47:565-96.

Stroupe C, Collins KM, Fratti RA, Wickner W. Purification of active HOPS complex reveals its affinities for phosphoinositides and the SNARE Vam7p. The EMBO Journal. 2006;25:1579-89.

Subramanian S, Woolford CA, Jones EW. The Sec1/Munc18 protein, Vps33p, functions at the endosome and the vacuole of *Saccharomyces cerevisiae*. Molecular biology of the cell. 2004;15:2593-605.

Sutherland MC, Nguyen TL, Tseng V, Vogel JP. The *Legionella* IcmSW complex directly interacts with DotL to mediate translocation of adaptor-dependent substrates. PLoS Pathog. 2012;8:e1002910.

Sutton RB, Fasshauer D, Jahn R, Brunger AT. Crystal structure of a SNARE complex involved in synaptic exocytosis at 2.4 Å resolution. Nature. 1998;395:347-53.

Suzuki K, Kirisako T, Kamada Y, Mizushima N, Noda T, Ohsumi Y. The pre-autophagosomal structure organized by concerted functions of APG genes is essential for autophagosome formation. The EMBO journal. 2001;20:5971-81.

Suzuki K, Kamada Y, Ohsumi Y. Studies of cargo delivery to the vacuole mediated by autophagosomes in *Saccharomyces cerevisiae*. Developmental cell. 2002;3:815-24.

Swanson MS, Isberg RR. Association of *Legionella pneumophila* with the macrophage endoplasmic reticulum. Infection and immunity. 1995;63:3609-20.

Schuh AL, Audhya A. The ESCRT machinery: from the plasma membrane to endosomes and back again. Critical reviews in biochemistry and molecular biology. 2014;49:242-61.

Tall GG, Hama H, DeWald DB, Horazdovsky BF. The phosphatidylinositol 3-phosphate binding protein Vac1p interacts with a Rab GTPase and a Sec1p homologue to facilitate vesicle-mediated vacuolar protein sorting. Molecular Biology of the Cell. 1999;10:1873-89.

Tan Y, Luo ZQ. *Legionella pneumophila* SidD is a deAMPylase that modifies Rab1. Nature. 2011;475:506-9.

Tatlock H. A Rickettsia-like Organism Recovered from Guinea Pigs. Experimental Biology and Medicine. 1944;57:95-9.

Teis D, Saksena S, Emr SD. Ordered assembly of the ESCRT-III complex on endosomes is required to sequester cargo during MVB formation. Developmental cell. 2008;15:578-89.

Teo H, Perisic O, González B, Williams RL. ESCRT-II, an endosome-associated complex required for protein sorting: crystal structure and interactions with ESCRT-III and membranes. Developmental cell. 2004;7:559-69.

Teo H, Gill DJ, Sun J, Perisic O, Veprintsev DB, Vallis Y, Emr SD, Williams RL. ESCRT-I core and ESCRT-II GLUE domain structures reveal role for GLUE in linking to ESCRT-I and membranes. Cell. 2006;125:99-111.

Tilney LG, Harb OS, Connelly PS, Robinson CG, Roy CR. How the parasitic bacterium *Legionella pneumophila* modifies its phagosome and transforms it into rough ER: implications for conversion of plasma membrane to the ER membrane. Journal of Cell Science. 2001;114:4637-50.

Toshima JY, Sato Y, Yamamoto W, Furukawa D, Siekhaus DE, Sawaguchi A, Toshima J. Bifurcation of the endocytic pathway into Rab5-dependent and-independent transport to the vacuole. Nature communications. 2014;5.

Toulabi L, Wu X, Cheng Y, Mao Y. Identification and structural characterization of a *Legionella* phosphoinositide phosphatase. Journal of Biological Chemistry. 2013;288:24518-27.

Touz MC, Kulakova L, Nash TE. Adaptor protein complex 1 mediates the transport of lysosomal proteins from a Golgi-like organelle to peripheral vacuoles in the primitive eukaryote *Giardia lamblia*. Molecular biology of the cell. 2004;15:3053-60.

Trajkovic K, Hsu C, Chiantia S, Rajendran L, Wenzel D, Wieland F, Schwille P, Brügger B, Simons M. Ceramide triggers budding of exosome vesicles into multivesicular endosomes. Science. 2008;319:1244-7.

Trumbly RJ, Bradley GA. Isolation and characterization of aminopeptidase mutants of *Saccharomyces cerevisiae*. Journal of bacteriology. 1983;156:36-48.

Ungermann C, Von Mollard GF, Jensen ON, Margolis N, Stevens TH, Wickner W. Three v-SNAREs and two t-SNAREs, present in a pentameric cis-SNARE complex on isolated vacuoles, are essential for homotypic fusion. The Journal of cell biology. 1999;145:1435-42.

Ullrich O, Stenmark H, Alexandrov K, Huber LA, Kaibuchi K, Sasaki T, Takai Y, Zerial M. Rab GDP dissociation inhibitor as a general regulator for the membrane association of rab proteins. Journal of Biological Chemistry. 1993;268:18143-50.

Urwyler S, Nyfeler Y, Ragaz C, Lee H, Mueller LN, Aebersold R, Hilbi H. Proteome analysis of *Legionella* vacuoles purified by magnetic immunoseparation reveals secretory and endosomal GTPases. Traffic. 2009;10:76-87.

van der Kant R, Jonker CT, Wijdeven RH, Bakker J, Janssen L, Klumperman J, Neefjes J. Characterization of the Mammalian CORVET and HOPS Complexes and Their Modular Restructuring for Endosome Specificity. Journal of Biological Chemistry. 2015;290:30280-90.

Venkataraman C, Haack BJ, Bondada S, Kwaik YA. Identification of a Gal/GalNAc lectin in the protozoan *Hartmannella vermiformis* as a potential receptor for attachment and invasion by the Legionnaires' disease bacterium. The Journal of experimental medicine. 1997;186:537-47.

Vida TA, Emr SD. A new vital stain for visualizing vacuolar membrane dynamics and endocytosis in yeast. The Journal of cell biology. 1995;128:779-92.

Vincent CD, Friedman JR, Jeong KC, Buford EC, Miller JL, Vogel JP. Identification of the core transmembrane complex of the *Legionella* Dot/Icm type IV secretion system. Molecular microbiology. 2006;62:1278-91.

Vollmer P, Will E, Scheglmann D, Strom M, Gallwitz D. Primary structure and biochemical characterization of yeast GTPase-activating proteins with substrate preference for the transport GTPase Ypt7p. European journal of biochemistry. 1999;260:284-90.

Vollenweider F, Kappeler F, Itin C, Hauri HP. Mistargeting of the lectin ERGIC-53 to the endoplasmic reticulum of HeLa cells impairs the secretion of a lysosomal enzyme. The Journal of cell biology. 1998;142:377-89.

Vogel JP, Andrews HL, Wong SK, Isberg RR. Conjugative transfer by the virulence system of *Legionella pneumophila*. Science. 1998;279:873-6.

Von Der Haar T. Optimized protein extraction for quantitative proteomics of yeasts. PloS one. 2007;2:e1078.

von Mollard GF, Nothwehr SF, Stevens TH. The yeast v-SNARE Vti1p mediates two vesicle transport pathways through interactions with the t-SNAREs Sed5p and Pep12p. The Journal of cell biology. 1997;137:1511-24.

Voth WP, Wei Jiang Y, Stillman DJ. New 'marker swap'plasmids for converting selectable markers on budding yeast gene disruptions and plasmids. Yeast. 2003;20:985-93.

Walz HA, Shi X, Bue CA, Navaroli DM, Hayakawa A, Zhou QL, Nadler J, Leonard DM, Corvera S. Isoform-specific regulation of Akt signaling by the endosomal protein WDFY2. Journal of Biological Chemistry. 2010;285:14101-8.

Wang CW, Stromhaug PE, Shima J, Klionsky DJ. The Ccz1-Mon1 protein complex is required for the late step of multiple vacuole delivery pathways. Journal of biological chemistry. 2002;277:47917-27.

Wang L, Seeley ES, Wickner W, Merz AJ. Vacuole fusion at a ring of vertex docking sites leaves membrane fragments within the organelle. Cell. 2002;108:357-69.

Wang YJ, Wang J, Sun HQ, Martinez M, Sun YX, Macia E, Kirchhausen T, Albanesi JP, Roth MG, Yin HL. Phosphatidylinositol 4 phosphate regulates targeting of clathrin adaptor AP-1 complexes to the Golgi. Cell. 2003;114:299-310.

Weber S, Wagner M, Hilbi H. Live-cell imaging of phosphoinositide dynamics and membrane architecture during *Legionella* infection. MBio. 2014;5:e00839-13.

Weber-Boyvat M, Aro N, Chernov KG, Nyman T, Jäntti J. Sec1p and Mso1p C-terminal tails cooperate with the SNAREs and Sec4p in polarized exocytosis. Molecular biology of the cell. 2011;22:230-44.

Weidman PJ, Melançon P, Block MR, Rothman JE. Binding of an N-ethylmaleimide-sensitive fusion protein to Golgi membranes requires both a soluble protein (s) and an integral membrane receptor. The Journal of cell biology. 1989;108:1589-96.

Weisman LS, Wickner W. Molecular characterization of VAC1, a gene required for vacuole inheritance and vacuole protein sorting. Journal of Biological Chemistry. 1992;267:618-23.

Weiss ER, Göttlinger H. The role of cellular factors in promoting HIV budding. Journal of molecular biology. 2011;410:525-33.

Whyte JR, Munro S. Vesicle tethering complexes in membrane traffic. Journal of Cell Science. 2002;115:2627-37.

Wigren E, Bourhis JM, Kursula I, Guy JE, Lindqvist Y. Crystal structure of the LMAN1-CRD/MCFD2 transport receptor complex provides insight into combined deficiency of factor V and factor VIII. FEBS letters. 2010;584:878-82.

Wollert T, Wunder C, Lippincott-Schwartz J, Hurley JH. Membrane scission by the ESCRT-III complex. Nature. 2009;458:172-7.

Xu L, Luo ZQ. Cell biology of infection by *Legionella pneumophila*. Microbes and Infection. 2013;15:157-67.

Xu Y, Su L, Rizo J. Binding of Munc18-1 to synaptobrevin and to the SNARE four-helix bundle. Biochemistry. 2010;49:1568-76.

Yao D, Cherney M, Cygler M. Structure of the N-terminal domain of the effector protein LegC3 from *Legionella pneumophila*. Acta Crystallographica Section D: Biological Crystallography. 2014;70:436-41.

Yeung BG, Phan HL, Payne GS. Adaptor complex-independent clathrin function in yeast. Molecular biology of the cell. 1999;10:3643-59.

Yu IM, Hughson FM. Tethering factors as organizers of intracellular vesicular traffic. Annual review of cell and developmental biology. 2010;26:137-56.

Yu Z, Gonciarz MD, Sundquist WI, Hill CP, Jensen GJ. Cryo-EM structure of dodecameric Vps4p and its 2: 1 complex with Vta1p. Journal of molecular biology. 2008;377:364-77.

Yuga M, Gomi K, Klionsky DJ, Shintani T. Aspartyl aminopeptidase is imported from the cytoplasm to the vacuole by selective autophagy in *Saccharomyces cerevisiae*. Journal of Biological Chemistry. 2011;286:13704-13.

Zhang B, Cunningham MA, Nichols WC, Bernat JA, Seligsohn U, Pipe SW, McVey JH, Schulte-Overberg U, de Bosch NB, Ruiz-Saez A, White GC. Bleeding due to disruption of a cargo-specific ER-to-Golgi transport complex. Nature genetics. 2003;34:220-5.

Zhu W, Hammad LA, Hsu F, Mao Y, Luo ZQ. Induction of caspase 3 activation by multiple *Legionella pneumophila* Dot/Icm substrates. Cellular microbiology. 2013;15:1783-95.

Zusman T, Yerushalmi G, Segal G. Functional similarities between the icm/dot pathogenesis systems of *Coxiella burnetii* and *Legionella pneumophila*. Infection and immunity. 2003;71:3714-23.

Zusman T, Aloni G, Halperin E, Kotzer H, Degtyar E, Feldman M, Segal G. The response regulator PmrA is a major regulator of the icm/dot type IV secretion system in *Legionella pneumophila* and *Coxiella burnetii*. Molecular microbiology. 2007;63:1508-23.

Zwilling D, Cypionka A, Pohl WH, Fasshauer D, Walla PJ, Wahl MC, Jahn R. Early endosomal SNAREs form a structurally conserved SNARE complex and fuse liposomes with multiple topologies. The EMBO Journal. 2007;26:9-18.

APPENDIX 1

In order to determine if the overexpression of any genes were able to suppress LegC7 induced toxicity we selected a representative group of endosome genes and expressed them from *GAL1* promoters. Only overexpression of *VAC1* was able to partially compensate for LegC7 toxicity. Interestingly overexpression of *VPS3, VPS33, PEP12, YKT6,* or *VPS34* was not able to suppress LegC7 toxicity. Overexpression of *VPS21* proved to be toxic meaning we are unable to determine what effect overexpression of this gene has on LegC7 induced toxicity. Overexpression of *VAC1* was previously noted to compensate for mutations in the CORVET complex, supporting the hypothesis that LegC7 may manipulate CORVET functionality (Cabrera 2013). Overexpression of *VPS34* was not able to suppress toxicity consistent with the idea that LegC7 does not cause a defect in PI(3)P synthesis, but instead may cause a defect in the localization of PI(3)P synthesis. Further overexpression analysis will be required in order to ascertain additional genetic suppressors of LegC7 toxicity.

Table 6.1 Plasmids used in this study

Plasmid	**Characteristics**	**Source**
pVJS81	pYES2/NT C, *VPS33, URA3*	This Study
pVJS82	pYES2/NT C, *VPS3, URA3*	This Study
pVJS83	pYES2/NT C, *VPS21, URA3*	This Study
pVJS84	pYES2/NT C, *VPS34, URA3*	This Study
pVJS85	BG1805, *GAL1*, *URA3, HA:YKT6*	GE Dharmacon
pVJS86	BG1805, *GAL1*, *URA3, HA:PEP12*	GE Dharmacon
pVJS87	BG1805, *GAL1*, *URA3, HA:VAC1*	GE Dharmacon

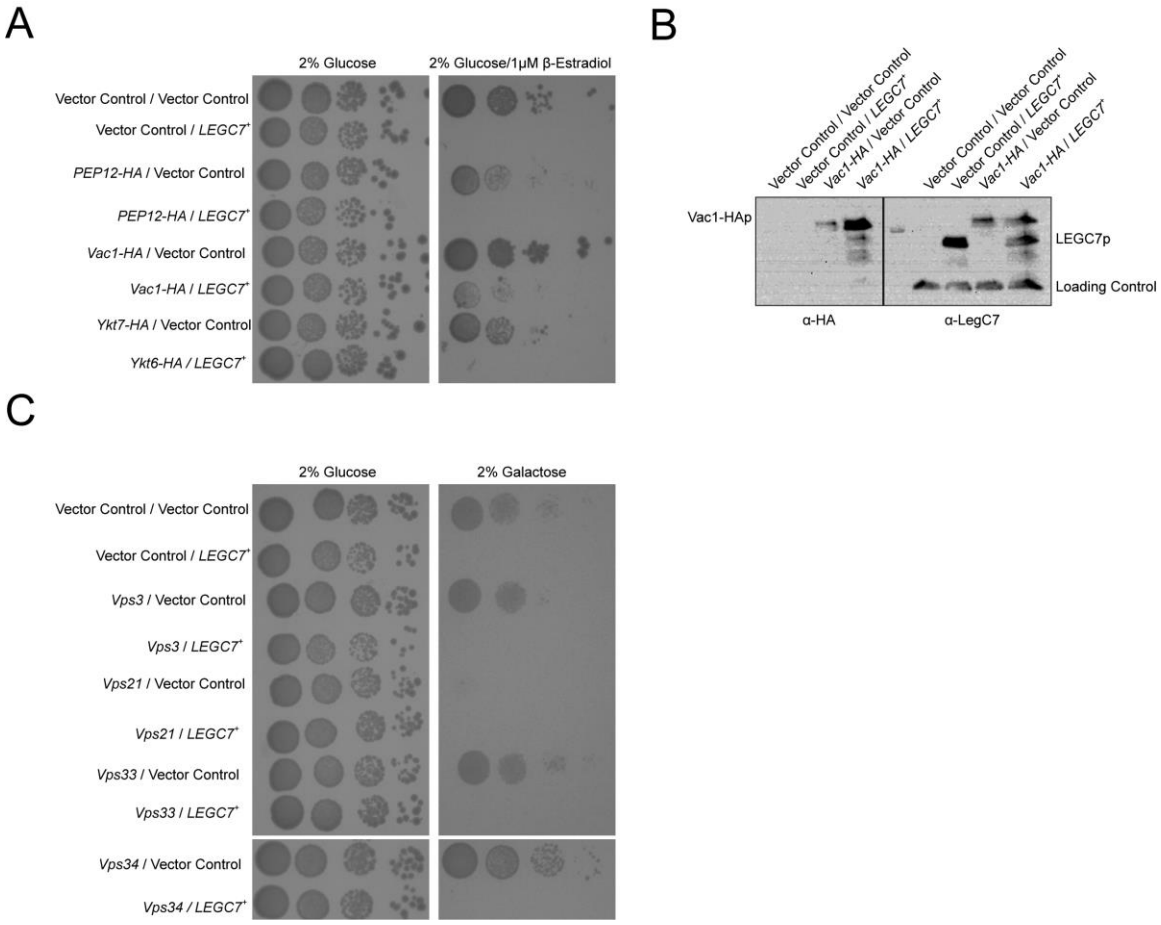

Figure 6.1: Overexpression of Vac1 suppresses LegC7 toxicity.
A. BY4742 pACT1 cells containing either pVJS53 or the vector control and either HA-Vac1, HA-Ykt6, or HA-Pep12 were grown in CSM-uracil-lysine for 16 hours at 30°. Cells were serially diluted and spotted to CSM-uracil-lysine media containing either 2% glucose or 2% glucose and 1μM β-estradiol and grown for 72 hours at 30°.
B. BY4742 pACT1 cells containing HA-Vac1 and either pVJS53 or the vector control were grown in CSM-uracil-lysine for 16 hours at 30°. Cells were collected by centrifugation, washed with sterile water and suspended in CSM-uracil-lysine media containing 2% glucose and 1μM β-estradiol and grown for 16 hours at 30°. 1 OD of cells was then harvested and total protein was extracted (von der Haar 2007). Samples were immunodetected for HA (1:1000 Mouse) and LegC7 (1:1000 Rabbit).
C. BY4742 cells containing either pVJS53 or the vector control and either pYES2/NTc-Vps3, pYES2/NTc-Vps21, pYES2/NTc-Vps33 were grown in CSM-uracil-lysine containing 2% glucose for 16 hours at 30°. Cells were serially diluted and spotted to CSM-uracil-lysine media containing either 2% glucose or 2% galactose and incubated for 72 hours at 30°.